Flinders UNIVERSITY
ADELAIDE · SOUTH AUSTRALIA

Quantitating tonic muscle activity in head and neck for artefact removal or disease understanding

by

Azinsadat Janani

Thesis
Submitted to Flinders University
for the degree of

PhD

College of Science and Engineering
15/08/2019

Abstract

Scalp electrical recordings using surface electrodes are traditionally used to record brain signals (EEG) but such recordings contain other biological signals such as cranial and upper cervical muscle signals (EMG), cardiac signals (ECG), etc.

Recent studies have shown that even during the "relaxed" condition, sitting or reclining, many cranial and upper cervical muscles are involuntarily contracted to maintain posture, facial expression, etc. Their activity has a broad-band spectrum that overlaps the spectrum of brain and exceeds it in power. Hence, the effect of tonic muscle activity during a usual scalp electrical recording is too large to be ignored.

On the one hand, separating and removing (pruning) these tonic muscle signals from scalp electrical recordings is an issue in brain studies. On the other hand, separating and keeping these tonic muscle signals (quantitating) is valuable for treatment and/or understanding of the role of muscle in some medical conditions, such as headache.

In this thesis, using the unique database of pharmacologically induced paralysis subjects, I evaluate the effectiveness of some current advanced signal processing algorithms (blind source separation) in the automated reduction of tonic cranial and upper cervical muscle activity from scalp electrical recordings. I then study one poorly-performing algorithm (canonical correlation analysis) in detail, and propose an extension with improved results. I also propose a completely new approach to muscle pruning, based on source localisation. Acknowledging the difference in approach between these algorithms, I explore the complementary effect of double pruning approaches targeting different features of muscle signals, and show that tonic muscle reduction using double pruning approaches is significantly more effective than single pruning approaches.

I also describe an "inverted" use of muscle pruning algorithms, and propose a new holistic cranial and upper cervical muscle quantitation approach using a high-density EEG cap. This

approach is validated using scalp electrical recordings from subjects suffering from diseases associating with increased muscle tension. Applying this approach on scalp electrical recordings of migraineurs and controls reveals that there is more cranial and upper cervical muscle activity in migraineurs than controls. This result diminishes one of the conceptual distinctions between migraine and tension-type headache.

Contents

List of Figures

List of Tables

Declaration

I certify that this thesis does not incorporate without acknowledgment any material previously submitted for a degree or diploma in any university; and to the best of my knowledge and belief, does not contain any material previously published or written by another person except where due reference is made in the text.

Azinsadat Janani 

Date: 18/01/2019

Acknowledgements

This PhD was supported by an Australian Government Research Training Program Scholarship. Many people helped and supported me throughout my PhD journey. Firstly, I would like to express my sincere thanks to my supervisors Assoc. Prof. Kenneth Pope and Prof. John Willoughby for their continuous support, great advice, patience, motivation, and immense knowledge. Their guidance helped me in all the time of research and writing of my thesis and papers, and I learnt a lot from them.

My sincere thanks also goes to Dr Trent Lewis, Dr Emma Whitham, and Dr Dylan DeLosAngeles who helped me in data recording. It would not be possible to conduct this research without their precious support.

I thank my fellow lab mate Tyler Grummett who have always supported me with his great suggestions. I also sincerely thank my friend Hanieh Bakhshayesh for her precious help especially during the first couple of months of my PhD, and for all the fun we have had in the last four years.

My special thanks goes to my mother, father and brothers who always supported me in achieving my goals. I appreciate my parents for the selfless love, care, dedicated efforts and sacrifices they did to shape my life. I would never be able to pay back the love showered upon me by my parents.

I owe thanks to a very special person, my husband Ali, for his continued and unfailing love, support and understanding during my PhD journey. I could not finish my PhD without his support and encouragement.

List of abbreviations

ICHD: International Classification of Headache Disorders

SER: Scalp Electrical Recording

EMG: ElectroMyoGraph

EEG: ElectroEncephaloGraph

ECG or EKG: ElectroCardioGraph

EOG: ElectroOculoGraph

MEG: MagnetoEncephaloGraphy

BSS: Blind Source Separation

JBSS: Joint Blind Source Separation

ICA: Independent Component Analysis

CCA: Canonical Correlation Analysis

IVA: Independent Vector Analysis

PDF: Probability Density Function

SCM: Source Component Matrix

sLORETA: standardized LOw Resolution Electromagnetic Tomography

VSSR: Visual Steady State Response

ASSR: Auditory Steady State Response

AERP: Auditory Event-Related Potential

ANOVA: ANalysis Of VAriance

SMU: Single Motor Unit

BEM: Boundary Element Method

PD: Parkinson's Disease

CAE: Childhood Absence Epilepsy

Chapter 1

Introduction

Headache is the most common neurological disorder, and any person is likely to experience headache during their lifetime. There are many types of headache disorder. The first categorisation of headache is into primary headache and secondary headache, where secondary headaches are rarer and more serious. They usually arise from other serious medical conditions which can cause headache, whereas primary headaches are thought to arise from biological dysfunction without any obvious medical issue.

Within primary headache, the sensory qualities of the pain are the primary features for categorisation. Migraine and tension-type headache are the most common types of primary headaches. The distinction between tension-type headache and migraine can be difficult to make. Increased pericranial muscle tenderness, which can be detected easily by palpation, is the most common abnormality in tension-type headache. Moreover, the International Classification of Headache Disorders (ICHD) considers muscle to be relevant in tension-type headache and uses other names such as muscle contraction headache and myogenic headache to refer to the tension-type headache.

So, one distinction that was made between tension-type headache and migraine was excess muscle activity (tension), allowing us to conclude that muscle does not contribute to migraine with or without aura. The word “muscle” is not even mentioned in the ICHD’s definition of migraine. However, there are now a small but significant number of quantitative studies, and roughly three times as many qualitative studies, that report increased muscle activity in

migraine sufferers. Their findings weaken the thinking that increased muscle activity is a feature only of tension-type headache and, therefore, changes our thinking about muscle activity and headache.

1.1 Research question

Consistent with this changing view, the initial research question of my thesis was: **"Is cranial and cervical muscle activity variant in different types of headache at rest, and can it be regarded as a feature to diagnose different types of headache"?**

There is a lack of studies providing *comprehensive* quantification of resting cranial and cervical muscle activity in headache patients. Previous research evaluating muscle tension in headache sufferers can be separated into qualitative research and quantitative research. Qualitative research evaluated the location and the level of muscle tension by asking participants to respond to questions targeting the quality of their pain and tenderness, or evaluating their pressure-pain sensitivity and muscle tenderness by palpation. The quantitative research used electromyography (EMG) from one or more muscles to measure the level of muscle tension. The findings of previous studies are not consistent, in that they have not pointed to a defined alteration in muscle activity. There are limitations in the methodologies in these studies:

- Most of the previous studies are qualitative rather than quantitative. Examining muscle tenderness by palpation cannot provide a reliable measurement of the level of muscle tension.
- The quantitative studies recorded EMG from only a few muscles, which cannot provide a reliable conclusion about the overall cranial and upper cervical muscle activity.
- Some of the quantitative studies recorded EMG from muscles while the participant was reclined, so that most of the cranial and upper cervical muscles holding the

posture of head and neck are at rest. The difference in muscle activity between reclined and seated is not well understood, hence posture is a confounding factor.

So, there is still a need for a comprehensive quantitative study or studies which can answer the question about the relationship between tonic muscle activity and different types of headache.

1.2 Experimental design

To answer my research question about the relationship between muscle activity and headache, I recorded data from both headache sufferers and healthy controls, and quantified the activity of cranial and upper cervical muscles in headache and headache-free phases. This relationship, if found, should give a better understanding of headache pathophysiology as well as a more appropriate and useful classification of primary headaches.

The main difference between my study and all previous qualitative studies is that, instead of recording surface EMG from a few specific groups of upper cervical or cranial muscles, I collected scalp electrical recordings using a passive high-density electroencephalograph (EEG) cap. Scalp electrical recordings using surface electrodes are traditionally used to record EEG, but such recordings contain other signals such as EMG, electrooculograms (EOG), electrocardiograms (ECG or EKG), mains power frequencies, white noise and other artefacts. So, the term EEG has been used both for the brain activity alone, and also for the scalp recording that includes many biological and non-biological signals. In this thesis, it is important to make this distinction clear. Hence, I use EEG to mean brain electrical activity alone, and I use the term Scalp Electrical Recording (SER) to refer to the measurements of electrical signals on the scalp which include EEG, EMG, EOG, ECG, mains power frequencies and environmental noise.

A high-density SER cap includes electrodes over muscles such as the frontalis, temporalis etc., and close to other muscles. Given modern methods of signal analysis, it is now possible

to extract EMG activity and other contaminants from SERs. At frequencies above 10-20 Hz, EMG signals are the largest contributors to SERs. Using such methods, therefore, it is equally feasible to obtain 'clean' EEG and to accurately quantitate power corresponding to EMG activity. Hence SERs can be valuable in quantitating muscle activity.

The cap used for my recordings included 64 electrodes distributed over cranial muscles such as the frontalis, orbicularis and temporalis, and also close to nuchal (upper cervical) muscles. Six bipolar surface electrodes were attached to record the activity of upper cervical muscles: sternomastoid (left and right), paraspinal (left and right) and trapezius (left and right). Therefore, the recorded signals could cover the activity of all cranial and upper cervical muscles and provide a higher resolution of the cranial and upper cervical muscle activity.

Participants were asked to perform two baseline tasks (5 minutes each), sitting in a chair in a relaxed position with closed eyes, and reclining with closed eyes, besides some contraction tasks (10 seconds each) such as frowning, raising their eyebrows, chewing, moving their head to the right and left, and shrugging their shoulders. The main target was to quantitate resting (baseline tasks) cranial and upper cervical muscle activity. The contraction tasks were included to assist in extracting EMG from the SERs. The resulting quantitated muscle activity could then be compared between groups, such as controls versus headache sufferers.

1.3 Participant selection criteria and the sample size

Participant selection was governed by the exclusion and inclusion criteria specified below.

Exclusion criteria:

- People with any other neurological disorder or history of head surgery;
- People with infection or skin problems;
- People with internal electrical devices such as a pacemaker.

Inclusion criterion:

- Diagnosis, by a neurologist, of severe (intense and frequent) migraine (with or without aura), tension-type headache or cervicogenic headache.

Additionally, participants with headache were expected to attend once without headache, and then again once or twice more during headache with and/or without aura. Participants were encouraged to have a friend or partner willing to accompany and support them for the recordings during a headache. All participants were required to sign a consent form and to fill in a questionnaire to record their headache characteristics.

To determine the appropriate sample size, a predicted effect size is required. One study has conducted a reduced form of my experiment on migraine patients, and evaluated muscle activity on sternomastoid muscle. The mean and variance of muscle activity are reported in headache-free phase and headache phase. By using this result and performing a standard power analysis, I estimated that I would need 25 subjects for each type of headache. Hence, I needed to record data from around 100 headache sufferers (migraine with aura, migraine without aura, tension-type headache, cervicogenic headache), and 50 controls to provide effective matches with the headache participants.

1.4 Recruitment of participants

The participants were recruited from four sources.

1. Individuals managed by neurologists at the Flinders Medical Centre who were diagnosed as having primary headache. Potential participants were advised of the study by their clinical consultant at the time of their presentation to the Neurology outpatient clinic or to the hospital wards, and invited to participate. If they showed interest in this study, the neurologist would outline the process.
2. Individuals managed by Watson Headache Clinic. Potential participants were advised of the study by their physiotherapist, and invited to participate in the study if they were interested.

3. Colleagues and staff of Flinders Medical Centre were invited to participate in the study through a poster advertisement.
4. Colleagues, families or friends of the investigators, with and without headache, who showed interest were also invited to participate in the study.

After one year of recording, 27 participants were recorded, 12% control and 88% headache sufferers. 8% of headache sufferers were recruited from neurology department of Flinders Medical Centre, 21% from Watson Headache Clinic, and the rest were families and friends of the investigators.

It was originally expected that more than 80% of headache sufferers would be recruited from sources one and two, but most of the interested volunteers changed their mind after being informed about the procedure of the study. They gave up due to various difficulties such as: the location of the study (it was too far for them), the duration of study (approximately 1.5 hours), and the severity of their headache (which made it hard for them to tolerate the study). All of the headache participants were suffering from more than one type of headache. In other words, they had a mixture of two or three types of headache, mostly tension-type headache and migraine. Additionally, all of the headache sufferers had only undergone recording during their non-headache phase.

It was clear that, at this rate of recruitment, I was unlikely to record sufficient participants to meet the aims of the study, in particular to have sufficient statistical power to appropriately address the research question.

1.5 The revised research questions

Since my purpose was to quantitate cranial muscle activity at rest by recording scalp measurement using a high-density SER cap, it meant that muscle activity had to be extracted or isolated from the SER. A consequence of this is that we are left with reconstructed SERs that contain mainly EEG, i.e. with reduced EMG, ideally EMG-free. I call such reconstructed

signals “pruned”. Turning this thinking in reverse, we can quantitate muscle activity by using algorithms that extract muscle activity from SERs and retaining rather than discarding the muscle activity.

Blind Source Separation (BSS) methods are the most commonly used methods for the task of separating SERs into their different biological or non-biological sources, such as brain activity, muscle activity, cardiac activity, environmental noise, etc. After a BSS algorithm has identified components, they are classified and either retained or discarded. The retained components are then re-mixed to yield pruned signals. The standard approach to testing the effectiveness of these methods has been to prune SERs with high amplitude phasic muscle activity and compare them to baseline relaxed signals. But, it is known that even during the baseline relaxed condition lots of muscles are activated to maintain head posture and facial expression, and hence baseline SERs include tonic muscle activity. Therefore, this approach can only evaluate the effectiveness of BSS algorithms in removing phasic muscle activity. A more nuanced and powerful evaluation has recently been published, that tests both the removal of low amplitude tonic muscle components and the retention of brain responses, despite the overlap of their spectra. However, this study has only used AMICA as the BSS algorithm, which is not commonly used in neuroscience and brain research due to its high computational cost. Hence, there are still many questions about the effectiveness of the current BSS methods in reducing tonic muscle activity without affecting the brain activity.

To fully test tonic muscle reduction, there is a need for two sets of SERs: one that is free from tonic muscle signals and one that includes them. With access to this kind of dataset, it is possible to apply any BSS algorithms to the second set of SERs (brain with tonic muscle) and then to compare the pruning results to the first set of SERs (brain without tonic muscle). To collect SERs of normal brain activity without tonic muscle activity, it essentially requires the participants to be awake while paralysed. This condition is invasive and ethically challenging.

To the best of my knowledge, only one dataset has been collected under this paralysed condition which makes it unique in the domain of brain research.

I have access to this unique dataset. This dataset consists of high-density SERs from six healthy participants recorded in two conditions, once before and once during pharmacologically-induced paralysis (EMG-contaminated and EMG-free). It is expected that the application of BSS algorithms to EMG-contaminated data should yield pruned signals whose characteristics are similar to those of EMG-free signals. This comparison provides almost all of the advantages of testing on simulated data while retaining the advantage of being "real" data. Additionally, it is expected that the application of BSS algorithms to EMG-free signals should result in no pruning. This unique dataset of paralysed subjects enables me to answer, with much more rigour than otherwise, my revised research question: **"How effectively can the current signal analysis methods reduce tonic muscle activity from scalp measurements without affecting brain activity, and can modified or new approaches with better effectiveness be proposed?"**.

Two other datasets were also accessible to me. The first dataset consists of high-density SERs of 13 healthy participants undertaking a series of tasks. The task of particular interest for this thesis is an auditory stimulation task, where a known brain response is expected. The second dataset includes high-density SERs of 626 subjects, including 93 controls, completing a series of tasks. Again, for this thesis, a visual stimulation task is used. All three datasets were examined to evaluate, using statistical analyses, the effectiveness of previous and proposed approaches in reducing tonic cranial muscle activity while retaining brain activity such as visual steady state response (VSSR), auditory steady state response (ASSR), auditory event-related potential (AERP), and the Berger effect.

The third (large sample) dataset includes SERs of participants who have zero, one or more diagnoses of neurological or psychiatric disorders. In particular, it contains 65 control

subjects with no history of headache and 26 non-chronic migraine sufferers. Consequently, I had access to enough data for migraine and control subjects to quantitate and compare the cranial muscle activity between migraine and control groups. So, this dataset enables me to address my initial research question in a reduced form: **"Is resting muscle activity increased in migraineurs?"**

After quantitating the cranial muscle activity, statistical analyses such as ANalysis Of VAriance (ANOVA) and regression were used to find if there is an increased resting muscle activity in migraineurs and, if there is, whether the muscle activity is related to the severity of headache or not. Answering this question could improve our understanding of migraine and its characteristics.

1.6 Thesis structure

In Chapter 2, the various sources of electrical activity recorded during a standard SER are discussed, particularly focussing on EEG and EMG. Then, a literature review of signal processing methods proposed to separate SERs into components is presented. Finally, the limitations of previous studies in reducing muscle activity from SERs are discussed.

Chapter 3 evaluates the effectiveness of a range of BSS algorithms in reducing tonic muscle activity from scalp measurements while retaining brain responses. All algorithms are applied to all three databases and the statistical results are discussed.

In Chapter 4, a new approach to reduce the effect of tonic muscle activity at scalp recordings is discussed. The results of applying this approach on all three databases are presented.

Chapter 5 presents the results of extending one of the popular signal separation methods. The limitations and possible improvement of the traditional method are discussed, and the results of applying the extended method on all three databases are presented.

Chapter 6 shows how some muscle reduction approaches can complement each other and how combinations of them can provide an improved muscle reduction when compared to each alone.

In Chapter 7, I propose a new holistic cranial and upper cervical muscle quantitation approach. This approach is validated using SERs of subjects suffering from diseases associated with increased muscle tension. Then it is applied to SERs of non-severe migraineurs and controls to compare their level of cranial and upper cervical muscle activity.

Finally, in Chapter 8, I discuss my contributions, my suggestions for further research, and provide answers for my revised research questions.

Chapter 2

Literature review

2.1 Electroencephalography (EEG)

Electroencephalography is the procedure of recording the electrical activity of groups of brain cells, i.e. neurons, typically from the scalp. EEG signals result from ionic currents flowing within the neurons of the brain (Petsche, Pockberger & Rappelsberger 1984), and was first implemented by Hans Berger in 1929 (Berger 1929; Petsche, Pockberger & Rappelsberger 1984; Haas 2003). EEG is frequently used in studying brain activity and in diagnosing medical diseases (Vinhas, Oliveira & Reis 2008).

Recording neural activity, EEG, is achieved by recording differential voltages on the scalp. During a normal scalp recording, other biological signals are also recorded along with EEG, such as muscle activity (EMG), eye movement artefacts (EOG), heart electrical activity (ECG), or non-biological signals such as mains power frequencies or environmental noise. Traditionally, the purpose of a scalp recording is to measure the brain activity or EEG, and so the term EEG has been used both for the brain activity alone, and also for the scalp recording that includes many biological and non-biological signals. As mentioned in Section 1.2, in this thesis, I use EEG to mean brain electrical activity alone, and I use the term SER to refer to the scalp measurements which include EEG, EMG, EOG, ECG, mains power frequencies and environmental noise.

In order to record brain signals, many small electrodes connected to a recording machine must be attached to the scalp of the subject. Because of the resistance of the scalp surface and

the large distances of electrodes from brain cells, the magnitude of the recorded potentials is very small and needs to be amplified (Barlow 1993). Consequently, a modern recording machine first amplifies the detected signals, then quantises them and records them on a computer.

2.1.1 EEG montage

The number of electrodes attached to the scalp of the subject differs in various studies. Nowadays, 16, 21, 64, 128, and even 256 electrodes are common in SER (Klem et al., 1999). The positioning pattern of the electrodes is called a montage. One of the most common montages in SER is the 10-20 international system, which is the basis of almost all other montages. The term 10-20 implies the space between nearby electrodes. It is either 10% or 20% of the overall distance from inion to nasion (back to front) or between the preauricular points (left to right), as shown in Figure 2-1.

Figure 2-1: 10-20 international system (Mansor, Rani & Wahy 2011).

The 10-20 system is the standard clinical montage, however in EEG research, SER with higher resolution may be needed. So, the standard 10-20 system is extended by adding some

extra electrodes. For example, Figure 2-2 shows the extended 10-20 system with 32 electrodes.

Adding extra electrodes with 10% divisions, which fill in the middle sites of the 10-20 international system as shown in Figure 2-3, provides a 74-channel montage called the 10-10 system. A further extension to 128 channels is called the 10-5 system, which adds extra electrodes with 5% divisions to the 10-10 system, as shown in Figure 2-4 (Oostenveld et al., 2001).

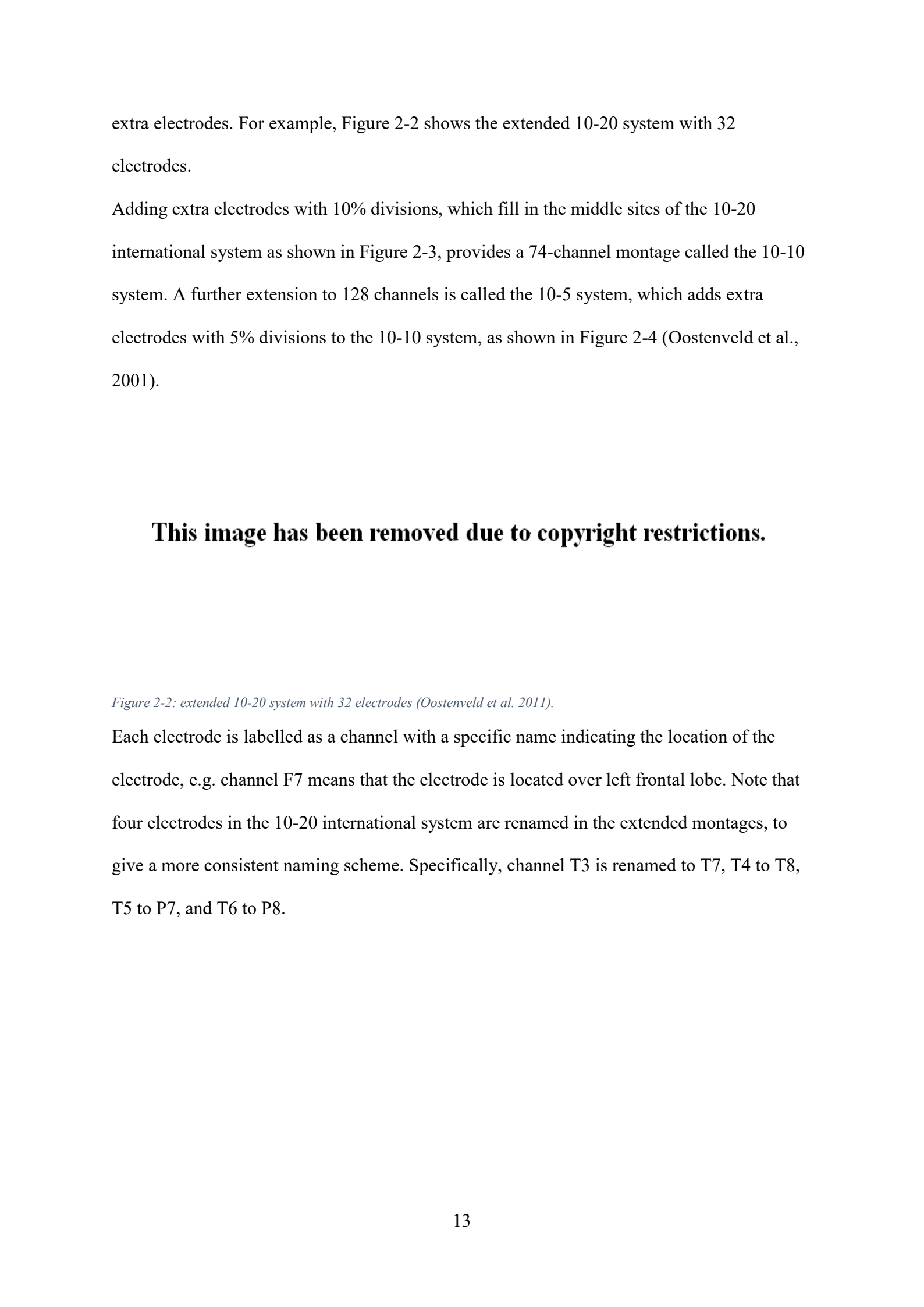

Figure 2-2: extended 10-20 system with 32 electrodes (Oostenveld et al. 2011).

Each electrode is labelled as a channel with a specific name indicating the location of the electrode, e.g. channel F7 means that the electrode is located over left frontal lobe. Note that four electrodes in the 10-20 international system are renamed in the extended montages, to give a more consistent naming scheme. Specifically, channel T3 is renamed to T7, T4 to T8, T5 to P7, and T6 to P8.

Figure 2-3: Montage of the extended 10-10 system. The black circles show the location of the electrodes in the underlying 10-20 international system (Oostenveld & Praamstra 2001).

Figure 2-4: Montage of the extended 10-5 system. The black circles and grey circles show the location of the electrodes in the underlying 10-20 international system and 10-10 system respectively. Including electrodes at the white circles increases this to 142 channels, and also including electrodes at the black dots extends this to over 300 channels. (Oostenveld & Praamstra 2001).

2.1.2 Brain waves

Clinical EEG usually considers a frequency spectrum in the range 1-30 Hz (Tatum 2014; Urigüen & Garcia-Zapirain 2015). EEG spectral power is high at lower frequency, but decreases at a rate of approximately 1/f with by increasing frequency (Fitzgibbon et al. 2016). EEG waveforms are divided by frequency into different bands, known as delta, theta, alpha, and beta (Figure 2-5). Delta has a frequency range between 0.5 and 4 Hz, which makes it the brain's slowest wave, but it has the highest amplitude. It is normally seen frontally in adults and posteriorly in children during the sleep (Kirmizi-Alsan et al. 2006; Teplan 2002; Urigüen & Garcia-Zapirain 2015). Theta has a frequency range between 4 and 7 Hz, and is mostly seen in drowsiness in adults or when meditating (DeLosAngeles et al. 2016; Kirmizi-Alsan et al. 2006; Teplan 2002). The frequency range of alpha is from 8 to 13 Hz (Kisley & Cornwell 2006; Teplan 2002; Urigüen & Garcia-Zapirain 2015) and is mainly distributed laterally with higher amplitude posteriorly. Alpha occurs at larger amplitude when the eyes are closed and the brain is in a relaxed state (Kirmizi-Alsan et al. 2006; Teplan 2002). Beta has a frequency range of 14 to 30 Hz, and is more prominent when the subject is focusing or thinking (Kisley & Cornwell 2006; Teplan 2002; Urigüen & Garcia-Zapirain 2015). Beta rhythm has a key role in information processing (Muthuraman et al. 2012). Cognitive, sensory and motor processing can cause beta power decreases and increases, called event-related desynchronization and synchronization respectively (Meirovitch et al. 2015; Muthuraman et al. 2012).

Another EEG waveform, discovered later, is called gamma, and has a frequency range of 30 to 100 Hz (Jia & Kohn 2011; Vanderwolf 2000). Earlier studies on EEG using analogue recording devices could only record rhythms less than 25 Hz (Hughes 2008). But later, with the invention of digital recording systems, rhythms with lower amplitudes and higher frequencies could be measured (Hughes 2008), and hence researchers could explore high

frequency EEG rhythms. Gamma was first considered as noise, especially when compared with other high amplitude and slow rhythms. However, nowadays, the general view of gamma rhythms has changed. It is suggested that gamma rhythms represent a group of different types of neurons synchronised together in order to carry out certain active cognitive functions (Engel et al. 1999; Singer 2001). Note that gamma is not as well understood as the other bands, and there are many open research questions (Vanderwolf 2000).

Figure 2-5: Different brain waves classified based on their frequency bands. From the top down, the frequency of the brain wave increases while the its amplitude typically decreases.(Jung, C-Y & Saikiran 2016).

2.1.3 Event-related potentials

Stereotyped small voltage changes in the EEG in response to a specific stimulus are called event-related potentials (ERP) (Blackwood & Muir 1990). They are time-locked EEG changes that can be provoked by various motor, sensory or cognitive events. The ERP waveform is usually broken down into separate components, whose amplitude and latency typically depend on the stimulus, and can also depend on psychiatric or neurological disorders. Figure 2-6 illustrates the components seen during an auditory oddball stimulus, the only ERPs studied in this thesis.

N100 or N1 wave is a negative peak appearing usually between 90 and 200 ms after the presentation of target or non-target stimulus (Sur & Sinha 2009). P200 or P2 wave is a positive peak appearing usually between 100 and 250 ms after the presentation of a target or

non-target stimulus (Sur & Sinha 2009). P300 or P3 is a positive wave that usually appears between 250 and 400 ms after the presentation of a target stimulus (Sur & Sinha 2009). The oddball paradigm is mostly used to elicit the P3. In the oddball paradigm, a series of stimuli are presented such that one of them is infrequent. Subjects are instructed to respond in some way to the infrequent or target stimulus, and to not react to the frequent or non-target stimulus.

Figure 2-6: Typical ERP wave to a target stimulus from an oddball paradigm. The N1, P2, and P3 components appear at different latencies after the onset of the stimulus (Olbrich & Arns 2013).

2.1.4 Steady state response

The steady state response of the brain (SSR) is produced by the synchronous activity of a large group of neurons in response to any kind of stimulus (Brenner et al. 2009). When subjects undertake a photic stimulation task with a predefined frequency, their brain response to that stimulation can be measured as a peak in the power spectra at the same frequency, called a visual steady state response (VSSR). Figure 2-7 shows the VSSR peak in the power spectrum when the subject is exposed to a LED flickers with a frequency of 14 Hz. The brain response to auditory stimulation at a specific frequency can be measured as a peak in the power spectrum at the same frequency, called an auditory steady state response (ASSR). To elicit an ASSR, a high carrier frequency, such as 1500 Hz, has to be modulated by a lower

stimulation frequency, such as 40 Hz. This generates a signal that is high enough in frequency to be easily heard, but has a slow enough stimulation frequency to allow neural circuits to synchronise with it (DeLosAngeles 2010). SSRs are usually used to gain better understanding of sensory processing in the brain and to find how sensory pathways in the brain can be impaired by disease or injury.

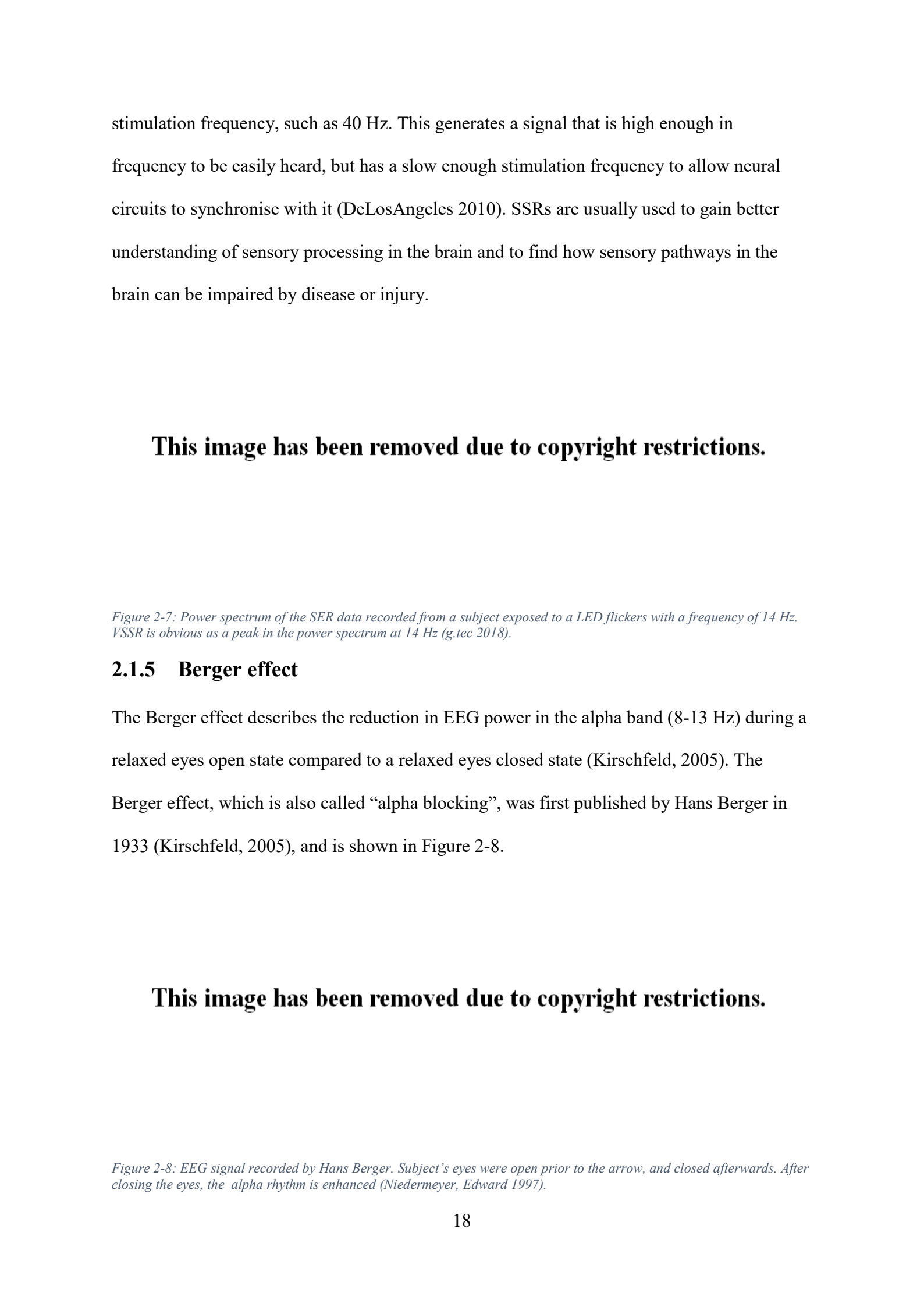

Figure 2-7: Power spectrum of the SER data recorded from a subject exposed to a LED flickers with a frequency of 14 Hz. VSSR is obvious as a peak in the power spectrum at 14 Hz (g.tec 2018).

2.1.5 Berger effect

The Berger effect describes the reduction in EEG power in the alpha band (8-13 Hz) during a relaxed eyes open state compared to a relaxed eyes closed state (Kirschfeld, 2005). The Berger effect, which is also called "alpha blocking", was first published by Hans Berger in 1933 (Kirschfeld, 2005), and is shown in Figure 2-8.

Figure 2-8: EEG signal recorded by Hans Berger. Subject's eyes were open prior to the arrow, and closed afterwards. After closing the eyes, the alpha rhythm is enhanced (Niedermeyer, Edward 1997).

2.2 Extracting EEG from SER: muscle is the main issue

As discussed in Section 2.1, during a typical SER, other biological and non-biological sources are recorded along with EEG. Traditionally the purpose of SER is to record only neural activity (EEG), so other non-neural recorded signals are called “EEG contamination” or “EEG artefact”. Hence, the first step in studying SER is to extract the neural activity, EEG, from the recorded SER.

SERs are often susceptible to electromagnetic interference at the harmonics of 50 or 60 Hz mains frequency (Charlton & O'Brien 2001; Reddy & Narava 2013), as shown in Figure 2-9. This non-biological artefact is due to mains-powered electrical devices in the environment. Shielded recording rooms can be used to reduce the effect of this contamination (Charlton & O'Brien 2001), but our recent study, shown in Figure 2-10, indicates that the most important factor in reducing this contamination is to use DC power for all SER equipment.

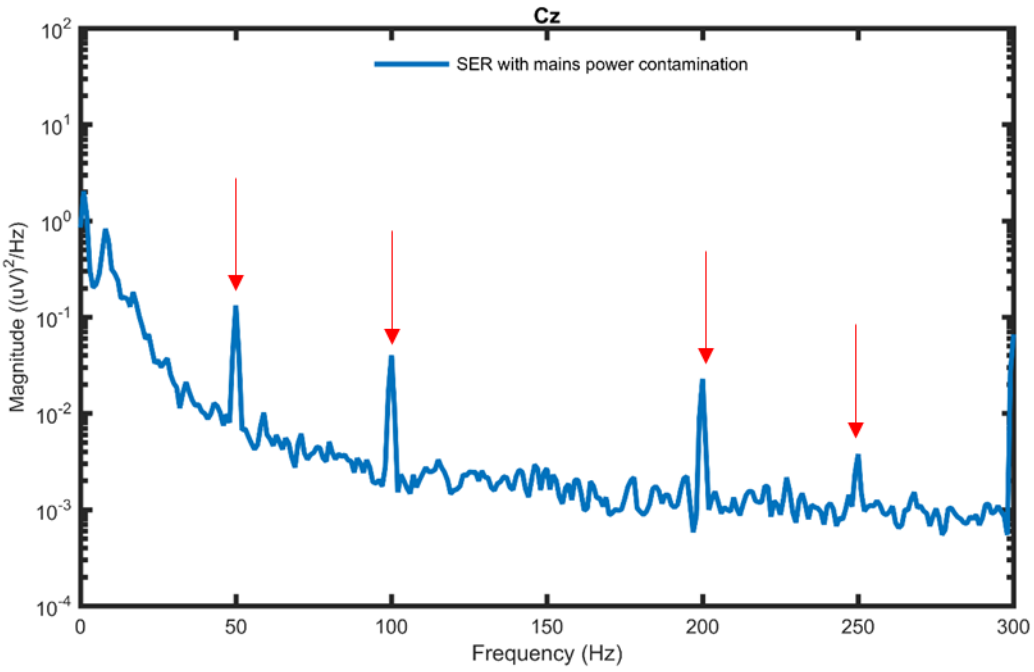

Figure 2-9: EEG spectrum contaminated by harmonics of 50 Hz, generated from a previously collected database described in (Whitham, Emma M et al. 2007).

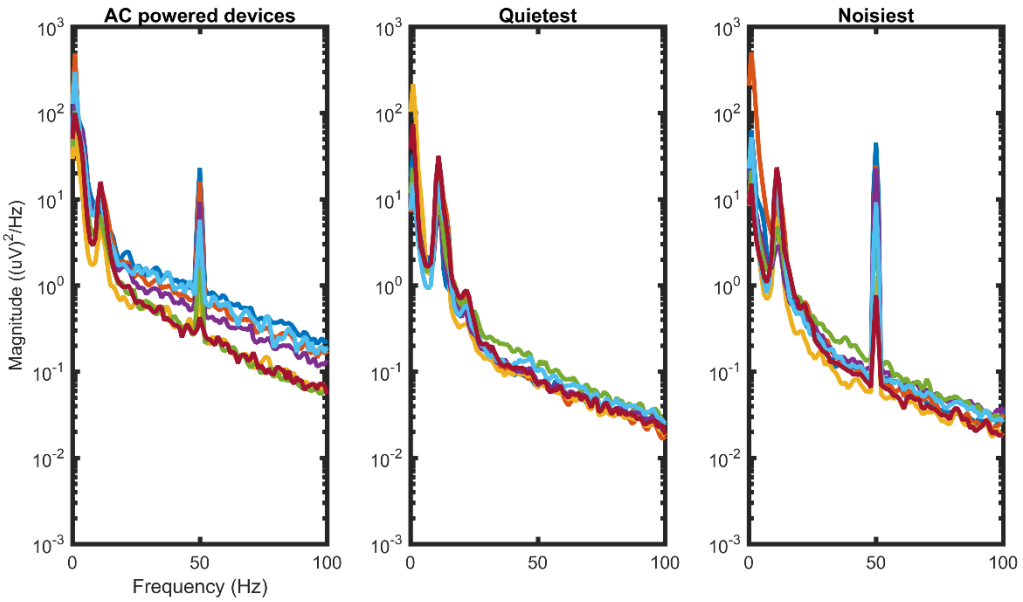

*Figure 2-10: Left shows a 7-channel SER while **AC** powered devices are inside the cage: active 50 Hz electromagnetic interference cancellation is **on**, lights are **off**, and there is **no** wireless transmission. Middle shows the 7-channel SER in the quietest condition: all devices **DC** powered, active 50 Hz electromagnetic interference cancellation is **on**, lights are **off**, and there is **no** wireless transmission. Right shows the 7-channel SER in the noisiest condition: all devices **AC** powered, active 50 Hz electromagnetic interference cancellation is **off**, lights are **on**, and recording computer is using **Wi-Fi**. Generated from unpublished data collected to evaluate the performance of the SER setup.*

Electrode drift is another non-biological source of contamination of EEG signals. This low frequency (<1 Hz) contamination is caused by gentle displacement of electrodes because of subject respiration or movement, and accentuated by poor contact of electrodes with the scalp (Reddy & Narava 2013). Electrode drift can be reduced by using a high-pass filter. However, very low frequency neural information may be lost due to the imperfectness of the filter.

There is a potential difference between the front and back of the eye, so that the eye can be modelled electrically as a dipole. Hence eye movements will change the voltage measured by nearby electrodes. To measure the eye movement, pairs of electrodes are usually attached to the left and right of the eye, horizontal EOG, or above and below the eye, vertical EOG. As shown in Figure 2-11, the low frequency VEOG signal appears as an artefact in SER channels, most strongly frontally (Romero, Mañanas & Barbanoj 2008; Urigüen & Garcia-Zapirain 2015). It is recommended that vertical and horizontal EOG are explicitly recorded simultaneously with SER, to maximise their usefulness in cancelling EOG from the SERs (Croft et al. 2005; Pham et al. 2011; Urigüen & Garcia-Zapirain 2015).

The electrical activity of the heart, ECG, produces a very regular and characteristic pattern which can affect some SER channels, as shown in Figure 2-12 (Urigüen & Garcia-Zapirain 2015). Its amplitude on the scalp is usually low and depends on body type and electrode location (Sörnmo & Laguna 2005). Figure 2-12 indicates that temporal channels, which are near the ear, are affected more than other channels. As with EOG, a reference ECG signal may be recorded along with the SER to assist in noise cancellation (Urigüen & Garcia-Zapirain 2015).

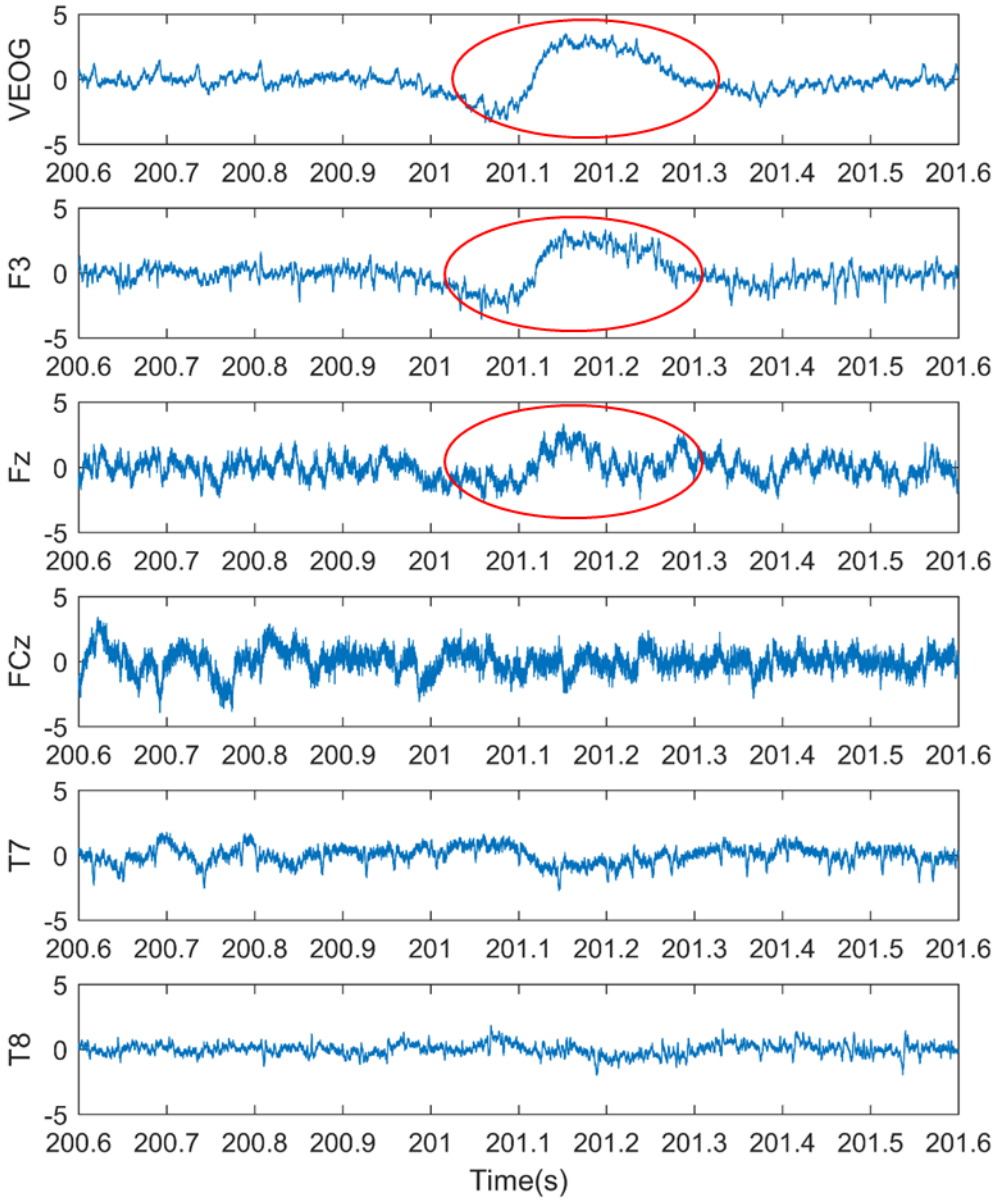

Figure 2-11: Effect of EOG on SER channels. Eye movement, obvious as a low frequency voltage change in VEOG (red oval), seriously affects F3 and Fz (red ovals) as a low-frequency distortion in the signal, generated from data recorded for an ongoing experiment.

Figure 2-12: Effect of ECG on the EEG signal (Correa et al. 2007). Temporal channels (eg T6-O2, the fourth red line) reflect the effect of ECG (bottom line) more than other channels.

Contamination of EEG signals due to muscle activity or EMG is an unavoidable issue in experimental and clinical studies (Akay & Daubenspeck 1999; Anderer et al. 1992; Fu, Daly & Cavusoglu 2006; Goncharova et al. 2003). The shape and degree of muscle contamination depends on the type of the muscle and the amount of muscle contraction, hence there is no stereotype for EMG contamination (Urigüen & Garcia-Zapirain 2015).

Phasic muscle contractions of cranial, facial and neck muscles produce signals of high amplitude overlapping the frequency bands of interest in EEG (Fitzgibbon, SP et al. 2015). Generally, the amplitude of phasic EMG contamination is sufficiently high that the artefact can be detected easily by eye or mathematical algorithm, and the contaminated part of data can be thrown away from all channels (Fitzgibbon, SP et al. 2015; Freeman et al. 2003; Goncharova et al. 2003). To reduce the occurrence of phasic contractions in EEG recordings, subjects are asked to sit or lie down in a relaxed position.

To date, researchers have focused on the characteristics of the phasic activity of cranial muscles. For example, Goncharova, et al. (2003) studied phasic cranial EMG topographies and their spectra in order to develop a better understanding of phasic EMG and to help in cranial muscle activity detection. According to their study, shown in Figure 2-13 the spectra

of the frontalis muscles (during eyebrow raising) have maximum power in the range 16–38 Hz and the spectra of the temporalis muscles (during teeth clenching) exhibit maximum power in the range 13–34 Hz.

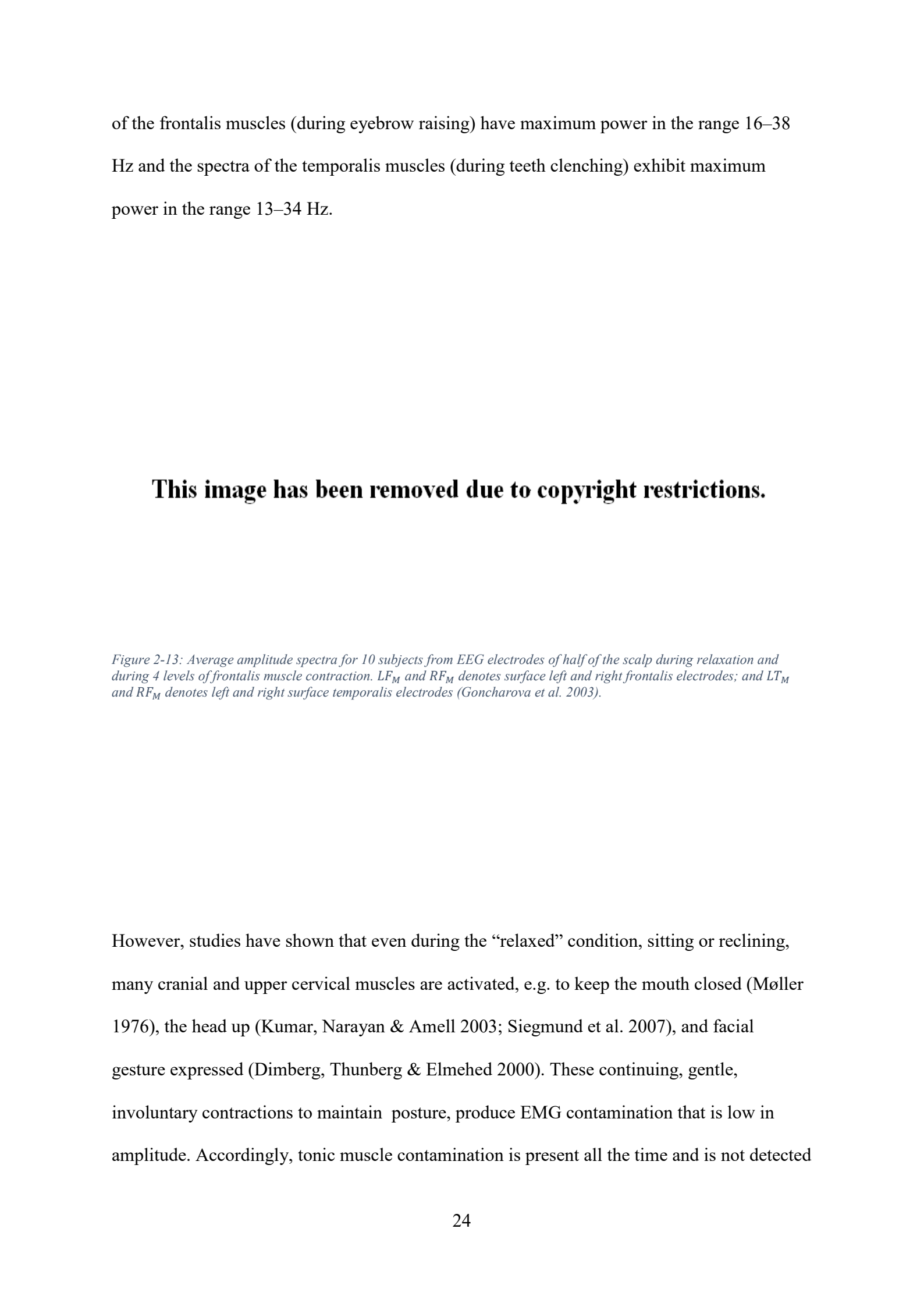

Figure 2-13: Average amplitude spectra for 10 subjects from EEG electrodes of half of the scalp during relaxation and during 4 levels of frontalis muscle contraction. LF_M and RF_M denotes surface left and right frontalis electrodes; and LT_M and RF_M denotes left and right surface temporalis electrodes (Goncharova et al. 2003).

However, studies have shown that even during the "relaxed" condition, sitting or reclining, many cranial and upper cervical muscles are activated, e.g. to keep the mouth closed (Møller 1976), the head up (Kumar, Narayan & Amell 2003; Siegmund et al. 2007), and facial gesture expressed (Dimberg, Thunberg & Elmehed 2000). These continuing, gentle, involuntary contractions to maintain posture, produce EMG contamination that is low in amplitude. Accordingly, tonic muscle contamination is present all the time and is not detected

by traditional methods. Approaching tonic muscle contamination (if it could be detected) in the same way as phasic contamination would result in rejecting much data. But, tonic muscle contamination does significantly alter the spectral characteristics of the scalp recordings (Pope, K. J. et al. 2009; Whitham, E. M. et al. 2008).

To date, the effect of cranial and upper cervical tonic muscle activity on EEG has been widely ignored, and a few studies have conducted to evaluate this issue. Yilmaz and colleague (2014) studied the effect of a single motor unit (SMU) on the SER during a relaxed condition. They recorded the activity of a left-temporalis motor unit by inserting a needle electrode and undertook muscle-unit time-locked signal averaging. Their result, shown in Figure 2-14, is that the presence of SMU spikes is reflected in spikes in EEG channels. More distant EEG channels typically have reduced spike amplitudes, and inversions can be seen. Their result emphasises the susceptibility of EEG to tonic cranial and upper cervical muscle activity, hence tonic muscle artefacts are an unavoidable issue in SER.

Figure 2-14: The effect of SMU spikes on the simultaneously recorded EEG signal (Yilmaz et al. 2014).

Studies conducted on paralysed conscious subjects endorse the importance of the presence of tonic EMG in SER, even when relaxed (Pope, K. J. et al. 2009; Whitham, E. M. et al. ; Whitham, Emma M et al. 2007). Figure 2-15 compares the average of 9-channel SER from

six subjects in two conditions: pharmacologically-paralysed (blue) and unparalysed (orange). The difference in the spectra is just the effect of tonic muscle contamination. It is clear that low amplitude, continual EMG contamination, by the tonic activity of extracranial and upper cervical muscles, exceeds EEG strength from above low frequencies (e.g. 15 to 20 Hz). Moreover, its power in some regions of the cranium (e.g. peripherally) can be 200 times greater than EEG power at high frequencies (Pope, K. J. et al. 2009; 2008; Whitham, Emma M et al. 2007). This study emphasizes that the effect of tonic muscle activity during a usual SER is large enough that it cannot be simply ignored.

Figure 2-15: Example of 9 channels of SER spectra during an eyes closed task in six unparalysed (orange) and paralysed (blue) subjects, generated from a previously collected database described in (Whitham, Emma M et al. 2007).

These studies confirm that the properties of cranial EMG make it more difficult to address EMG contamination than the other artefacts in SER. EMG has a broad-band spectrum that overlaps the spectrum of EEG and exceeds it in power (Pope, K. J. et al. 2009; Whitham, E. M. et al. ; Whitham, Emma M et al. 2007). EMG has a less repetitive pattern compared with other biological signals (such as ECG and EOG) and is harder to characterise. This is because EMG comprises the activity of different muscle groups, with distinct spectral and topographic characteristics, which are functionally independent (Goncharova et al. 2003).

Due to volume conduction of cranial and upper cervical myogenic signals, EMG can affect almost all the electrodes attached across the head (Goncharova et al. 2003; McMenamin et al. 2010).

Therefore, detection and cancellation of EMG is the main issue in EEG research, and simple signal processing algorithms such as low-pass filtering, adaptive filtering, and regression cannot account for EMG contamination perfectly.

2.3 Blind Source Separation (BSS), as a solution

Consider a room with two recording microphones, in which two people are speaking simultaneously. The microphones are located in different places. Each microphone records a weighted sum of the speech signals produced by each individual. These weights are parameters dependent on factors such as the distance between microphones and speaker. The problem is to extract the speech signal of each speaker alone from the mixed signals recorded by microphones. This problem is known as the "cocktail party problem" (Hyvärinen & Oja 2000).

Blind Source Separation attempts to solve the cocktail party problem (Figure 2-16), i.e. it tries to separate a set of measurements into its original sources (commonly also called components). The term 'blind' is used because the algorithm does not use information about the source signals or the method of combination (Jung, C-Y & Saikiran 2016; Pope, Kenneth J & Bogner 1996).

Figure 2-16: BSS block diagram, modified from (Abd et al. 2016).

The BSS method has been investigated since 1991 (Comon, Jutten & Herault 1991; Jutten & Herault 1991). It has been implemented in different areas of interest such as higher-order statistics, noise cancellation, speech enhancement, and neural networks.

In EEG noise cancellation using the BSS approach, the set of scalp measurements at time k can be presented as:

$$X(k) = [x_1(k), x_2(k), \dots, x_C(k)]$$

where C is the number of electrodes and $X(k)$ is assumed to be a linear mixture of unknown sources, namely:

$$X(k) = MS(k)$$

where M is the unknown mixing matrix and $S(k)$ is the set of unknown source signals. The aim is to estimate the unknown mixing matrix and find the original sources by:

$$\hat{S}(k) = WX(k)$$

where W is the de-mixing (or weight) matrix, ideally equal to the pseudo-inverse of the mixing matrix M.

To find the de-mixing matrix and solve the BSS problem, several approaches to BSS have been proposed. However, Independent Components Analysis (ICA) (Fitzgibbon, S et al. 2016; McMenamin et al. 2011; Shackman et al. 2009) and Canonical Correlation Analysis (CCA) (De Clercq et al. 2006; Karhunen, Hao & Ylipaavalniemi 2012) are the most common BSS approaches to removing muscle activity from SERs.

2.3.1 Independent Component Analysis

ICA is the most popular approach to solve the BSS problem (Capizzi, Coco & Laudani 2007). ICA calculates a weight matrix to generate statistically independent components, equal in number to the input SER channels (Delorme et al. 2012; Pope, Kenneth J & Bogner 1996).

Two variables, x and y, are said to be independent if information about either of them does not give any information about the other one. Independence is technically defined as the separability of the joint probability density function (pdf):

$$p(x, y) = p(x)p(y)$$

where $p(x)$ and $p(y)$ are the marginal probability density functions of variable x and y respectively, and $p(x, y)$ denotes the joint probability density function of x and y.

This definition can be extended to n random variables, in which case, the joint pdf equals the product of n marginal pdfs. Since testing the joint pdf separability is impossible in practice, especially for a finite number of samples, it is commonly approximated with higher-order statistics as:

$$E\{x, y\} = E\{x\}E\{y\}$$

where E{.} is the statistical expectation.

Most ICA methods find the components by optimising an explicit objective function. The objective function, which is also known as cost function or contrast function, is a measure of statistical independence which should be optimised (Acharya & Panda 2008). Some of the popular measurements of independence, frequently used as the basis for an objective function, are non-gaussianity and mutual information. Based on the central limit theorem, the non-gaussianity of independent identically distributed random variables is greater than any mixture (Acharya & Panda 2008). Entropy is a quantitative measure of non-gaussianity (Acharya & Panda 2008). The entropy $H(s)$ of variable s with the pdf $p(s)$ is defined as:

$$H(s) = -\int p(s) \log\big(p(s)\big)\, ds$$

For variables with the same fixed variance, $H(s)$ has the greatest value for more unpredictable and random variables. Thus, the entropy of Gaussian variables is greater than other variables with the same variance. This means that entropy can provide a measure of non-gaussianity.

Another measure of independence between two variables is mutual information. Mutual information measures the information one variable has on another variable. As shown in Figure 2-17, it can be expressed in terms of marginal, conditional and joint entropies as:

$$\begin{aligned} I(X;Y) &= H(X) - H(X|Y) \\ &= H(Y) - H(Y|X) \\ &= H(X) + H(Y) - H(X,Y) \\ &= H(X,Y) - H(X|Y) - H(Y|X) \end{aligned}$$

where $I(X;Y)$ defines the mutual information between X and Y, $H(Y)$ and $H(X)$ are the marginal entropies, $H(X,Y)$ denotes the joint entropy of X and Y, $H(X|Y)$ and $H(Y|X)$ are the conditional entropies. So, minimising the mutual information between two variables decreases their dependency, and ideally results in having independent variables.

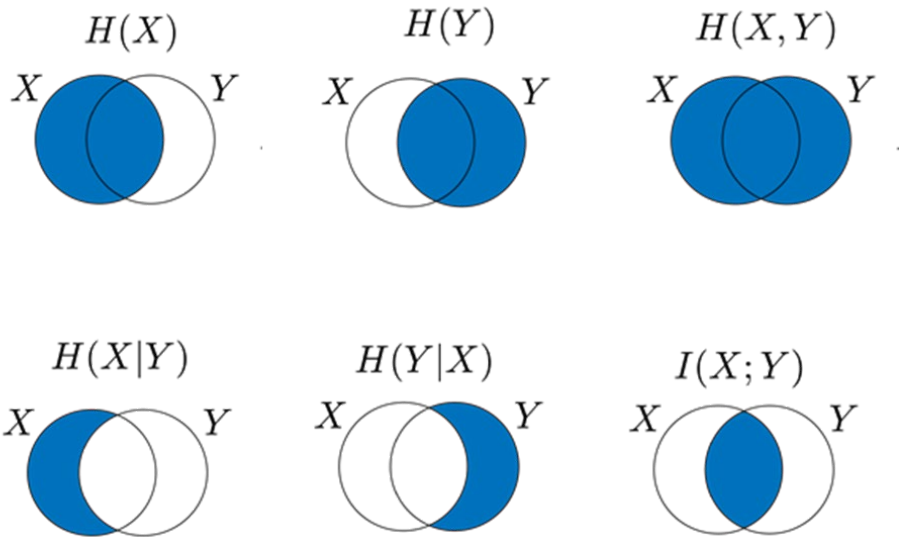

Figure 2-17: Diagram showing the relationship between mutual information and entropy. Mutual information is the difference between a conditional and marginal entropy (either the first column or second column), or as the subtraction of joint entropy from the summation of marginal entropies (first row).

Consider the source signals, with more than two variables, as:

$$S(k) = [s_1(k), s_2(k), \dots, s_C(k)]$$

where $k = 1,2, \dots, N, N$ is the number of samples and C is the number of components which is equal to the number of SER channels. The mutual information means the information that

variable s_i , a member of S, has on other members. The mutual information based on entropy can be defined as:

$$I(s_1; s_2; \dots; s_C) = \sum_i H(s_i) - H(S)$$

Considering $S = WX$, then we have equation:

$$I(s_1; s_2; , \dots; s_C) = \sum_i H(s_i) - H(X) - log|\det(W)|$$

Since $H(X)$ is a constant dependent on the observations, the mutual information can be presented as following:

$$I(s_1; s_2; \dots; s_C) = \sum_i H(s_i) - log|\det(W)| - Constant$$

Based on the choice of the objective function and the optimisation process, different ICA algorithms have been proposed such as Infomax (Bell & Sejnowski 1995), AMICA (Palmer, Kreutz-Delgado & Makeig 2012), FastICA (Hyvarinen 1999), Jade (Cardoso & Souloumiac 1993), SOBI (Belouchrani et al. 1997), ORICA (Akhtar et al. 2012) etc.

Delorme et al. (2012) performed a comparative study on various ICA algorithms to compare the performance of these algorithms based on three measures: the amount of mutual information reduction, the average of remaining pairwise mutual information, and the dipolarity of the components (Delorme et al. 2012). The last one, dipolarity, is based on the assumption that brain and non-brain components have spatially fixed source location and orientation in addition to having independent time courses.

Based on their result, reproduced in Figure 2-18, Infomax and AMICA , with 25 - 30% of components being dipolar-like, perform better than other algorithms in the separation of sources. In other words, using AMICA, only 30% of the estimated components are “pure” brain or “pure” muscle, and about 70% of them are still a “mixture” of different sources.

The performance of FastICA is not as good as AMICA and Infomax, as only about 20% of its components are pure. Despite this, it is popular due to its faster computational time, as implied by the name “FastICA”.

Figure 2-18: Comparison of components dipolarity derived from ICA methods (Delorme et al. 2012).

A comparative study between Infomax and AMICA indicates that AMICA is more effective than Infomax in separating and removing phasic muscle activity of SERs (Leutheuser et al. 2013).

From these comparison studies, it can be concluded that AMICA and Infomax has the best performance among ICA algorithms in estimating independent components, and FastICA is the most popular one, which is implemented in current EEG analysis toolboxes such as EEGLAB (Delorme & Makeig 2004) and FieldTrip (Oostenveld et al. 2011).

2.3.2 BSS-CCA

CCA is a statistical method that defines the correlation structure between two multivariate datasets using a linear transformation (Hotelling 1936). As the name indicates, it quantifies the relationship with correlation coefficients (Friman 2003). CCA seeks to find components U and V of each of two datasets X and Y such that the components are uncorrelated within

each dataset and are maximally correlated between datasets. Solving this maximization problem results in the following eigenvalue problem (Friman 2003; Friman et al. 2001):

$$\begin{cases} C_{xx}^{-1}C_{xy}C_{yy}^{-1}C_{yx}w_x = \rho^2 w_x \\ C_{yy}^{-1}C_{yx}C_{xx}^{-1}C_{xy}w_y = \rho^2 w_y \end{cases}$$

where C_{xy}, C_{xx}, and C_{yy} are the cross-covariance and auto-covariance matrices of X and Y respectively. Each solution to the above equations yields two eigenvectors w_x and w_y and a common eigenvalue ρ^2, where ρ is the canonical correlation coefficient and equals the correlation between the two eigenvectors. Then, components U is derived by multiplying X by a linear transformation matrix composed of the vertical stacking of the set of w_x^T. Similarly, components V is derived by multiplying Y by a linear transformation matrix composed of the vertical stacking of the set of w_y^T.

The CCA approach in solving the BSS problem (BSS-CCA) was firstly introduced by Clercq (2006) to separate myogenic and neurogenic signals from SER. This approach uses the scalp recordings as the first dataset X and a temporally delayed copy of the recordings as the second dataset Y.

$$Y(k) = X(k-1)$$

Because the datasets are now statistically very similar, CCA calculates components (or sources) that are maximally auto-correlated and mutually uncorrelated (De Clercq et al. 2006). The components U for the first dataset X become the estimated sources S in the BSS problem. Traditionally, Y is delayed by one sample, and hence "maximally autocorrelated" means the optimisation calculates components with the maximum autocorrelation at lag one. The delay of one sample is also used to identify whether a component is muscle-like or brain-like, as muscle is regarded as similar to white noise and hence has a low autocorrelation coefficient at lag one, whereas brain is a slower, more correlated signal and hence has a high autocorrelation coefficient at lag one.

2.3.3 Independent Vector Analysis

Joint Blind Source Separation (JBSS) is proposed as a generalization of the BSS problem when more than one dataset is observed (Andersonet al. 2014). The aim of JBSS algorithms is to solve the BSS problem on multiple datasets concurrently. They can achieve this purpose by balancing two conditions: the estimated sources within each dataset are maximally independent, and the sources across the datasets are maximally dependent (Chen et al. 2014). Independent Vector Analysis (IVA), one specific formulation of JBSS, is introduced by Kim et al. (Kim, Eltoft & Lee 2006). It is considered as an extension of ICA from one dataset to multiple datasets. Initially, it was designed to solve the permutation problem in separating acoustic signals (Kim, Eltoft & Lee 2006). In 2012, it was formulated as a JBSS algorithm by Anderson et al. (2012). As shown in Figure 2-19, the model of IVA is composed of a set of ICA models such that the univariate sources across all the layers are dependents (Lee, Kim & Lee 2007). In other words, IVA estimates sources independent within each dataset while corresponding sources across datasets are dependent (Anderson, Adali & Li 2012).

Figure 2-19: Schematic of IVA with F datasets. A denotes the mixing matrix, X and S are the measured and source data, respectively (Lee, Kim & Lee 2007).

The model of source component matrix (SCM) is defined for IVA (Andersonet al. 2014). Each SCM is a matrix which is independent from other SCMs while containing components dependent to each other (Anderson et al. 2014; Chen et al. 2017). The c th SCM can be presented as:

$$s_c = [s_c^{[1]}, s_c^{[2]}, s_c^{[3]}, \dots, s_c^{[F]}]^T$$

Where $c = 1,2, \dots C$ is the number of components (SER channels), and T means transpose. The symbol $s_c^{[f]}$ with $f = 1,2, \dots F$ defines the c th component in the f th dataset, which can be presented as:

$$s_c^{[f]} = [s_c^{[f]}(1), s_c^{[f]}(2), \dots s_c^{[f]}(K)]$$

where $k = 1,2, \dots K$ is the set of time samples.

IVA tries to achieve its goal by minimising mutual information among SCMs. The mutual information of IVA can be defined as (Anderson et al. 2014; Chen et al. 2017; Laney et al. 2015):

$$I_{IVA} = I[s_1; s_2; \dots, s_c]$$

$$= \sum_{c=1}^{C} (\sum_{f=1}^{F} H(s_c^{[f]}) - I(s_c)) - \sum_{f=1}^{F} \log\left|\left(\det\left(W^{[f]}\right)\right)\right| - Constant$$

where $I(s_c)$ represents the mutual information within c th SCM, H means entropy, and $W^{[f]}$ is the de-mixing matrix of f th dataset.

Based on the above equation, if the objective function of IVA is minimised, the entropy of each component, $H\left(s_c^{[f]}\right)$, would be minimised meanwhile the mutual information within each estimated SCM, $I(s_c)$, would be maximised (Anderson et al. 2014; Chen et al. 2017). Minimising the entropy of each component leads to maximally independent components within each dataset, while maximising the mutual information within each SCM results in having maximal dependence across datasets.

In can be inferred that IVA is implementing the advantageous of both CCA and ICA approaches. Applying ICA on multiple datasets can only provide independent sources within each dataset without considering the dependency of corresponding sources across the datasets. On the other hand, applying CCA on multiple datasets ($F = 2$) provides sources that are correlated across datasets, but only decorrelated (not independent) within each dataset (Chen et al. 2017). Hence, the IVA algorithm can be interpreted as a method that integrates CCA and information-theoretic ICA in one algorithm.

To implement IVA, the form of the probability density function of SCMs must be selected. The most popular IVA method is IVA-L, which assumes a second-order uncorrelated multivariate Laplace distribution for each SCM (Kim, Eltoft & Lee 2006). It exploits higher-order dependencies, but not utilising the linear dependencies (Anderson et al. 2013; Kim et al. 2007; Kim, Eltoft & Lee 2006). The other popular IVA method is IVA-G which explicitly exploits the linear dependencies using a multivariate Gaussian distribution for each SCM (Anderson, Adali & Li 2012; Anderson et al. 2013). IVA-GL combines the two approaches, and has been shown to have a robust and better performance than either of them (Chen et al. 2017; Laney et al. 2015). First, it estimates the linear dependence among the components of each SCM using IVA-G. Then the estimated de-mixing matrices derived by applying the IVA-G are used to initialise the IVA-L (Chen et al. 2017; Laney et al. 2015). In another word, it applies IVA-L on the observed dataset while setting the initial values of de-mixing matrices to the values estimated by applying IVA-G on the datasets.

2.4 Detecting muscle components

After applying a BSS algorithm to the SERs and separating the sources, it is needed to classify muscle (myogenic) and brain (neurogenic) components.

Components with transient (phasic) muscle activity usually have a sufficiently high amplitude, in comparison to the brain components, that can be classified easily by eye or

mathematical algorithm (Fitzgibbon et al. 2015; Freeman et al. 2003; Goncharova et al. 2003). However the constant, low amplitude, tonic muscle components are the main issue. Generally, they are such low in amplitude that cannot be recognised just by using their temporal characteristics. Other features of tonic muscle components such as spectral characteristics or topographic maps should be considered in classifying them (Fitzgibbon et al. 2016).

Previous studies, dealing with phasic muscle activity, have used temporal characteristic and topographic maps to classify and reject phasic muscle components manually by visual inspection, after applying ICA method. This visual inspection is usually time-consuming and dependent to the decision making of the operator or the expert (Mognon et al. 2011; Radüntz et al. 2015; Viola et al. 2009).

Viola et al. (2009) proposed a semi-automatic algorithm to classify neural components from non-neural components. Their method is based on the component similarity using a correlation procedure. In other words, it correlates ICA inverse weights to a user-defined template. So, their algorithms relies on the subjective selection of the templates.

Radüntz et al. (2015) suggested an automatic components classification algorithm. Using the topographic map of a component and image processing, a feature vector is extracted for each component. These feature vectors are then classified by linear discriminant analysis. Figure 2-20 shows the topographic maps of five typical artefact components, along with a neural component. Although, their proposed method shows a good accuracy rate, its computational complexity is high.

Figure 2-20: Topographic maps of non-neural components and neural components. Topographic maps of five typical artefact components (eye blink, EOG, ECG, EMG, and impedance) and a neural component in two sets of channels configuration: 25-channel SER (first row) and 30-channel SER (second row) (Radüntz et al. 2015).

In 2016, by analysing SERs of pharmalogically paralysed conscious subjects, Fitzgibbon et al. (2016) indicated that unavoidable tonic muscle contamination is the main issue in EEG analysis and proposed an automated algorithm to recognise these components.

They have shown that muscle components are typically spatially localised and have spectra that increase approximately linearly between 7-75 Hz log-log scale, whereas the spectra of brain components decreases approximately linearly in this frequency band, as shown in Figure 2-21 (Fitzgibbon et al. 2016).

Figure 2-21: Topographic map and spectrum of a brain IC (components) and a muscle IC (component). The red line fits a linear polynomial to the spectrum between 7 to 75 Hz (Fitzgibbon et al. 2016).

Based on their result, tonic muscle components can be labelled reliably based on their spectral gradient. Their results indicated that the gradient (in the range 7-75 Hz) of components in paralysis (EMG-free) condition is different from unparalysed (EMG-contaminated) condition. As shown in Figure 2-22, the EMG-contaminated data has a wide histogram with more positive-slope components, while EMG-free data has a narrow histogram with the maximum gradient of -0.31 bel/decade. The gradient of -0.31 can be considered as a safe threshold in labelling muscle components. In other words, components whose spectral gradient is greater than this threshold can be reliably considered as muscle and components with a spectral gradient less than this threshold can be considered as brain. From Figure 2-22, it can be concluded that ICA cannot separate components perfectly, and most of the components are a mixture of two or more sources. If ICA enables a clean

separation, it would be expected to see a dipolar histogram for the gradient of components in EMG-contaminated data.

Fitzgibbon and colleagues have also suggested other thresholds to decrease the effect of muscle contamination on scalp measurement: a threshold at the crossover point of the EMG-contaminated and EMG-free histograms, and a threshold at the highest peak of the EMG-free histogram. The former is a conservative balancing of the removal of myogenic contamination with the loss of neurogenic signal, and the latter removes more muscle and more brain, which may be appropriate in some situations.

Figure 2-22: The histogram of the gradient of components derived by applying AMICA on EMG-contaminated and EMG-free data from six subjects. The red line and purple line show the histograms of EMG-free and EMG-contaminated components respectively. The four grey dashed lines indicates four different threshold (at zero gradient, at maximum gradient of EMG-free components, and at peaks of gradient in EMG-free components) that can be used to classify muscle components automatically (Fitzgibbon, S et al. 2016).

On the other hand, correlation of components is another feature usually used after applying BSS-CCA method to label brain components and muscle components. It is assumed that the broad band spectrum of EMG, resembling white noise, and its concomitant low autocorrelation are exploited to identify muscle components (Chen 2014; De Clercq et al. 2006; Gao, Zheng & Wang 2010; Karhunen, Hao & Ylipaavalniemi 2012). This approach actually relies more on muscle autocorrelation being small in comparison to brain autocorrelation, rather than muscle being like white noise.

As an example, Figure 2-23 shows the derived components after applying the BSS-CCA method on 21 channels of SER data (De Clercq et al. 2006). Based on the results reported in (De Clercq et al. 2006), the last three components, whose autocorrelation coefficients are much smaller than the rest of the components, are considered as muscle components. This approach is subjective to the decision of the user and is not automated.

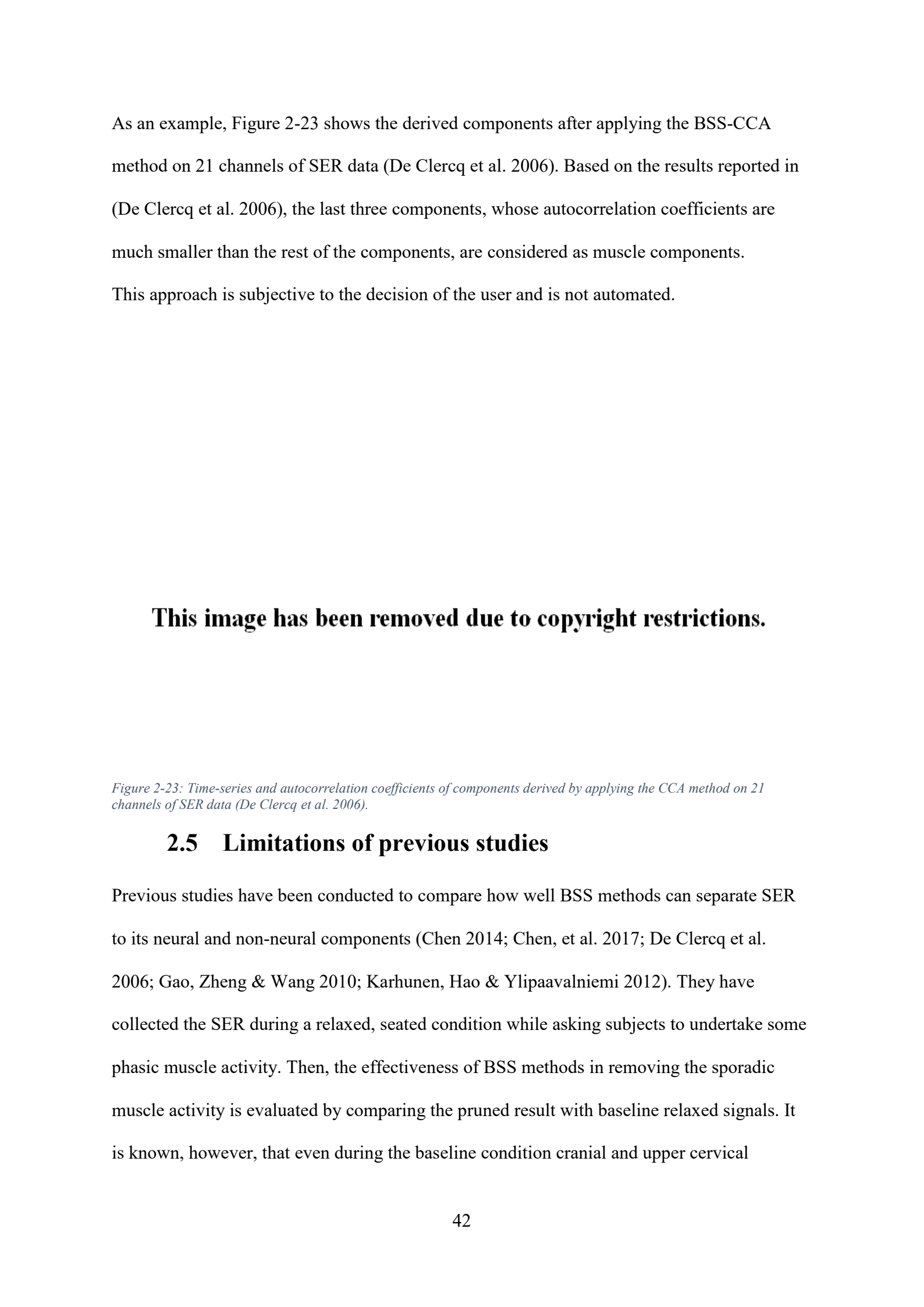

Figure 2-23: Time-series and autocorrelation coefficients of components derived by applying the CCA method on 21 channels of SER data (De Clercq et al. 2006).

2.5 Limitations of previous studies

Previous studies have been conducted to compare how well BSS methods can separate SER to its neural and non-neural components (Chen 2014; Chen, et al. 2017; De Clercq et al. 2006; Gao, Zheng & Wang 2010; Karhunen, Hao & Ylipaavalniemi 2012). They have collected the SER during a relaxed, seated condition while asking subjects to undertake some phasic muscle activity. Then, the effectiveness of BSS methods in removing the sporadic muscle activity is evaluated by comparing the pruned result with baseline relaxed signals. It is known, however, that even during the baseline condition cranial and upper cervical

muscles are activated, and hence baseline SERs record tonic muscle activity. Therefore, the previous results are only evaluating the effectiveness of BSS methods in removing phasic muscle activity, and the effectiveness of these methods in separating low amplitude tonic muscle components is not addressed. However, by recording SERs from pharmacologically-paralysed subjects, Fitzgibbon et al. (2016) have shown that tonic, low-amplitude muscle activity is a significant issue in SERs. Using their proposed automatic algorithm, they have evaluated the effectiveness of AMICA in removing tonic muscle activity from SERs, and also whether the algorithm retained or disclosed high frequency cognitive brain responses, typically hidden by muscle power. However, they didn't evaluate other BSS algorithms which are more popular, such as Infomax and FastICA. Hence, there is still a need to evaluate the effectiveness of current popular BSS algorithms in removing tonic muscle activity from SERs while retaining high frequency brain activity, and to see if modified or new approaches with better effectiveness can be proposed.

The number of SER channels used in muscle-removal algorithm is likely to have an effect in muscle reduction. Many previous studies have recorded scalp measurement using a 21-channel SER cap (Chen 2014; Chen et al. 2017; De Clercq et al. 2006; Gao, Zheng & Wang 2010; Karhunen, Hao & Ylipaavalniemi 2012). As BSS algorithms produces a number of components equal to the number of SER channels, the number of sources that can be truly separated is similarly limited. The brain has a vast numbers of sources (neurons), far greater than could ever individually be recorded. Hence, it seems the number of SER channels might be an important issue in separating neurogenic and myogenic sources, and using more channels in a BSS algorithm may result in better separation of brain from muscle and hence improved muscle reduction. This issue has not been studied, so there is a need to evaluate the effect of the number of SER channels in reducing tonic muscle activity.

Chapter 3

Evaluation of existing methods in removing tonic cranial muscle activity

In this chapter, using three different existing datasets, I evaluate the effectiveness of popular BSS algorithms, introduced in Chapter 2, in reducing cranial muscle activity while retaining neural activity from SERs.

The number of SER channels used in muscle-removal algorithms is likely to have an effect in muscle reduction. BSS algorithms produce components ideally corresponding to separate sources, but the number of components is limited by the number of SER channels. So, using more channels in a BSS algorithm should result in better separation of brain from muscle and improved muscle reduction. I also test the effect of the number of SER channels in one of the BSS-based muscle-removal algorithms which can achieve a good result in a reasonable time.[1]

3.1 Datasets

To evaluate the effectiveness of different BSS methods in quantitating tonic muscle activity, I applied them to three different existing datasets recorded from healthy participants. All participants signed a consent form and these experiments were approved by the Clinical Research Ethics Committee of Flinders Medical Centre and Flinders University.

The first dataset contains SERs from six participants as described in Table 3-1. All participants were recruited between 2006 and 2008. They were asked to complete a series of

[1] A subset of this chapter, specifically the testing of the effect of the number of SER channels, has been published. The conference paper can be found in Appendix B-1.

tasks including baseline eyes closed, baseline eye open, auditory verbal learning, serial subtraction, auditory oddball, and exposure to a strobe light with three different frequencies, 16 Hz, 40 Hz, and 59 Hz. The tasks were performed twice, once before and once during pharmacologically-induced paralysis. So, the first set of these data contained muscle activity (pre-paralysis or EMG-contaminated) while the second has no muscle activity (post-paralysis or EMG-free) (Whitham, E. M. et al. 2008; Whitham, Emma M et al. 2007). During the paralysis condition, brain activity was unaffected (Whitham, E. M. et al. 2008). Consequently, this unique dataset of paralysed subjects provides many of the advantages of simulated data while retaining the advantage of being "real" data. The results of the pruned data can be compared to EMG-free data (paralysis condition) and EMG-contaminated data (pre-paralysis condition). Note that the pruned data are processed from the EMG-contaminated data, and hence the pruned and EMG-contaminated data are drawn from data recorded at the same time, and a different time to the EMG-free data.

Under the paralysed condition, participants could not open their eyes by themselves, so, the left eye was held open (passive opening) using a swab-on-a-stick during the eye open task. The tasks listed above were undertaken by the participants with two exceptions: only five participants undertook the strobe 40 Hz and 59 Hz tasks. Additionally, the data from the oddball task for one participant were too noisy, hence, oddball data from only five participants were considered in the analyses. The total recording time for each participant was approximately 12 minutes, and data were collected from 115 SER channels at a sampling frequency of 5000 Hz.

The second dataset consists of 13 participants as described in Table 3-1. All participants were recruited between 2007 and 2009. An auditory stimulus, one of the tasks to be used in this study, with a 1500 Hz carrier amplitude modulated by a 40 Hz message was presented to all participants under three meditation conditions, as described in DeLosAngeles et al. (2010).

Under all conditions, the brain should exhibit an ASSR to this stimulus. The total recording time was approximately six minutes, and data were collected from 112 SER channels at a sampling frequency of 2000 Hz.

The third dataset consists of 626 SERs collected from controls and from participants with a range of neurological and psychological disorders. The original purpose was to use the dataset to investigate changes in brain rhythms with disease. All participants were recruited from the clinics and staff of the Flinders Medical Centre, or their relatives, between 2004 and 2007. Some participants had more than one diagnosis and were not used in this study. There were 93 healthy participants who were used in this study as controls. Their demographic details are described in Table 3-1. Scalp electrical activity was recorded from each participant while sitting and completing a series of tasks including eyes closed, eyes open, auditory discrimination, visual discrimination, visual rotation, finger tapping, maze, serial subtraction, auditory verbal learning task, and reading (Whitham, E. M. et al. 2008). Participants typically took 22 minutes to complete all the tasks, and data were collected from 124 SER channels at a sampling frequency of 2000 Hz.

Table 3-1: Subject demographics and SER parameters of all three datasets.

Dataset number	Females	Males	Age	Number of SER channels	Reference channel	Sampling frequency (Hz)	Length of data (min)
1	1	5	28-73	115	Left ear	5000	12
2	7	6	7-80	112	Left ear	2000	6
3	48	45	29-62	124	Linked-ears	2000	22

3.2 Methods

3.2.1 Pre-processing

All pre-processing and processing of data was performed using code written in MATLAB (The Mathworks, Natick, MA, USA). All recordings were resampled to 1000 Hz and were re-referenced with common average head referencing. SER electrodes were labelled based on

the 10-5 international system (Oostenveld & Praamstra 2001). Transient high-amplitude phasic muscle activity was eliminated from further analysis using the EEGLAB toolbox (Delorme et al. 2011; Kothe & Makeig 2013) to mark out identified segments. To reduce electrode drift, data were passed through a fourth-order elliptical high pass filter with a cut-off frequency of 0.5 Hz.

3.2.2 ICA pruning

There are several ICA algorithms aiming to provide independent components. However, in this study, the ones which have better performance would be evaluated. Better performance can be defined by separating components effectively or converging fast. Best separation of components is measured by dipolarity of components, in other words, they are either neural or muscular, not a mixture. AMICA and Infomax with 25% and 30% dipolar-like components are the best of the ICA approaches (Delorme et al. 2012). Although the performance of FastICA in providing dipolar-like components is not as good as AMICA and Infomax, it is popular due to its fast computation time. Because of this feature, it is widely used in current EEG analysis toolboxes such as EEGLAB (Delorme & Makeig 2004) and FieldTrip (Oostenveld et al. 2011). So, I evaluated the performance of three ICA algorithms in my analyses: AMICA, Infomax, and FastICA.

To prune tonic muscle activity from the scalp recordings automatically, the process described in (Fitzgibbon, S et al. 2016) was followed. Firstly, each of the chosen ICA algorithms, AMICA, Infomax and FastICA, were applied separately to the EMG-contaminated and EMG-free data from the first dataset, yielding two sets of components and two mixing matrices per algorithm. Secondly, the spectral gradient of each component was calculated by fitting a straight line to the log-log spectrum between 7 Hz and 75 Hz. Thirdly, the maximum gradient of EMG-free components was set as a threshold. This choice of threshold ensures that all components with a gradient above the threshold must contain at least some muscle.

Fourthly, EMG-contaminated components with a spectral gradient greater that the threshold were labelled as muscle-containing components and were rejected (set to zero). Finally, SERs were reconstructed using the preserved components and the mixing matrix, yielding signals named to identify the ICA algorithm used. For example, pruned signals derived by applying AMICA are called pruned-AMICA.

After finding the specific threshold by applying the ICA approach on the first dataset, SERs from datasets two and three were pruned automatically as described.

3.2.3 BSS-CCA pruning

BSS-CCA removes muscle components from SER. Components are identified using CCA applied to a dataset and a delayed version of itself, then the components are classified as myogenic or neurogenic on the basis of their correlation coefficients. The delay of one sample is used to identify whether a component is muscle-like or brain-like, as muscle is modelled as similar to white noise and hence has a low autocorrelation coefficient at lag one, whereas brain is a slower, more correlated signal and hence has a high autocorrelation coefficient at lag one. However, BSS-CCA requires the user to specify the correlation threshold for the classification of components, and hence the process is not automatic.

An automated pruning process based on BSS-CCA and using our unique database of paralysed subjects is proposed as follows:

1. The EMG-contaminated and EMG-free data from dataset one were subjected to BSS-CCA approach separately. This gives two sets of components and correlation coefficients.
2. The histogram of correlation coefficients from the EMG-free components were investigated to identify a minimum correlation coefficient from EMG-free data, to be used as a threshold.

3. EMG-contaminated components with a correlation coefficient less than the threshold were labelled as muscle-containing components and were rejected.
4. SERs were reconstructed using the retained components and the mixing matrix, yielding signals called pruned-CCA.

The correlation coefficient threshold from dataset one is then used on SERs from other datasets, yielding an automated pruning procedure described by steps 3 and 4 above.

3.2.4 IVA pruning

IVA, an extension of ICA from one dataset to multiple datasets, can be used to remove muscle activity from scalp recordings by using a delayed version of the recordings as the second dataset (Chen, X, Peng, et al. 2017). In the pruning case considered here, this produces one SCM per SER channel, each SCM containing two components as there are two datasets (SERs and their delayed version). IVA then maximises the mutual information between the two components within each SCM, and minimises the entropy of all first components and all second components (separately) across SCMs. This yields components that are maximally independent within datasets and maximally dependent to their corresponding components across datasets.

Different IVA approaches have been proposed, each with different models for the probability density function of the SCMs. I selected IVA-GL, as it is robust and has the best performance (Chen, X, Peng, et al. 2017; Laney et al. 2015).

After applying IVA-GL on both EMG-contaminated and EMG-free data (dataset one), the spectral gradients of all derived components were calculated and the threshold was set as described in Section 3.2.2. Components whose gradients were greater that the specified threshold were rejected as muscle-containing components. Finally, SERs were reconstructed using the preserved components. We call these signals pruned-IVA.

This approach was applied to datasets two and three using the threshold from dataset one, to calculate muscle-pruned SERs.

3.2.5 ICA pruning with different numbers of SER channels

From the ICA algorithms, Infomax, which is a popular choice in neuroscience and provides a good separation of components in a reasonable time (Dharmaprani et al. 2016), was selected to evaluate the effect of the number of SER channels on tonic muscle reduction. I applied the Infomax algorithm on EMG-contaminated data four times; each time with a different number of input SER channels. Each application of Infomax results in a set of components, equal in number to the number of input SER channels, and an associated mixing matrix. Infomax was applied to each dataset with its original number of channels, and with subsets of channels corresponding substantially to the 10-10 (64 channels, Figure 3-1), extended 10-20 (32 channels, Figure 2-2) and 10-20 (21 channels, Figure 2-1) systems (Oostenveld et al. 2011). As described in Section 3.2.2, components whose spectral gradient was greater than the (Infomax-derived) threshold were labelled as muscle-containing components and were discarded (set to zero). Finally, pruned signals were reconstructed by multiplying the components and mixing matrix. These pruned signals were named according to their number of channels: e.g. pruned-64, pruned-32, and pruned-21.

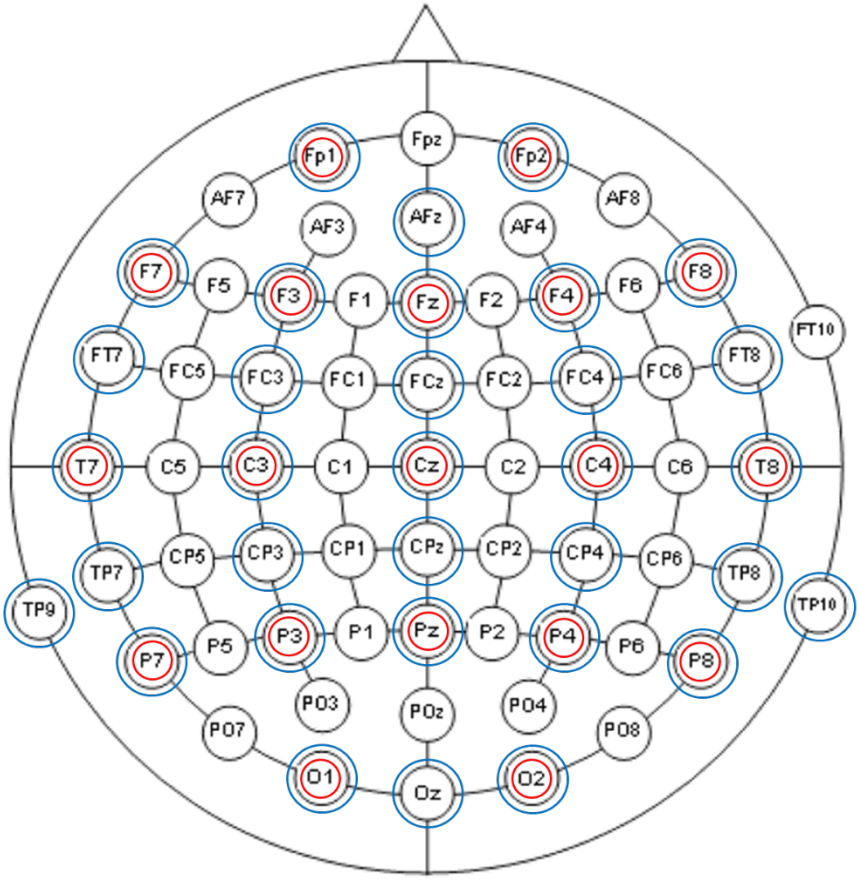

Figure 3-1: Montage of the subset of channels, with 64 electrodes, corresponding to the 10-10 system (black circles). Red circles and blue circles show other subsets of channels based on 10-20 (21 channels) and extended 10-20 systems (32 channels).

3.2.6 Comparisons and statistical analysis

Using Welch's modified periodogram (Welch 1967), with Hanning windows of length 1 s, the power spectra of all EMG-contaminated, pruned and EMG-free signals were calculated. For statistical analysis, spectral power was averaged in bands related to neural activity that also contained significant muscle activity. The selected bands were gamma1 (25-35 Hz), gamma2 (35-45 Hz), gamma3 (52-98 Hz), and muscle (102-198 Hz). Comparisons were made in baseline tasks, and in tasks that elicit a neural response. This enabled testing of the efficacy of muscle removal, and for the retention of neurophysiological signals.

After confirming the data were normally distributed using a Lilliefors test, statistical comparisons between EMG-contaminated data, pruned and/or EMG-free data were

performed with 3-way parametric ANOVAs or with 1-way parametric ANOVAs, depending on the purpose of the analysis. When the purpose of comparison was on the efficacy of algorithms in removing tonic muscle activity, a 3-way ANOVA was selected to provide comparison based on the signal, region and band. When the purpose of comparison is on the efficacy of algorithms in retaining neurophysiological responses, a 1-way ANOVA is chosen, because neural responses are always at a specific channel, and at a specific frequency or narrow band or specific time points of the time-domain signal. For the 1-way ANOVA, the height of steady state response is defined as the ratio of the power at the stimulus frequency to the geometric mean of the power at 2 Hz either side of the stimulus frequency. Where a significant effect was found, post hoc comparisons were performed to identify statistically significant differences between pairs of signals, using Tukey's honest significant difference test to account for the multiple comparisons. All tests used a threshold for significance of $p = 0.05$.

3.3 Results of comparing BSS algorithms

I examined all three datasets to evaluate the effectiveness of BSS approaches in reducing tonic muscle activity while retaining/disclosing brain neurophysiological responses.

3.3.1 The selection of thresholds

Figure 3-2 shows the histogram of the gradients of the derived components by three different ICA algorithms and the IVA algorithm for EMG-contaminated and EMG-free signals from the first dataset. A negative spectral gradient is expected for purely neurogenic components, whereas purely myogenic components should have a positive gradient. In other words, ideally, the histogram of EMG-contaminated components should be bimodal. However, as shown in Figure 3-2, most of the components have negative spectral gradients, independent of the BSS algorithm. This implies there are many components that are a mixture of myogenic and neurogenic signals.

The threshold for rejecting the muscle-containing components is set at the maximum gradient of the EMG-free components. This selection of threshold ensures that all rejected components contain at least some myogenic signal (conservative threshold). So, the thresholds for the AMICA, Infomax, FastICA, and IVA methods were set at -0.31,-0.28, -0.36, and -0.11 bel/decade respectively.

Figure 3-3 displays the histogram of correlation coefficients after applying BSS-CCA on both the EMG-contaminated (orange) and EMG-free (blue) data from first dataset. Clearly, the distributions completely overlap. Hence, it is not possible to set a threshold based on the correlation coefficient to classify components as putatively muscle or brain, and the procedure specified in Section 3.2.3 will not achieve useful pruning.

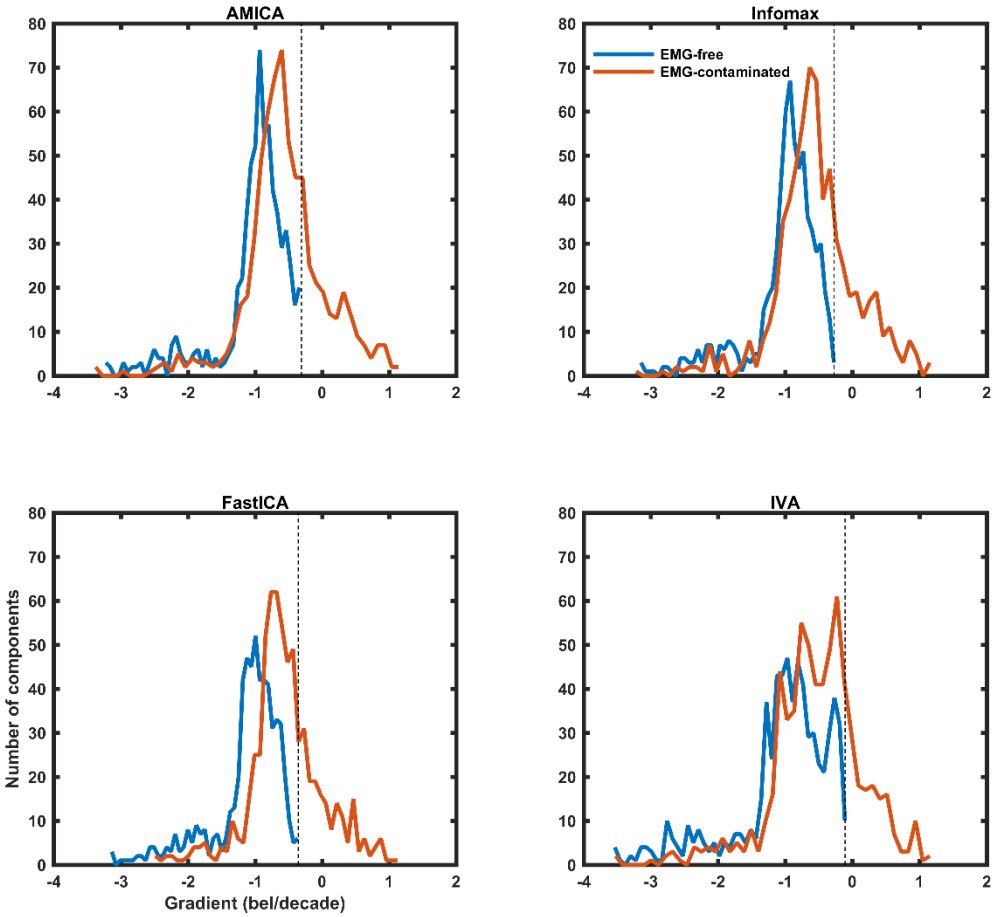

Figure 3-2: From database 1, histograms of the gradients of EMG-contaminated (orange) and EMG-free (blue) components derived by applying AMICA (top-left), Infomax (top-right), FastICA (bottom-left) and IVA (bottom-right). For each approach, the threshold was set at the maximum gradient of EMG-free components.

It might be suggested that a possible choice of threshold is at the minimum cross point of EMG-contaminated and EMG-free data, around 0.05. When testing this suggestion, I could detect no visible difference between the pruned spectra and the EMG-contaminated spectra, meaning this method of determining the threshold is not useful.

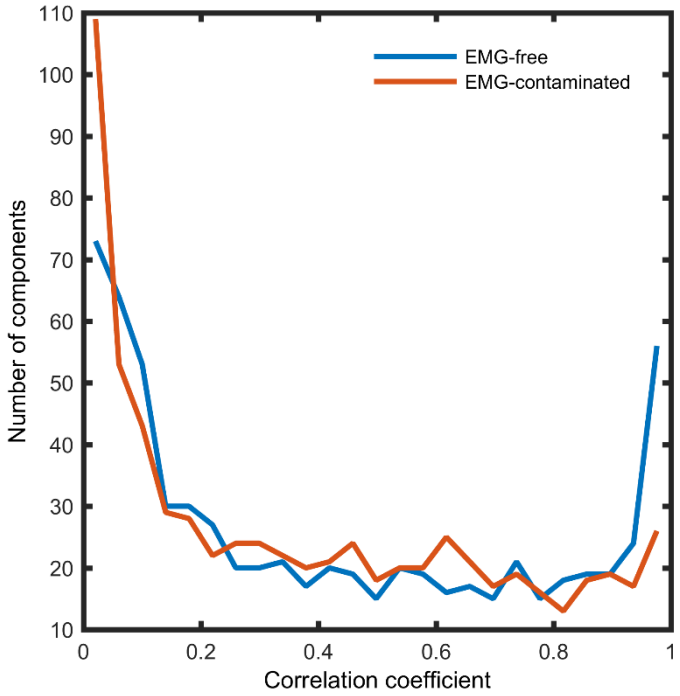

Figure 3-3: From database 1, histograms of the correlation coefficients of EMG-contaminated (orange) and EMG-free (blue) components derived by applying CCA.

Therefore, since traditional BSS-CCA cannot be automated, I exclude it from the analyses and comparisons in this chapter. In Chapter 5, investigations into extending BSS-CCA is described, with the aim of automating the detection and rejection of muscle-containing components to yield useful pruning. Investigations on the spectral gradient of components and characterising different sources (e.g. white noise as well as muscle components) resulted in a new BSS-CCA approach called extended-CCA.

3.3.2 Tonic muscle activity reduction

Figure 3-4 compares the amount of muscle activity in EMG-contaminated, pruned, and EMG-free data (during baseline eyes closed) in nine channels spread evenly across the head,

namely F7, Fz, F8, T7, Cz, T8, O1, Oz, and O2. The orange and the dark blue lines correspond to EMG-contaminated and EMG-free data respectively. Better pruning has spectra closer to EMG-free spectra.

It is observed that in all pruned signals, muscle reduction starts at low frequencies, about 20 Hz. High frequency power, associated with muscle, has been reduced by all pruning approaches, but there is still substantial muscle contamination compared to EMG-free data, especially at peripheral channels where cranial and upper cervical muscles are located.

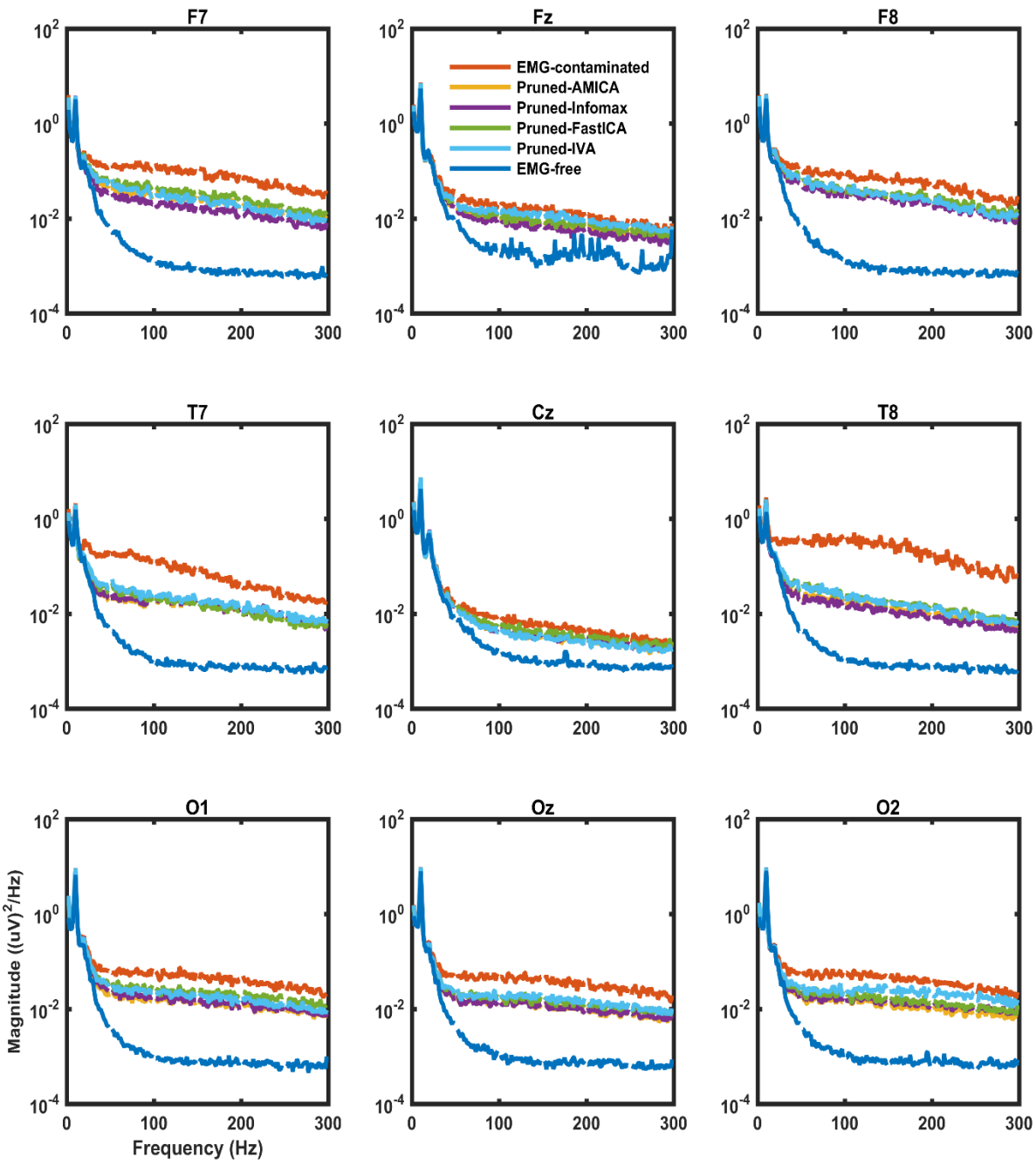

Figure 3-4: From dataset 1, mean of six subjects' power spectra during baseline eyes closed task. Mains power artefacts, i.e. harmonics of 50 Hz, have not been displayed.

Figure 3-5 displays, in the four frequency bands of interest, the topographic maps of relative spectra of EMG-contaminated to EMG-free and pruned to EMG-free data. The scale from dark blue to dark red indicates how much a region is affected by muscle activity. Dark red areas indicate strong muscle activity, whereas dark blue areas are almost muscle-free. The power of the pruned signals is comparable to the EMG-free signal in frequencies up to 35 Hz

in central channels. Although none of the pruning algorithms completely remove muscle activity at higher frequencies, they reduced muscle contamination, especially in peripheral channels. For example, at 102-198 Hz (muscle band), the average power of EMG-contaminated spectra at temporal channels was about 300 times greater than EMG-free spectral power, but after pruning this value decreased to about 30 times.

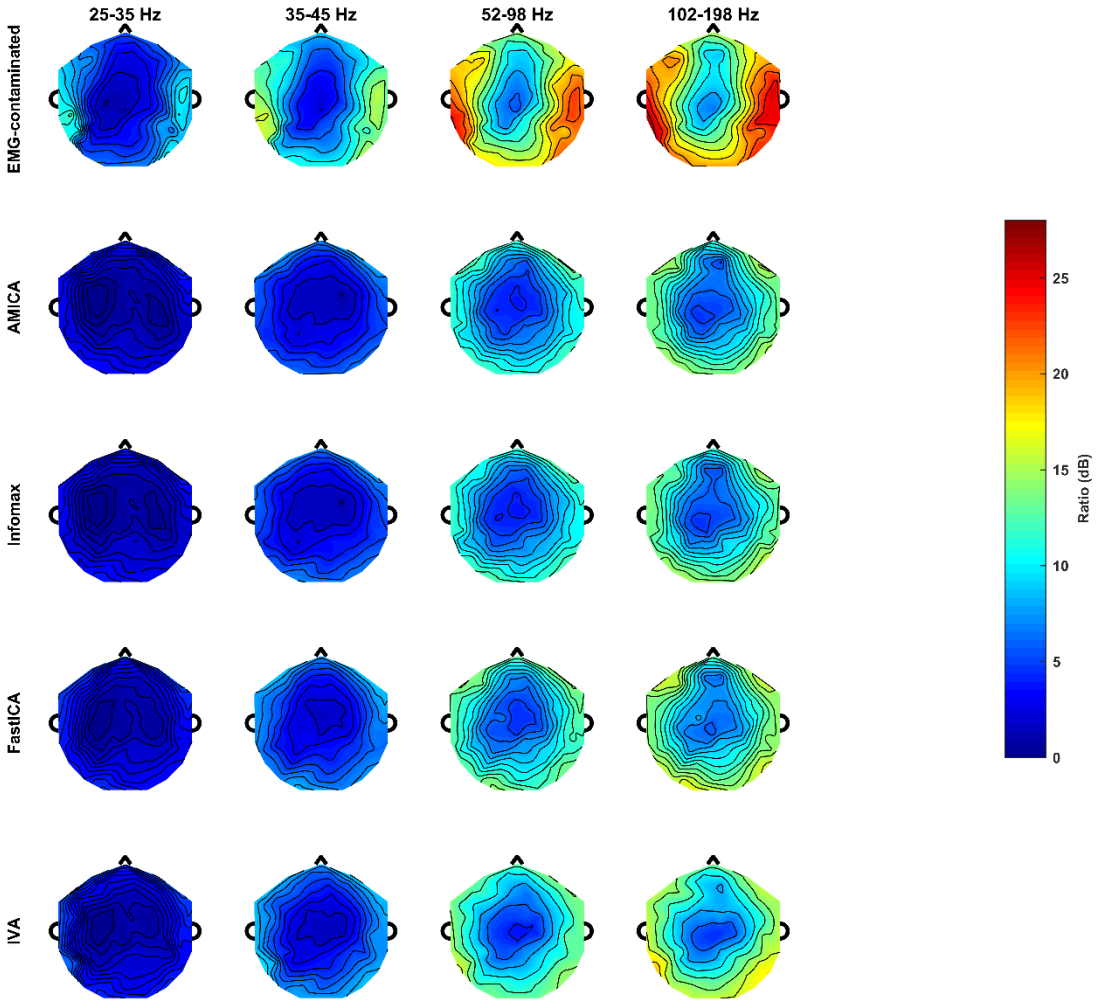

Figure 3-5: From dataset 1, topographic maps of relative spectra of EMG-contaminated/EMG-free (first row), and pruned signals/EMG-free (subsequent rows) in the four frequency bands of interest (columns). Each topography is looking down on the head, with ears and nose indicated, conforming to the montage in Figure 2-4. Note that differences within frequency band are strongest at peripheral channels.

Two groups of channels were considered: central channels (Fz, FCz, Cz, C1, C2, CPz, and Oz), and peripheral channels (T7, T8, F7, F8, O1, and O2). Average power spectra of all signals in each group of channels and each frequency band were calculated. Figure 3-6

illustrates the average and standard deviation of power of all signals in each region and each frequency band. Visually, AMICA and Infomax result in better pruning than the other methods, especially in higher frequency bands.

To test these observations statistically, a 3-way parametric ANOVA was performed to compare the average power for six different signals (EMG-contaminated, four pruned, and EMG-free signals) over two regions and four frequency bands. Hence, the independent variable is average power and the dependent variables or factors are signal, region, and band. Table 3-2 shows the result of the ANOVA for each factor and all interactions of factors.

Table 3-2: Results of ANOVA. The average power is different over each factor, and each two-way interaction

Analysis of Variance

Source	Sum of squares	Mean square	F	p
Signal	120	24.8	105.58	**< 0.001**
Band	174	58.1	254.94	**< 0.001**
Region	379	37.9	166.15	**< 0.001**
Signal*Band	27.9	1.80	7.89	**< 0.001**
Signal*Region	19.3	3.85	16.90	**< 0.001**
Band*Region	6.74	2.24	9.84	**< 0.001**
Signal*Band*Region	2.03	0.135	0.59	0.87

The ANOVA shows that the average power is different over each factor (signal, band, and region), and each two-way interaction (signal∗band, signal∗channel, and band∗channel). Hence, six post-hoc tests were performed to identify statistically significant differences between pairs of signals.

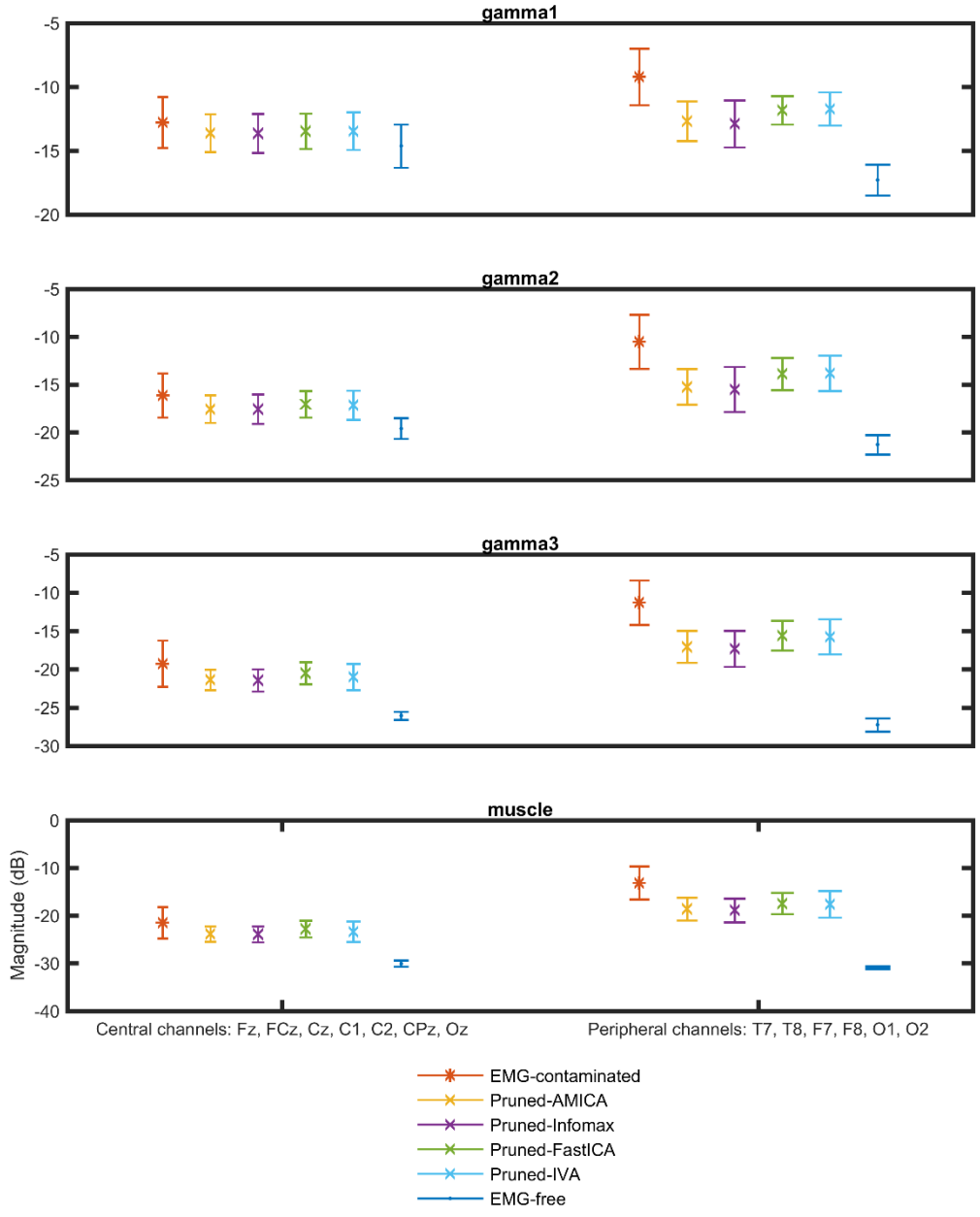

Figure 3-6: From dataset 1, average and standard deviation of power in each frequency band in EMG-contaminated, EMG-free and pruned data for 6 subjects.

Table 3-3 shows the post hoc results for factor of signal. All pruned data are statistically different to both EMG-contaminated and EMG-free. This means that all pruning methods are reducing cranial muscle activity significantly but the amount of reduction is not sufficient to reach the level of EMG-free.

Table 3-3: Post hoc test for the factor of signal. All pruned data are statistically different to both EMG-contaminated and EMG-free.

	EMG-contaminated	Pruned-AMICA	Pruned-Infomax	Pruned-FastICA	Pruned-IVA	EMG-free
EMG-contaminated		**<0.001**	**<0.001**	**<0.001**	**<0.001**	**<0.001**
Pruned-AMICA			0.99	0.24	0.37	**<0.001**
Pruned-Infomax				0.07	0.12	**<0.001**
Pruned-FastICA					1.00	**<0.001**
Pruned-IVA						**<0.001**
EMG-free						

Table 3-4 shows the post hoc results for the interaction of signal and region. All pruned data are statistically different to EMG-free data in both central (lower triangle) and peripheral (upper triangle) channels, and also to EMG-contaminated data in peripheral channels. In central channels, however, only pruned-AMICA and pruned-Infomax are significantly different to EMG-contaminated data. This demonstrates that AMICA and Infomax outperform FastICA and IVA in tonic muscle reduction at central channels.

Table 3-4: Post hoc test for the interaction of signal and region. AMICA and Infomax outperform FastICA and IVA in tonic muscle reduction at central channels.

Peripheral / Central	EMG-contaminated	Pruned-AMICA	Pruned-Infomax	Pruned-FastICA	Pruned-IVA	EMG-free
EMG-contaminated		**<0.001**	**<0.001**	**<0.001**	**<0.001**	**<0.001**
Pruned-AMICA	**0.02**		1.00	0.73	0.80	**<0.001**
Pruned-Infomax	**0.01**	1.00		0.27	0.35	**<0.001**
Pruned-FastICA	0.42	0.99	0.98		1.00	**<0.001**
Pruned-IVA	0.29	0.99	0.99	1.000		**<0.001**
EMG-free	**<0.001**	**<0.001**	**<0.001**	**<0.001**	**<0.001**	

Table 3-5 shows the post hoc results for the interaction of signal and band. All pruned data are statistically different to EMG-contaminated and EMG-free signals at the two higher

frequency bands (gamma3 and muscle). This means that all pruning algorithms are reducing tonic muscle activity significantly at higher frequency bands, but the amount of reduction is not sufficient to reach the level of EMG-free signal. At the lowest frequency band, gamma1, none of the pruned data is statistically different to either EMG-contaminated or EMG-free data, although EMG-contaminated and EMG-free data are statistically different. Hence all pruning algorithms are reducing muscle, but the amount of reduction is not significant. However at gamma2, all pruned data are statistically different to EMG-free data, but only pruned-AMICA and pruned-Infomax are significantly different to EMG-contaminated data. This again demonstrates that AMICA and Infomax outperform FastICA and IVA at tonic muscle reduction, here in the gamma2 band.

Table 3-5: Post hoc test for interaction of signal and band. AMICA and Infomax outperform FastICA and IVA at tonic muscle reduction in the gamma2 band. (Note: two analyses shown per sub-table).

Gamma2 / Gamma1	EMG-contaminated	Pruned-AMICA	Pruned-Infomax	Pruned-FastICA	Pruned-IVA	EMG-free
EMG-contaminated		**0.008**	**0.002**	0.30	0.26	**<0.001**
Pruned-AMICA	0.61		1.00	1.00	1.00	**0.004**
Pruned-Infomax	0.47	1.00		0.99	1.00	**0.01**
Pruned-FastICA	0.91	1.00	1.00		1.00	**<0.001**
Pruned-IVA	0.93	1.00	1.00	1.00		**<0.001**
EMG-free	**0.002**	0.96	0.98	0.74	0.69	

Muscle / Gamma3	EMG-contaminated	Pruned-AMICA	Pruned-Infomax	Pruned-FastICA	Pruned-IVA	EMG-free
EMG-contaminated		**<0.001**	**<0.001**	**0.003**	**0.001**	**<0.001**
Pruned-AMICA	**<0.001**		1.00	1.00	1.00	**<0.001**
Pruned-Infomax	**<0.001**	1.00		0.99	0.99	**<0.001**
Pruned-FastICA	**0.010**	0.99	0.98		1.00	**<0.001**
Pruned-IVA	**0.003**	1.00	0.99	1.00		**<0.001**
EMG-free	**<0.001**	**<0.001**	**<0.001**	**<0.001**	**<0.001**	

Since, the purpose of this chapter is to compare the efficacy of existing algorithms in removing tonic muscle activity, post hoc tests on the factor of signal and two-way interactions of signal∗band, and signal∗region have been presented in detail. Post hoc tests for the factor of region and the factor of band show peripheral channels have more power than central channels ($p < 0.001$), and lower frequency bands have more power than higher frequency bands (all $p < 0.001$). Post hoc result on the interaction of region and band is shown in Figure 3-7, but not discussed in detail because it is beyond the purpose of this chapter.

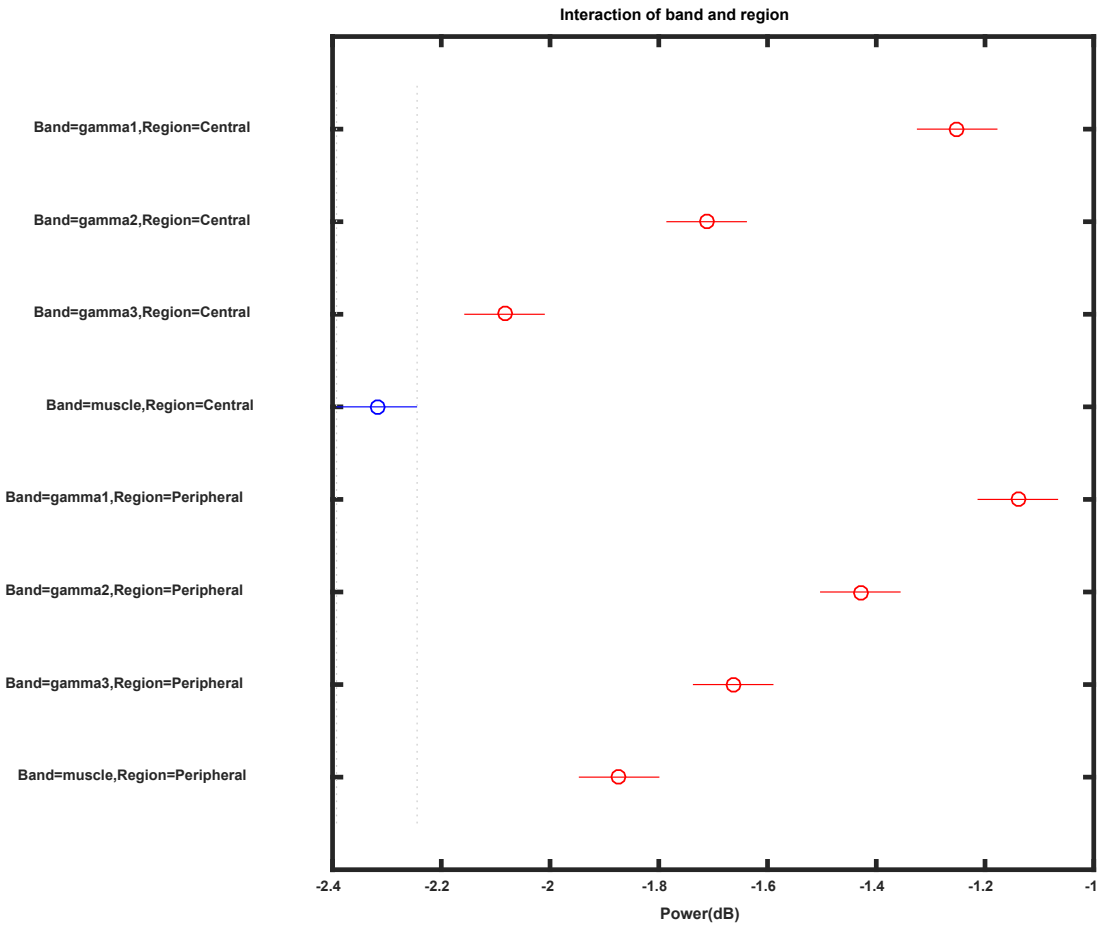

Figure 3-7: Post-hoc tests for the interaction of band and region. In each band, peripheral region has more power than central region, and in each region, lower frequency bands have more power than higher frequency bands.

To sum up, all pruning algorithms are reducing tonic muscle activity significantly but the amount of reduction is not sufficient to reach the level of EMG-free data. AMICA and Infomax outperform FastICA and IVA at tonic muscle reduction, because they can reduce tonic muscle activity significantly at central channels and in the lower frequency band (gamma2), whereas FastICA and IVA are not significantly effective either in this region or at this band.

3.3.3 Retention of neurophysiological responses

A second requirement of a good muscle-removal algorithm is that it should not remove desired neural signals. Hence we investigated the effect of each pruning method on brain neurophysiological responses, namely the Berger effect, auditory event-related potentials (AERP), visual steady state responses (VSSR), and auditory steady state response (ASSR).

3.3.3.1 Berger effect

The Berger effect describes the reduction in EEG power in the alpha band (8-13 Hz) during a relaxed eyes open state compared to a relaxed eyes closed state (Kirschfeld 2005). Figure 3-8 displays the Berger effect as raw spectra of eyes closed (left) and left eye open (right) at an occipital channel (Oz) for dataset 1. Figure 3-9 illustrates the same data as relative spectra of eyes closed over left eye open. Both figures show the expected higher power in the eyes closed task for all data.

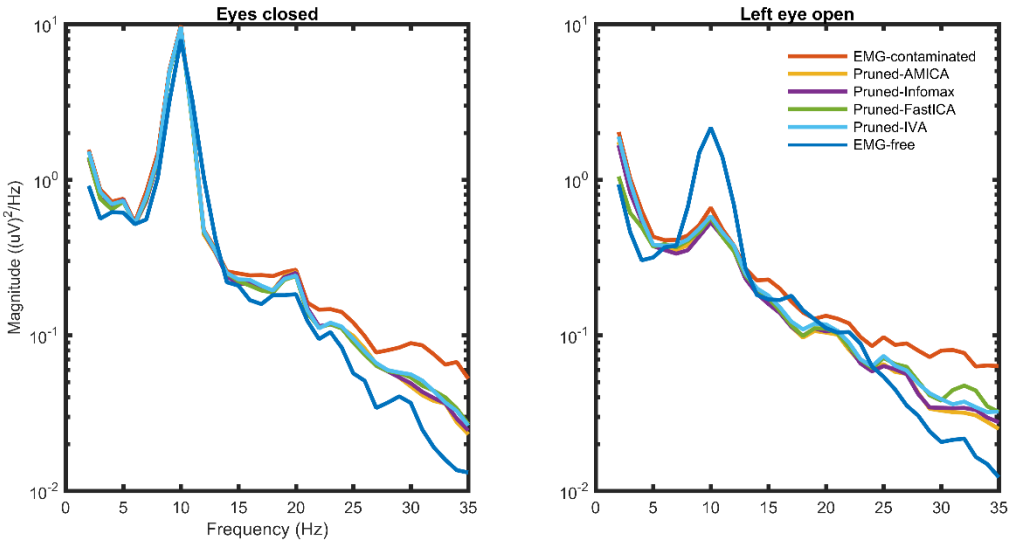

Figure 3-8: From dataset 1, average of six subjects' eyes closed spectra (left) and left eye open spectra (right) at Oz. Alpha activity, the peak around 10 Hz, is noticeably smaller with the eye open. Note that the pruned spectra are processed from the EMG-contaminated data, and hence the pruned and EMG-contaminated spectra are drawn from data recorded at the same time, and at a different time to the EMG-free data.

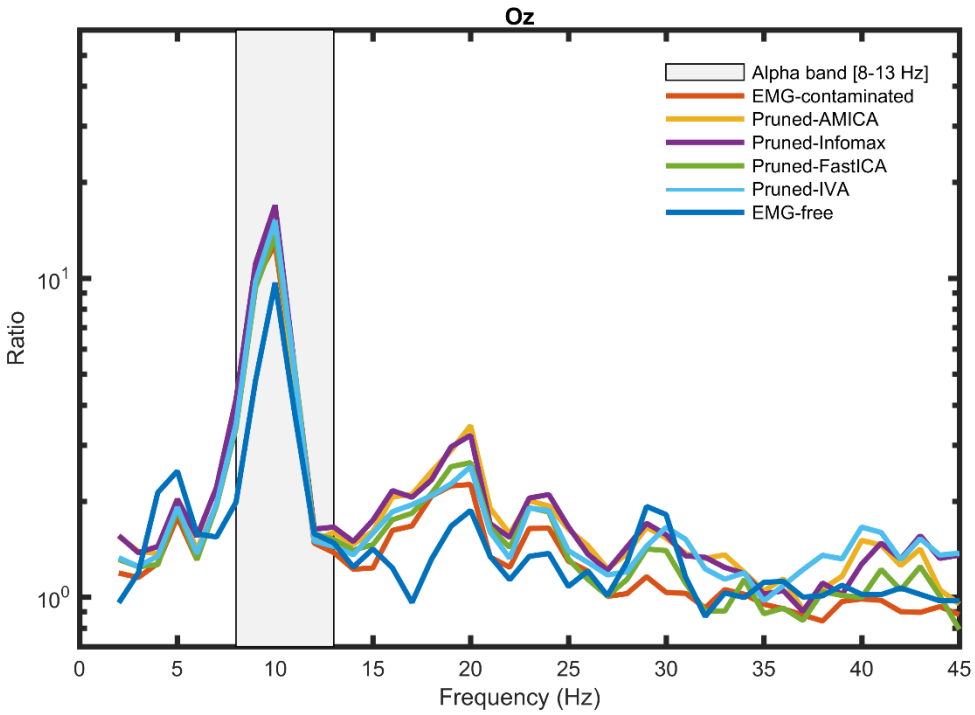

Figure 3-9: From dataset 1, average of six subjects' relative power spectra (eyes closed to left eye open) at Oz. Alpha activity, the power at frequencies 8-13 Hz, is not statistically significantly different in any pair of EMG-contaminated, EMG-free, and pruned signals.

Using a single ANOVA test, the alpha power (average power in the band 8-13 Hz) of all signals was compared. The result showed no effect for signal, ie no evidence of difference

between signals (F = 0.02, p = 0.99). This is consistent with all pruning approaches having no substantial effect on the measurement of this low frequency cognitive response.

3.3.3.2 Auditory oddball

The effect of each pruning method was evaluated on the oddball task from dataset 1. Figure 3-10 illustrates the mean of AERPs at channel Fz for five subjects. It is visually clear that the N1 and P2 components, which are brain responses to all tones, and the P3 component, which is a brain response to the target high tone, have been preserved in all pruning methods.

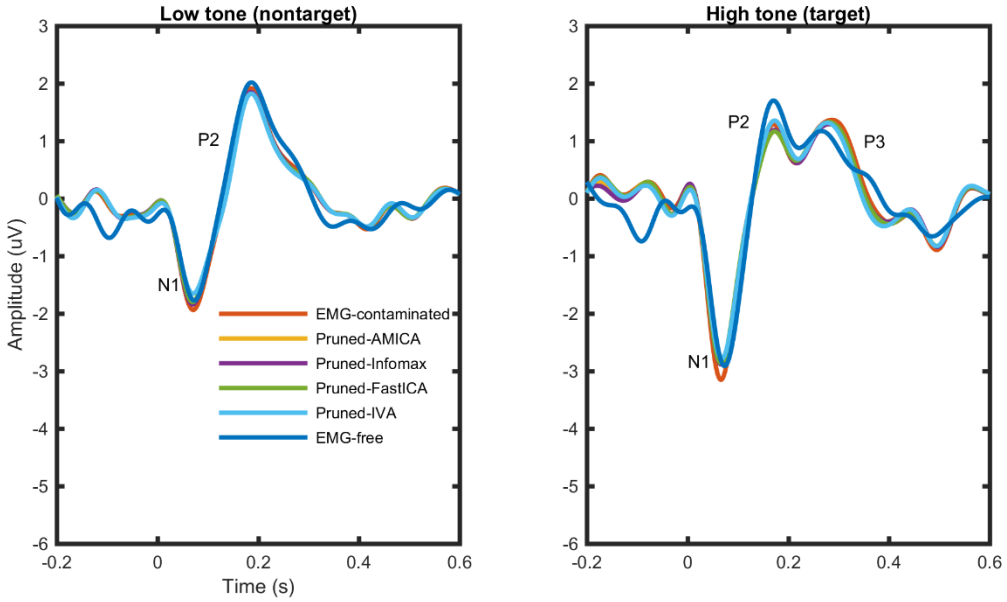

Figure 3-10: From dataset 1, averaged auditory event-related potentials (AERPs) of five subjects in the oddball task at channel Fz. The N1 and P2 components of the response to the non-target low tone (left) and the N1, P2, and P3 components of the response to the target high tone (right) have been preserved in all pruning approaches.

To test this observation statistically, separate ANOVAs were performed for each component (N1, P2, and P3) to compare their power in all data. The results shows no significant effect for the factor of signal (N1: F = 0.13, p = 0.98; P2: F = 0.34, p = 0.88; P3: F = 0.02, p = 1). Note that the apparently larger P2 complex in EMG-free signals was not statistically different. This result shows that all of the pruning approaches do not significantly affect the measurement of AERPs.

3.3.3.3 Photic stimulation

To investigate the effect of the different muscle-removal approaches on the measurement of VSSRs, I applied them to the photic stimulation tasks (strobe at 16 Hz, 40 Hz, and 59 Hz) of dataset 1. Figure 3-11 shows the mean of the power spectra for all subjects at Oz. Brain response to photic simulation could only be visually identified at the strobe frequency of 16 Hz in all data. The steady state responses at strobe 40 Hz and 59 Hz were not clear in EMG-contaminated data, but after pruning, they could be identified visually.

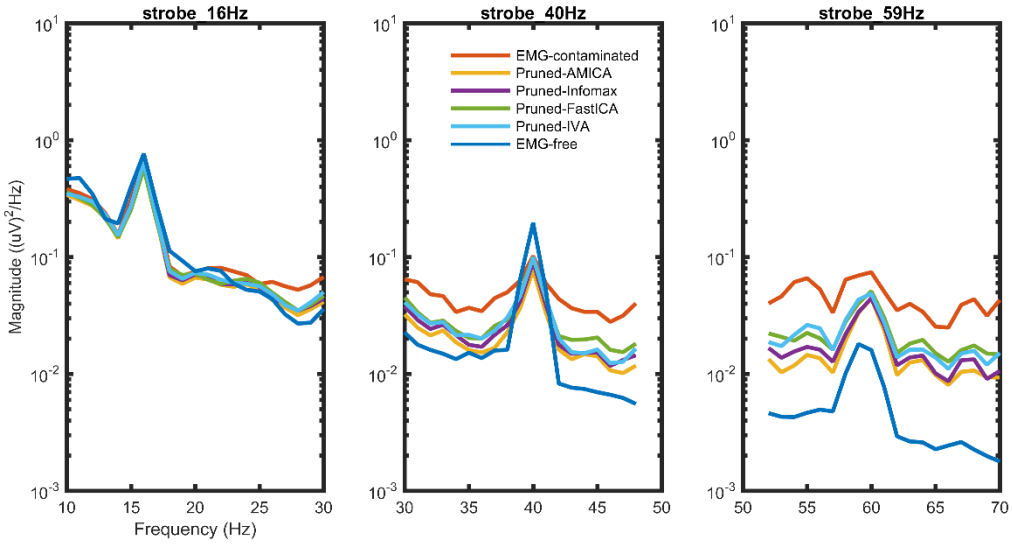

Figure 3-11: From dataset 1, mean power spectra at Oz in response to photic simulation at 16Hz, 40Hz, and 59Hz. All pruning methods reduce the power away from the stimulus frequency, while substantially retaining the power at the stimulus frequency. The VSSR becomes apparent as a peak at the stimulus frequency.

Qualitatively, the pruned data show spectra lying between the EMG-contaminated spectra and the EMG-free spectra. The height of the VSSR was defined as the ratio of the power at the stimulus frequency to the geometric mean of the power at 2 Hz either side of the stimulus frequency. Three separate ANOVAs (three frequencies) revealed no statistical difference for the factor of signal in their height of the VSSR at 16 Hz, 40 Hz, and 59 Hz (16 Hz: $F = 0.24$, $p = 0.93$; 40 Hz: $F = 0.93$, $p = 0.47$; 60 Hz: $F = 0.67$, $p = 0.64$).

3.3.3.4 Auditory stimulation

To evaluate the effect of the muscle-removal approaches on ASSRs, I applied the methods to the 40 Hz auditory stimulation task of dataset 2. The power spectra averaged over the 13 subjects is displayed in Figure 3-12 for channels T7, FCz and T8. The figure shows a substantial reduction in power at muscle frequencies peripherally, and less reduction at the central channel. A 40 Hz peak at FCz is clear in all data, whereas peripherally (where there is more muscle contamination) the peak is only clear in pruned data.

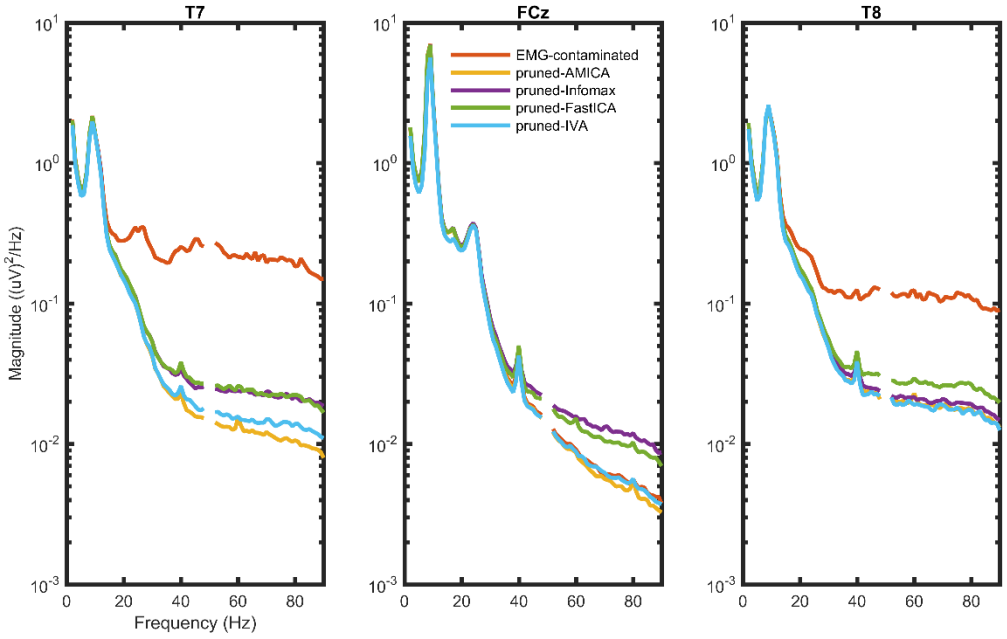

Figure 3-12: From dataset 2, mean of power spectra in response to auditory simulation at 40 Hz. Mains power artefact at 50 Hz has not been displayed. All muscle pruning approaches show a considerable reduction in power above 20 Hz at temporal channels, and all reveal a brain response not seen in the EMG-contaminated data.

The height of the ASSR was defined as the ratio of the power at the stimulus frequency to the geometric mean of the power at 2 Hz either side of the stimulus frequency. Three separate ANOVAs (three channels) revealed no significant effect for the factor of signal at any channel (T7: $F = 0.4$, $p = 0.8$; T8: $F = 0.53$, $p = 0.71$; FCz: $F = 0.37$, $p = 0.82$). These results are consistent with the pruning methods reducing cranial muscle activity while retaining brain signal.

3.3.4 Large sample

Manual pruning on a large number of data is time-consuming and often impractical, making an automatic muscle-removal approach attractive. To investigate the effect of the pruning approaches on a large sample, I applied them on dataset 3, which consists of a large number of healthy participants. Figure 3-13 shows the Berger effect, i.e. reduction of alpha activity in eyes open task, and the VSSR caused by the 60 Hz refresh rate of the monitor, i.e. a peak at 60 Hz in the eyes open task but not in the eyes closed task. Figure 3-14 shows the relative spectra of eyes closed to eyes open to illustrate the Berger effect and 60 Hz VSSR more noticeably. The Berger effect is substantially unchanged by pruning, and the expected VSSR peak is enhanced by pruning.

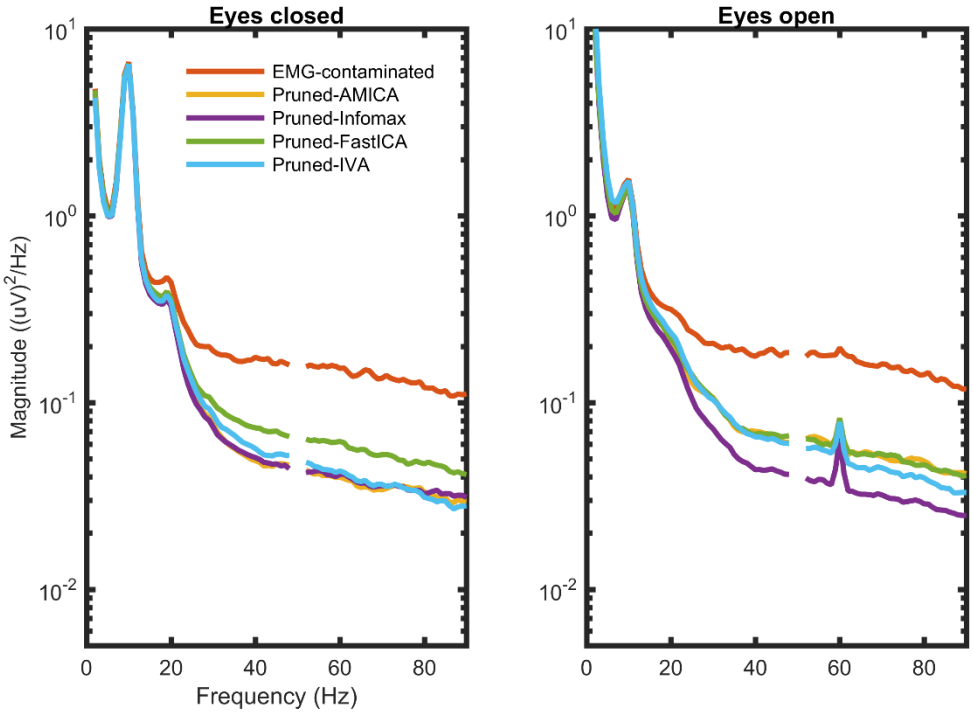

Figure 3-13: From dataset 3, mean of 93 subjects' spectra (eyes closed and eyes open) at Oz. The power at 10 Hz, alpha activity, is decreased in the eyes-open task.

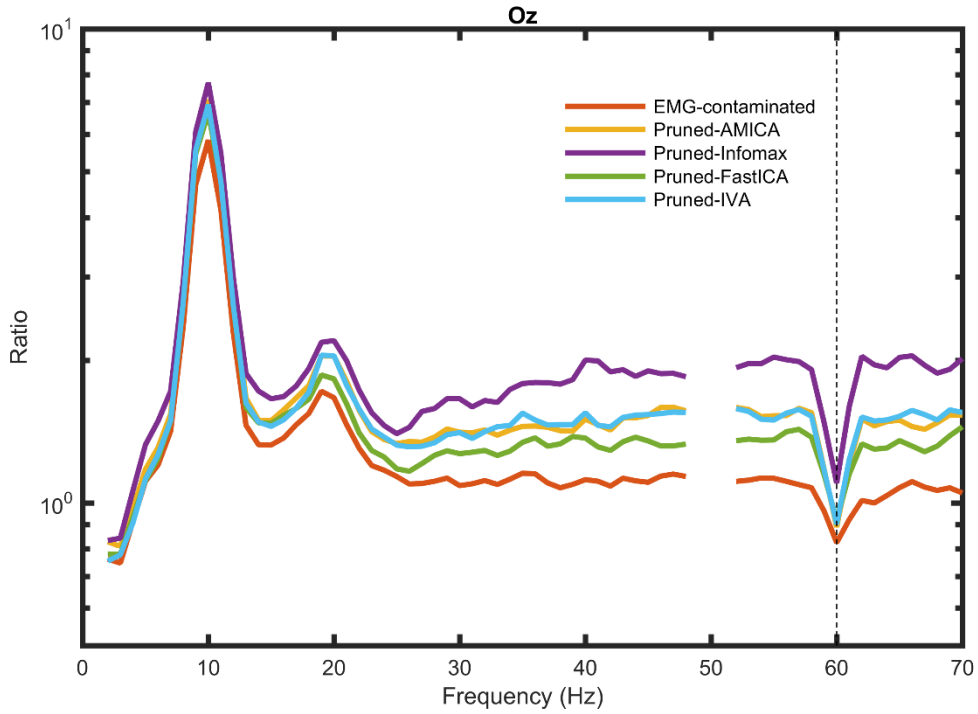

Figure 3-14: From dataset 3, averaged relative power spectra (eyes closed to eyes open) of healthy 93 subjects at Oz. The Berger effect is substantially unchanged by pruning, and the expected VSSR peak is enhanced by pruning.

A one-way ANOVA was performed to compare the height of the VSSR between EMG-contaminated and pruned data in eyes open task. Statistically, there is a significant difference in the VSSR peak height in the eyes open task ($F = 6.23$, $p<0.001$). As shown in Table 3-6, post hoc tests indicate that every pruned data is significantly different to the EMG-contaminated data, but no significant difference is found between any pair of pruned data.

Table 3-6: Post hoc tests for VSSR peak height in the eyes open task. Every pruned data is significantly different to the EMG-contaminated data.

	EMG-contaminated	Pruned-AMICA	Pruned-Infomax	Pruned-FastICA	Pruned-IVA
EMG-contaminated		**<0.001**	**<0.001**	**0.01**	**0.01**
Pruned-AMICA			0.94	0.87	0.97
Pruned-Infomax				0.52	0.67
Pruned-FastICA					0.83
Pruned-IVA					

ANOVA analysis showed that there is no statistically significant effect for the factor of signal in the power in the alpha band (8-13 Hz) in relative spectra ($F = 0.29$, $p = 0.88$).

These results are consistent with all pruning approaches reducing muscle contamination while preserving or enhancing brain activity.

I observed a possible difference in power between pruned data in relative spectra, and I decided to test it statistically in the gamma2 band (35-45 Hz) as it seemed most likely to show a difference. Hence I performed a 1-way ANOVA on the factor of signal, and found a statistically significant difference in the average power of signals in the gamma2 band ($F = 3.49$, $p = 0.008$). Figure 3-15 shows the results of the post hoc tests. None of the pruned data except Infomax are statistically different to the EMG-contaminated data (all $p > 0.051$). However, there is significant difference between EMG-contaminated and Infomax ($p = 0.004$). This is consistent with Infomax outperforming other algorithms in removing tonic muscle activity. No statistical difference was found between any pair of pruned signals (all $p > 0.6$). It should be noted that the means of the ratios are all over one, which is consistent with the pruning algorithms removing more muscle in the eyes open task than the eyes closed task.

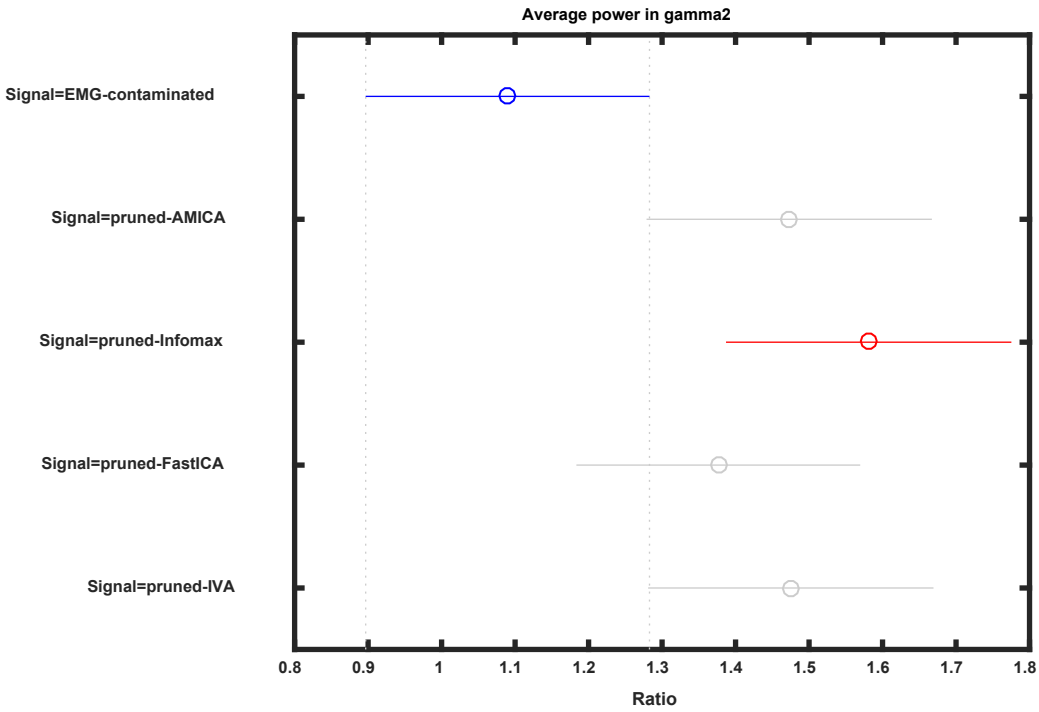

Figure 3-15: Post hoc results for the factor of signal in the gamma2 band. Only pruned-Infomax is statistically different to EMG-contaminated. Note that the means of the ratios (circles) are all over one, which is consistent with the pruning algorithms removing more muscle in the eyes open task than the eyes closed task. Red conditions are significantly different to the blue condition, and light grey conditions are not significantly different to the blue condition.

3.4 Results from comparing the number of SER channels used in ICA

In this section, the effect of the number of SER channels on tonic muscle reduction is evaluated. As described in Section 3.2.5, Infomax was applied to each dataset with their original number of channels, and with subsets of channels corresponding substantially to the 10-10 (64 channels), extended 10-20 (32 channels) and 10-20 (21 channels) systems.

3.4.1 Tonic muscle activity removal

Figure 3-16 compares the averaged power spectra of six subjects from dataset one pruned by Infomax using different numbers of SER channels, during the baseline eyes closed task in nine channels spread evenly across the head. Note that Oz is not present in the international 10-20 system, hence I use Pz instead in the figure, making it slightly different to earlier similar figures. Visually, it seems that tonic muscle activity is reduced in all pruned data, but

better reduction is achieved by pruned-64 and pruned-115 in channels closer to upper cervical muscles.

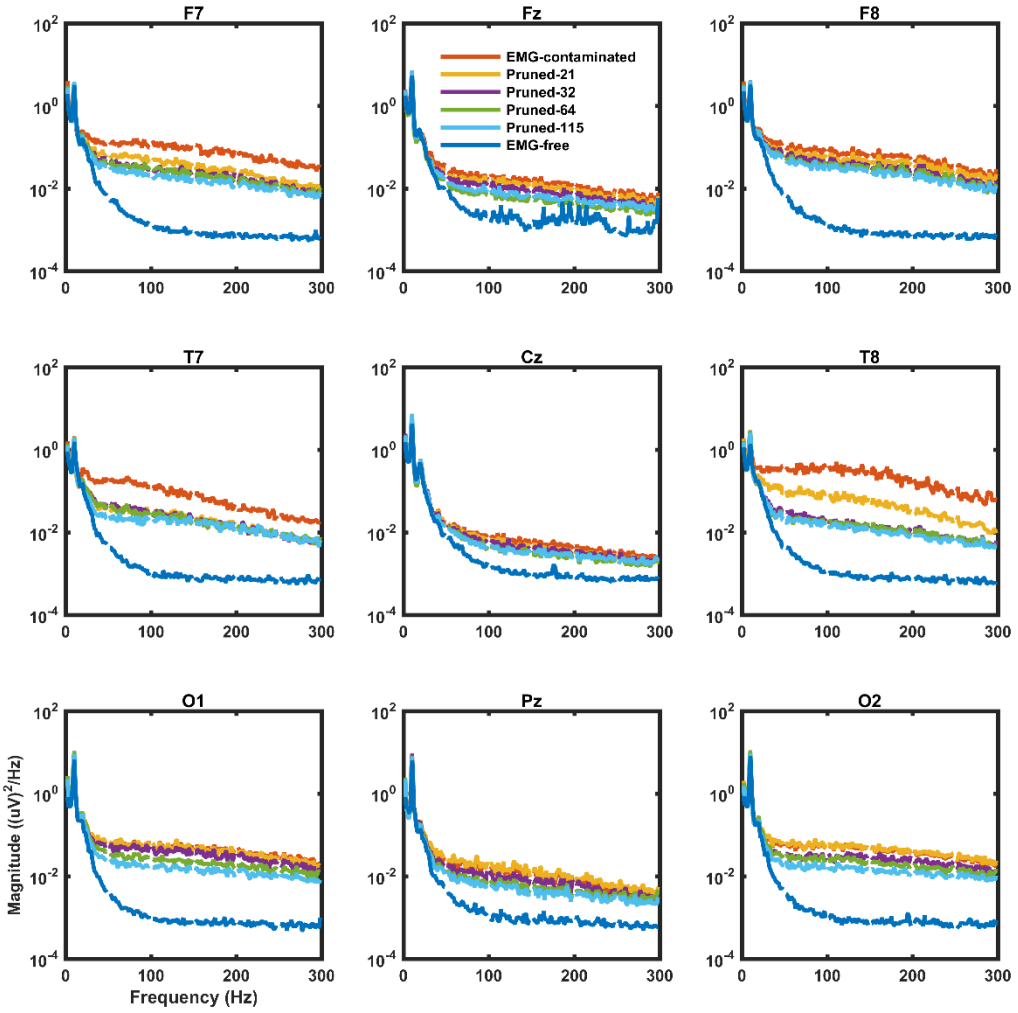

Figure 3-16: From dataset 1, mean of six subjects' power spectra, derived by Infomax pruning using different numbers of EEG channels, during baseline eyes closed task. Note that channels Pz is used in this montage as Oz is not present in the international 10-20 system.

Figure 3-17 displays the topographic maps of relative spectra of EMG-contaminated to EMG-free and pruned to EMG-free in the four frequency bands of interest.

It is observed that the average power of EMG-contaminated spectra at peripheral channels was about 300 times greater than EMG-free spectral power, but after pruning by Infomax this decreased to about 100 times and 35 times using 21 and 32 channels respectively. Visually, pruning with 64 and 115 input channels gives similar results around 20 times greater than EMG-free, nearly half the power of ICA with 32 input channels.

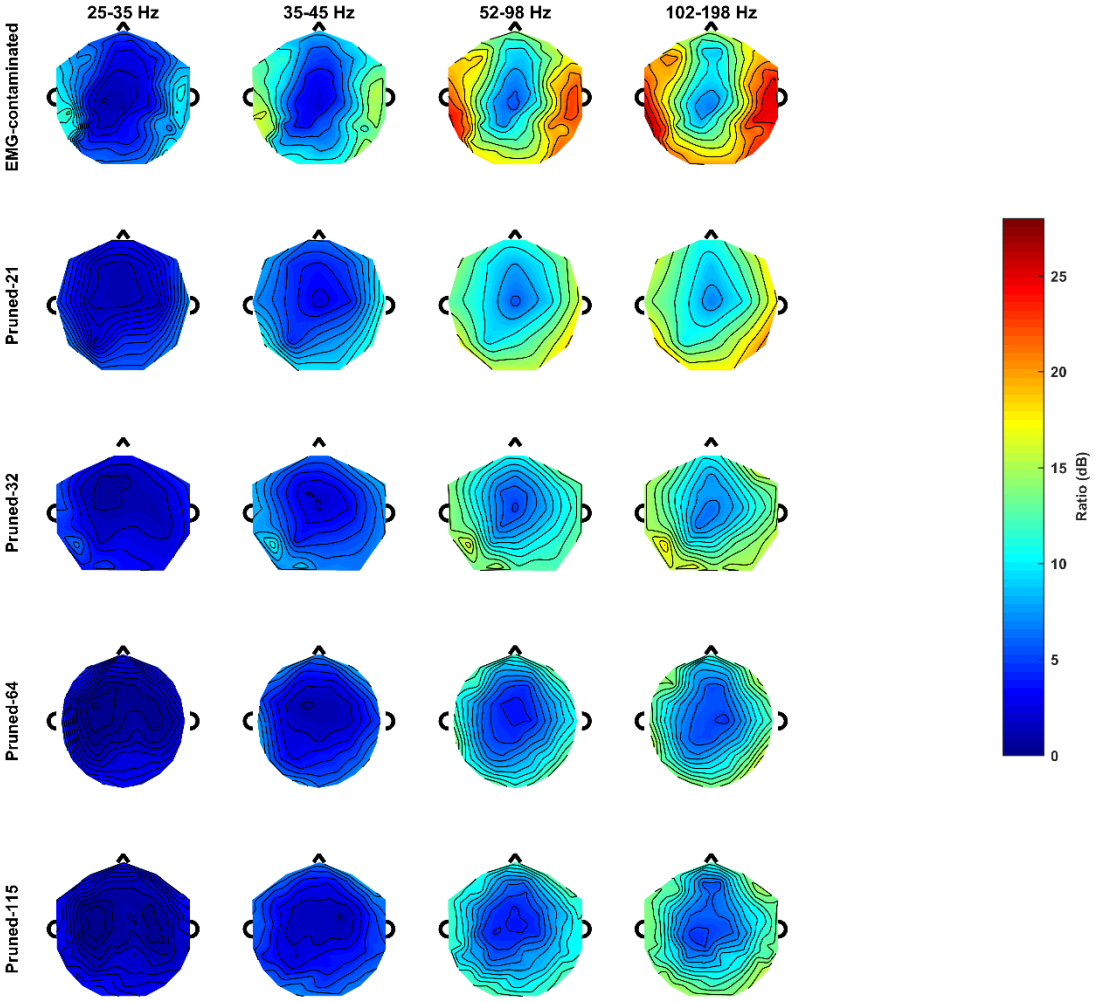

Figure 3-17: Topographic maps of relative spectra of EMG-contaminated and pruned signals relative to EMG-free (rows) in the four frequency bands of interest (columns). Note that the differences are clearest in peripheral channels.

Two groups of channels were considered: central channels (Fz, Cz, C1, C2, and Pz), and peripheral channels (T7, T8, F7, F8, O1, and O2). Again, compared to earlier analyses, I have substituted Pz for Oz in our set of central channels, as Oz is not present in the pruned-21 channel set. Average power spectra of all signals in each group of channels and each frequency band were calculated. Figure 3-18 illustrates the average and standard deviation of power of all signals in each region and each frequency band. Visually, ICA pruning using 115 channels and 64 channels results in better pruning than the other methods.

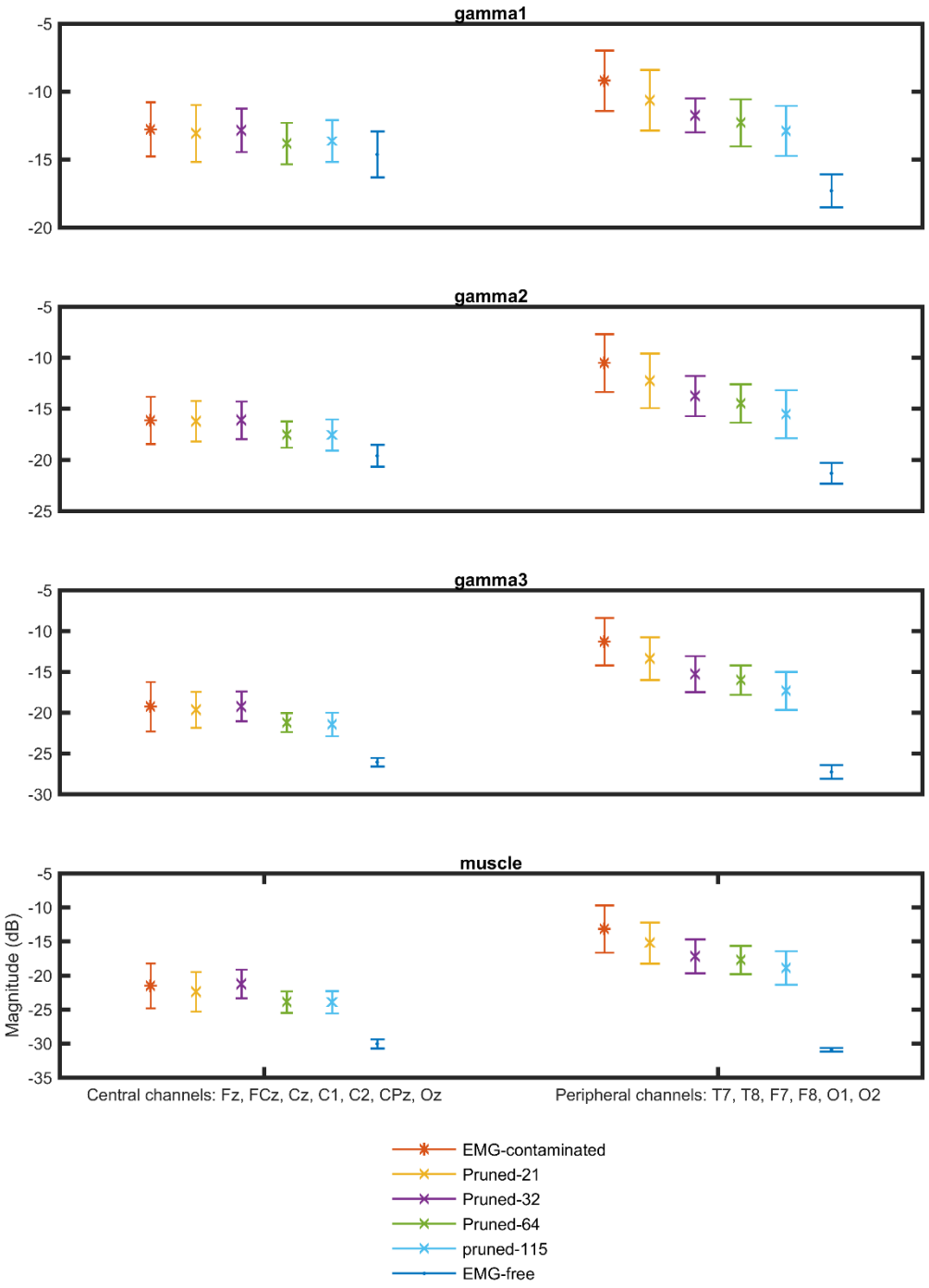

Figure 3-18: From dataset 1, mean and standard deviation of six subjects' power in each frequency band in EMG-contaminated, EMG-free and pruned data with different number of SER channels as input to the ICA.

To test these observations statistically, a 3-way parametric ANOVA was performed to compare the average power for six different signals (EMG-contaminated, EMG-free, and four pruned signals with different numbers of channels input to the ICA) over two regions and four frequency bands. As shown in Table 3-7, The ANOVA showed that the average power

was different over each factor (signal, band, and region), and each two-way interaction (signal∗band, signal∗channel, and band∗channel), all $p < 0.001$. Since the purpose of this section is to compare the number of SER channels used in ICA in removing tonic muscle activity, post-hoc tests were only performed on the factor of signal and on the two-way interactions of signal∗band and signal∗channel to identify statistically significant differences between pairs of signals. The post hoc results on the other factors (region and band) and their two-way interaction is similar to the previous results described in Section 3.3.2.

Table 3-7: Results of three-way ANOVA to compare the power of signals over two regions and four frequency bands.

Analysis of Variance

Source	Sum of squares	Mean square	F	p
Signal	1.32e+02	2.63e+01	104.21	**< 0.001**
Band	1.60e+02	5.33e+01	211.01	**< 0.001**
Region	4.19e+01	4.19e+01	165.67	**< 0.001**
Signal*Band	2.92e+01	1.94	7.70	**< 0.001**
Signal*Region	2.12e+01	4.24	16.76	**< 0.001**
Band*Region	7.13	2.37	9.39	**< 0.001**
Signal*Band*Region	2.25	1.50e-01	0.59	0.87

Table 3-8 shows the post hoc results for factor of signal. All pruned data are statistically different to both EMG-contaminated and EMG-free data. This means that all prunings are reducing cranial muscle activity significantly but the amount of reduction is not sufficient to reach the level of EMG-free data. In addition, pruned-21 is statistically different to pruned-64 and pruned-115 data, which means the amount of muscle reduction using 21 channels is significantly less than achieved using 64 and 115 channels. Similarly, a statistically significant difference between pruned-32 and pruned-115 data demonstrates that significantly more tonic muscle is removed using 115 channels compared to 32 channels. No statistically significant difference was found between pruned-21 and pruned-32, between pruned-32 pruned-64, and between pruned-64 and pruned-115 data.

Table 3-8: Post hoc test for the factor of signal. All pruned data are statistically different to both EMG-contaminated and EMG-free data.

	EMG-contaminated	Pruned-21	Pruned-32	Pruned-64	Pruned-115	EMG-free
EMG-contaminated		**0.001**	**<0.001**	**<0.001**	**<0.001**	**<0.001**
Pruned-21			0.910	**0.008**	**<0.001**	**<0.001**
Pruned-32				0.156	**0.001**	**<0.001**
Pruned-64					0.605	**<0.001**
Pruned-115						**<0.001**
EMG-free						

Table 3-9 shows the post hoc results for the interaction of signal and region. All pruned data are statistically different to EMG-free data in both central and peripheral channels, and also to EMG-contaminated data in peripheral channels. In central channels, however, only pruned-115 is significantly different to EMG-contaminated data. This demonstrates that pruning with 115 channels outperforms pruning with fewer channels in tonic muscle reduction at central channels.

Statistically significant differences of pruned-21 data to pruned-64 and pruned-115 data at peripheral channels indicate that the muscle reduction achieved using 21 channels is significantly less than 64 and 115 channels peripherally.

Table 3-9: Post hoc test for the interaction of signal and region. ICA with any number of SER channels can reduce tonic muscle activity at peripheral channels significantly.

Peripheral / Central	EMG-contaminated	Pruned-21	Pruned-32	Pruned-64	Pruned-115	EMG-free
EMG-contaminated		**0.002**	**<0.001**	**<0.001**	**<0.001**	**<0.001**
Pruned-21	0.92		0.38	**0.03**	**<0.001**	**<0.001**
Pruned-32	1.00	0.99		0.99	0.18	**<0.001**
Pruned-64	0.09	0.94	0.36		0.78	**<0.001**
Pruned-115	**0.03**	0.78	0.16	1.00		**<0.001**
EMG-free	**<0.001**	**<0.001**	**<0.001**	**<0.001**	**<0.001**	

Table 3-10 shows the post hoc results for the interaction of signal and band. At the lowest frequency band, gamma1, none of the pruned data is statistically different to either EMG-contaminated or EMG-free, although EMG-contaminated and EMG-free are statistically different. Hence all pruning methods are reducing muscle, but the amount of reduction is not significant. However at gamma2, all prunings are statistically different to EMG-free, but only pruned-115 is significantly different to EMG-contaminated. This demonstrates that pruned-115 outperforms other methods at tonic muscle reduction in the gamma2 band. At the two higher frequency bands (gamma3 and muscle), again, all prunings are statistically different to EMG-free, but only pruned-115 and pruned-64 are significantly different to EMG-contaminated. This demonstrates that pruned-115 and pruned-64 outperform pruned-21 and pruned-32 at tonic muscle reduction at the higher frequency bands.

Table 3-10: Post hoc test for interaction of signal and band. At higher frequency bands, all prunings are statistically different to EMG-free, but only pruned-115 and pruned-64 are significantly different to EMG-contaminated.

Gamma2 / Gamma1	EMG-contaminated	Pruned-21	Pruned-32	Pruned-64	Pruned-115	EMG-free
EMG-contaminated		0.99	0.79	0.09	**0.006**	**<0.001**
Pruned-21	1.00		1.00	0.97	0.60	**<0.001**
Pruned-32	0.99	1.00		1.00	0.97	**<0.001**
Pruned-64	0.78	1.00	1.00		1.00	**0.001**
Pruned-115	0.58	1.00	1.00	1.00		**0.02**
EMG-free	**0.004**	0.27	0.59	0.96	0.99	

Muscle / Gamma3	EMG-contaminated	Pruned-21	Pruned-32	Pruned-64	Pruned-115	EMG-free
EMG-contaminated		0.45	0.29	**0.001**	**<0.001**	**<0.001**
Pruned-21	0.77		1.00	0.98	0.37	**<0.001**
Pruned-32	0.27	1.00		0.99	0.55	**<0.001**
Pruned-64	**0.002**	0.91	0.99		1.00	**<0.001**
Pruned-115	**<0.001**	0.18	0.64	1.00		**<0.001**
EMG-free	**<0.001**	**<0.001**	**<0.001**	**<0.001**	**<0.001**	

To summarise, all applications of ICA with different numbers of input SER channels are reducing tonic muscle activity significantly at peripheral channels. However the significant difference of pruned-21 to pruned-64 and pruned-115 at peripheral channels indicates that tonic muscle reduction using pruned-21 is significantly less than pruned-64 and pruned-115. Pruned-115 outperform other methods at tonic muscle reduction, because it can reduce tonic muscle activity significantly at central channels and in all tested frequency bands except gamma1. Pruned-64 outperforms pruned-21 and pruned-32 due to its significant tonic muscle reduction at the two higher frequency bands (gamma3 and muscle).

3.4.2 Retention of neurophysiological responses

I investigated the effect of the number of SER channels used in Infomax pruning on the measurement of neurophysiological responses: Berger effect, VSSR, AERP, and ASSR.

3.4.2.1 Berger effect

Figure 3-19 shows the mean of six subjects' eyes closed and left eye open spectra at one of the occipital channels (Pz). In all data pruned with different numbers of SER channels, the power of the alpha band has decreased significantly in the eyes open task comparing to eyes closed task.

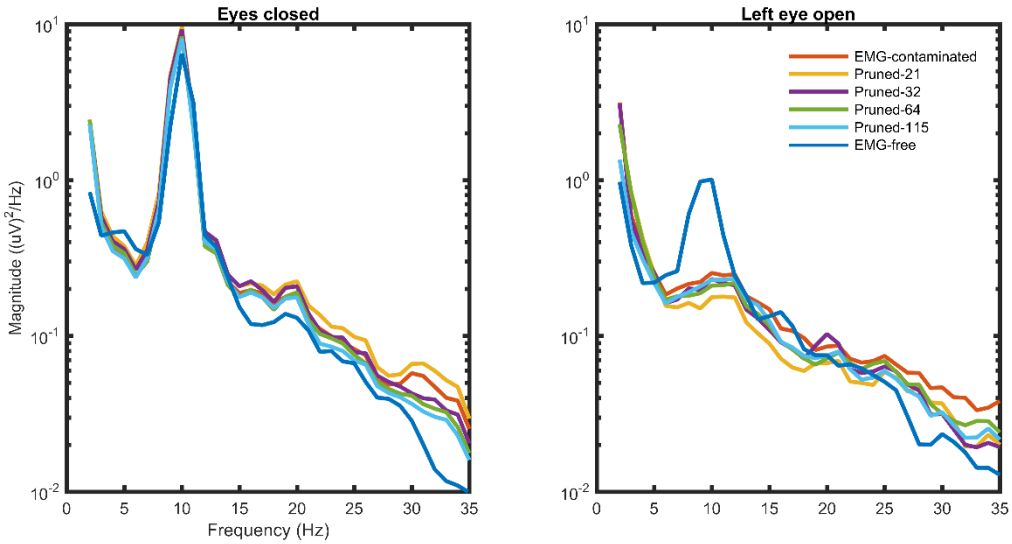

Figure 3-19: From dataset 1, average of six subjects' power spectra at Pz during eyes closed (left) and left eye open (right) tasks. In all signals pruned with different numbers of SER channels, the alpha activity (power at 8-13 Hz) has decreased in the left eye open task. Note that the pruned spectra are processed from the EMG-contaminated data, and hence the pruned and EMG-contaminated spectra are drawn from data recorded at the same time, and a different time to the EMG-free data.

Figure 3-20 shows the averaged relative spectra of the six subjects at Pz. The peak around 10 Hz, due to the reduction of power in the eyes open task, is clear in all signals. Despite the apparent differences in alpha power ratio, statistical analysis revealed no significant difference between EMG-contaminated, pruned and EMG-free signals ($F = 0.16$, $p = 0.97$).

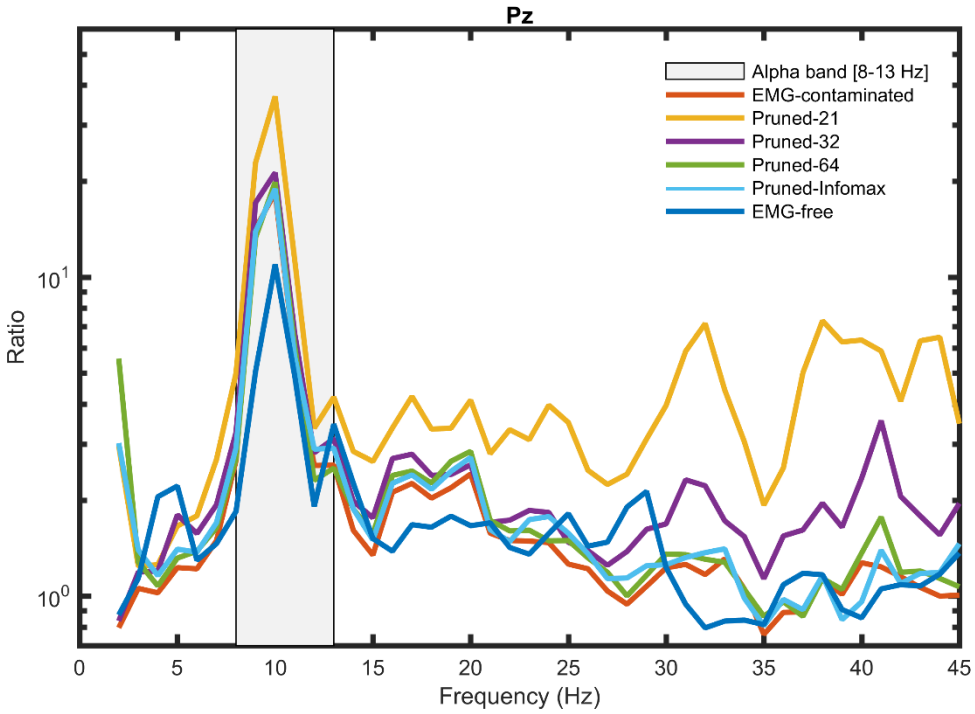

Figure 3-20: From dataset 1, mean of six subjects' relative spectra (eyes closed to left eye open) at channel Pz. The higher power of the pruned-21 spectrum in the alpha band is not statistically significantly different to other spectra.

3.4.2.2 Auditory oddball

The effect of pruning with different numbers of SER channels was evaluated on the AERPs during an oddball task. Figure 3-21 illustrates mean AERPs at channel Fz for five subjects. It is clear that the N1 and P2 components, which are responses to any tone, and the P3 component, which is the response to the target high tone, have been preserved in all pruning methods. Statistical analysis showed no significant difference between any pair of signals (N1: $F = 0.43$, $p = 0.82$; P2: $F = 0.62$, $p = 0.68$; P3: $F = 0.02$, $p = 1$). This result shows that none of the pruning approaches affected the measurement of AERPs. Moreover, the observation that there is no statistical difference between EMG-free and EMG-contaminated is consistent with the process of measuring AERPs (time-locked signal averaging) avoiding muscle contamination, even with few channels.

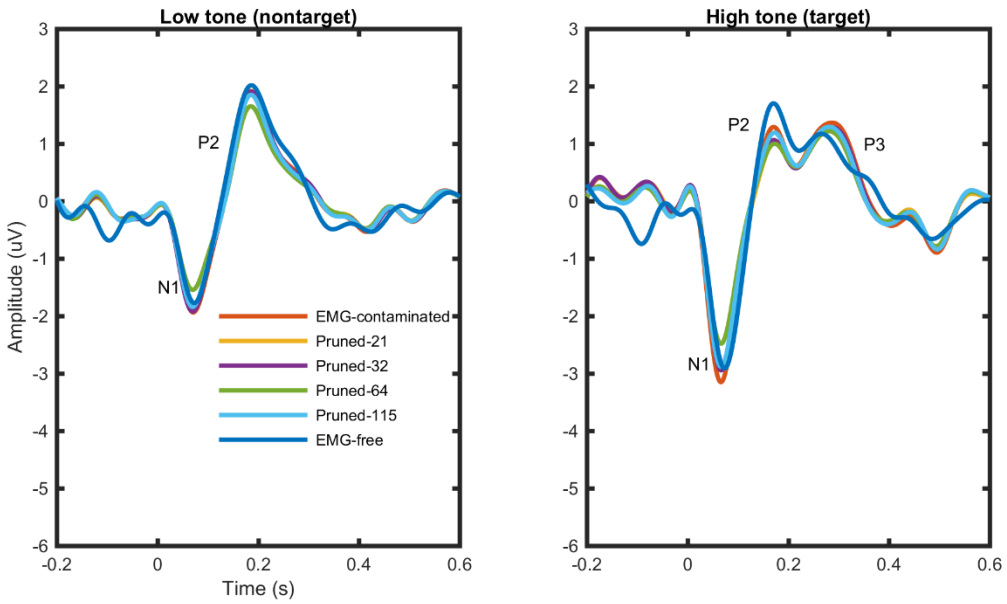

Figure 3-21: From dataset 1, averaged auditory event-related potentials (AERPs) of five subjects in an oddball task at channel Fz. The N1, P2, and P3 components to non-target low tone (left) and target high tone (right) have been preserved in all signals pruned with different numbers of SER channels.

3.4.2.3 Photic stimulation

Figure 3-22 shows the mean of dataset1 subjects' power spectra at Pz in response to photic stimulation at 16 Hz, 40 Hz and 59 Hz. The 16 Hz VSSR is visually apparent in all pruned data, whereas at 40 Hz there is no clear peak in EMG-contaminated and pruned-21 spectra, and at 59 Hz there is no clear peak in EMG-contaminated. Three separate ANOVAs (corresponding to the three strobe frequencies) revealed no significant difference between EMG-contaminated, EMG-free and pruned signals in their spectral power at 16 Hz ($F = 0.12$, $p = 0.98$), 40 Hz ($F = 0.63$, $p = 0.67$) and 59 Hz ($F = 0.40$, $p = 0.83$). These results are consistent with preservation of brain activity in all pruning approaches with different numbers of SER channels.

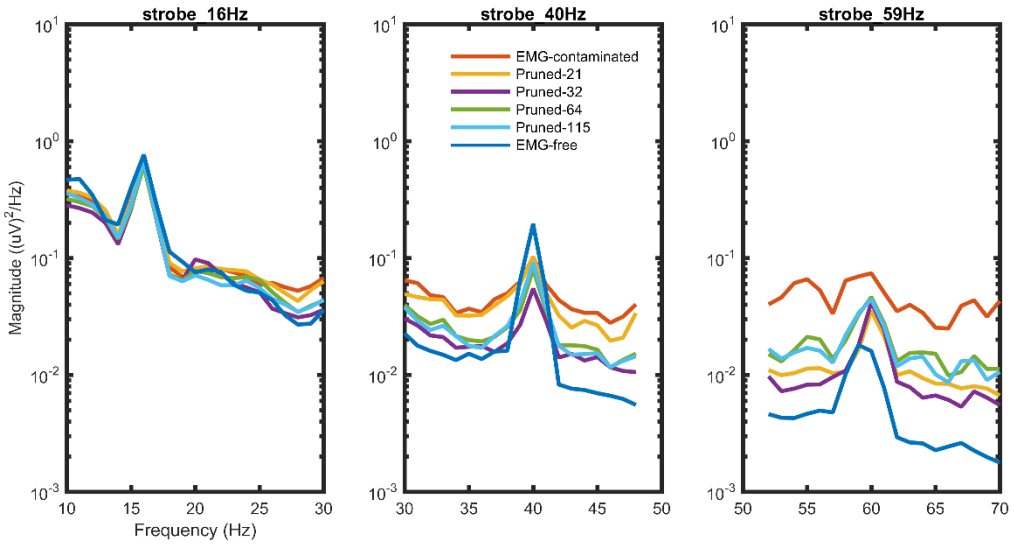

Figure 3-22: From dataset 1, mean power spectra at Pz in response to photic stimulation at 16 Hz, 40 Hz and 59 Hz. There is no statistically significantly difference between the amplitudes of the steady state responses of all datra pruned with different numbers of SER channels.

3.4.2.4 Auditory stimulation

I applied the Infomax algorithm to scalp recordings from dataset 2 using different numbers of SER channels to evaluate its effect on the steady state response to 40 Hz auditory stimulation. Figure 3-23 shows the average power spectra for 13 subjects. The amplitude of the steady state response is disclosed in all pruned data. Three separate ANOVAs (corresponding to the three channels) revealed no significant difference between EMG-contaminated and pruned signals (T7: $F = 0.43$, $p = 0.78$; T8: $F = 0.77$, $p = 0.54$; FCz: $F = 0.83$, $p = 0.47$). These observations are consistent with all the pruning approaches reducing cranial muscle activity while retaining brain signal.

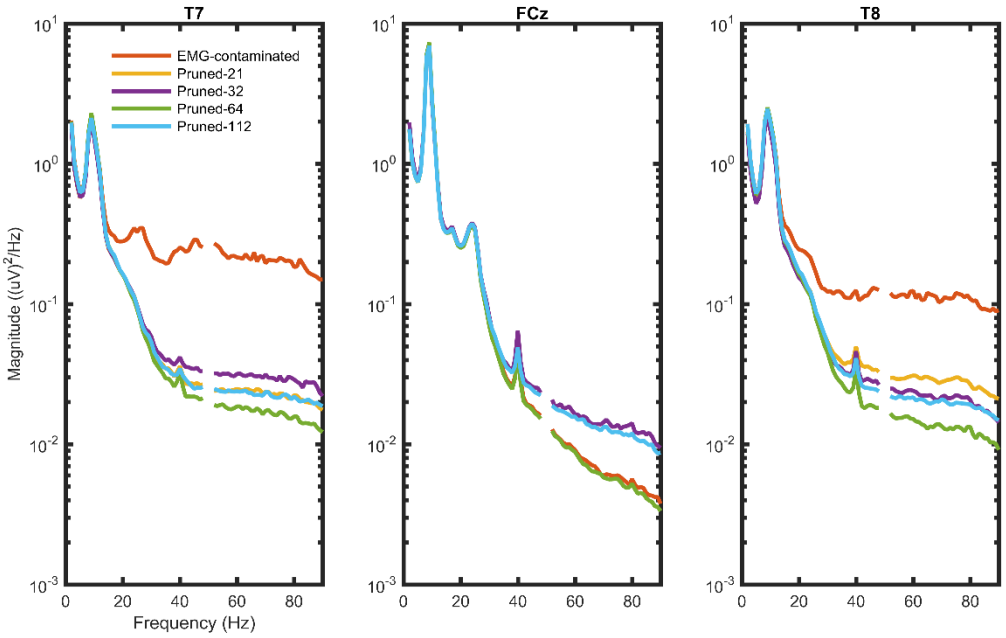

Figure 3-23: From dataset 2, mean of thirteen subjects' power spectra at T7 (left), FCz (middle), and T8 (right) in response to auditory simulation at 40 Hz. There is no statistically significant difference in the amplitudes of the steady state responses between all data pruned with different numbers of SER channels.

3.4.3 Large sample

Infomax was also applied to dataset 3, consisting of large number of healthy participants, using different numbers of SER channels. Figure 3-24 displays the mean of 93 healthy subjects' power spectra at Pz. It shows the Berger effect, i.e. reduction of alpha activity in eyes open task compared to the eyes closed task, and the VSSR caused by the 60 Hz refresh rate of the monitor, i.e. a peak at 60 Hz in the eyes open task only. Figure 3-25 shows the relative spectra of eyes closed to eyes open to illustrate the Berger effect and 60 Hz VSSR more noticeably. The Berger effect is substantially unchanged by the pruning, and the expected VSSR peak is enhanced by pruning using 115 SER channels. ANOVA analysis on the relative spectra showed that there is no statistically significant difference between any of the signals in the relative power of the alpha band ($F = 0.08$, $p = 0.97$). One-way ANOVA was performed for eyes open task to compare the height of the VSSR between EMG-contaminated and pruned data. No significant difference was found between signals in the height of the VSSR ($F = 1.22$, $p = 0.29$).

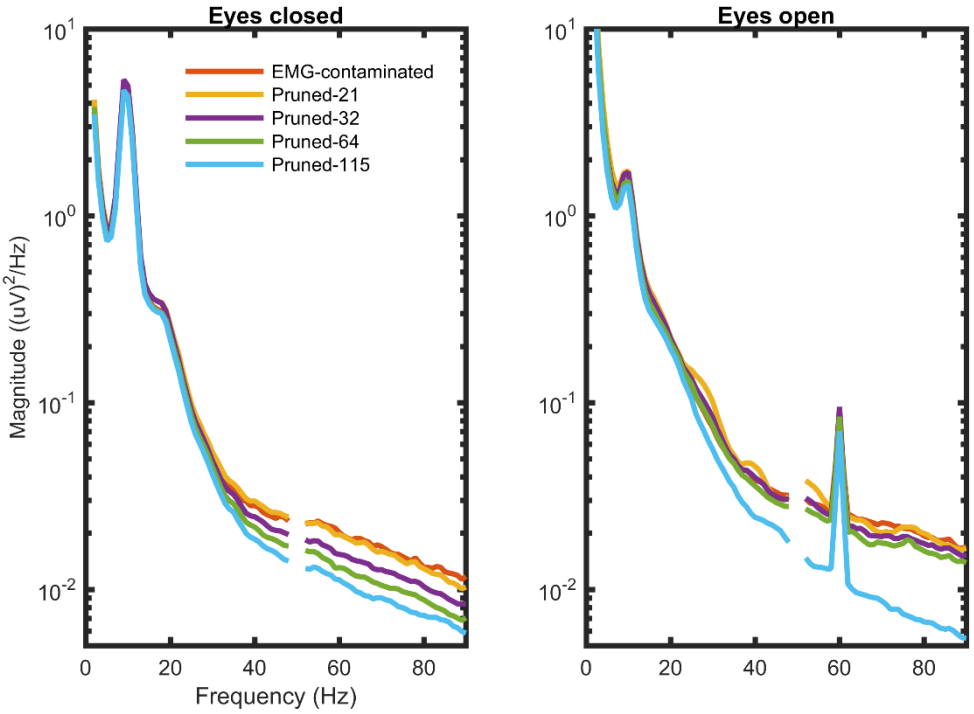

Figure 3-24: From dataset 3, mean of 93 subjects' spectra at Pz during the eyes closed task (left) and the eyes open task (right). The power at 10 Hz, alpha activity, is decreased in the eyes open task, but a VSSR response to the screen refresh rate at 60 Hz is apparent.

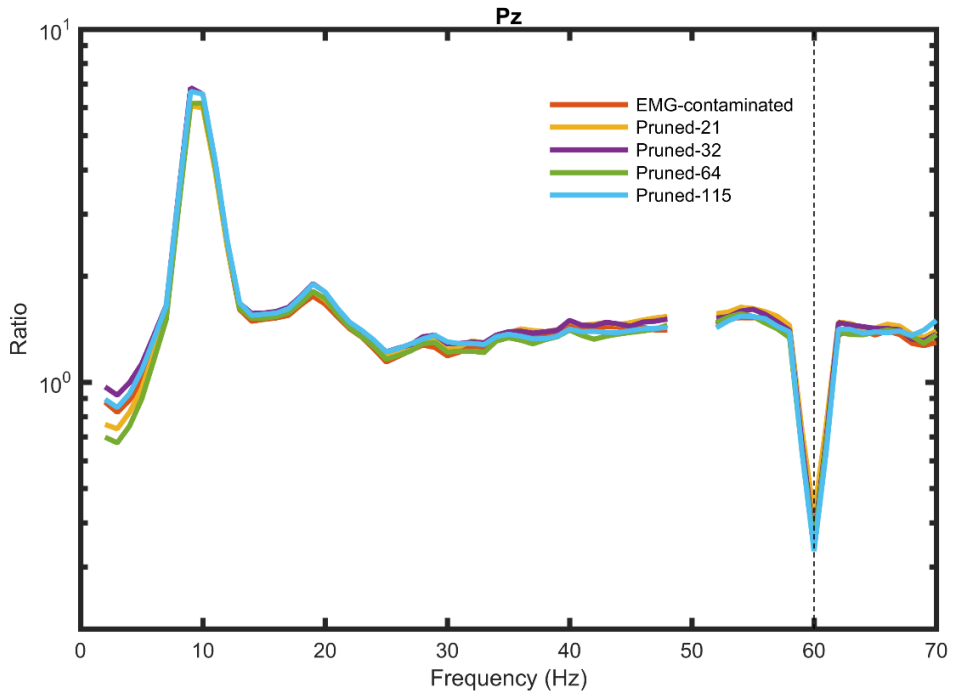

Figure 3-25: From dataset 3, averaged relative power spectra (eyes closed to eyes open) of 93 healthy subjects at Pz. The Berger effect and the expected VSSR peak are substantially unchanged by pruning with different numbers of SER channels.

3.5 Discussion and conclusion

The effect of five BSS algorithms (AMICA, Infomax, FastICA, CCA, and IVA) in the automated removal of tonic cranial and upper cervical muscle activity was evaluated. Using the unique database of pharmacologically-induced paralysed subjects and the spectral gradient of components, a gradient threshold could be set for all algorithms except CCA. Based on the results, the traditional BSS-CCA approach cannot classify components automatically, so the classification of components remains subjective. Chapter 5 investigates the traditional BSS-CCA algorithm and considers possible extensions to automate the classification of muscle components.

The unique dataset of paralysed subjects provides many of the advantages of simulated data while retaining the advantage of being "real" data. The results of the pruned data were compared to EMG-free data (paralysis condition) and EMG-contaminated data (pre-paralysis condition).

The main effect of signal shows that all pruned data were significantly different to both EMG-contaminated and EMG-free data, but not different to other pruned data. Therefore, the amount of muscle reduction is not sufficient to reach the level of EMG-free data and there is still residual tonic muscle activity in pruned SERs. Likely the most significant reason is that these algorithms cannot provide a sufficient number of sufficiently pure muscle or pure brain components. In fact, most of the components are mixtures of myogenic and neurogenic signals (Delorme et al. 2012). This can be concluded even by visual inspection of the histogram of EMG-free and EMG-contaminated components derived by applying each algorithm, Figure 3-2. A negative spectral gradient is expected for purely neurogenic components, whereas purely myogenic components should have a positive gradient. In other words, ideally, the histogram of EMG-contaminated components should be bimodal. However, most of the components have negative spectral gradients, independent of the BSS

algorithm. This implies there are many components that are a mixture of myogenic and neurogenic signals. Hence, there is still a need for an algorithm that gives components that are better separated. This will be discussed further in Section 8.2.

Considering the interaction with region, the statistical analyses reveal that in central channels only AMICA and Infomax can reduce muscle activity significantly. However, all of the algorithms can significantly reduce tonic muscle activity at peripheral channels, which are the channels most affected by cranial and upper cervical muscles.

Considering the interaction with band, FastICA and IVA can only significantly reduce tonic muscle contamination at higher frequency bands (above 52 Hz). But AMICA and Infomax can achieve a significant muscle reduction from lower frequency bands (above 35 Hz). The results indicate AMICA and Infomax outperform FastICA and IVA in reducing tonic muscle activity. This is consistent with others' results showing that AMICA and Infomax produce components that are at best 30% and 25% dipolar-like respectively, which are better percentages that all other ICA approaches (Delorme et al. 2012). They can achieve better separation of pure components, pure muscle or pure brain, and hence better muscle reduction. Moreover, Albera et al. (2012) have shown that, ignoring the computational complexity, Infomax outperforms FastICA and some less popular ICA algorithms in removing muscle activity from simulated EMG-contaminated data. Although, Leutheuser et al. (2013) have shown that AMICA outperforms Infomax in non-automated phasic muscle reduction, my results did not endorse this outperformance in tonic muscle reduction. Moreover, it is indicated that FastICA can separate SERs to their composed components faster than Infomax (Dharmaprani et al. 2016; Sahonero-Alvarez et al. 2017). Hence, FastICA is a better choice than Infomax in studies where computation time is more important than optimum tonic muscle reduction.

IVA, as an algorithm combining the advantages of both CCA and ICA, has recently been applied in studies of the removal of phasic muscle from SER (Chen, X, Liu, et al. 2017; Chen, X, Peng, et al. 2017). Although, it has shown better performance than both ICA and CCA algorithm in phasic muscle reduction or in removing muscle contamination from EEG with low signal-to-noise ratio (Chen, X, Liu, et al. 2017; Chen, X, Peng, et al. 2017), my results indicate that AMICA and Infomax outperform IVA in tonic muscle reduction.

The statistical results indicate that none of the applied BSS algorithms has a significant effect on any brain neurophysiological responses. Therefore, the aim of retaining brain neurophysiological responses can be achieved using any of the four algorithms.

Comparing Figure 3-24 to Figure 3-13, it can be observed that the VSSR peak is not apparent in EMG-contaminated data at Oz (Figure 3-13), but it is visible at Pz (Figure 3-24). This is likely due to the activity of upper cervical and paraspinal muscles more severely affecting the occipital channels located close to these muscles.

The relationship between the number of SER channels used in ICA and the reduction of tonic cranial muscle activity was also evaluated. Although ICA pruning based on 21 and 32 channels of SER showed good results in reducing phasic muscle contamination (Jung, T-P et al. 2000; Radüntz et al. 2015), the results of my analyses show that their application achieved no significant tonic muscle reduction at any frequency band (averaged across both regions), but there was significant tonic muscle reduction at peripheral channels (averaged across all bands). Moreover, the amount of peripheral muscle removal achieved by applying ICA with 21 channels is significantly less than the amount of muscle removal achieved by applying ICA with 64 or 115 channels. This indicates an advantage of applying ICA to data with a higher number of SER channels. Application of ICA with 64 SER channels results in a significant muscle reduction at both higher frequencies (above 45 Hz), and in peripheral channels. However, application of ICA with 115 SER channels results in a significant muscle

reduction both centrally and peripherally, and also at higher frequencies (above 35 Hz). Hence, as the number of channels increases, the amount of muscle reduction increases, as does the range of frequencies achieving significant reduction. Lau et al. (2012) have evaluated the number of SER channels in brain imaging. They have shown that by reducing the number of SER channels, the percentage of pure (myogenic or neurogenic) components is decreased. This can be interpreted as follows: by reducing the number of SER channels, less pure components can be separated and more components are mixtures of myogenic and neurogenic signals.

Increasing the number of channels increases the time, expense and difficulty of collecting the data, and the computational time and cost of processing the data. Hence, the choice of number of channels should depend on the purpose of study. For example, for studies which need to reduce tonic muscle activity peripherally, ICA with 32 channels is likely sufficient. Studies which need to reduce the effect of tonic muscle activity centrally or at lower frequencies should use a higher number of SER channels.

I found no evidence that the application of ICA significantly affects any brain neurophysiological responses. Therefore, the aim of retaining brain neurophysiological responses can be achieved using ICA with any number of SER channels.

Chapter 4

Source localisation as a muscle-removal method

Source localisation is based on the assumption that electrical signals recorded at the scalp originate as electrical dipoles in the brain (sources), and propagate through the volume of the head to the scalp (sensors). Source localisation estimates the source signals, given the measured SERs and a volume conduction model of the head (Grech et al. 2008). Hämäläinen and Ilmoniemi (1984) proposed the first solution for this inverse problem in 1984, and many other methods have been proposed since.

It has been shown that source signals have reduced **phasic** muscle contamination at **source level** as compared to sensor signals (Hipp, Engel & Siegel 2011). However, my aim is to reduce the effect of **tonic** muscle activity at **sensor level**. Hence, my approach is a new use of source localisation which is different to the traditional approach in two ways, as highlighted.[2]

4.1 Beamformer

Beamforming is used to describe the processing of data from an array of sensors that can be viewed as implementing a spatial filter, originally in radar and sonar (Sekihara et al. 2001). Systems receiving spatially broadcast signals usually have problems with unwanted or interfering signals. Traditional spectral-based filtering is not able to separate the desired and unwanted signals if these signals have overlapping frequency bands. On the other hand, the sources of desired and unwanted signals usually have different spatial locations. This

[2] The proposed approach and most of the results presented in this chapter are published in the journal paper attached in Appendix A-1. This chapter also includes a more detailed statistical analysis and expanded discussion and conclusion.

different spatial origin is exploited in a spatial filter to separate the desired signals from unwanted ones (Van Veen & Buckley 1988). Hence, the aim of a beamformer or spatial filter is to recognise the signal radiating from a particular direction or location in the presence of other unwanted or interfering signals.

Beamformer gives an output which is more sensitive to signals from particular directions or locations using a linear combination (a weighted sum) of sensor signals. In traditional radar applications, where the sensors are arrange with equal separation along a line, the sensitivity of this output with direction is often characterised using a radiation pattern, where a high gain in one direction is clear from the large beam pointing in that direction. An algorithm that adjusts the weightings to control the direction of the beam or beams is therefore called a beamforming algorithm, or beamformer.

When the sensors have a more complex spatial arrangement, the sensitivity of the output depends on location, not simply direction. Characterising the sensitivity of the output only by direction is now not possible. Hence the output is better described as spatially filtered, rather than beamformed. Despite this, the names beamformer and spatial filter are both used somewhat interchangeably.

The concept of beamforming or spatial filtering is being used in several applications, such as communications, geophysics, astrophysics, imaging, biomedical and brain research (Van Veen & Buckley 1988). In brain research, spatial filtering is being used for source localisation. Despite the array of sensors denying a radiation pattern characterisation, the literature traditionally refers to this as beamforming.

Beamforming source localisation is a method based on source analysis that is most commonly used in magnetoencephalography (MEG) research, but can also be applied to SERs (Hipp, Engel & Siegel 2011). Using the volume conduction **model of the head** and the defined **location of the sources** and **SER electrodes**, leadfields at each source location are

calculated. The **leadfields** represent the geometric properties of the conductive medium between submerged sources and surface electrodes. They are used in the **forward** problem, transforming source signals to sensor signals. In contrast, beamformers solve the **inverse** problem by calculating **spatial filters** that transform sensor signals to source signals (Huang, MX et al. 2004b). The inverse problem is an underdetermined problem which is difficult to solve. There are many source configurations which can produce the same SER, hence achieving a unique answer requires some additional assumptions, commonly regarding regularisation and the number, location and orientation of sources (Van Oosterom 1991). Based on the chosen additional assumptions, beamformer algorithms can be categorised into two main families: minimum-norm beamformers and minimum-variance beamformers (Jonmohamadi et al. 2014). Minimum-norm beamformers estimate the activity of all sources such that their propagation to and combination at the scalp sensors (SER electrodes) has the minimum difference to the measured signals. So the aim of minimum-norm beamformers is to accurately model the SER measurements. In contrast, minimum-variance beamformers do not have this constraint. This allows them to perform better than minimum-norm beamformers in other ways, such as achieving a higher spatial resolution when mapping brain activity. But it does mean they cannot be used to reconstruct surface SER signals, and so cannot be used for the proposed sensor-level muscle-removal method.

4.2 sLORETA

One of the popular minimum-norm beamformers is sLORETA (standardized low resolution electromagnetic tomography) which has shown reliable performance in source localisation (Pascual-Marqui 2002).

Based on the forward solution, the scalp electrical potential with common average reference can be described as:

$$\Phi = LJ$$

where Φ is a vector of the measured scalp potentials at $i = 1,2,3, \ldots, M$ electrodes and J is the source current density defined as:

$$J = (J_1^T, J_2^T, J_3^T, \ldots J_N^T)^T$$

where $J_\ell^T = (J_\ell^x, J_\ell^y, J_\ell^z)$ contains the three unknown dipole moments at $\ell = 1,2,3, \ldots, N$ source locations, and the superscript T denotes the transpose.

The leadfield L has the following structure:

$$L = \begin{bmatrix} l_{1,1} & l_{1,2} & \ldots. & l_{1,N} \\ l_{2,1} & l_{2,2} & \ldots. & l_{2,N} \\ \vdots & \vdots & & \vdots \\ l_{M,1} & l_{M,2} & & l_{M,N} \end{bmatrix}$$

$l_{i,\ell} = (l_{i,\ell}^x, l_{i,\ell}^y, l_{i,\ell}^z)$ describes the surface SER at the i^{th}electrode due to a unit strength dipole at each orientation (x, y, z) at the ℓ^{th} source location. The leadfield matrix represents the geometric properties of the conductive medium between submerged sources and surface electrodes (Van Veen et al. 1997). In other words, it is only dependent on the volume conduction model of the head, the locations of the electrodes and the locations of the dipoles (voxels).

The aim of the inverse solution is to estimate the source current density at each source location. The sLORETA source estimation method solves the inverse problem by minimising the following function with respect to J for known Φ and L (Pascual-Marqui 2002):

$$F = \|\Phi - LJ\|^2 + \alpha \|J\|^2$$

α is the regularisation parameter. Solving this minimisation problem gives the estimated source signals as:

$$\hat{J} = W\Phi$$

where the spatial filter weight matrix W is given by:

$$W = \frac{(G_\Omega + \alpha I)^{-1} L}{\sqrt{L^T G_\Omega^{-1} L}}$$

$$G_{\Omega} = \sum_{\Omega} LL^{T}$$

G_{Ω} is called the gram matrix and Ω is the region of interest (i.e. inside the brain) (Jonmohamadi et al. 2014).

4.3 Approaching sLORETA as a muscle-removal method

In order to reduce muscle activity at the sensor level using sLORETA, the following processing steps were implemented.

Firstly, using the MATLAB Fieldtrip toolbox (Oostenveld et al. 2010) and boundary element method (BEM), a generic volume conduction model of the head was constructed which included three layers: brain, skull, and scalp (Figure 4-1). Secondly, a set of source locations (voxels) located on a regular grid with a 1 mm spacing was culled to retain only those voxels that were in either the brain layer or the scalp layer. It is assumed that the bone of the skull does not generate any electrical activity. This resulted in 1619 sources distributed inside the brain, and 1115 sources distributed within the scalp. Thirdly, having the volume conduction model of the head, electrode locations, and defined source locations (voxels), the leadfield vectors, L, were calculated. Finally, the beamforming technique sLORETA provided estimates of the spatial filters,W, and source signals, J.

Using the derived leadfields, the surface SER signal was reconstructed, forward modelling, using only sources inside the brain.

$$\hat{\Phi}_{brain} = L_{brain}\hat{J}_{brain}$$

Sources in the scalp layer were considered to be extracranial muscle activity and were therefore discarded in the forward modelling. **Error! Reference source not found.** shows the step-wise algorithm.

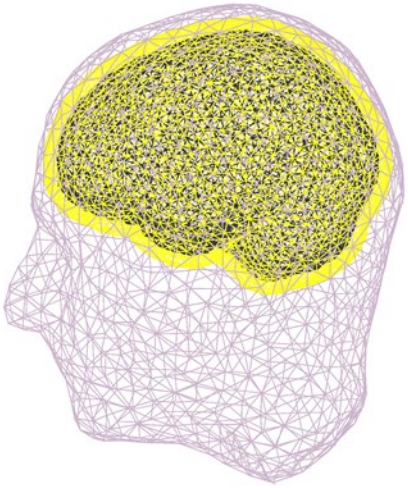

Figure 4-1: Volume conduction model of the head with three layers: brain (black), skull (yellow), and scalp (light mauve).

Table 4-1: The step-wise algorithm of the proposed pruning method.

sLORETA as a muscle-removal method
1. Using the boundary element method, construct a generic volume conduction model of the head consisting of three layers: scalp, skull, and brain.
2. Locate a set of sources on a regular grid with a 1mm spacing, and retain those sources that lie inside either the brain layer or the scalp layer.
3. Using the head model, electrode locations and source locations, calculate the leadfields.
4. Estimate the source signals at each source location using sLORETA method.
5. Discard the estimated sources within the scalp volume (putatively muscle).
6. Reconstruct surface SER signals (forward model) using the retained sources within the brain volume (putatively brain) and their corresponding leadfields.

The proposed approach was applied on all three datasets to evaluate its effectiveness in the automated removal of cranial and upper cervical muscle activity while retaining neurophysiological responses. The signals pruned by this approach are called pruned-sLORETA. In this chapter, I will use three datasets to quantitate the performance of this algorithm. In Chapter 6, its effectiveness will be compared to several other pruning algorithms.

4.4 Results

This section shows the results of applying the proposed method to all three datasets. It includes both baseline tasks and neurophysiological responses such as the Berger effect, AERPs, VSSRs, and ASSRs.

4.4.1 Brain source vs muscle source

The time series and spectra of two sources are shown in Figure 4-2; one is from a source inside the brain (intracranial, A) and the other is from inside the scalp (extracranial, B). The times series in A and B are consistent with typical brain and muscle time series, respectively, with B showing more high amplitude spikes. The spectrum in A decreases rapidly after a peak at 10 Hz, consistent with the brain exhibiting alpha activity. On the other hand, the spectrum in B exhibits a positive gradient between 7 Hz and 75 Hz, consistent with the presumed muscular origin of this source (Fitzgibbon, S et al. 2016).

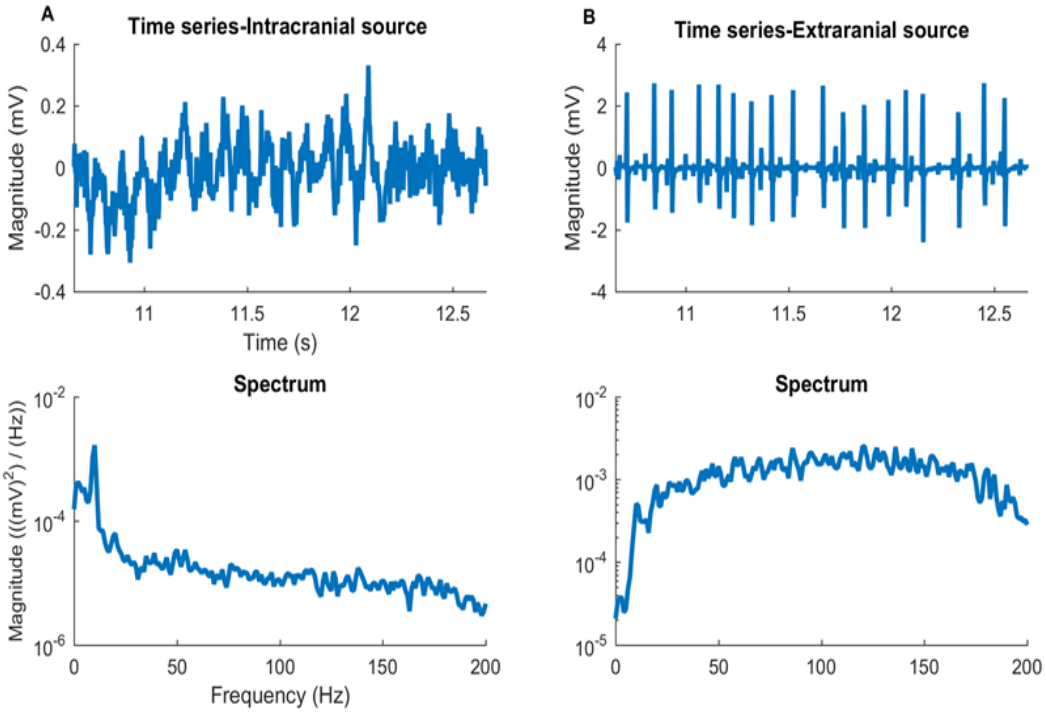

Figure 4-2: Time series and spectra of head sources. A, from an intracranial source and B, from an extracranial source.

4.4.2 Tonic muscle activity removal

Figure 4-3 compares the average of muscle removed using the sLORETA method with EMG-free data and EMG-contaminated data in nine channels spread evenly across the head.

I observe that using the sLORETA method, muscle reduction starts at frequencies as low as 20 Hz. High frequency power, associated with muscle, has been reduced, but there is still muscle contamination compared to EMG-free data. Its effectiveness in reducing cranial muscle activity is clearer at peripheral channels.

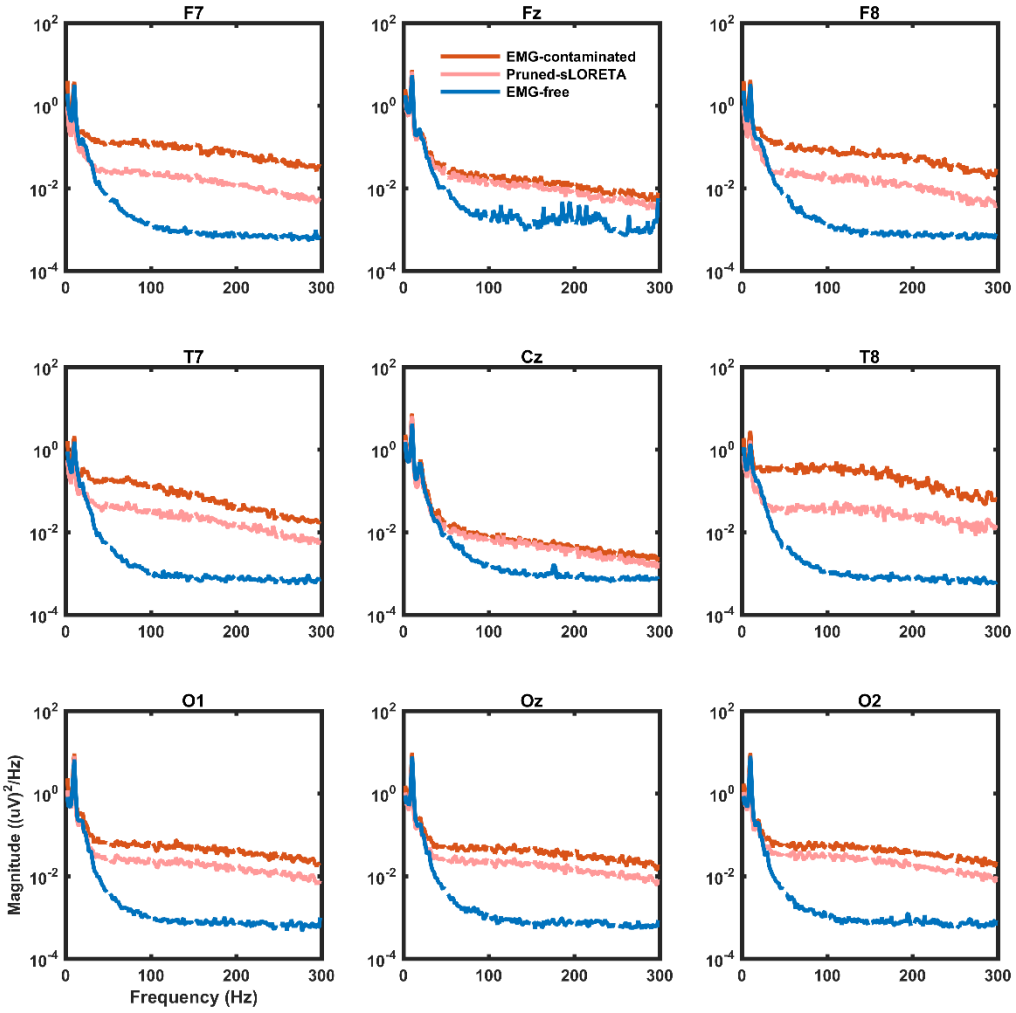

Figure 4-3: From dataset 1, mean of six subjects' power spectra during baseline eyes closed task. Using the sLORETA method, muscle reduction starts at frequencies as low as 20 Hz, but there is still muscle contamination compared to EMG-free data.

Figure 4-4 displays the topographic maps of relative spectra of EMG-contaminated to EMG-free, and pruned sLORETA to EMG-free in the four frequency bands of interest. It is observed that the proposed sLORETA method is more effective in reducing muscle activity peripherally than centrally. For example, the average power at 102-198 Hz (muscle band) at temporal channels in EMG-contaminated data was about 300 times greater than in EMG-free data, whereas after pruning with sLORETA this value decreased to about 60 times.

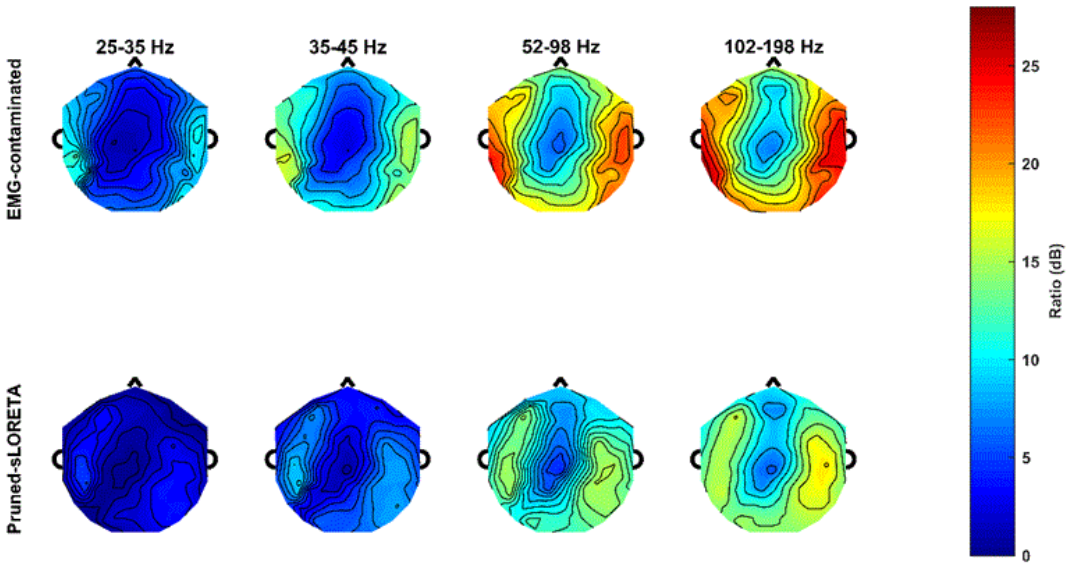

Figure 4-4: From dataset 1, topographic maps of relative spectra in EMG-contaminated/EMG-free, and pruned signals/EMG-free (rows)in different frequency bands (columns). It is observed that the proposed sLORETA method is more effective in reducing muscle activity peripherally than centrally. Each topography is looking down on the head, with ears and nose indicated, conforming to the montage in Figure 2-4.

Two groups of channels were considered for statistical analysis: central channels (Fz, Cz, C1, C2, and Oz), and peripheral channels (T7, T8, F7, F8, O1, and O2). The average power spectra of all signals in each group of channels and each frequency band were calculated. Figure 4-5 compares the mean and standard deviation of six subjects' power in each frequency band within each region. Visually, the proposed sLORETA method does not appear to be effective in reducing muscle activity at central channels, while its performance appears better peripherally.

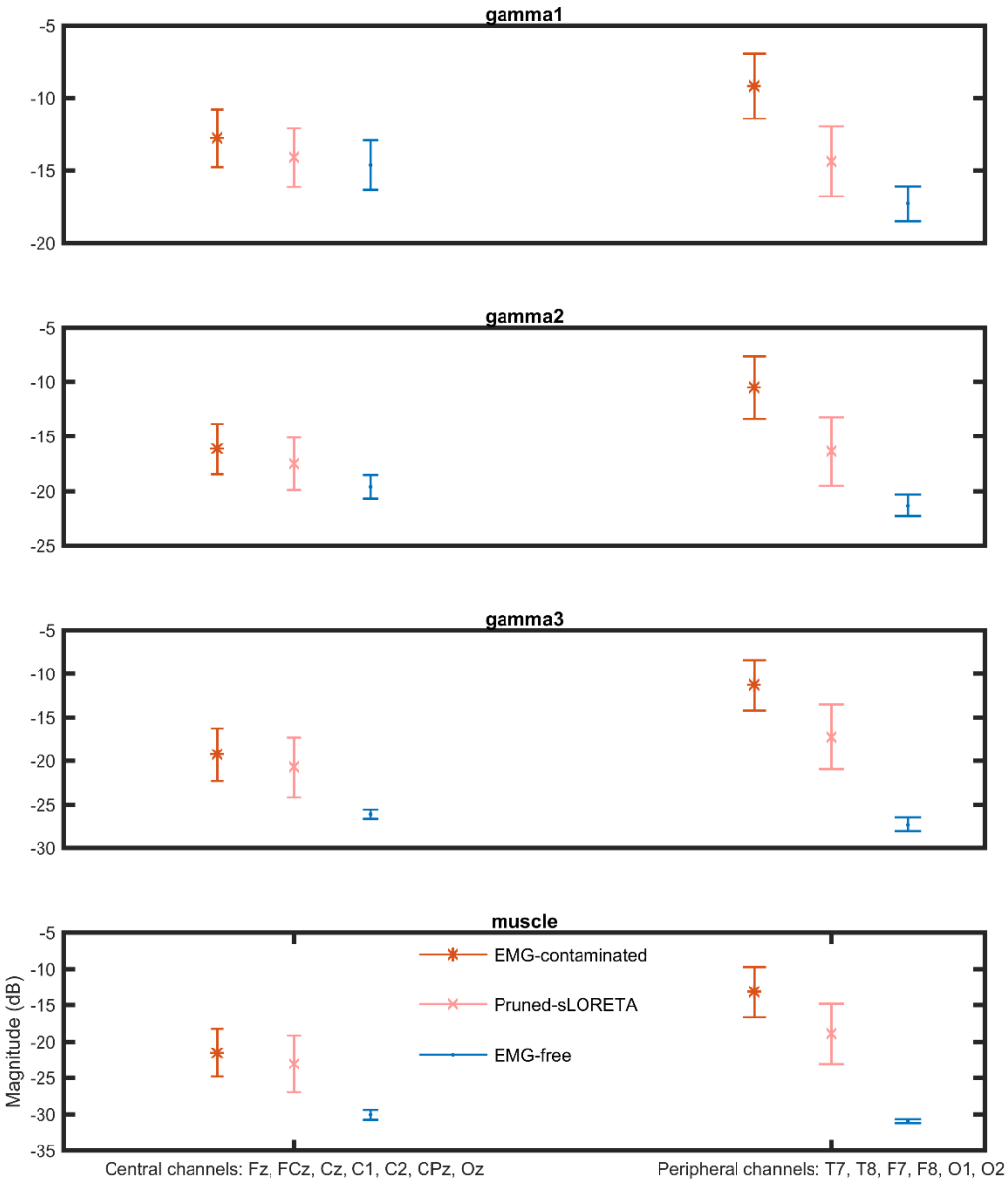

Figure 4-5: From dataset 1, mean and standard deviation of pruned-sLORETA power compared with EMG-contaminated and EMG-free data, for each region and each frequency band.

To test these observations statistically, a 3-way parametric ANOVA (as described in 3.2.6) was performed to compare the average power for EMG-contaminated, EMG-free, and pruned-sLORETA data over two regions and four frequency bands. The statistical analysis showed that the average power was different over each factor (signal, band, and region), and for the two-way interactions of signal∗band and signal∗region (all $p < 0.001$). Since the purpose of this section is to evaluate the effectiveness of the proposed method in removing

tonic muscle activity, post-hoc tests were only performed on the factor of signal and on the two-way interactions of signal∗band and signal∗channel to identify statistically significant differences between pairs of signals.

Table 4-2 shows the post hoc results for the factor of signal. Pruned-sLORETA is statistically different to both EMG-contaminated and EMG-free data. This means that it is reducing cranial and upper cervical muscle activity significantly, but the amount of reduction is not sufficient to reach the level of EMG-free data.

Table 4-2: Post hoc test for the factor of signal. Pruned-sLORETA is significantly different to EMG-contaminated and EMG-free.

	EMG-contaminated	Pruned-sLORETA	EMG-free
EMG-contaminated		<0.001	<0.001
Pruned-sLORETA			<0.001
EMG-free			

Table 4-3 shows the post hoc results for the interaction of signal and region. No significant difference was found between pruned-sLORETA and EMG-contaminated at central region. Hence, sLORETA pruning does not significantly reduce tonic muscle activity centrally. On the other hand, there is a statistically significant difference between pruned-sLORETA and EMG-contaminated peripherally. Hence, this pruning method is effective in reducing peripheral tonic muscle activity.

Table 4-3: Post hoc test for the interaction of signal and region. Pruned-sLORETA only reduces muscle significantly at peripheral channels.

Peripheral / Central	EMG-contaminated	Pruned-sLORETA	EMG-free
EMG-contaminated		<0.001	<0.001
Pruned-sLORETA	0.26		<0.001
EMG-free	<0.001	<0.001	

Table 4-4 shows the post hoc results for the interaction of signal and band. At the lowest frequency band, gamma1, pruned-sLORETA is not statistically different to either EMG-contaminated or EMG-free data, although EMG-contaminated and EMG-free data are statistically different. Hence this method is reducing muscle, but the amount of reduction is not significant. However, at gamma2, pruned-sLORETA is significantly different to EMG-contaminated but not different to EMG-free. This means that the amount of reduction is significant enough to reach the level of EMG-free data. At higher frequency bands, gamma3 and muscle, pruned-sLORETA is statistically different to both EMG-free and EMG-contaminated. This demonstrates that the proposed method can reduce tonic muscle contamination significantly at higher frequency bands, but the amount of reduction is not sufficient to reach the level of EMG-free data.

Table 4-4: Post hoc test for interaction of signal and band. Pruned-sLORETA is significantly different to EMG-contaminated at all bands except gamma1.

Gamma2 / Gamma1	EMG-contaminated	Pruned-sLORETA	EMG-free
EMG-contaminated		**0.01**	**<0.001**
Pruned-sLORETA	0.08		0.16
EMG-free	**0.02**	1	

Muscle / Gamma3	EMG-contaminated	Pruned-sLORETA	EMG-free
EMG-contaminated		**0.01**	**<0.001**
Pruned-sLORETA	**0.008**		**<0.001**
EMG-free	**<0.001**	**<0.001**	

To sum up, the proposed muscle reduction approach using sLORETA can significantly remove tonic muscle activity at peripheral channels, and also at higher frequency bands (above 35 Hz). However, the amount of muscle reduction is not sufficient to reach the level of EMG-free data except at the frequency range 35 to 45 Hz.

4.5 Retention of neurophysiological responses

A second requirement of a good muscle-removal method is that it should not affect desired neural activity. Hence, the effect of the proposed sLORETA muscle-removal approach in the measurement of neurophysiological responses was investigated.

4.5.1 Berger effect

Figure 4-6 shows the Berger effect as raw spectra of eyes closed (left) and left eye open (right) at an occipital channel (Oz) for dataset 1. The alpha activity (power at 8-13 Hz) has decreased in the eye open task in all signals.

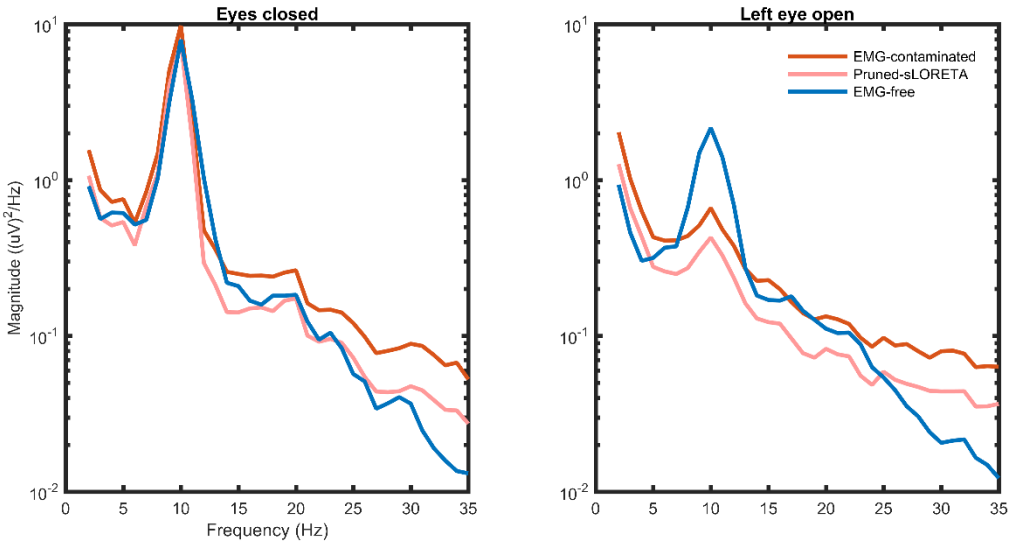

Figure 4-6: From dataset 1, average of six subjects' power spectra at Oz during eyes closed (left) and left eye open (right) tasks. The alpha activity (power at 8-13 Hz) has decreased in the eye open task in all signals. Note that the pruned spectra are processed from the EMG-contaminated data, and hence the pruned and EMG-contaminated spectra are drawn from data recorded at the same time, and a different time to the EMG-free data.

Figure 4-7 displays the same data as relative spectra of eyes closed over left eye open. It shows the expected higher power (peak) around 10 Hz for all data. Statistical analysis revealed no significant difference between EMG-contaminated, pruned and EMG-free signals ($F = 0.08$, $p = 0.91$). This is consistent with the pruning approach not affecting brain activity.

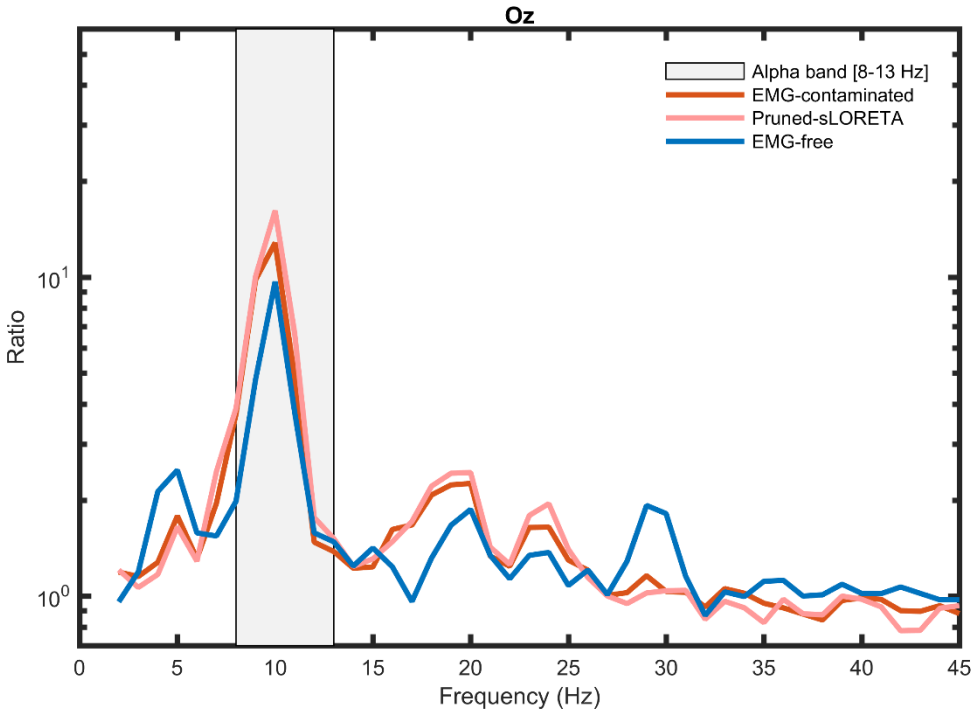

Figure 4-7: From dataset 1, mean of six subjects' relative spectra (eyes closed to left eye open) at channel Oz. The power of alpha activity in pruned-sLORETA is not significantly different to the other spectra.

4.5.2 Auditory oddball

The effect of pruning with sLORETA was evaluated on the AERPs during an oddball task. Figure 4-8 illustrates the mean AERP at channel Fz for five subjects. It is clear that the N1 and P2 components, which are responses to both low and high tones, and the P3 component, which is the response to the target high tone, have been preserved in pruning with sLORETA method. Statistical analysis showed no significant difference between any signals (N1: F = 0.24, p = 0.78; P2: F = 0.94, p = 0.40; P3: F = 0007, p = 0.99). This result shows that sLORETA pruning approach did not affect the measurement of AERPs.

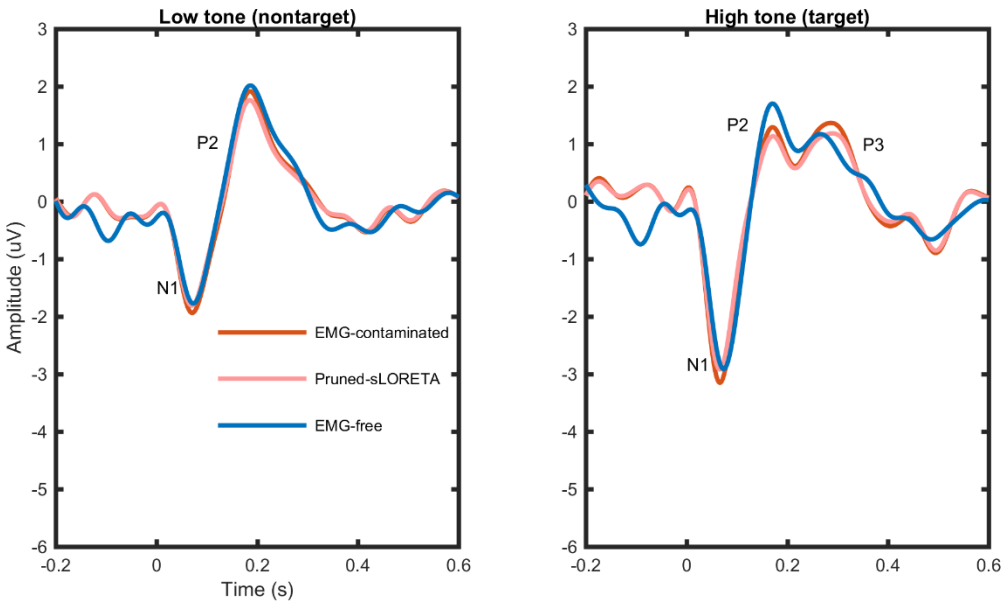

Figure 4-8: From dataset 1, averaged auditory event-related potentials (AERPs) of five subjects in an oddball task at channel Fz. The N1, P2, and P3 components to non-target low tone (left) and target high tone (right) have been preserved in the pruned-sLORETA spectra.

4.5.3 Photic stimulation

Figure 4-9 shows the mean power spectra at Oz in response to photic stimulation at 16 Hz, 40 Hz and 59 Hz. The 16 Hz VSSR is visually apparent in all spectra, whereas at 40 Hz and 59 Hz there is no clear peak in the EMG-contaminated spectrum. Three separate ANOVAs (three frequencies) revealed no significant difference between EMG-contaminated, EMG-free and pruned-sLORETA in their spectral power at 16 Hz, 40 Hz and 59 Hz (16 Hz: $F = 0.07$, $p = 0.92$; 40 Hz: $F = 1.91$, $p = 0.20$; 59 Hz: $F= 1.39$, $p = 0.28$). These results are consistent with the preservation of brain activity by the sLORETA muscle-removal approach.

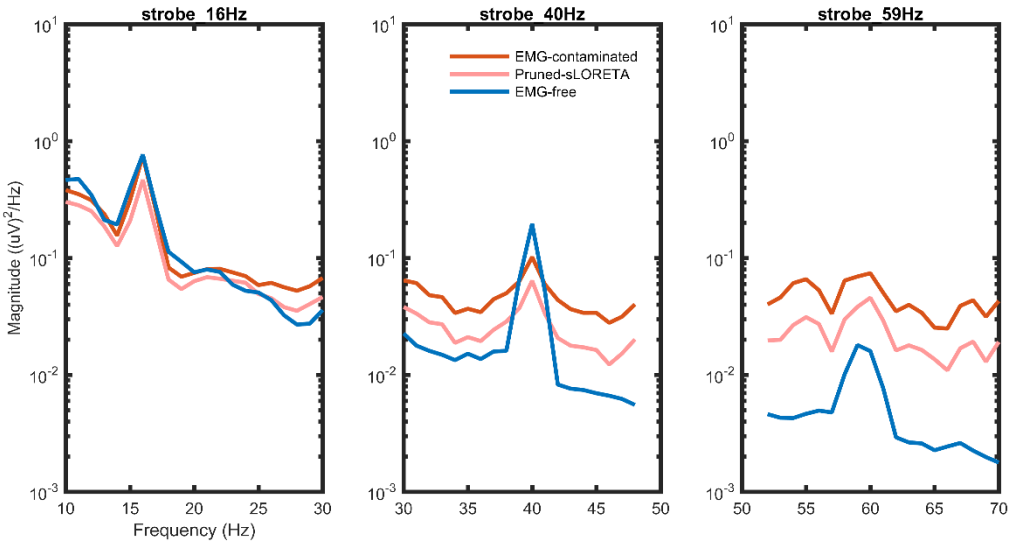

Figure 4-9: From dataset 1, mean power spectra at Oz in response to photic stimulation at 16 Hz, 40 Hz and 59 Hz. The amplitude of the steady state response is retained in pruned-sLORETA spectra.

4.5.4 Auditory stimulation

The sLORETA muscle-removal approach was applied to scalp recordings from dataset 2 to evaluate its effect on the steady state response to 40 Hz auditory stimulation.

Figure 4-10 shows the average power spectra for 13 subjects. A steady state response peak at 40 Hz is revealed in pruned-sLORETA spectra in all channels, but most obviously at T7. However, three separate ANOVAs (three channels) found no significant difference between EMG contaminated and pruned-sLORETA (T7: $F = 3.21$, $p = 0.07$; T8: $F = 1.12$, $p = 0.29$; FCz: $F = 0.93$, $p = 0.33$). These observations are consistent with the sLORETA muscle-removal approach reducing tonic muscle activity while retaining brain signal.

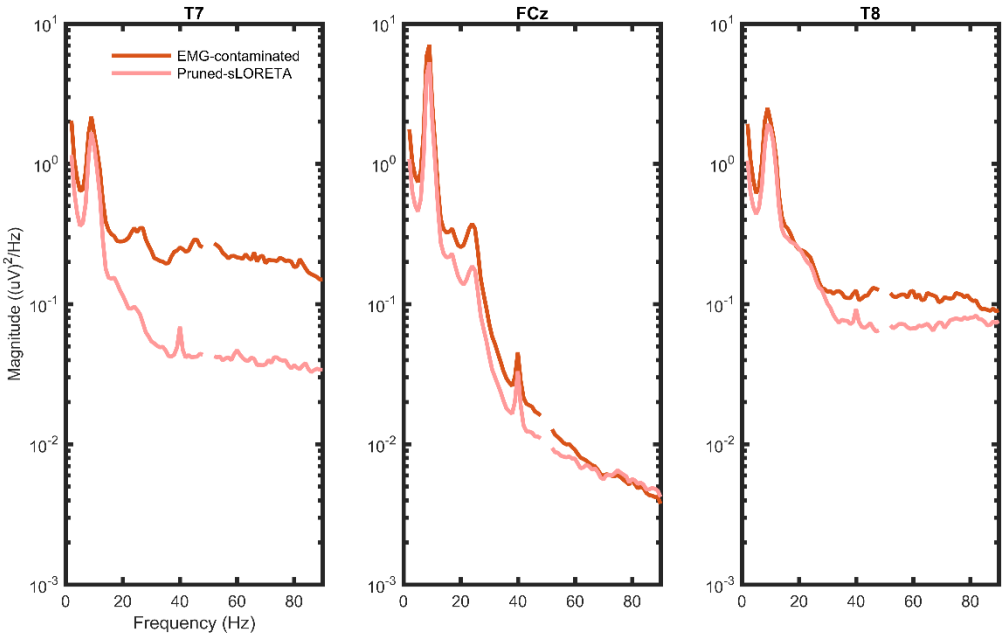

Figure 4-10: From dataset 2, mean of thirteen subjects' power spectra at T7 (left), FCz (middle), and T8 (right) in response to auditory simulation at 40 Hz. A steady state response peak is revealed in pruned-sLORETA spectra in all channels, but most obviously at T7.

4.5.5 Large sample

To investigate the effect of the sLORETA muscle-removal approach on a large sample, it was applied on dataset 3 consisting of 93 healthy participants. Participants undertook both an eyes closed and an eyes open baseline task, enabling us to test the Berger effect. Additionally, the 60 Hz refresh rate of the monitor induced a VSSR in the eyes open task. Figure 4-11 shows the raw spectra for both tasks and for both EMG-contaminated and pruned-sLORETA data. The Berger effect, i.e. reduction of alpha activity in the eyes open task, is clearly visible, whereas the 60 Hz VSSR is not. Figure 4-12 shows the relative spectra of eyes closed to eyes open, and now the Berger effect and the 60 Hz VSSR are both clearly visible.

Both the raw and relative spectra show that the Berger effect is substantially unchanged by the sLORETA pruning. Similarly, the VSSR peak is not substantially changed by the sLORETA pruning, though this is only apparent in the relative spectra.

ANOVA showed that there is no statistical difference between EMG-contaminated and pruned-sLORETA in the power of alpha band (8-13 Hz) in the relative spectra ($F = 0.13$, $p =$

0.71). Moreover, ANOVA was performed on the raw spectra from the eyes open task to compare the height of the VSSR peaks (as defined in 3.2.6) in EMG-contaminated and pruned-sLORETA data. No significant difference was found ($F = 2.08$, $p = 0.15$). These statistical results are consistent with the effectiveness of this method in retaining brain activity while reducing muscle contamination. However, in contrast to the BSS algorithms discussed in 3.3.4, this approach did not reveal a robust VSSR peak in the raw spectra, suggesting it removes less tonic muscle activity than BSS pruning algorithms at occipital channels.

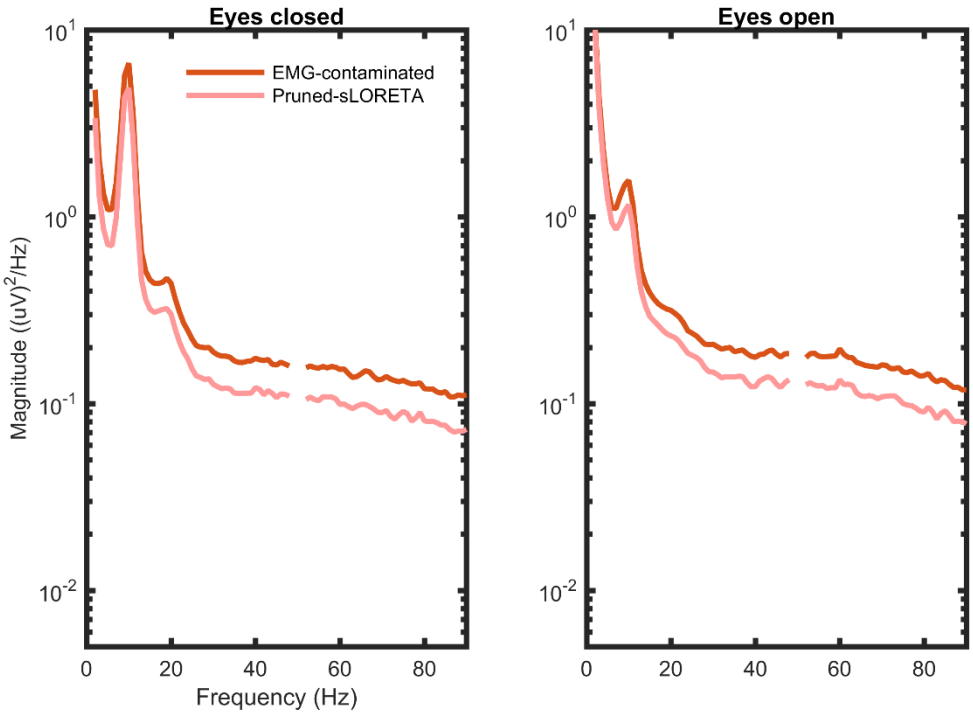

Figure 4-11: From dataset 3, mean of 93 subjects' spectra, eyes closed (left) and eyes open (right) at Oz. The power at 10 Hz, alpha activity, is decreased in the eyes open task. The expected 60 Hz VSSR peak in the eyes open task is not barely discernible in either spectra.

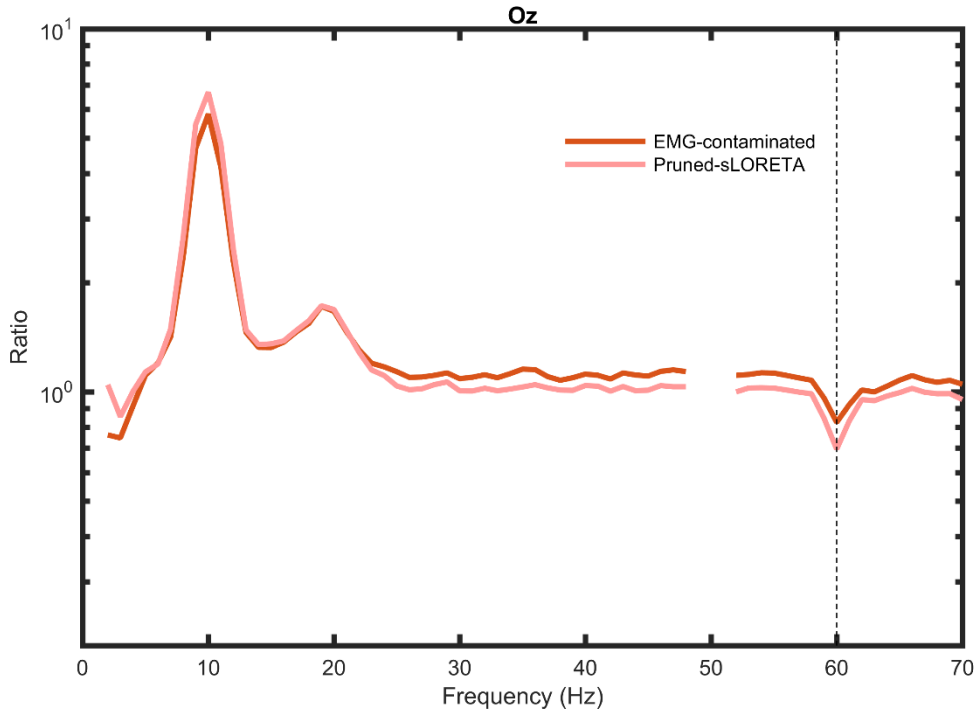

Figure 4-12: From dataset 3, averaged relative power spectra (eyes closed to eyes open) of healthy subjects at Oz. The alpha peak (Berger effect) and the VSSR at 60 Hz in the EMG-contaminated data are not significantly different to the peaks in the pruned-sLORETA data.

4.6 Discussion and conclusion

I have demonstrated that the signals from sources in the brain and in the scalp, as calculated by the beamformer method, are qualitatively similar to cognitive and muscle signals, respectively. When applied to the paralysis and pre-paralysis data, the pruning typically shows a significant but incomplete removal of muscle artefact. The pruning is most pronounced at peripheral fronto-temporal channels, less pronounced at posterior channels, and had little effect at midline frontal and central channels. Additionally, the pruning algorithm has no significant effect on the Berger effect, VSSRs and an ASSR. Hence, all results are consistent with the interpretation that the proposed pruning algorithm reduces muscle artefact but retains cognitive activity, i.e. an improvement in signal-to-noise ratio. One can ask: "Why is there still high frequency muscle activity in pruned data in comparison to EMG-free data if all the muscle sources outside the brain are discarded?" This may be the

effect of using a minimum-norm algorithm, that enables us to reconstruct scalp EEG, to estimate the dipole moment at each source location (Pascual-Marqui 2002). sLORETA estimates the activity of all sources such that their propagation to and combination at the scalp sensors (SER electrodes) has the minimum difference to the measured signals (Pascual-Marqui 2002; Sekihara, Sahani & Nagarajan 2005). This condition leads to a low spatial resolution, as implied by its name: standardized low resolution electromagnetic tomography (Jonmohamadi et al. 2014). This low spatial resolution may result in a mixture of brain and muscle activities in sources close to the boundary between brain and scalp. Moreover, this imprecise separation has been observed in high resolution beamforming analyses, using minimum variance algorithms and individual head models (Brookes et al. 2008; Huang, MX et al. 2004a; Van Veen et al. 1997). Hence, it is an inherent limitation of source analysis, rather than specific to minimum-norm beamformers. In addition, some of the muscle contamination in the scalp recording is caused by cervical muscles (trapezius and paraspinal) in the neck and shoulders (Fehrenbach & Herring 2015; Johnson et al. 1994). Since these sources are located below the extent of the head model, their contribution to the SERs is poorly modelled. This difference in modelling capability is seen in Figure 4-3, where the amount of pruning (separation between pruned-sLORETA and EMG-contaminated) is small at occipital channels in comparison to peripheral fronto-temporal channels, where the local muscles (e.g. temporalis) are located inside the head model.

While it would be expected that using a subject's own sMRI for the head model will result in better pruning, this requires the sMRI to be collected, and then processed. This is an additional expense in time and money, may require time-consuming manual segmentation to generate the head model (depending on the quality of the sMRI and the skill and experience of the analyst), and may simply not be possible in all subjects (e.g. those with pacemakers)

(Chen, Y & Ostoja-Starzewski 2010; Huang, Y et al. 2013; Kane, Balint & Sturrock 2003). Hence, it is more practicable to apply the proposed algorithm with a generic head model. This study provides quantitative evidence of the effectiveness of minimum-norm based beamformer as a tonic muscle-removal method at sensor level. The minimum-variance beamformer technique has been shown to reduce muscle and eye movement artefacts (i.e. phasic muscle artefacts) at the source level by using sMRI data (Hipp & Siegel 2013). However, previously, it was not possible to quantify the amount of artefact removal. Using a minimum-norm beamformer and the paralysis dataset, the effectiveness of the tonic muscle-removal algorithm at the sensor level can now been quantified.

Another advantage of this technique is that it can be reliably applied on any length of recorded data that captures the dynamics of the signals of interest (Gudmundsson et al. 2007; Shim, Im & Lee 2017). The disadvantages of this technique are (1) its assumption of a head model, used in the forward and inverse modelling (Neugebauer et al. 2017; Song et al. 2015), and (2) its accuracy depends on the number and spatial extent of the SER channels (Sohrabpour et al. 2015; Song et al. 2015).

Based on these results, minimum-norm beamforming can be used for reducing muscle activity at the sensor level. However, its performance is imperfect, as there is still a significant difference between pruned-sLORETA and EMG-free signals, especially at higher frequencies. As the proposed method only uses source location to prune, it contrasts with BSS pruning, which uses component signal properties (e.g. spectral gradient) to identify muscle components. Therefore, it is possible that these methods are complementary, and a combination of them may further improve the reduction of muscle contamination of SERs. Therefore, in Chapter 6, I evaluate the effectiveness of combinations of this approach with other BSS algorithms in reducing tonic cranial muscle activity, and also compare this method with the BSS-based methods described in Chapter 3

Chapter 5

A new approach to BSS-CCA method

The traditional BSS-CCA approach was not studied in Chapter 3 as it could not automatically detect and reject muscle components. In this chapter, investigations into extending BSS-CCA are described, with the aim of automating the detection and rejection of muscle-containing components to yield useful pruning. Investigations into the spectral gradient of components and how to characterise additional sources (e.g. white noise and mains noise) result in a new BSS-CCA approach called extended-CCA. Its performance in removing tonic muscle artefact while retaining neurogenic signals is examined.[3]

5.1 Limitations of traditional BSS-CCA

The standard approach to muscle reduction using CCA has some limitations. First, muscle activity, both phasic and tonic, does not have a flat spectrum like white noise (Bertrand & Tallon-Baudry 2000; Engel et al. 1992; Goncharova et al. 2003). For example, Fitzgibbon et al. (2016) have shown that the spectral power of muscle components increases with frequency in the range 7-75 Hz. Second, there is little discussion about how to choose which components are discarded. Perhaps the clearest advice is to discard components with low correlation coefficient one by one until enough muscle contamination is removed (Górriz, Lang & Ramírez 2011), where "enough" is a subjective choice. Third, the effect of

[3] The investigations, proposed extension and most of the results presented in this chapter are published in the journal paper attached in Appendix A-2. This chapter also includes a more detailed statistical analysis and expanded discussion and conclusion. The journal paper includes some extensions (e.g. comparing different thresholds) not included in the thesis as they do not contribute to the direct comparison of this approach to the alternatives considered in other chapters.

environmental noises in the recorded mixtures are ignored. Two significant sources are mains power noise and white noise, which have autocorrelation indices in the range of brain and muscle respectively. Fourth, while the effectiveness of the approach in removing phasic muscle contamination has been tested, its effect on tonic muscle has not been addressed. It has been shown that constant tonic muscle contamination of EEG is significant even in resting positions (Whitham, Emma M et al. 2007).

5.2 Investigations

First, I tested the assumptions regarding the difference between the autocorrelation of brain signals and muscle signals, and their comparison to white noise. Using the source-reconstruction approach, I selected a representative source from inside the brain volume with a negative spectral gradient (putatively brain) and a representative source within the scalp volume (putatively muscle). I calculated the correlation function of the signals from these sources and compared them with the correlation function of simulated white Gaussian noise. I also repeated this process by using two ICA-derived components, one with positive spectral gradient (putatively muscle) and one with negative spectral gradient (putatively brain). The ICA-derived components and source-reconstruction-derived sources showed substantially the same characteristics, across the majority of components and sources. Figure 5-1 shows (top) the time series of an example of each of the three signals, (lower left) their autocorrelation functions for temporal delays in the interval [-10 ms, 10 ms], and (lower right) their spectra. Note that as all data is sampled at 1 kHz, each lag corresponds to 1 ms.

Figure 5-1 shows clear differences between muscle and white noise. First, the time series of muscle contains more and higher amplitude spikes than the Gaussian white noise. Second, its spectrum is not flat, it rises in power at low frequencies to a broad peak around 120 Hz and then decreases slowly. Third, its autocorrelation function differs from white noise most noticeably at a delay of 2 ms, where muscle is negatively correlated. Hence correlation

coefficient at this delay (lag two here, as we are sampling at 1 kHz) may be useful in separating muscle from white noise. Note that exploiting this anti-correlation requires sampling at a minimum rate of 500 Hz.

The traditional BSS-CCA approach relies more on brain correlation coefficient being large in comparison to muscle correlation coefficient, rather than muscle being like white noise. Figure 5-1 clearly shows this is true at a range of small delays. Hence using correlation to separate brain from both muscle and white noise has merit. Note that traditional BSS-CCA uses lag one, which will correspond to a particular delay depending on the sampling frequency. At high sampling rates, lag one will be at a short delay, and therefore correlation coefficient will enable good separation between brain and muscle components. However, as the sampling frequency decreases, the differentiation in correlation coefficient will decrease, and hence so will its usefulness. For example, in Figure 5-1 a lag one at a sampling frequency of 100 Hz corresponds to a delay of 10 ms, and the differentiation between brain and muscle is clearly becoming difficult.

It is known that scalp recordings can be contaminated by environmental noises, particularly electrical line noise (50 Hz in Australia). To evaluate the effect of this noise, I applied the BSS-CCA approach (using a temporal delay of two samples on data sampled at 1 kHz) on previously recorded data from a separate testing study inside the Faraday cage with the 64-channel SER cap completely immersed in water (environmental noise test). The experiment was run with the same equipment at two different locations, one with visible mains power contamination and one without. Figure 5-2 shows (top) the spectra of two components (one contaminated with harmonics of the 50 Hz and other visually uncontaminated), (lower left) the canonical correlation coefficients from the contaminated recording in descending order, and (lower right) the canonical correlation coefficients from the visually uncontaminated recordings in descending order.

The presence of mains power contamination clearly increases the correlation coefficient of some components, and those components having the highest contamination were noted as also having the highest correlation index. Critically, high contamination can result in a correlation index as high as brain signals. Usefully, where there is no visually apparent contamination, all the components have correlation coefficients less than 0.19.

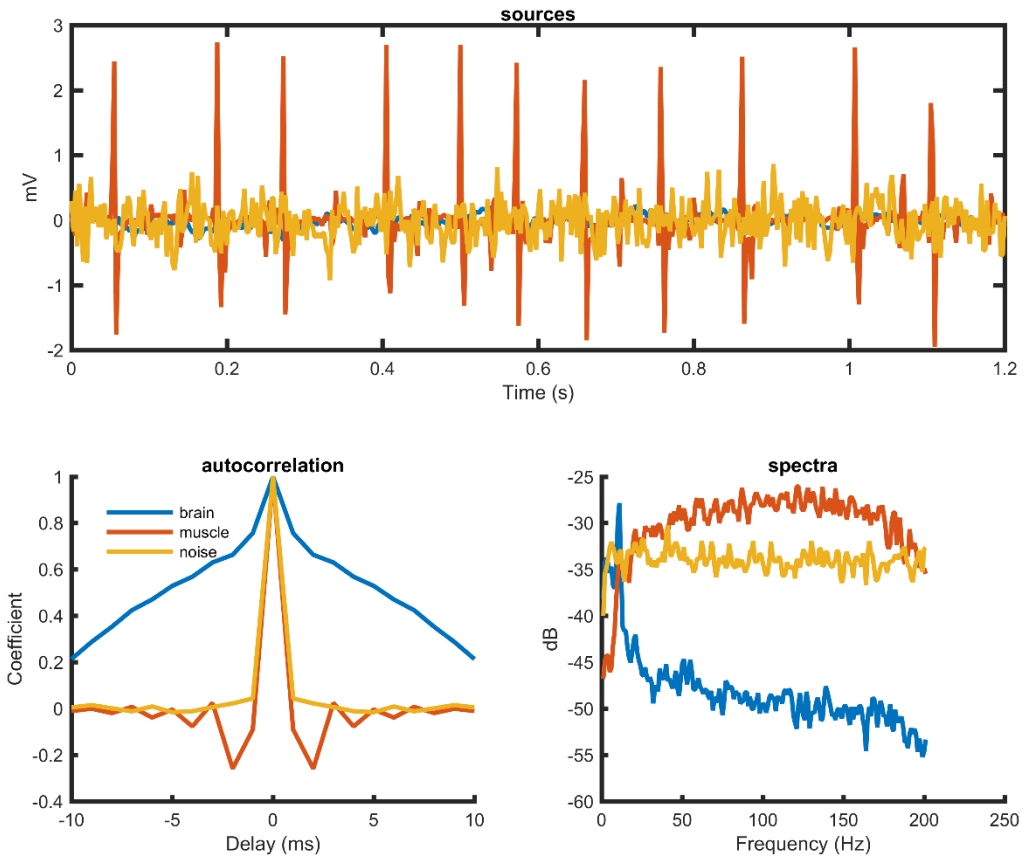

Figure 5-1: Characterisations of brain, muscle and white noise sources. (top) The time series of a putative brain source (blue) from source-reconstruction of dataset 1, a putative muscle source (orange) from source-reconstruction of dataset 1, and simulated white noise (yellow) signal; (lower left) their autocorrelation coefficients at temporal delays in the interval [-10 ms, 10 ms]; and (lower right) their spectra.

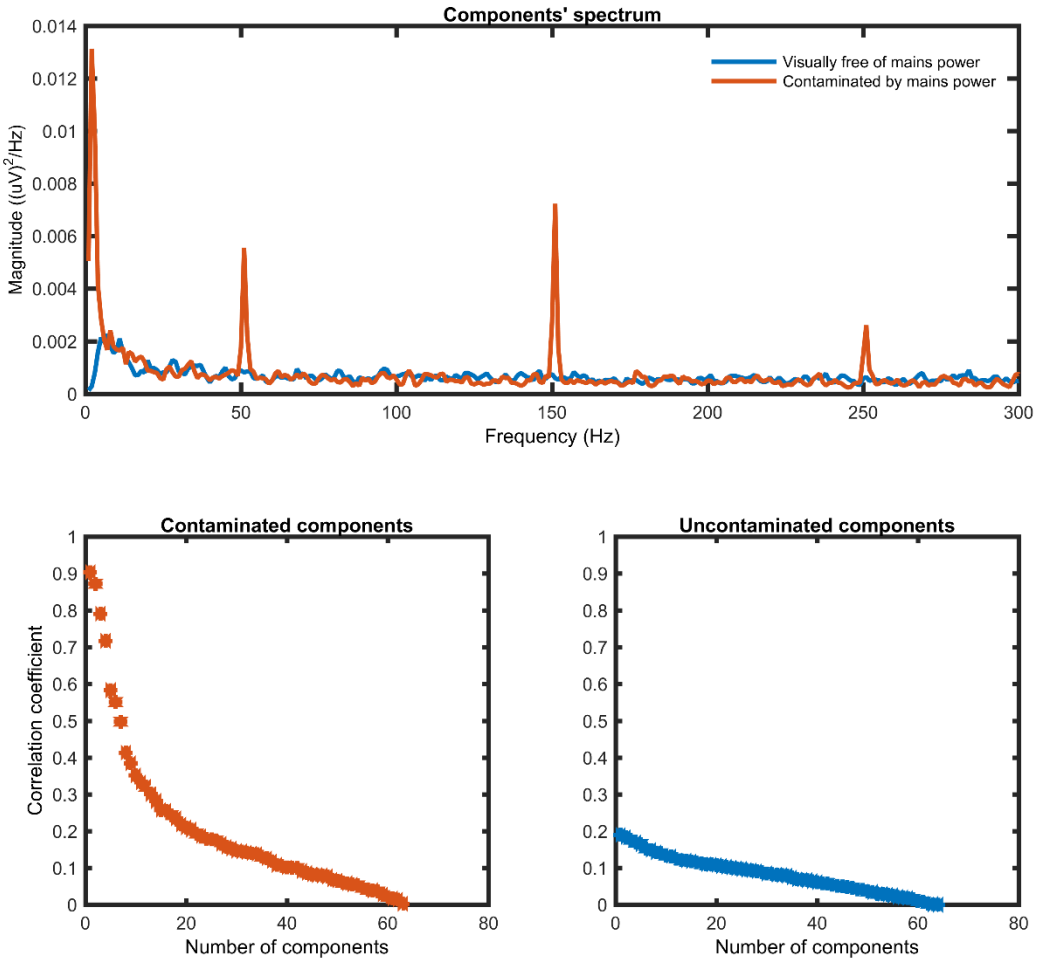

Figure 5-2: Characterisation of environmental noise components. (top) Spectrum of a component contaminated by 50 Hz harmonics (blue) and a component visually free of mains power contamination (orange); (lower left) correlation coefficients of contaminated components; (lower right) correlation coefficients of components not visually contaminated by mains power.

5.3 Extended BSS-CCA method

The traditional BSS-CCA approach identifies components as muscle simply by their correlation coefficient being low. The previous section has shown that mains power signals and white noise complicate this approach, and that extending the approach may give better results. Two possible extensions are to use correlation at lag two, or to use spectral gradient in the range 7-75 Hz (Fitzgibbon, S et al. 2016) as a discriminator for selecting components. Note I have chosen to use correlation at lag 2, which corresponds to a delay of 2 ms at my sampling rate of 1 kHz, to maximise the possibility of separating white noise, muscle and brain from each other, not simply separating brain from muscle and white noise.

First, I applied the BSS-CCA method on dataset 1 (paralysis dataset) to compare the correlation coefficients and spectral gradient of a set of components from scalp recordings containing brain, muscle, and noise (pre-paralysis or EMG-contaminated data) to another set from recordings without muscle (paralysis or EMG-free data).

Figure 5-3 is a scatterplot of the correlation coefficients against spectral gradients for the two sets of components. It shows an inverse relationship, where components with the highest correlation coefficients have the lowest gradients (very negative), consistent with expectations of a component of neural origin. Similarly, myogenic components should have low correlation coefficients and high (positive) spectral gradients. However, as most components have negative spectral gradients, this implies that there are few components that are purely myogenic. The smooth spread of components from the two extremes also suggests most components are mixtures of brain, muscle and noise. Clearly, simply thresholding components on the basis of their correlation coefficient will remove both myogenic and neurogenic signals, and a more nuanced approach would be preferable.

Comparing the EMG-contaminated and the EMG-free data, there is overlap at high (> 0.9) and low (< 0.1) correlation coefficients, and separation between the two in the mid-range (between 0.2 and 0.7). The inclusion of significant myogenic signal power in the EMG-contaminated data causes the spectral gradients of components to increase relative to the EMG-free data, most noticeably in the mid-range. At high correlation coefficients, it is likely both data have components that are substantially neurogenic. At low correlation coefficients, it is likely both data have components that are substantially white noise. This result, in combination with the environmental noise test, suggests that components with a correlation coefficient less than 0.19 are substantially environmental noise and can be discarded. Figure 5-3 shows that EMG-free and EMG-contaminated data both cover the same range of correlation coefficients and spectral gradients, making it difficult to discriminate components

that are substantially muscle. Figure 5-4 (left) shows the histogram of spectral gradients for all components, which also illustrates this point and demonstrates that a simple thresholding is problematic. However, if components with a correlation coefficient of less than 0.19 are first removed, a repeat of the histogram of spectral gradient without those components can be seen in Figure 5-4 (right). It shows that now there is a difference in extent between the EMG-contaminated and EMG-free data, and that thresholding on spectral gradient is likely to result in a reduction of muscle contamination.

The choice of threshold is not simple, as I previously concluded that almost no components are purely myogenic. Hence varying the threshold would vary both the amount of myogenic signal removed as well as the amount of neurogenic signal removed. Figure 5-4 (right) suggests a threshold set to the maximum gradient of EMG-free components (-0.48) should theoretically remove only those components that are substantially myogenic.

The proposed artefact-removal algorithm therefore has three stages:

1. Components with a correlation coefficient less than 0.19 are discarded.
2. Remaining components with a spectral gradient greater than -0.48 are discarded.
3. Retained components are projected back to produce pruned SER.

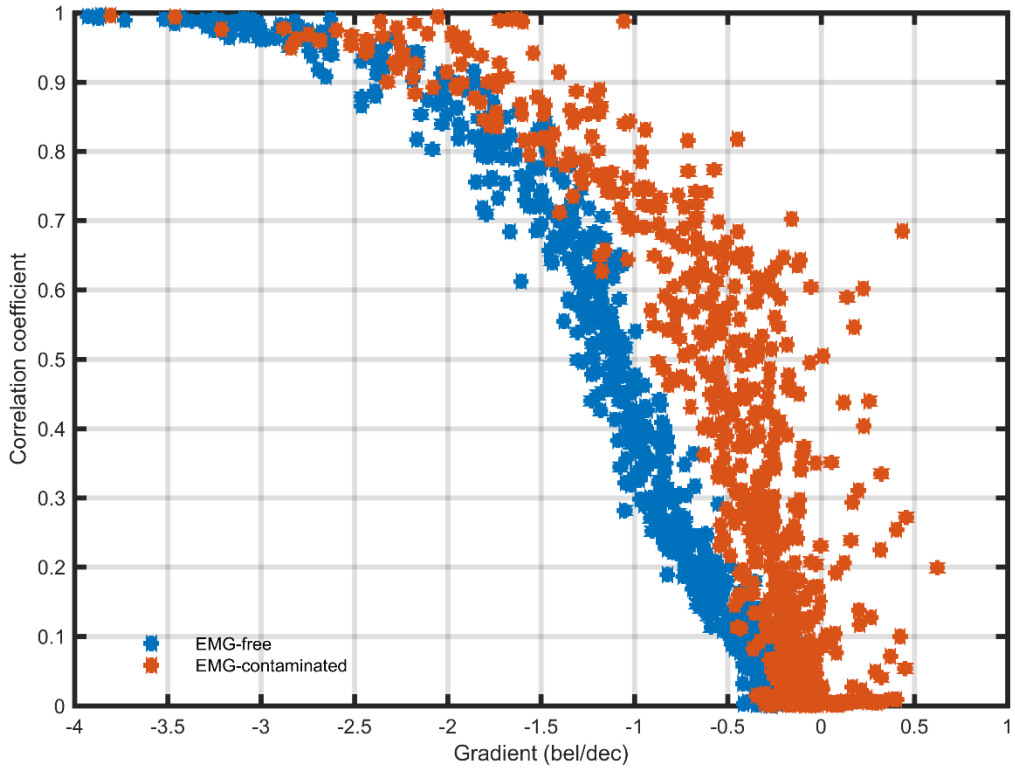

Figure 5-3: Scatterplot of correlation coefficient and spectral gradient for both EMG-contaminated components and EMG-free components.

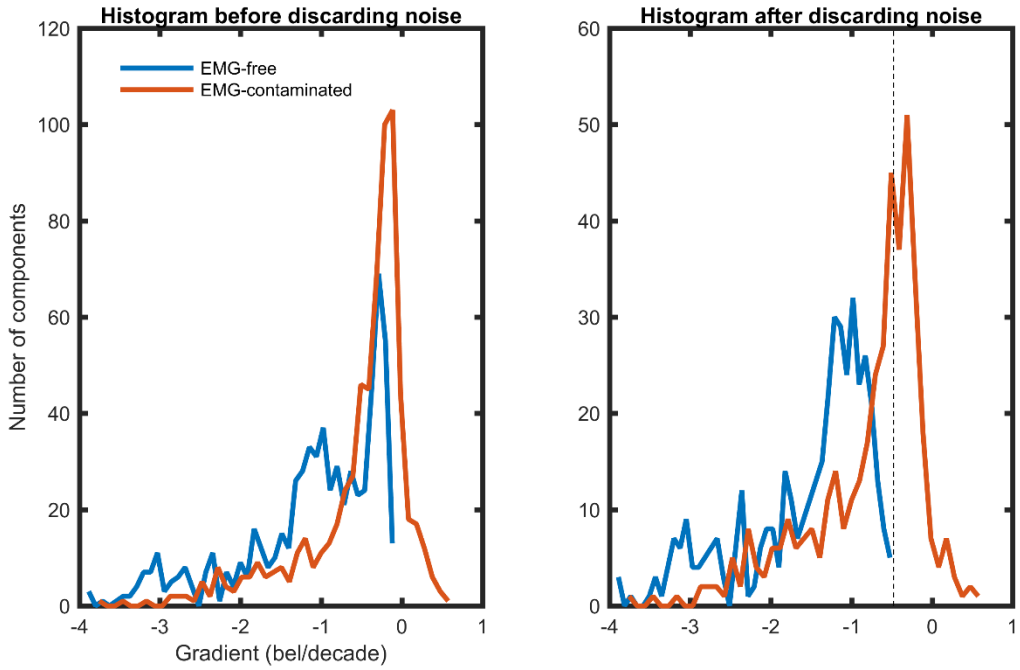

Figure 5-4: From dataset 1, histogram of the spectral gradient of components from EMG-contaminated data (blue) and EMG-free data (orange). The histogram on the left is before discarding noise components, while on the right is after discarding noise components. The right histogram also shows the proposed threshold (grey dashed line).

5.4 Results

The proposed extended-CCA method was applied on all three datasets to evaluate its effectiveness in the automated removal cranial muscle activity while retaining brain activity. Signals pruned by this approach are called pruned-CCA. The effectiveness of this proposed method is compared to other BSS algorithms in Chapter 6.

5.4.1 Tonic muscle activity removal

Figure 5-5 compares the spectra of EMG-contaminated data, pruned-CCA data, and EMG-free data in nine channels spread evenly across the head.

I observe that the extended-CCA approach reduces muscle power from low frequencies, about 20 Hz. However, there is still muscle contamination compared to EMG-free data. Tonic muscle reduction is greater at peripheral channels.

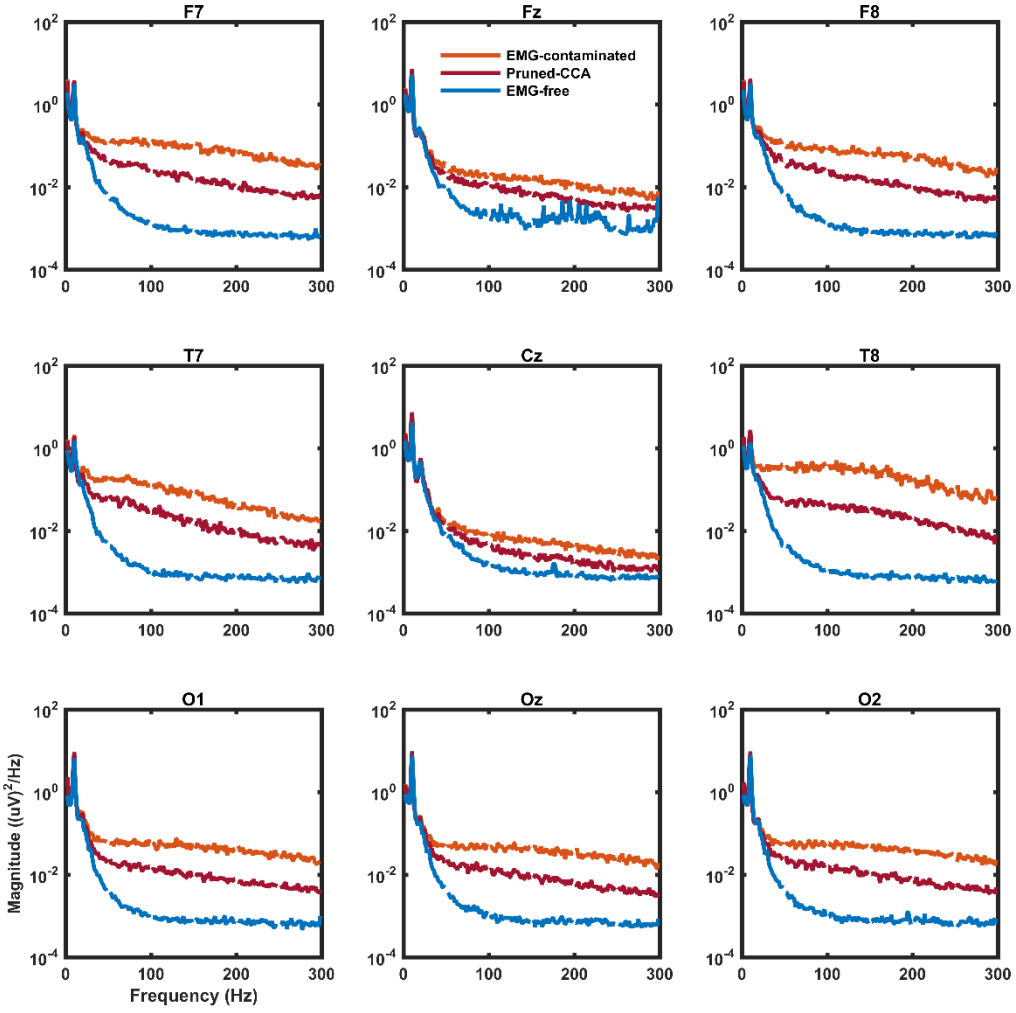

Figure 5-5: From dataset 1, mean of six subjects' power spectra during baseline eyes closed task. Using the extended-CCA method, muscle reduction starts at frequencies as low as 20 Hz, but there is still muscle contamination compared to EMG-free data.

Figure 5-6 displays the topographic maps of relative spectra of EMG-contaminated to EMG-free, and pruned-CCA to EMG-free in the four frequency bands of interest. Although the extended-CCA algorithm did not completely remove muscle activity at higher frequencies, it reduced muscle contamination, especially at peripheral channels. For example, at 102-198 Hz (muscle band), the average power at temporal channels of EMG-contaminated spectra was about 300 times greater than EMG-free spectral power, but after pruning with extended-CCA method this value decreased to about 30 times.

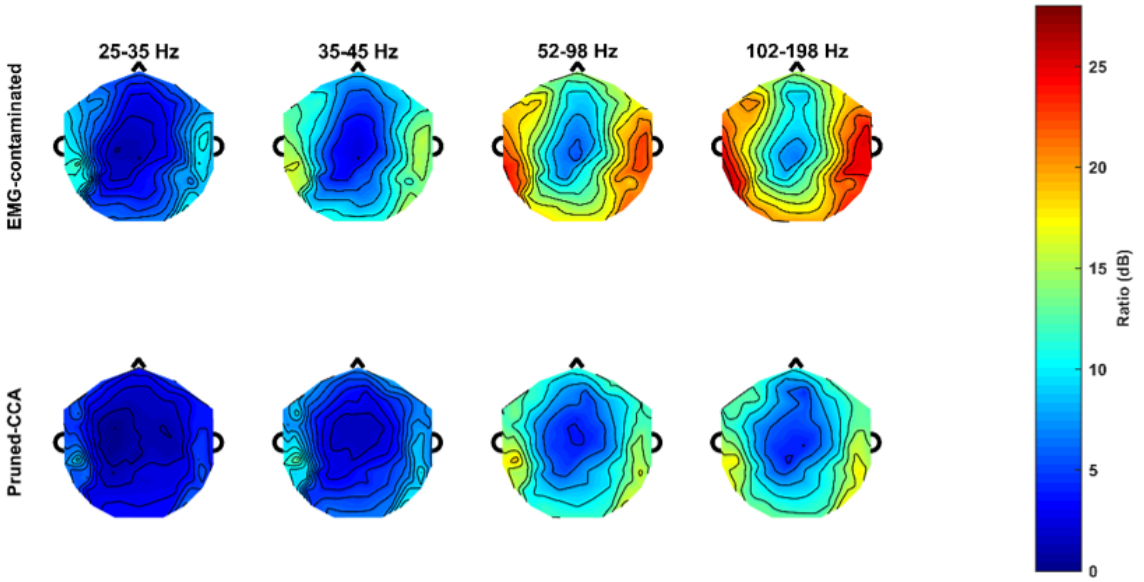

Figure 5-6: From dataset 1, topographic maps of relative spectra in EMG-contaminated/EMG-free (first row), and pruned-CCA/EMG-free (second row) in different frequency bands (columns). The extended-CCA method reduces muscle contamination, especially at peripheral channels. Each topography is looking down on the head, with ears and nose indicated, conforming to the montage in Figure 2-4.

Two groups of channels were considered: central channels (Fz, Cz, C1, C2, and Oz), and peripheral channels (T7, T8, F7, F8, O1, and O2). The average power spectra of all signals in each group of channels and each frequency band were calculated. Figure 5-7 compares the mean and standard deviation of six subjects' power in each frequency band within each region. Visually, the proposed extended-CCA method is partially effective in reducing tonic muscle contamination more peripherally and in higher frequency bands.

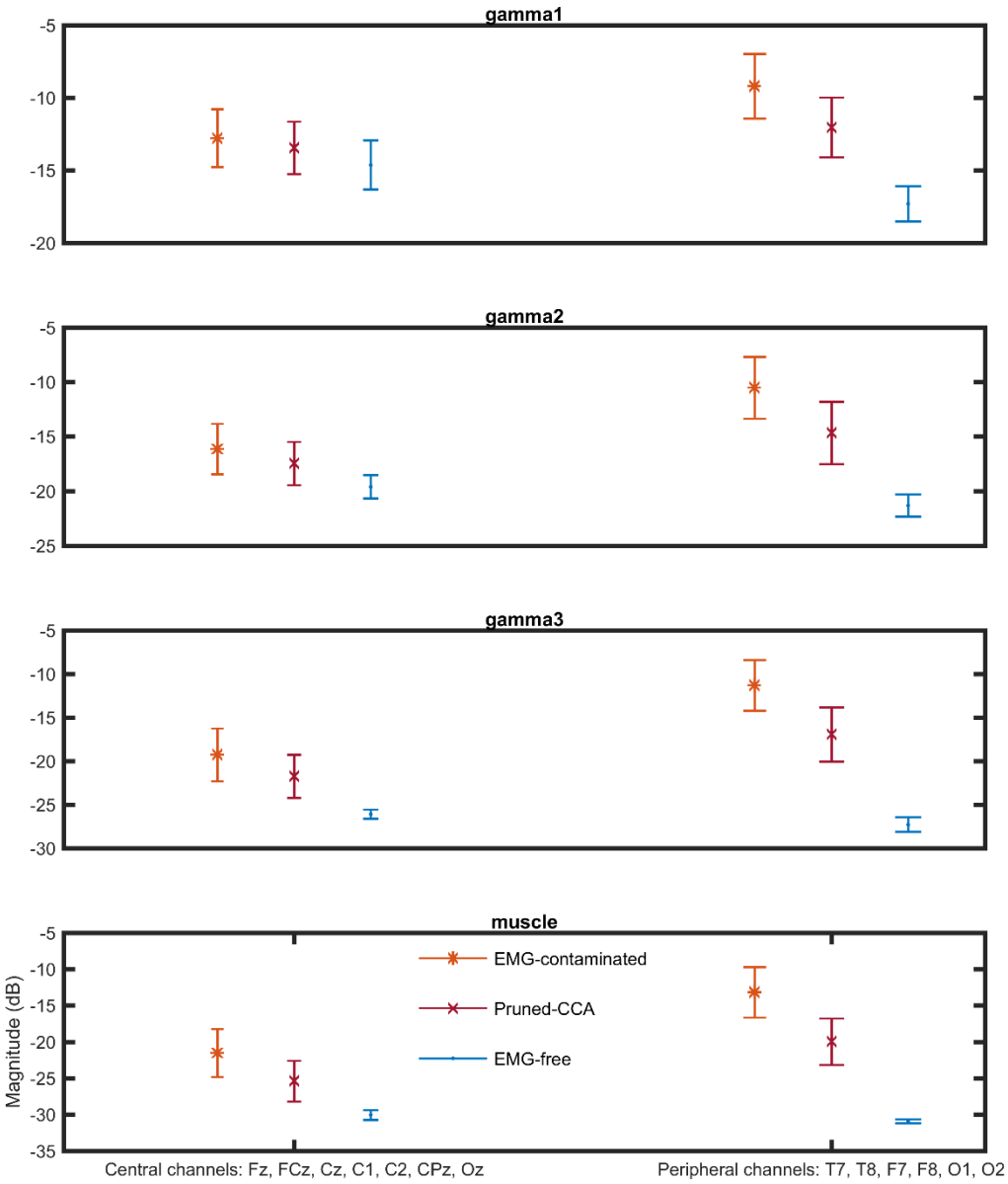

Figure 5-7: From dataset 1, mean and standard deviation of pruned-CCA power compared with EMG-contaminated and EMG-free power within each region and each frequency band.

To test these observations statistically, a 3-way parametric ANOVA was performed to compare the average power for EMG-contaminated, EMG-free, and pruned-CCA over two regions and four frequency bands. The statistical analysis showed that the average power was significantly different over each factor (signal, band, and region), and each two-way interaction of signal∗band, signal∗region, and band∗region (all $p < 0.001$). Since the purpose of this section is to evaluate the effectiveness of extended-CCA method in removing tonic

muscle activity, post-hoc tests were only performed on the factor of signal and on the two-way interactions of signal∗band and signal∗region to identify statistically significant differences between pairs of signals.

Table 5-1 shows the post hoc results for the factor of signal. Pruned-CCA is statistically different to both EMG-contaminated and EMG-free. This means that extended-CCA is reducing cranial muscle activity significantly but the amount of reduction is not sufficient to reach the level of EMG-free data.

Table 5-1: Post hoc test for the factor of signal. Pruned-CCA is significantly different to EMG-contaminated and EMG-free.

	EMG-contaminated	Pruned-CCA	EMG-free
EMG-contaminated		<0.001	<0.001
Pruned-CCA			<0.001
EMG-free			

Table 5-2 shows the post hoc results for the interaction of signal and region. There is a statistically significant difference between pruned-CCA and EMG-contaminated both peripherally and centrally. However, the significant difference between pruned-CCA and EMG-free means that the amount of muscle reduction is not sufficient to reach the level of EMG-free.

Table 5-2: Post hoc test for the interaction of signal and region. Pruned-CCA significantly reduces tonic muscle activity both at central and peripheral channels.

Central \ Peripheral	EMG-contaminated	Pruned-CCA	EMG-free
EMG-contaminated		<0.001	<0.001
Pruned-CCA	0.008		<0.001
EMG-free	<0.001	<0.001	

Table 5-3 shows the post hoc results for the interaction of signal and band. At the lowest frequency band, gamma1, pruned-CCA is not significantly different to either EMG-contaminated or EMG-free, although EMG-contaminated and EMG-free are significantly different. Hence this method is reducing muscle, but the amount of reduction is not significant. Similarly, at the gamma2 band, pruned-CCA is not significantly different to EMG-contaminated. This means that the method is not effective in reducing tonic muscle activity at gamma2. At higher frequency bands, gamma3 and muscle, pruned-CCA is statistically significantly different to both EMG-free and EMG-contaminated. This demonstrates that this method can reduce tonic muscle activity significantly at higher frequency bands, but the amount of reduction is not sufficient to reach the level of EMG-free data.

Table 5-3: Post hoc test for interaction of signal and band. Pruned-CCA is significantly different to EMG-contaminated at gamma3 and muscle bands.

Gamma2 / Gamma1	EMG-contaminated	Pruned-CCA	EMG-free
EMG-contaminated		0.11	**<0.001**
Pruned-CCA	0.79		**0.002**
EMG-free	**0.007**	0.62	

Muscle / Gamma3	EMG-contaminated	Pruned-CCA	EMG-free
EMG-contaminated		**0.001**	**<0.001**
Pruned-CCA	**0.001**		**<0.001**
EMG-free	**<0.001**	**<0.001**	

To sum up, the extended-CCA method can significantly remove tonic muscle activity both peripherally and centrally, and at higher frequency bands (above 45 Hz). However, the amount of muscle reduction is not sufficient to reach the level of EMG-free data.

5.4.2 Retention of neurophysiological responses

Another requirement of a good muscle-removal method is that it should not affect desired neurophysiological responses. Hence, the effect of the extended-CCA method on neurophysiological responses was investigated.

5.4.2.1 Berger effect

Figure 5-8 shows the Berger effect as raw spectra of eyes closed (left) and left eye open (right) at an occipital channel (Oz) for dataset 1. As expected, the alpha activity (power at 8-13 Hz) has decreased in the eye open task compared to the eyes closed task in all cases. Additionally, the pruned-CCA and EMG-contaminated spectra are visually indistinguishable below 15 Hz.

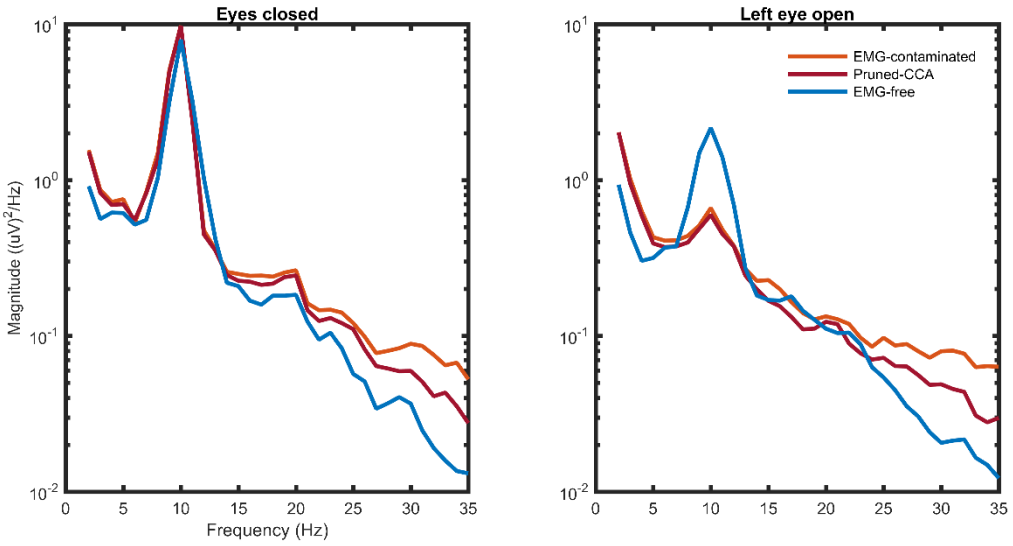

Figure 5-8: From dataset 1, average of six subjects' power spectra at Oz during eyes closed (left) and left eye open (right) tasks. The alpha activity (power at 8-13 Hz) has decreased in the eye open task in all signals.

Figure 5-9 shows the same data as relative spectra of eyes closed over left eye open. It illustrates the expected higher power (peak) around 10 Hz for all data. Statistical analysis revealed no significant difference in peak height between EMG-contaminated, pruned-CCA and EMG-free data ($F = 0.07$, $p = 0.92$).

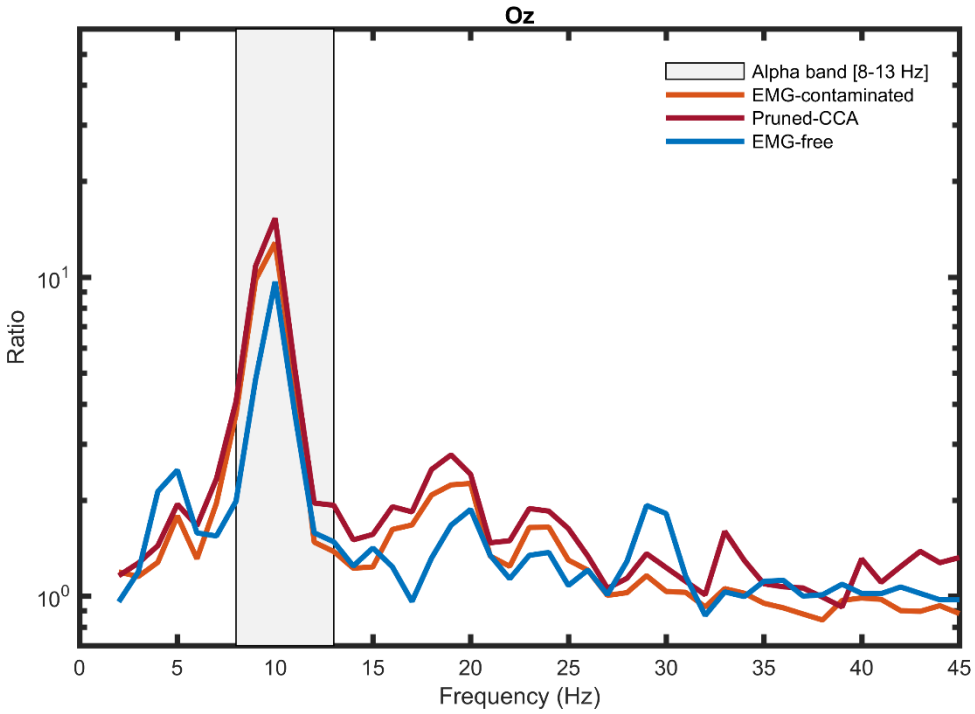

Figure 5-9: From dataset 1, mean of six subjects' relative spectra (eyes closed to eyes open) at channel Oz. The power of alpha activity in pruned-CCA is not significantly different to any other spectrum.

5.4.2.2 Auditory oddball

The effect of pruning with extended-CCA was evaluated on the event-related potentials during an auditory oddball task. Figure 5-10 illustrates mean AERP at channel Fz for five subjects. It is clear that the N1 and P2 components, which are responses to any tone, and the P3 component, which is the response to the target high tone, have been preserved in pruning with the extended-CCA method. Statistical analysis showed no significant difference between any signals (N1: $F = 0.26$, $p = 0.76$; P2: $F = 0.39$, $p = 0.67$; P3: $F = 0.005$, $p = 0.99$). These results show that the extended-CCA pruning approach did not affect the measurement of AERPs.

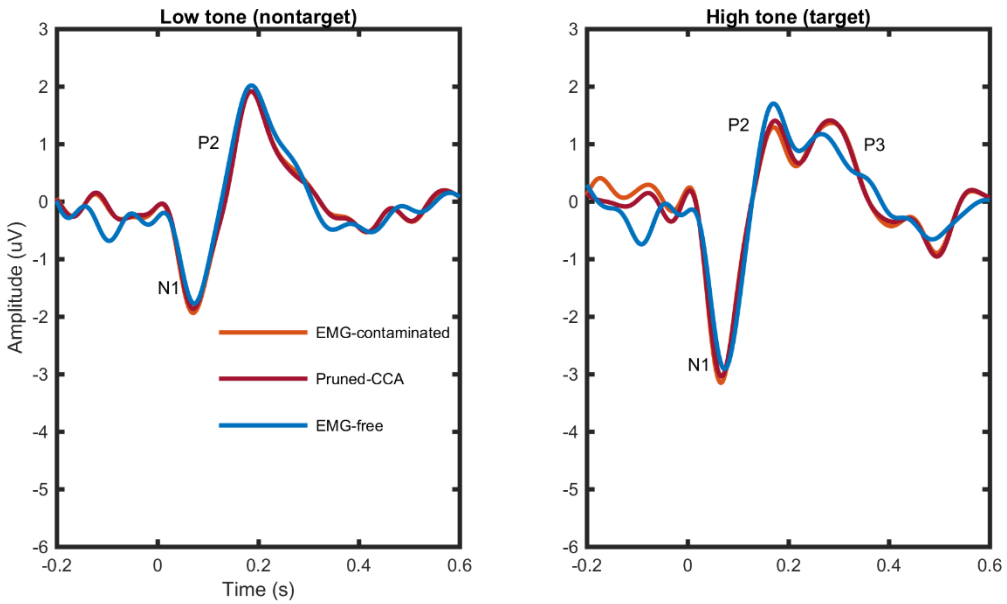

Figure 5-10: From dataset 1, averaged auditory event-related potentials (AERPs) of five subjects in an oddball task at channel Fz. The N1, P2, and P3 components to the non-target low tone (left) and target high tone (right) have been preserved in pruned-CCA.

5.4.2.3 Photic stimulation

Figure 5-11 shows the mean power spectra at Oz in response to photic stimulation at 16 Hz, 40 Hz and 59 Hz. The 16 Hz VSSR is visually apparent in all spectra, whereas at 40 Hz and 59 Hz there is no clear peak in the EMG-contaminated spectra. Three separate ANOVAs (three frequencies) revealed no significant difference between EMG-contaminated, EMG-free and pruned-CCA in their spectral power at 16 Hz, 40 Hz and 59 Hz (16 Hz: $F = 0.16$, $p = 0.84$; 40 Hz: $F = 1.73$, $p = 0.21$; 59 Hz: $F= 1.38$, $p = 0.28$). These results are consistent with preservation of brain activity in muscle pruning using the extended-CCA method.

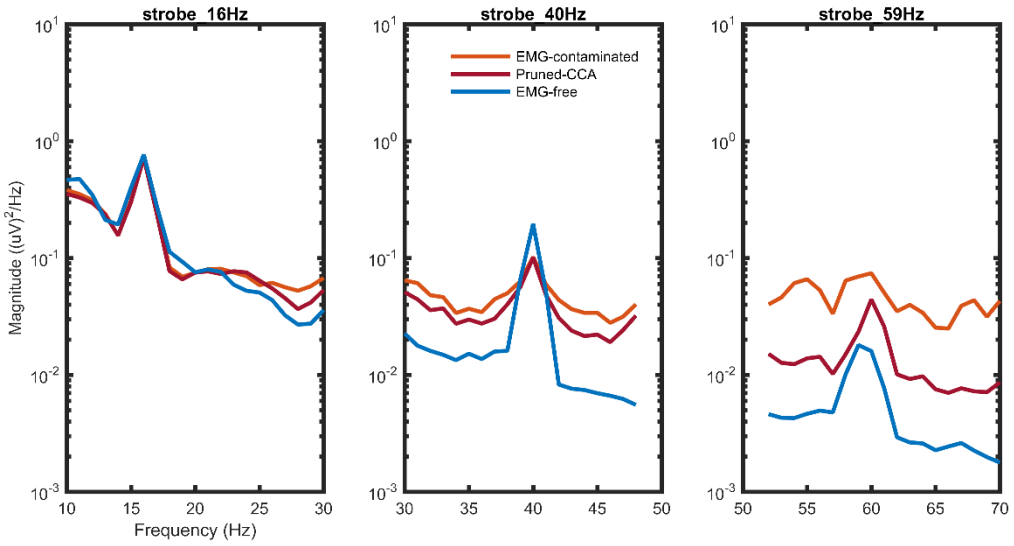

Figure 5-11: From dataset 1, mean power spectra at Oz in response to photic stimulation at 16 Hz, 40 Hz and 59 Hz. The amplitude of the steady state response is retained in the pruned-CCA spectra.

5.4.2.4 Auditory stimulation

The extended-CCA approach was applied to SERs from dataset 2 to evaluate its effect on the steady state response to 40 Hz auditory stimulation.

Figure 5-12 shows the average power spectra for 13 subjects at three channels. The steady state response peak is clear in FCz, perhaps visible in T8, and not apparent in T7. A 60 Hz peak is apparent at FCz, and at T8 after pruning, likely a screen refresh VSSR due to some participants opening their eyes during the task. Three separate ANOVAs (three channels) revealed no significant difference in peak height between EMG contaminated and pruned-CCA (T7: $F = 0.13$, $p = 0.71$; T8: $F = 0.55$, $p = 0.46$; FCz: $F = 0.01$, $p = 0.92$). These observations are consistent with the extended-CCA method reducing tonic muscle activity while retaining brain neurophysiological responses.

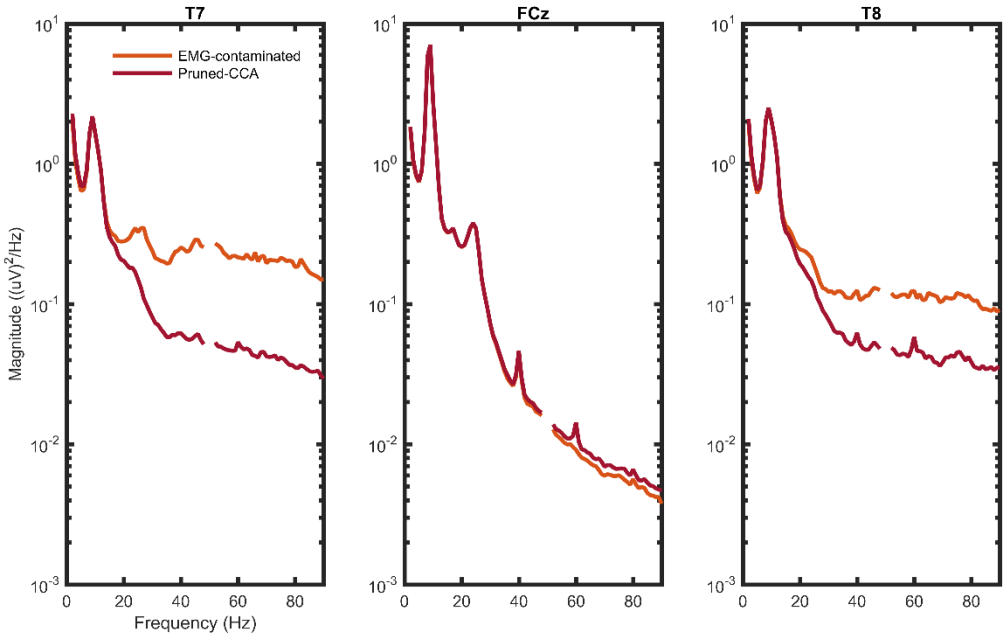

Figure 5-12: From dataset 2, mean of thirteen subjects' power spectra at T7 (left), FCz (middle), and T8 (right) in response to auditory simulation at 40 Hz. The steady state response peak is visible at FCz, perhaps visible at T8, but not apparent at T7.

5.4.3 Large sample

To investigate the effect of the extended-CCA method on a large sample, it was applied to dataset 3 consisting of a large number of healthy participants. Figure 5-13 shows the Berger effect, reduction of alpha activity in eyes open task, and the VSSR caused by the 60 Hz refresh rate of the monitor, a peak at 60 Hz in the eyes open task. The 60 Hz VSSR peak is disclosed in eyes open task in the pruned-CCA spectrum. Figure 5-14 shows the relative spectra of eyes closed to eyes open to illustrate the Berger effect and 60 Hz VSSR more clearly. The Berger effect is substantially unchanged by the extended-CCA pruning, and the expected VSSR peak is enhanced by pruning.

ANOVA analysis showed that there is no statistically significant difference between EMG-contaminated and pruned-CCA in the power of alpha band (8-13 Hz) in relative spectra ($F = 0.75$, $p = 0.38$). However, there is a significant difference in the VSSR peak height in the eyes open task between EMG-contaminated and pruned-CCA ($F = 8.42$, $p = 0.004$).

These results are consistent with the extended-CCA method reducing tonic muscle contamination while keeping or disclosing brain neurophysiological responses.

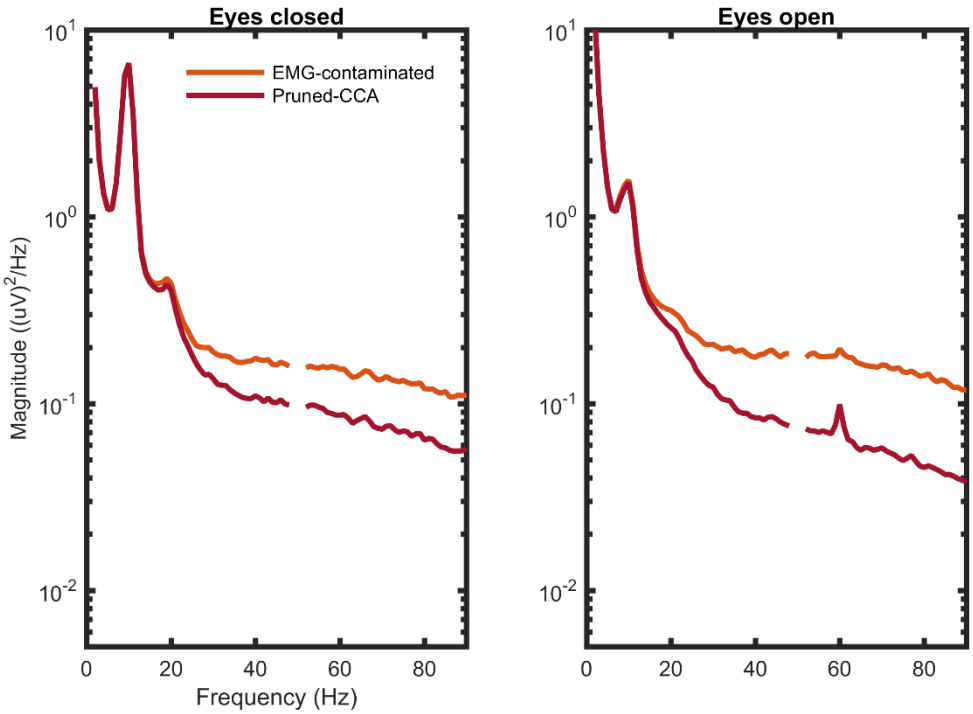

Figure 5-13: From dataset 3, mean of 93 subjects' spectra (eyes closed and eyes open) at Oz. The power at 10 Hz, alpha activity, is decreased in the eyes open task. The 60 Hz VSSR peak is disclosed in the eyes open task after pruning.

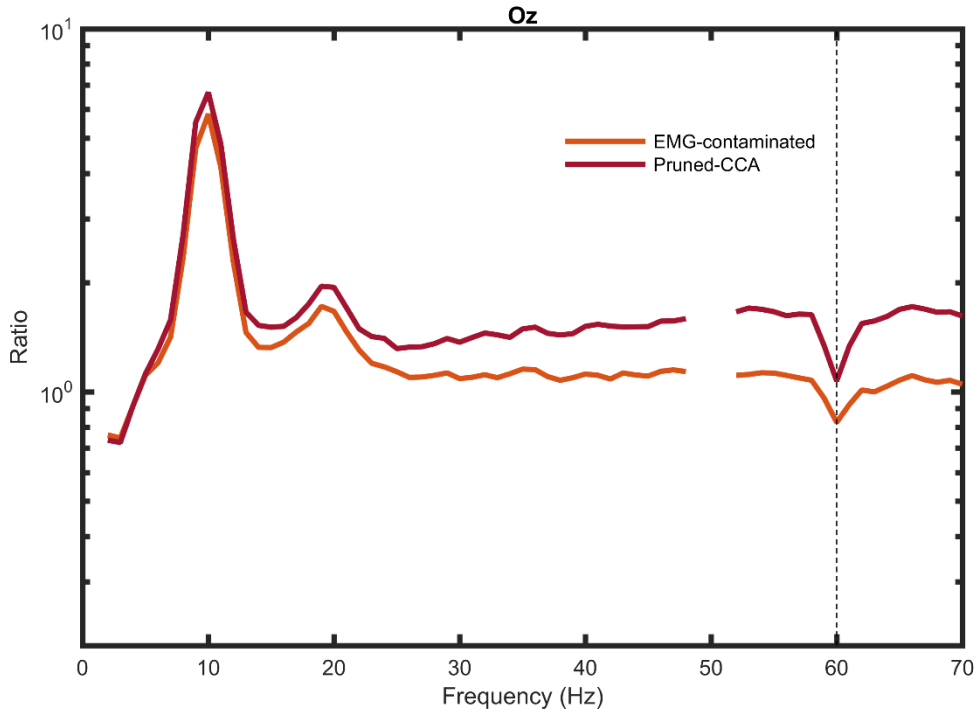

Figure 5-14: From dataset 3, averaged relative power spectra (eyes closed to eyes open) of 93 healthy subjects at Oz. The Berger effect is substantially unchanged by pruning, and the expected VSSR peak is enhanced by pruning.

5.5 Discussion and conclusion

I have proposed a muscle-removal approach that combines and extends traditional BSS-CCA and the spectral gradient of the derived components. This extended method is different to traditional BSS-CCA, which was first introduced by De Clercq et al. (2006), in several ways. Firstly, it considers other sources, such as mains power and white noise, and addresses the difficulty of the distribution of their correlation coefficients overlapping those of brain and/or muscle. Secondly, the extended-CCA method relies on a time delay (2 ms) rather than a number of lags (one) in traditional BSS-CCA, which provides more reliable separation between muscle, brain, and white noise regardless of sampling rate. Thirdly, the new method exploits both spectral gradient and correlation coefficient to classify muscle components. Fourthly, the new method is explicitly automated, as the unique dataset of paralysed subjects (EMG-free) provides clear evidence for the choice of thresholds.

Many studies have tested the effectiveness of the traditional BSS-CCA method in removing phasic muscle contamination from SERs (De Clercq et al. 2006; Gao, Zheng & Wang 2010; Hallez et al. 2009; Safieddine et al. 2012; Vergult et al. 2007). They applied the traditional BSS-CCA method to the SERs of subjects performing tasks requiring voluntary muscle contraction, such as frowning and biting (phasic muscle activity), or to the ictal muscle artefacts in SERs from subjects suffering from epilepsy (non-voluntary muscle contractions[4]). By comparing the results of pruning to a baseline relaxed condition, they have claimed that the traditional BSS-CCA method has good performance in removing muscle activity. Therefore, they have evaluated the effectiveness of BSS-CCA method only in removing **phasic** muscle activity, without considering tonic muscle activity or the retention of brain neurophysiological responses.

Hence, these studies are not directly comparable with the studies presented here based on the proposed extended-CCA method. I have used data from baseline or relaxed states, hence have quantified the effectiveness of the extended method in removing **tonic** muscle activity and in retaining brain neurophysiological responses. Therefore, I have provided a more thorough testing of the evaluation of the extended-CCA method.

There is a presumption that the proposed extended-CCA method would achieve significant muscle reduction when it is applied to SERs that contain phasic muscle contamination. This conclusion is based on preliminary results from an ongoing study. Figure 5-15 shows the histogram of the spectral gradient of components after applying BSS-CCA to SERs from various tasks. Tasks involving voluntary muscle contractions have histograms skewed to the right compared to baseline tasks, i.e. there are more components with larger spectral gradients during phasic muscle tasks. So, it would be expected that the extended-CCA method applied

[4] Muscle contractions during the seizure in people suffering from epilepsy is involuntary, but the amplitude of muscle activity is high enough to be treated as phasic muscle activity.

to SERs with phasic muscle should achieve at least as good a result as when applied to SERs including only tonic muscle activity. This should be tested thoroughly by conducting more experiments and investigation. It is, however, beyond the scope of this thesis, which is on quantitating the cranial and upper cervical **tonic** muscle activity.

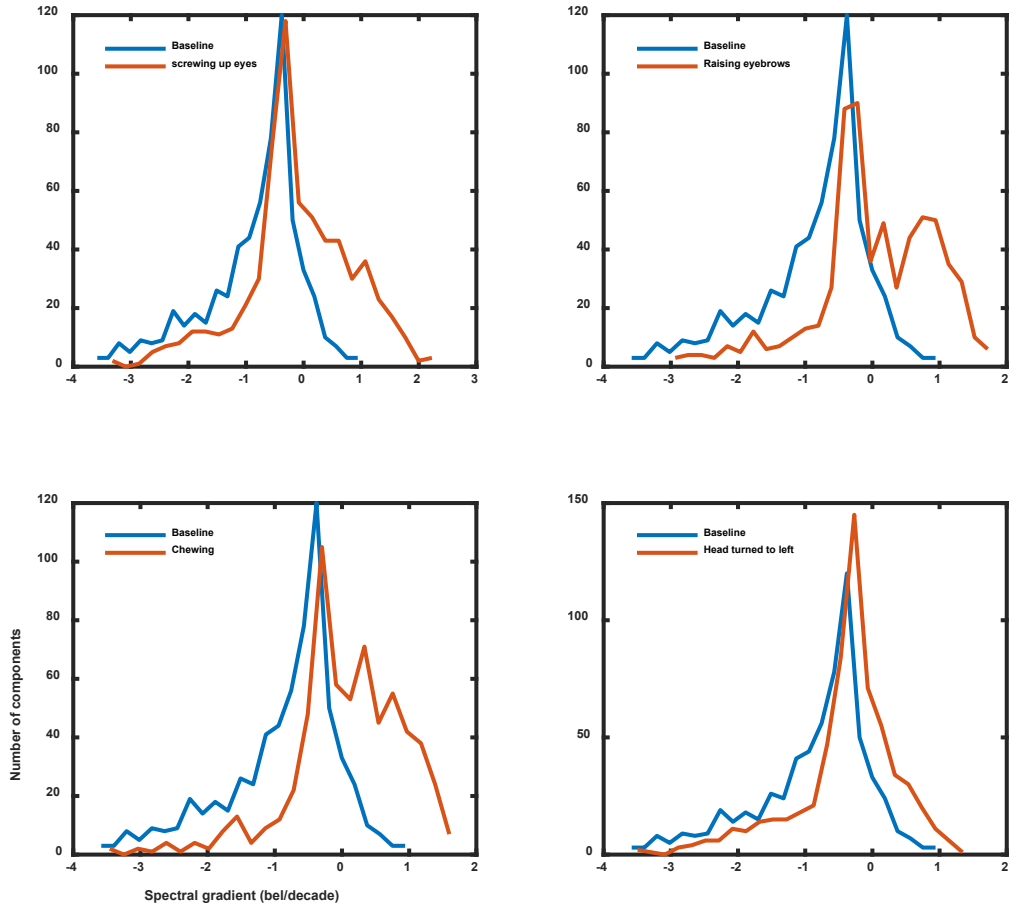

Figure 5-15: Histograms of the spectral gradients of the derived components during a baseline relaxed task (blue) and muscle activating tasks (orange) including screwing up the eyes[5] (top-left), raising eyebrows (top-right), chewing fictitious gum (bottom-left) and head turned to the left (bottom-right). The histograms of the spectral gradient during phasic muscle tasks have increased high gradient components.

The selection of the spectral gradient threshold may vary with the purpose of the study. A sensible choice with a clear interpretation is to set the threshold at the maximum spectral gradient of EMG-free components. This ensures that all pure brain components are preserved as no EMG-free component has a spectral gradient above this value. Other thresholds could be selected, e.g. at the intersection of the EMG-contaminated and EMG-free histograms, or at

[5] Activating face and eye muscles to maximally close the eyes.

the highest peak of the EMG-free histogram. These more aggressive thresholds do not have a straightforward interpretation, but correspond to a trade-off between removing more myogenic contamination while also removing more neurogenic activity (Fitzgibbon, S et al. 2016).

Although the extended BSS-CCA method showed significant results in reducing SER muscle activity, the statistically significant higher power of pruned data in comparison to EMG-free data demonstrates that this approach does not remove all muscle activity. Therefore, it is clear that at least some of the retained components contain a significant amount of muscle activity. A possible (likely?) explanation is that the algorithm does not effectively estimate components that are purely myogenic or neurogenic (or purely other source types), and there are many components which are mixtures of two or more sources. The scatterplot of correlation coefficient versus spectral gradient in EMG-contaminated and EMG-free data supports this (Figure 5-3). If the method could achieve pure components, one would expect to see a cluster of components for each source type, as illustrated in Figure 5-16.

The blue cluster consists of components with high correlation coefficient and negative spectral gradient, corresponding to brain components. It is generally accepted that the spectral power of brain components decreases with a rate of $1/(\text{frequency})^n$ with n in the range $1-2$ (Buzsáki, Anastassiou & Koch 2012). Additionally, the spectral gradient of intracranial brain recordings (electrocorticographs) have been measured, yielding $n = 2$ (Milstein et al. 2009). Exploring the histograms of the gradient of EMG-free components derived by different ICA algorithms and the extended-CCA method shows a broad range of negative gradients for putatively brain components. The blue cluster is a speculation based on this incomplete information. Further investigations are required to reveal a better understanding of the spectral characteristics of pure brain signals measured at the scalp.

Based on the previous information and investigation in Section 5.2, the orange cluster consists of components with a correlation coefficient about 0.2 (in absolute value) and a positive spectral gradient, corresponding to muscle components. The yellow cluster consist of components with a correlation coefficient less than 0.19 and a spectral gradient about zero, corresponding to white noise. Finally, the purple cluster consists of components whose correlation coefficients cover a broad range from low to high and their gradient is about zero, corresponding the mains power components. Hence, the extended BSS-CCA method does not achieve well-separated components, and perhaps a non-blind method, using the known spectral and correlation characteristics of different sources, may achieve an improved separation of components.

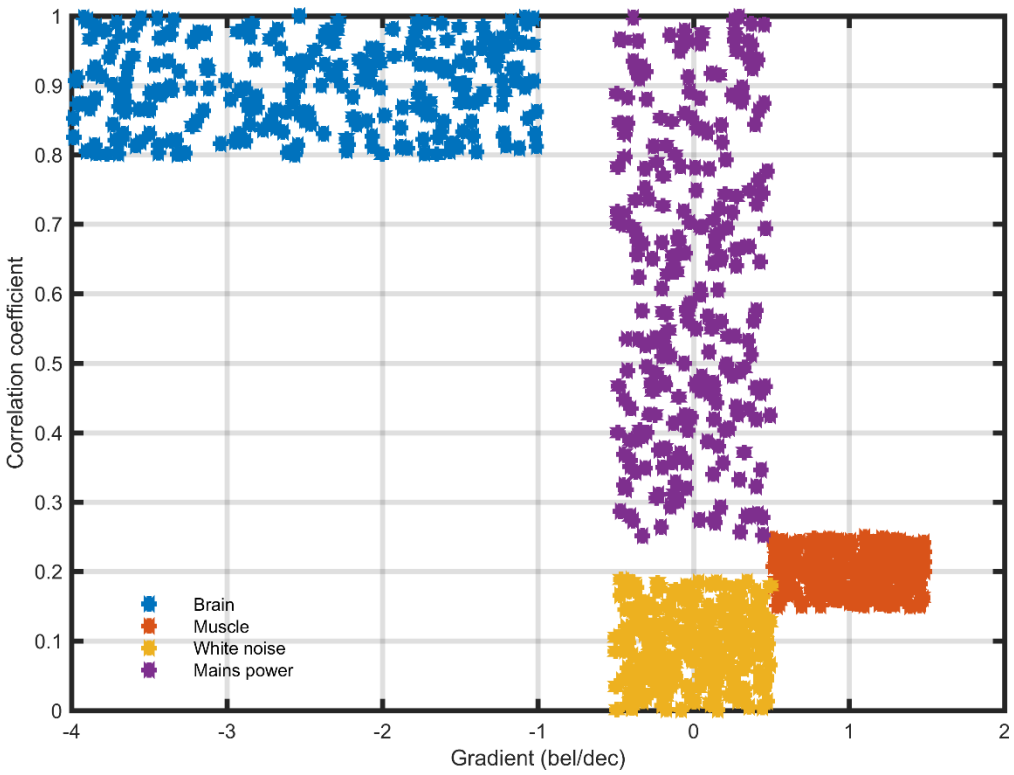

Figure 5-16: Hypothesised scatterplot of correlation coefficient and spectral gradient for pure brain (blue), muscle (orange), white noise (yellow), and mains power (purple) components.

The extended BSS-CCA technique relies on the correlation coefficients and spectral gradient features to identify muscle components, while the proposed minimum-norm beamforming muscle-reduction technique (Chapter 4) separates myogenic sources from neurogenic ones

based on their spatial location. Given the fundamentally different approaches, there may be some merit in combining these methods to further reduce muscle contamination of SERs. This is the subject of the next chapter.

Chapter 6

Complementary effect of beamforming and blind source separation in tonic muscle reduction

Using the beamforming technique, muscle sources are separated automatically based on their location; while using blind source separation, muscle components are separated based on their spectral gradient. The combination of these fundamentally different approaches may result in greater discrimination between muscle and brain signals, and hence allow a greater reduction in muscle activity in SERs.[6]

6.1 Complementary effect of sLORETA and BSS

In chapters 3 and 5, muscle-pruning algorithms based on BSS algorithms have been studied: Infomax, AMICA, FastICA, IVA, and extended CCA. These algorithms aimed to separate muscle and brain sources into different components. Muscle components were classified based on their spectral gradient. Discarding muscle components allowed reconstruction of cleaner SERs. Chapter 4 also studied the use of a decomposition algorithm (sLORETA) in reducing tonic muscle activity. Unlike BSS algorithms, sLORETA uses the spatial location of sources, i.e. it is non-blind. It has been used to separate SERs into source signals located within the head. By discarding sources distributed within the scalp layer, this technique significantly reduces muscle activity in reconstructed sensor signals.

[6] The published conference paper in Appendix B-2 contains some of the results presented in this chapter. It is restricted to using Infomax on dataset 1. Additionally, this chapter has a more detailed statistical analysis and expanded discussion and conclusion.

I have shown that none of the aforementioned methods works perfectly in reducing tonic muscle activity, and there is still residual cranial and upper cervical muscle activity in the pruned data. As these two approaches use different features to classify muscle signals, I hypothesise that their combination will be complementary. Hence, in this chapter I test if combinations of BSS and beamforming approaches reduce muscle contamination more than the individual approaches.

6.2 Method

To test the complementary effect of BSS and beamforming approaches in reducing tonic muscle activity of SER, the SER data pruned by each of BSS methods were also pruned by the sLORETA method. Additionally, this was repeated with the order of the two prunings reversed. The resulting doubled-pruned data is named with the first-applied method listed first. For example, the data pruned by Infomax and then sLORETA is called pruned-Infomax-sLORETA, while the data pruned by sLORETA and then Infomax is called pruned-sLORETA-Infomax. Note that pruned-CCA refers to data pruned using the automated extend-CCA approach Chapter 5.

The approach of double pruning was applied to all three datasets to evaluate its effectiveness in removing tonic muscle activity while retaining neurophysiological responses.

6.3 Results

In this section, every double-pruned signal is compared to other double-pruned, single-pruned, EMG-contaminated, and EMG-free data. Hence, a complete comparison of all algorithms in removing tonic muscle signals and keeping desired brain signals is provided.

6.3.1 Tonic muscle activity removal

Figure 6-1 compares the amount of muscle activity in EMG-contaminated, pruned, and EMG-free data in nine channels spread evenly across the head. The orange and the dark blue

lines correspond to EMG-contaminated and EMG-free data respectively. Better pruning has spectra closer to EMG-free spectra.

Two groups of channels were considered: central channels (Fz, FCz, Cz, C1, C2, CPz, and Oz), and peripheral channels (T7, T8, F7, F8, O1, and O2). Average power spectra of all signals in each group of channels and each frequency band were calculated. Figure 6-2 shows, for each group of channels, the spectra of EMG-contaminated, pruned and EMG-free data averaged across channels to provide better visual comparison between single pruning and double pruning approaches.

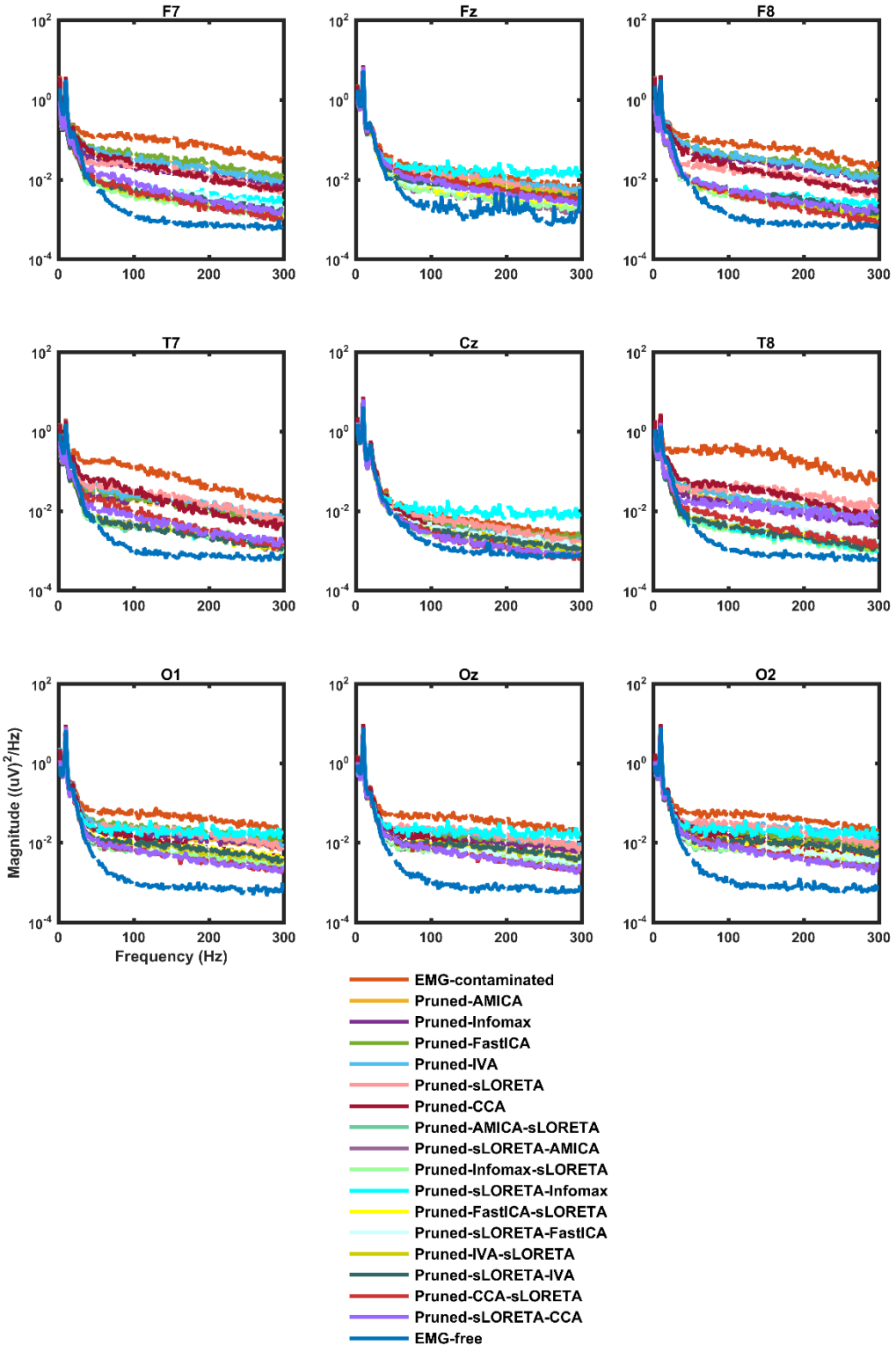

Figure 6-1: From dataset 1, mean of six subjects' power spectra during baseline eyes closed task. Visually, double-pruning approaches are reducing more tonic muscle activity than single-pruning approaches, especially at peripheral channels.

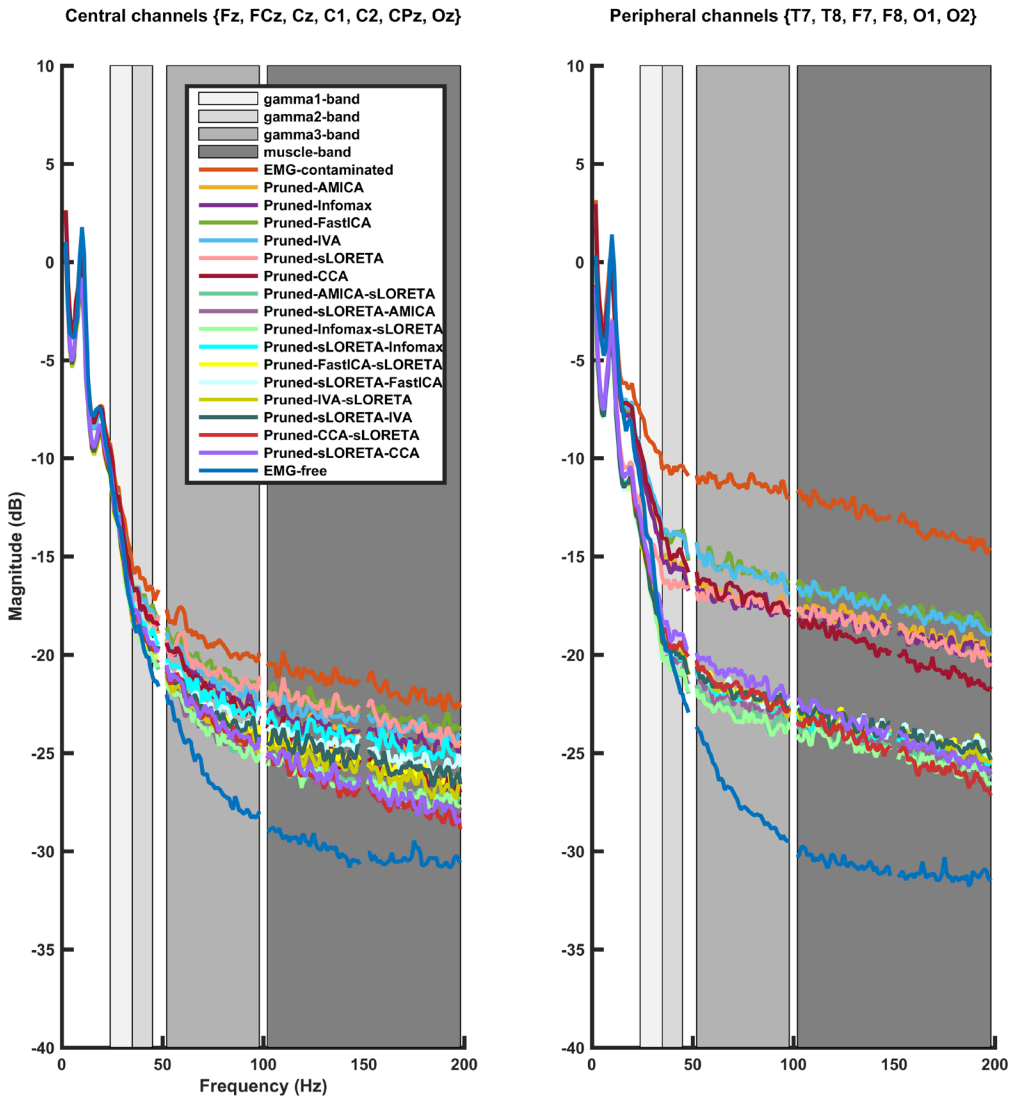

Figure 6-2: From dataset 1. Mean of six subjects' spectra in central channels (left) and peripheral channels (right) during baseline eyes closed task. Mains power artefact and harmonics of 50 Hz, have not been displayed. High frequency power, associated with muscle, has been reduced by all pruning approaches, but, visually, double-pruning approaches are reducing more tonic muscle activity than single-pruning approaches, especially at peripheral channels.

It is observed that in both single-pruned and double-pruned data, muscle reduction at peripheral channels starts at low frequencies, about 20 Hz. High frequency power, associated with muscle, has been reduced by all pruning approaches at most or all channels, but, visually, double-pruning approaches are reducing more tonic muscle activity than single-pruning approaches, especially at peripheral channels. All pruning algorithms still retain substantial muscle contamination compared to EMG-free data, especially at occipital channels (O1, Oz, and O2) where upper cervical muscles are located.

Figure 6-3 displays, in the four frequency bands of interest, the topographic maps of relative spectra of EMG-contaminated to EMG-free and pruned to EMG-free. The 25-35 Hz spectral power of all pruned-EEG signals is comparable to EMG-free centrally, and also peripherally for double-pruned signals. Although none of the pruning algorithms completely removed muscle activity at higher frequencies, double-pruning approaches reduced more muscle than single-pruning approaches, especially at peripheral channels. For example, at 102-198 Hz (muscle band), the average power of EMG-contaminated spectra at temporal channels was about 300 times greater than EMG-free spectral power, but after single pruning and double pruning this value decreased to an average of about 30 times and 10 times respectively. Visual inspection shows that AMICA and Infomax remove more muscle peripherally than the other single pruning algorithms. In addition, visually, more tonic muscle is removed occipitally in pruned-sLORETA-AMICA, pruned-AMICA-sLORETA, and pruned-Infomax-sLORETA, suggesting these approaches may outperform other double-pruning approaches. The order of pruning (first beamforming then BSS or first BSS then beamforming) results in no substantial difference in performance except with Infomax, where Infomax-sLORETA is more effective than sLORETA-Infomax.

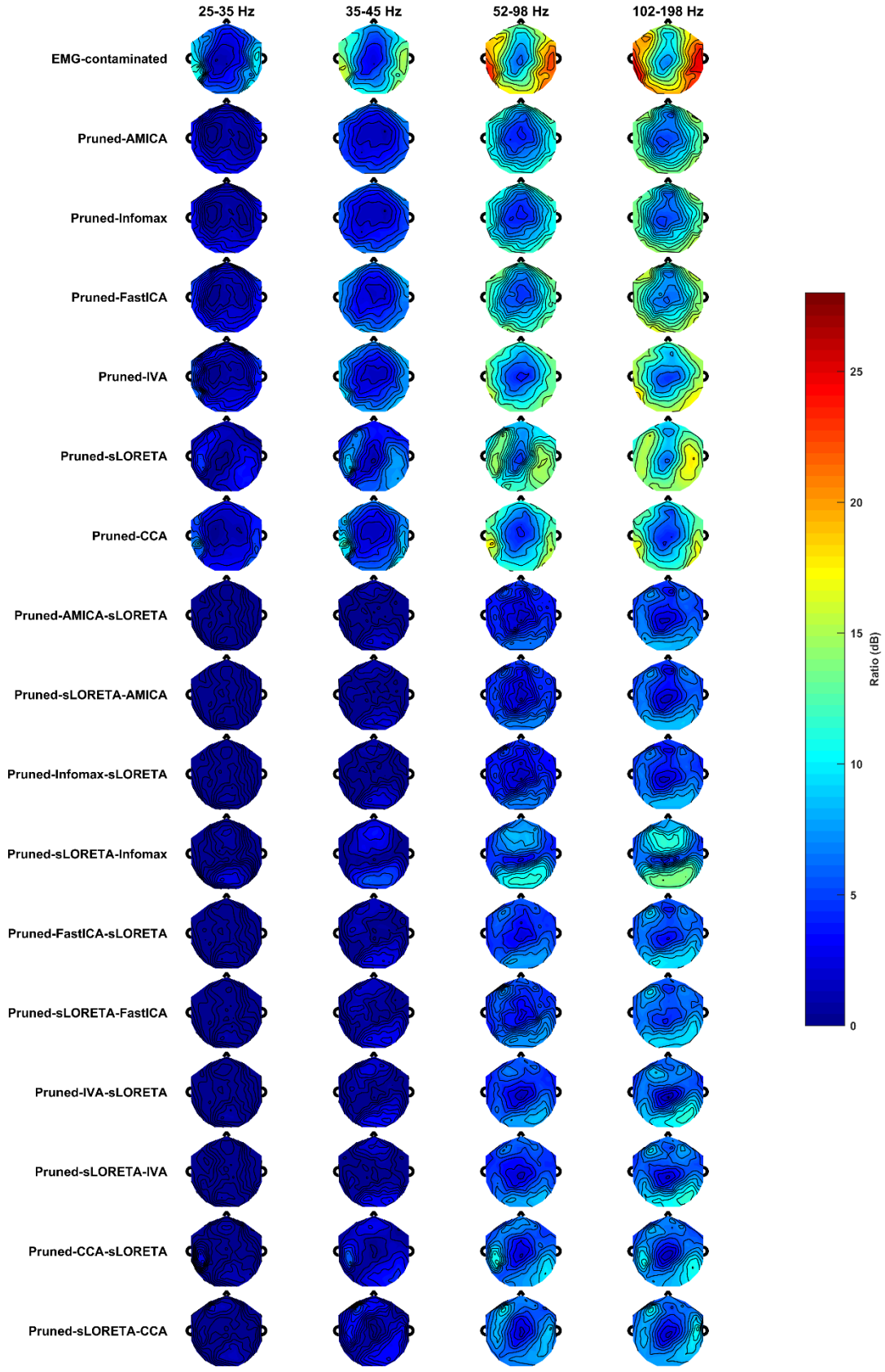

Figure 6-3: From dataset 1, topographic maps of relative spectra of EMG-contaminated/EMG-free (first row), and pruned data/EMG-free (subsequent rows) in the four frequency bands of interest. In almost all situations, double-pruning approaches reduce more muscle artefact than single-pruning approaches. Each topography is looking down on the head, with ears and nose indicated, conforming to the montage in Figure 2-4.

Figure 6-4 illustrates the mean and standard deviation of power of all signals in each region and each frequency band. Visually, it is hard to find any difference between single-pruned data and double-pruned data at central channels, but double-pruned data have lower average power than single-pruned data at peripheral channels. It can be observed that AMICA and Infomax have the best performance among the single-pruning algorithms, and sLORETA-AMICA, AMICA-sLORETA, and Infomax-sLORETA are the best among the double-pruning approaches.

To test these observations statistically, a 3-way parametric ANOVA was performed to compare the average power for all eighteen signals (EMG-contaminated, single-pruned, double-pruned, and EMG-free) over two regions (central and peripheral) and four frequency bands (gamma1, gamma2, gamma3, muscle).

Table 6-1 shows the result of the ANOVA for each factor and all interactions of factors. The ANOVA shows that the average power is different over each factor (signal, band, and region), and each two-way interaction (signal*band, signal*region, and band*region). Since the purpose of this section is to evaluate the effectiveness of double pruning and single pruning muscle-removal approaches, post-hoc tests were only performed on the factor of signal, and on the two-way interactions of signal*band and signal*region to identify statistically significant differences between pairs of signals.

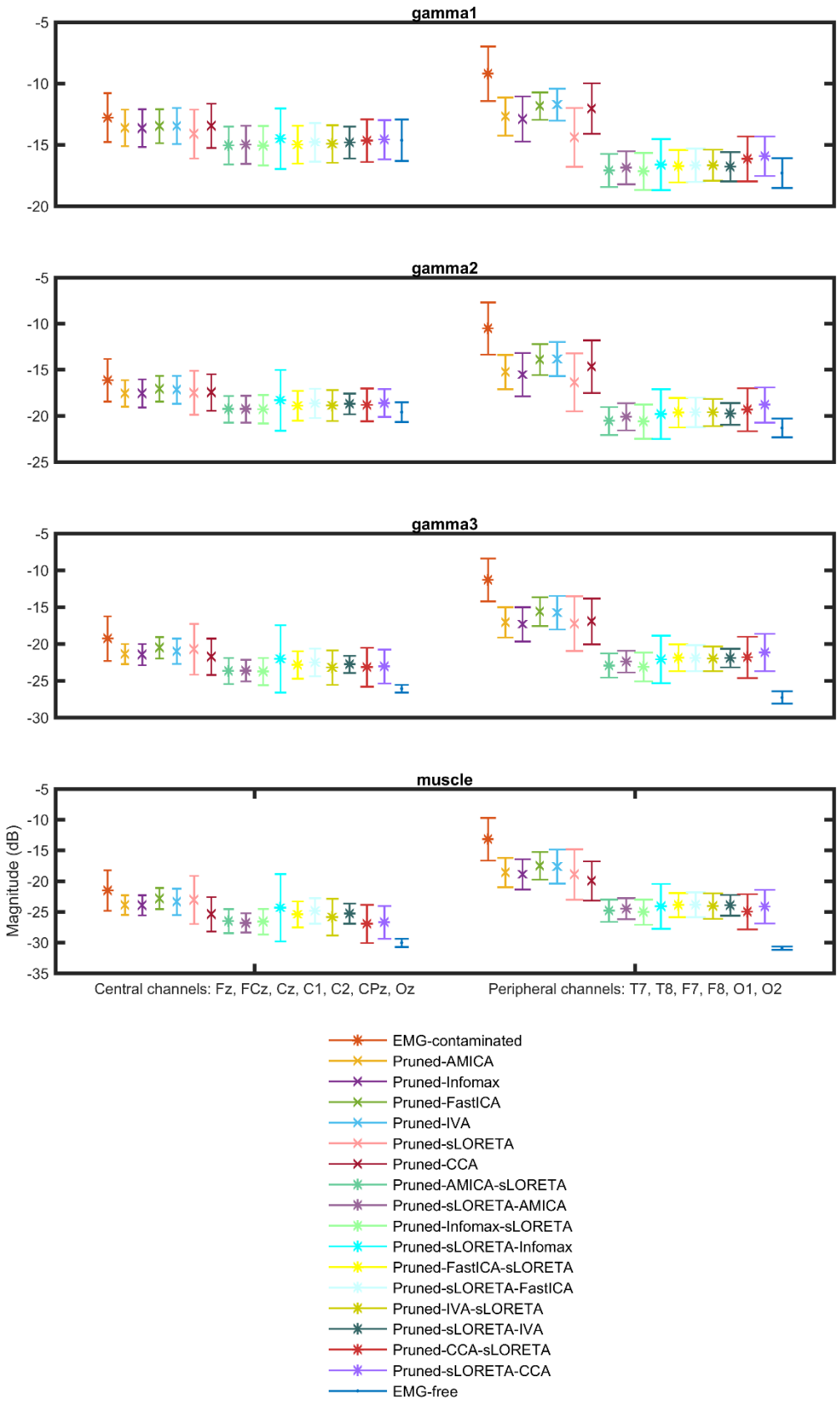

Figure 6-4: From dataset 1, average and standard deviation of power in each frequency band in EMG-contaminated, EMG-free and pruned data for 6 subjects. Visually double-pruned data have lower average power than single-pruned data at peripheral channels.

*Table 6-1: Results of ANOVA. The average power is different over each factor (signal, band, and region), and each two-way interaction (signal*band, signal*region, and band*region).*

Analysis of Variance

Source	Sum of squares	Mean square	F	p
Signal	237	13.9	52.72	**< 0.001**
Band	545	181	687.12	**< 0.001**
Region	195	19.5	73.85	**< 0.001**
Signal*Band	32.8	0.64	2.43	**< 0.001**
Signal*Region	51.1	3	11.36	**< 0.001**
Band*Region	2.72	7.61	28.79	**< 0.001**
Signal*Band*Region	2.03	0.05	0.20	1.00

Table 6-2 shows the post hoc results for factor of signal. All pruned data are statistically different to both EMG-contaminated and EMG-free data. This means that all pruning approaches are reducing tonic muscle activity significantly, but the amount of reduction is not sufficient to reach the level of EMG-free data. In addition, all double-pruned data are statistically different to single-pruned data. This indicates that all double-pruning approaches are significantly more effective than all single-pruning approaches in removing tonic muscle activity. However, no statistically significant difference was found between any pair of single-pruned data, or between any pair of double-pruned data.

Table 6-2: Post hoc test for the factor of signal. Double pruned-data are significantly different to EMG-contaminated, EMG-free and single-pruned data.

	EMG-contaminated	Pruned-AMICA	Pruned-Infomax	Pruned-FastICA	Pruned-IVA	Pruned-sLORETA	Pruned-CCA	Pruned-AMICA-sLORETA	Pruned-sLORETA-AMICA	Pruned-Infomax-sLORETA	Pruned-sLORETA-Infomax	Pruned-FastICA-sLORETA	Pruned-sLORETA-FastICA	Pruned-IVA-sLORETA	Pruned-sLORETA-IVA	Pruned-CCA-sLORETA	Pruned-sLORETA-CCA	EMG-free
EMG-contaminated		**<0.001**	**<0.001**	**<0.001**	**<0.001**	**<0.001**	**<0.001**	**<0.001**	**<0.001**	**<0.001**	**<0.001**	**<0.001**	**<0.001**	**<0.001**	**<0.001**	**<0.001**	**<0.001**	**<0.001**
Pruned-AMICA			1.00	0.85	0.94	1.00	1.00	**<0.001**	**<0.001**	**<0.001**	**<0.001**	**<0.001**	**<0.001**	**<0.001**	**<0.001**	**<0.001**	**<0.001**	**<0.001**
Pruned-Infomax				0.50	0.67	1.00	1.00	**<0.001**	**<0.001**	**<0.001**	**<0.001**	**<0.001**	**<0.001**	**<0.001**	**<0.001**	**<0.001**	**<0.001**	**<0.001**
Pruned-FastICA					1.00	0.58	0.93	**<0.001**	**<0.001**	**<0.001**	**<0.001**	**<0.001**	**<0.001**	**<0.001**	**<0.001**	**<0.001**	**<0.001**	**<0.001**
Pruned-IVA						0.74	0.98	**<0.001**	**<0.001**	**<0.001**	**<0.001**	**<0.001**	**<0.001**	**<0.001**	**<0.001**	**<0.001**	**<0.001**	**<0.001**
Pruned-sLORETA							1.00	**<0.001**	**<0.001**	**<0.001**	**<0.001**	**<0.001**	**<0.001**	**<0.001**	**<0.001**	**<0.001**	**<0.001**	**<0.001**
Pruned-CCA								**<0.001**	**<0.001**	**<0.001**	**<0.001**	**<0.001**	**<0.001**	**<0.001**	**<0.001**	**<0.001**	**<0.001**	**<0.001**
Pruned-AMICA-sLORETA									1.00	1.00	0.51	0.99	0.95	0.98	0.87	0.99	0.79	**0.008**
Pruned-sLORETA-AMICA										1.00	0.72	1.00	0.99	0.99	0.96	1.000	0.92	**0.003**
Pruned-Infomax-sLORETA											0.34	0.97	0.87	0.94	0.74	0.98	0.62	**0.02**
Pruned-sLORETA-Infomax												1.00	1.00	1.00	1.00	1.00	1.00	**<0.001**
Pruned-FastICA-sLORETA													1.00	1.00	1.00	1.00	1.00	**<0.001**
Pruned-sLORETA-FastICA														1.00	1.00	1.00	1.00	**<0.001**
Pruned-IVA-sLORETA															1.00	1.00	1.00	**<0.001**
Pruned-sLORETA-IVA																1.00	1.00	**<0.001**
Pruned-CCA-sLORETA																	1.00	**<0.001**
Pruned-sLORETA-CCA																		**<0.001**
EMG-free																		

Table 6-3 shows the post hoc results for the interaction of signal and region. In central channels (lower triangle), none of the single-pruned data is statistically different to EMG-contaminated data, however, all double-pruned data are significantly different to EMG-contaminated data. Hence, double-pruning approaches outperform single-pruning in removing tonic muscle activity centrally. Moreover, all double-pruning data except pruned-sLORETA-Infomax are not significantly different to EMG-free. This means that the amount of muscle reduction using nearly all double pruning approaches is sufficient to reach the level of EMG-free data. Among double pruned data, pruned-sLORETA-AMICA, pruned-AMICA-sLORETA, and pruned Infomax-sLORETA are significantly different to pruned-FastICA, pruned-IVA and pruned-sLORETA[7]. This indicates that these double-pruning approaches outperform FastICA, IVA, and sLORETA in reducing tonic muscle activity centrally. No significant difference is found between any pair of single-pruned data, or between any pair of double-pruned data.

In peripheral channels (upper triangle), there is more muscle artefact and so the differences between pruned data can be more clearly seen. All pruned data (single and double) are significantly different to EMG-contaminated data, and all of them are significantly different to EMG-free data except pruned-AMICA-sLORETA and pruned Infomax-sLORETA. This means all pruning approaches are reducing tonic muscle activity peripherally, but only in pruned-AMICA-sLORETA and pruned Infomax-sLORETA is the amount of muscle reduction sufficient to reach the level of EMG-free data. Hence, these two double-pruning approaches outperform all other pruning methods in removing peripheral tonic muscle activity. All the double-pruned data are significantly different to all single-pruned data. This indicates double pruning outperforms single pruning in reducing tonic muscle activity

[7] One of the nine comparisons described here is not strictly significant, but is close to significant ($p = 0.054$).

peripherally. However, no statistically significant difference was found between any pair of single-pruned data, or between any pair of double-pruned data.

Table 6-3: Post hoc test for the interaction of signal and region. Double pruning outperforms single pruning both centrally and peripherally.

Central \ Peripheral	EMG-contaminated	Pruned-AMICA	Pruned-Infomax	Pruned-FastICA	Pruned-IVA	Pruned-sLORETA	Pruned-CCA	Pruned-AMICA-sLORETA	Pruned-sLORETA-AMICA	Pruned-Infomax-sLORETA	Pruned-sLORETA-Infomax	Pruned-FastICA-sLORETA	Pruned-sLORETA-FastICA	Pruned-IVA-sLORETA	Pruned-sLORETA-IVA	Pruned-CCA-sLORETA	Pruned-sLORETA-CCA	EMG-free
EMG-contaminated		**<0.001**	**<0.001**	**<0.001**	**<0.001**	**<0.001**	**<0.001**	**<0.001**	**<0.001**	**<0.001**	**<0.001**	**<0.001**	**<0.001**	**<0.001**	**<0.001**	**<0.001**	**<0.001**	**<0.001**
Pruned-AMICA	0.27		1.00	0.99	1.00	1.00	1.00	**<0.001**	**<0.001**	**<0.001**	**<0.001**	**<0.001**	**<0.001**	**<0.001**	**<0.001**	**<0.001**	**<0.001**	**<0.001**
Pruned-Infomax	0.21	1.00		0.89	0.93	1.00	1.00	**<0.001**	**<0.001**	**<0.001**	**<0.001**	**<0.001**	**<0.001**	**<0.001**	**<0.001**	**<0.001**	**<0.001**	**<0.001**
Pruned-FastICA	0.96	1.00	1.00		1.00	0.41	1.00	**<0.001**	**<0.001**	**<0.001**	**<0.001**	**<0.001**	**<0.001**	**<0.001**	**<0.001**	**<0.001**	**<0.001**	**<0.001**
Pruned-IVA	0.90	1.00	1.00	1.00		0.51	1.00	**<0.001**	**<0.001**	**<0.001**	**<0.001**	**<0.001**	**<0.001**	**<0.001**	**<0.001**	**<0.001**	**<0.001**	**<0.001**
Pruned-sLORETA	0.80	1.00	1.00	1.00	1.00		0.99	**<0.001**	**<0.001**	**<0.001**	**<0.001**	**<0.001**	**<0.001**	**<0.001**	**<0.001**	**<0.001**	**<0.001**	**<0.001**
Pruned-CCA	0.07	1.00	1.00	1.00	1.00	1.00		**<0.001**	**<0.001**	**<0.001**	**<0.001**	**<0.001**	**<0.001**	**<0.001**	**<0.001**	**<0.001**	**<0.001**	**<0.001**
Pruned-AMICA-sLORETA	**<0.001**	0.35	0.43	**0.01**	**0.02**	0.054	0.75		1.00	1.00	1.00	1.00	1.00	1.00	1.00	1.00	0.94	0.18
Pruned-sLORETA-AMICA	**<0.001**	0.28	0.35	**0.009**	**0.01**	**0.03**	0.67	1.00		1.00	1.00	1.00	1.00	1.00	1.00	1.00	0.99	**0.04**
Pruned-Infomax-sLORETA	**<0.001**	0.26	0.33	**0.008**	**0.01**	**0.03**	0.64	1.00	1.00		1.00	1.00	1.00	1.00	0.99	1.00	0.85	0.310
Pruned-sLORETA-Infomax	**0.008**	1.00	1.00	0.98	0.996	0.99	1.00	0.98	0.96	0.96		1.00	1.00	1.00	1.00	1.00	1.00	**0.001**
Pruned-FastICA-sLORETA	**<0.001**	0.93	0.96	0.20	0.32	0.47	0.99	1.00	1.00	1.00	1.00		1.00	1.00	1.00	1.00	1.00	**0.002**
Pruned-sLORETA-FastICA	**<0.001**	0.99	0.99	0.51	0.67	0.81	1.00	1.00	1.00	1.00	1.00	1.00		1.00	1.00	1.00	1.00	**0.002**
Pruned-IVA-sLORETA	**<0.001**	0.96	0.98	0.26	0.40	0.55	0.99	1.00	1.00	1.00	1.00	1.00	1.00		1.00	1.00	1.00	**0.001**
Pruned-sLORETA-IVA	**<0.001**	0.99	0.99	0.55	0.71	0.84	1.00	1.00	1.00	1.00	1.00	1.00	1.00	1.00		1.00	1.00	**<0.001**
Pruned-CCA-sLORETA	**<0.001**	0.86	0.90	0.13	0.22	0.34	0.99	1.00	1.00	1.00	1.00	1.00	1.00	1.00	1.00		1.00	**0.002**
Pruned-sLORETA-CCA	**<0.001**	0.90	0.93	0.16	0.26	0.40	0.99	1.00	1.00	1.00	1.00	1.00	1.00	1.00	1.00	1.00		**<0.001**
EMG-free	**<0.001**	**<0.001**	**<0.001**	**<0.001**	**<0.001**	**<0.001**	**0.001**	0.95	0.97	0.98	**0.008**	0.41	0.15	0.33	0.13	0.55	0.49	

Table 6-4 (gamma1 and gamma2) and Table 6-5 (gamma3 and muscle) show the post hoc results for the interaction of signal and band. At gamma1, none of the single-pruned data are significantly different to EMG-contaminated data. However, all the double-pruned data are significantly different to EMG-contaminated data. Additionally, none of the single-pruned and double-pruned data are significantly different to EMG-free data. This means only double pruning could significantly reduce the muscle activity to reach the level of EMG-free. No significant difference is found between any pair of double-pruned and single-pruned data.

At gamma2, again, none of the single-pruned data are significantly different to EMG-contaminated, but all double-pruned data are significantly different to EMG-contaminated. This indicates double pruning outperforms single pruning in removing tonic muscle activity at gamma2. In addition, none of the pruned data are significantly different to EMG-free except pruned-FastICA, pruned-IVA, and pruned-CCA. Pruned-sLORETA-AMICA, pruned-AMICA-sLORETA, and pruned-Infomax-sLORETA are also statistically different to pruned-IVA, pruned-CCA, and pruned-FAstICA. No significant difference is found between any pair of double-pruned data, or any pair of single-pruned data. Hence, it can be concluded that AMICA, Infomax, and sLORETA are the best single pruning approaches at gamma2, and sLORETA-AMICA, AMICA-sLORETA, and Infomax-sLORETA are the best double pruning approaches at gamma2.

At gamma3, all pruned data except pruned-IVA and pruned-FastICA are significantly different to EMG-contaminated. This indicates other single-pruning approaches and double-pruning approaches outperform IVA and FastICA. Additionally, most of the double-pruned data are significantly different to pruned-FastICA, and pruned-IVA. This means that most double pruning approaches outperform single pruning using FastICA or IVA. Moreover, all pruned data are significantly different to EMG-free data except pruned-sLORETA-AMICA, pruned-AMICA-sLORETA, and pruned-Infomax-sLORETA. In addition, these three double-

pruned data are significantly different to all of the single-pruned data. These results indicate that these three double-pruning approaches can reduce tonic muscle activity sufficiently to reach the level of EMG-free, and they outperform the other double-pruning and all single-pruning approaches. No significant difference is found between any pair of double-pruned data, or between any pair of single-pruned data.

At muscle band, all pruned data are significantly different to both EMG-contaminated and EMG-free. This means that all pruning approaches can reduce tonic muscle activity but the amount of reduction is not sufficient to reach the level of EMG-free. In most comparisons, double pruned-data are significantly different to single-pruned data. However, none of the double-pruned data are significantly different to pruned-CCA. This indicates that at high frequency bands (>100 Hz), pruned-CCA is comparable to double-pruning approaches. Again, all double-pruned data are significantly different to pruned-FastICA, and pruned-IVA, which means that double pruning approaches outperform these two single prunings. No significant difference is found between any pair of double-pruned data, or between any pair of single-pruned data.

Table 6-4: Post hoc test for interaction of signal and band for gamma1 and gamma2.

Gamma1 \ Gamma2	EMG-contaminated	Pruned-AMICA	Pruned-Infomax	Pruned-FastICA	Pruned-IVA	Pruned-sLORETA	Pruned-CCA	Pruned-AMICA-sLORETA	Pruned-sLORETA-AMICA	Pruned-Infomax-sLORETA	Pruned-sLORETA-Infomax	Pruned-FastICA-sLORETA	Pruned-sLORETA-FastICA	Pruned-IVA-sLORETA	Pruned-sLORETA-IVA	Pruned-CCA-sLORETA	Pruned-sLORETA-CCA	EMG-free
EMG-contaminated		0.14	0.06	0.92	0.90	0.06	0.59	**<0.001**	**<0.001**	**<0.001**	**<0.001**	**<0.001**	**<0.001**	**<0.001**	**<0.001**	**<0.001**	**<0.001**	**<0.001**
Pruned-AMICA	0.99		1.00	1.00	1.00	1.00	1.00	0.09	0.18	0.07	0.88	0.54	0.67	0.64	0.70	0.84	0.98	0.08
Pruned-Infomax	0.98	1.00		1.00	1.00	1.00	1.00	0.20	0.35	0.17	0.97	0.76	0.86	0.84	0.88	0.95	0.99	0.19
Pruned-FastICA	1.00	1.00	1.00		1.00	1.00	1.00	**0.001**	**0.003**	**0.001**	0.104	**0.02**	**0.03**	**0.03**	**0.04**	0.08	0.27	**0.001**
Pruned-IVA	1.00	1.00	1.00	1.00		1.00	1.00	**0.001**	**0.004**	**0.001**	0.12	**0.02**	**0.04**	**0.04**	**0.05**	0.09	0.31	**0.001**
Pruned-sLORETA	0.18	1.00	1.00	1.00	1.00		1.00	0.44	0.64	0.39	0.99	0.94	0.97	0.97	0.98	0.99	1.00	0.42
Pruned-CCA	1.00	1.00	1.00	1.00	1.00	1.00		**0.009**	**0.022**	**0.007**	0.38	0.11	0.18	0.16	0.20	0.32	0.68	**0.008**
Pruned-AMICA-sLORETA	**<0.001**	0.76	0.88	0.37	0.33	1.00	0.37		1.00	1.00	1.00	1.00	1.00	1.00	1.00	1.00	1.00	1.00
Pruned-sLORETA-AMICA	**<0.001**	0.81	0.91	0.43	0.38	1.00	0.43	1.00		1.00	1.00	1.00	1.00	1.00	1.00	1.00	1.00	1.00
Pruned-Infomax-sLORETA	**<0.001**	0.71	0.84	0.32	0.28	1.00	0.32	1.00	1.00		1.00	1.00	1.00	1.00	1.00	1.00	1.00	1.00
Pruned-sLORETA-Infomax	**0.002**	0.98	0.99	0.82	0.78	1.00	0.82	1.00	1.00	1.00		1.00	1.00	1.00	1.00	1.00	1.00	1.00
Pruned-FastICA-sLORETA	**<0.001**	0.83	0.92	0.45	0.41	1.00	0.46	1.00	1.00	1.00	1.00		1.00	1.00	1.00	1.00	1.00	1.00
Pruned-sLORETA-FastICA	**0.001**	0.92	0.97	0.61	0.56	1.00	0.61	1.00	1.00	1.00	1.00	1.00		1.00	1.00	1.00	1.00	1.00
Pruned-IVA-sLORETA	**<0.001**	0.88	0.95	0.53	0.48	1.00	0.53	1.00	1.00	1.00	1.00	1.00	1.00		1.00	1.00	1.00	1.00
Pruned-sLORETA-IVA	**<0.001**	0.89	0.96	0.56	0.51	1.00	0.56	1.00	1.00	1.00	1.00	1.00	1.00	1.00		1.00	1.00	1.00
Pruned-CCA-sLORETA	**0.003**	0.99	0.99	0.88	0.85	1.00	0.88	1.00	1.00	1.00	1.00	1.00	1.00	1.00	1.00		1.00	1.00
Pruned-sLORETA-CCA	**0.006**	0.99	1.00	0.94	0.92	1.00	0.94	1.00	1.00	1.00	1.00	1.00	1.00	1.00	1.00	1.00		1.00
EMG-free	**0.004**	1.00	1.00	0.99	0.99	1.00	0.99	1.00	1.00	1.00	1.00	1.00	1.00	1.00	1.00	1.00	1.00	

Table 6-5: Post hoc test for interaction of signal and band for gamma3 and muscle.

Gamma3 \ Muscle	EMG-contaminated	Pruned-AMICA	Pruned-Infomax	Pruned-FastICA	Pruned-IVA	Pruned-sLORETA	Pruned-CCA	Pruned-AMICA-sLORETA	Pruned-sLORETA-AMICA	Pruned-Infomax-sLORETA	Pruned-sLORETA-Infomax	Pruned-FastICA-sLORETA	Pruned-sLORETA-FastICA	Pruned-IVA-sLORETA	Pruned-sLORETA-IVA	Pruned-CCA-sLORETA	Pruned-sLORETA-CCA	EMG-free
EMG-contaminated		**<0.001**	**<0.001**	**0.05**	**0.04**	**0.008**	**<0.001**	**<0.001**	**<0.001**	**<0.001**	**<0.001**	**<0.001**	**<0.001**	**<0.001**	**<0.001**	**<0.001**	**<0.001**	**<0.001**
Pruned-AMICA	**0.001**		1.00	1.00	1.00	1.00	1.00	**0.002**	**0.002**	**0.001**	0.70	0.13	0.23	0.20	0.50	**0.001**	**0.01**	**<0.001**
Pruned-Infomax	**<0.001**	1.00		1.00	1.00	1.00	1.00	**0.006**	**0.007**	**0.003**	0.90	0.29	0.45	0.41	0.76	**0.005**	**0.05**	**<0.001**
Pruned-FastICA	0.16	1.00	1.00		1.00	1.00	0.99	**<0.001**	**<0.001**	**<0.001**	**0.03**	**0.001**	**0.003**	**0.002**	**0.01**	**<0.001**	**<0.001**	**<0.001**
Pruned-IVA	0.06	1.00	1.00	1.00		1.00	1.00	**<0.001**	**<0.001**	**<0.001**	**0.05**	**0.002**	**0.005**	**0.004**	**0.02**	**<0.001**	**<0.001**	**<0.001**
Pruned-sLORETA	**0.006**	1.00	1.00	1.00	1.00		1.00	**<0.001**	**<0.001**	**<0.001**	0.19	**0.01**	**0.02**	**0.02**	0.09	**<0.001**	**0.001**	**<0.001**
Pruned-CCA	**0.004**	1.00	1.00	1.00	1.00	1.00		0.11	0.12	0.06	1.00	0.90	0.96	0.95	0.99	0.09	0.49	**<0.001**
Pruned-AMICA-sLORETA	**<0.001**	**0.008**	**0.02**	**<0.001**	**<0.001**	**0.001**	**0.001**		1.00	1.00	1.00	1.00	1.00	1.00	1.00	1.00	1.00	**<0.001**
Pruned-sLORETA-AMICA	**<0.001**	**0.02**	**0.07**	**<0.001**	**<0.001**	**0.003**	**0.004**	1.00		1.00	1.00	1.00	1.00	1.00	1.00	1.00	1.00	**<0.001**
Pruned-Infomax-sLORETA	**<0.001**	**0.003**	**0.013**	**<0.001**	**<0.001**	**<0.001**	**<0.001**	1.00	1.00		1.00	1.00	1.00	1.00	1.00	1.00	1.00	**<0.001**
Pruned-sLORETA-Infomax	**<0.001**	0.76	0.93	**0.02**	0.06	0.34	0.40	1.00	1.00	1.00		1.00	1.00	1.00	1.00	1.00	1.00	**<0.001**
Pruned-FastICA-sLORETA	**<0.001**	0.29	0.55	**0.002**	**0.007**	0.07	0.08	1.00	1.00	1.00	1.00		1.00	1.00	1.00	1.00	1.00	**<0.001**
Pruned-sLORETA-FastICA	**<0.001**	0.36	0.63	**0.003**	**0.01**	0.09	0.12	1.00	1.00	1.00	1.00	1.00		1.00	1.00	1.00	1.00	**<0.001**
Pruned-IVA-sLORETA	**<0.001**	0.24	0.48	**0.001**	**0.005**	0.054	0.06	1.00	1.00	1.00	1.00	1.00	1.00		1.00	1.00	1.00	**<0.001**
Pruned-sLORETA-IVA	**<0.001**	0.50	0.77	**0.006**	**0.02**	0.15	0.19	1.00	1.00	1.00	1.00	1.00	1.00	1.00		1.00	1.00	**<0.001**
Pruned-CCA-sLORETA	**<0.001**	0.37	0.65	**0.003**	**0.01**	0.10	0.12	1.00	1.00	1.00	1.00	1.00	1.00	1.00	1.00		1.00	**<0.001**
Pruned-sLORETA-CCA	**<0.001**	0.71	0.91	**0.01**	**0.050**	0.30	0.35	1.00	1.00	1.00	1.00	1.00	1.00	1.00	1.00	1.00		**<0.001**
EMG-free	**<0.001**	**<0.001**	**<0.001**	**<0.001**	**<0.001**	**<0.001**	**<0.001**	0.37	0.19	0.53	**0.001**	**0.01**	**0.008**	**0.01**	**0.004**	**0.008**	**0.001**	

To sum up, it can be said that double-pruning generally outperforms single pruning, especially at peripheral channels or at higher frequencies. Using double pruning, tonic muscle activity is reduced significantly both centrally and peripherally and in all frequency bands of interest. Among the double-pruning approaches, AMICA-sLORETA and Infomax-sLORETA have the best outcomes because they are not significantly different to EMG-free data except in the highest frequency band (> 100 Hz). Moreover, sLORETA-AMICA, AMICA-sLORETA, and Infomax-sLORETA are significantly different to single-pruning algorithms in most comparisons. Among the single-pruning algorithms, AMICA and Infomax are the best since they are not significantly different to any double-pruned data at central channels or at lower frequency bands (<50 Hz). Moreover, extended-CCA is as good as double-pruning approaches in removing tonic muscle activity at high frequencies (> 100 Hz).

6.3.2 Retention of neurophysiological responses

Another requirement of a good muscle-removal approach is that it should not affect desired brain signals. Hence, the effect of double-pruning approaches in the measurement of neurophysiological responses was investigated.

6.3.2.1 Berger effect

Figure 6-5 shows the Berger effect as raw spectra of eyes closed (left) and left eye open (right) at an occipital channel (Oz) for dataset 1. The alpha activity (power at 8-13 Hz) has decreased in the eye open task in all single-pruned and double-pruned spectra.

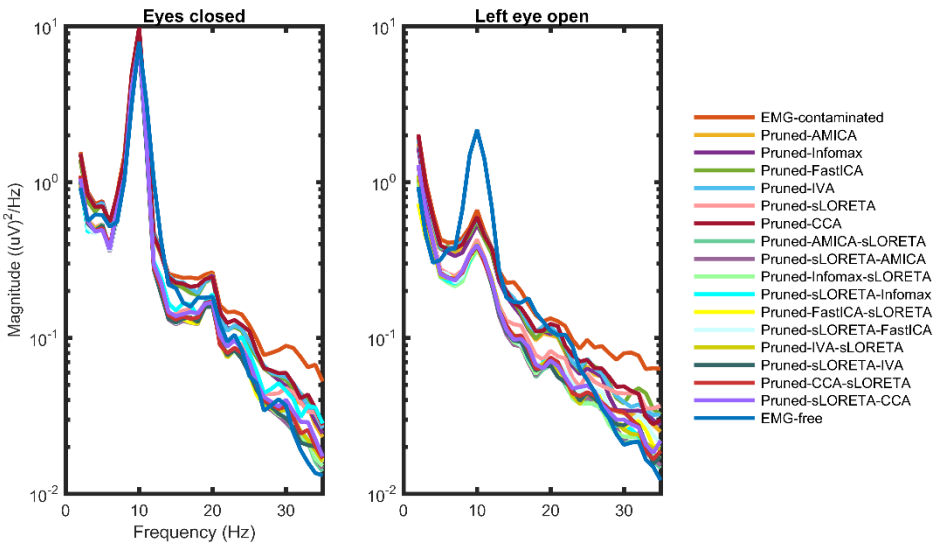

Figure 6-5: From dataset 1, average of six subjects' power spectra at Oz during eyes closed (left) and left eye open (right) tasks. As expected, the alpha activity (power at 8-13 Hz) has decreased in the eye open task in all double-pruned and single-pruned spectra.

Figure 6-6 shows the same data as relative spectra of eyes closed over left eye open. It illustrates the expected higher power (peak) around 10 Hz for all data. Statistical analysis (one-way ANOVA) revealed no significant effect for the factor of signal ($F = 0.02$, $p = 1$). In other words, there is no evidence that any pruning has a significant effect on the measurement of the Berger effect.

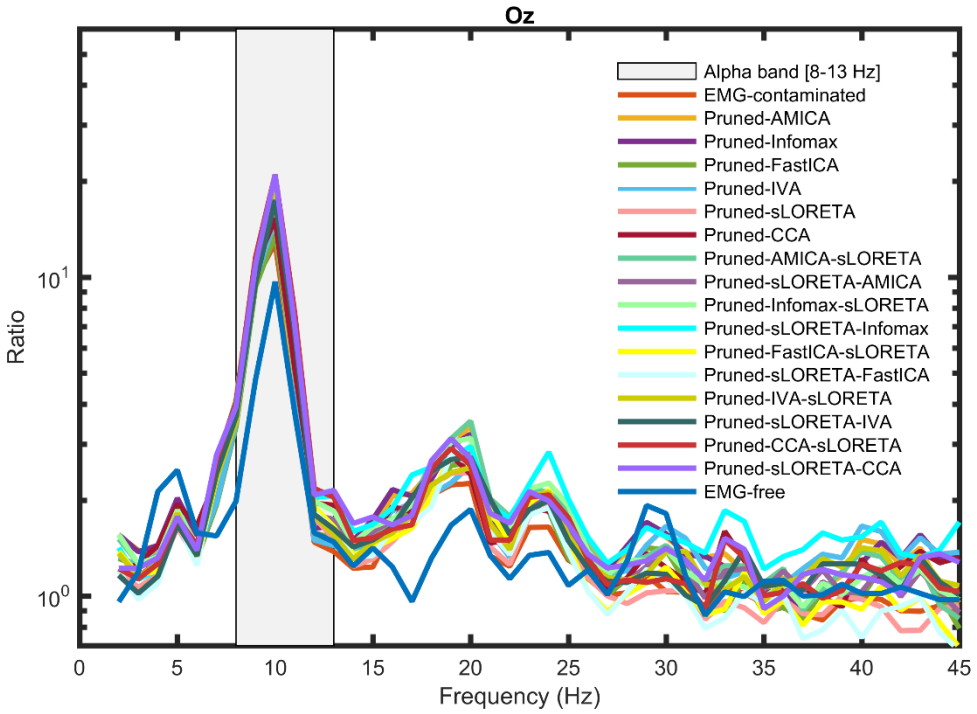

Figure 6-6: From dataset 1, mean of six subjects' relative spectra (eyes closed to left eye open) at channel Oz. Statistically, there is no difference in the relative power of alpha activity in EMG-contaminated, single-pruned, double-pruned, and EMG-free data.

6.3.2.2 Auditory oddball

The effect of double-pruning approaches was evaluated on the event-related potentials during an auditory oddball task. Figure 6-7 illustrates mean AERPs at channel Fz across five subjects for the low tone (left) and high tone (right) stimuli. It is clear that the N1 and P2 components, which are responses to any tone, and the P3 component, which is the response to the target high tone, have been preserved in all double-pruned and single-pruned data. Statistical analyses showed no significant difference for the factor of signal (N1: $F = 0.39$, $p = 0.98$; P2: $F = 0.32$, $p = 0.99$; P3: $F = 0.02$, $p = 1$). These results show that double-pruning approaches do not significantly affect the measurement of AERPs.

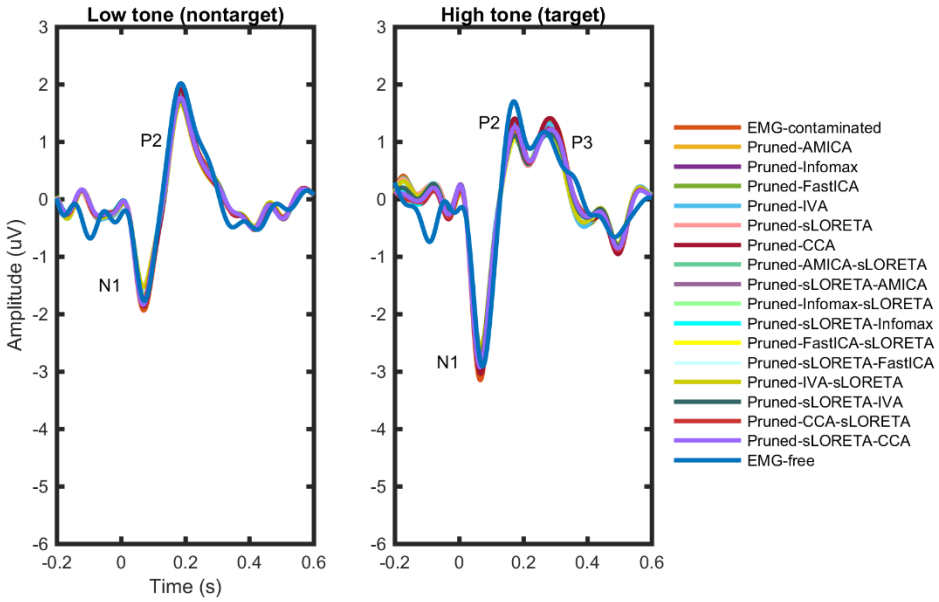

Figure 6-7: From dataset 1, averaged auditory event-related potentials (AERPs) of five subjects in an oddball task at channel Fz. The N1, P2, and P3 components to non-target low tone (left) and target high tone (right) have been preserved in all double-pruned and single-pruned data.

6.3.2.3 Photic stimulation

Figure 6-8 shows the mean of power spectra at Oz in response to photic stimulation at 16 Hz, 40 Hz and 59 Hz. The 16 Hz VSSR is visually apparent in all spectra, whereas it is much less clear at 40 Hz and 59 Hz in the EMG-contaminated spectra. The 59 Hz peak is apparent in all double-pruned and single-pruned data. However, due to more muscle reduction in double-pruned data, their spectra are closer to EMG-free. Three separate ANOVAs (three frequencies) revealed no significant effect for the factor of signal (16 Hz: $F = 0.10$, $p = 1$; 40 Hz: $F = 0.43$, $p = 0.97$; 59 Hz: $F= 0.13$, $p = 1$). These results are consistent with the preservation of brain activity when performing muscle removal using double-pruning approaches.

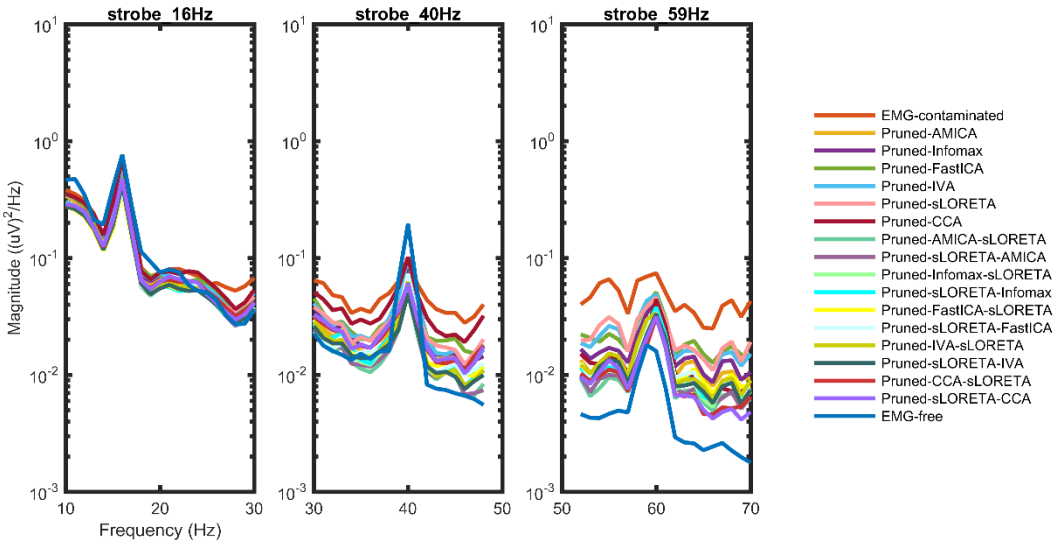

Figure 6-8: From dataset 1, mean power spectra at Oz in response to photic stimulation at 16 Hz, 40 Hz and 59 Hz. The steady state response peak is apparent in all double-pruned and single-pruned spectra.

6.3.2.4 Auditory stimulation

Double-pruning approaches were applied to scalp recordings from dataset 2 to evaluate their effect on the steady state response to 40 Hz auditory stimulation.

Figure 6-9 shows the average power spectra for 13 subjects. The peak of the steady state response is apparent in all single-pruned and double-pruned spectra despite it not being apparent in EMG-contaminated spectra T7 and T8. In some pruned spectra, a peak around 60 Hz is disclosed, because three subjects opened their eyes during this task. Hence, the 60 Hz refresh rate of the monitor caused a VSSR in their spectra. Three separate ANOVAs (three channels) revealed no significant effect for the factor of signal (T7: $F = 2.13$, $p = 0.15$; T8: $F = 1.58$, $p = 0.07$; FCz: $F = 0.54$, $p = 0.91$). These observations are consistent with double-pruning approaches reducing tonic muscle activity while retaining brain neurophysiological responses.

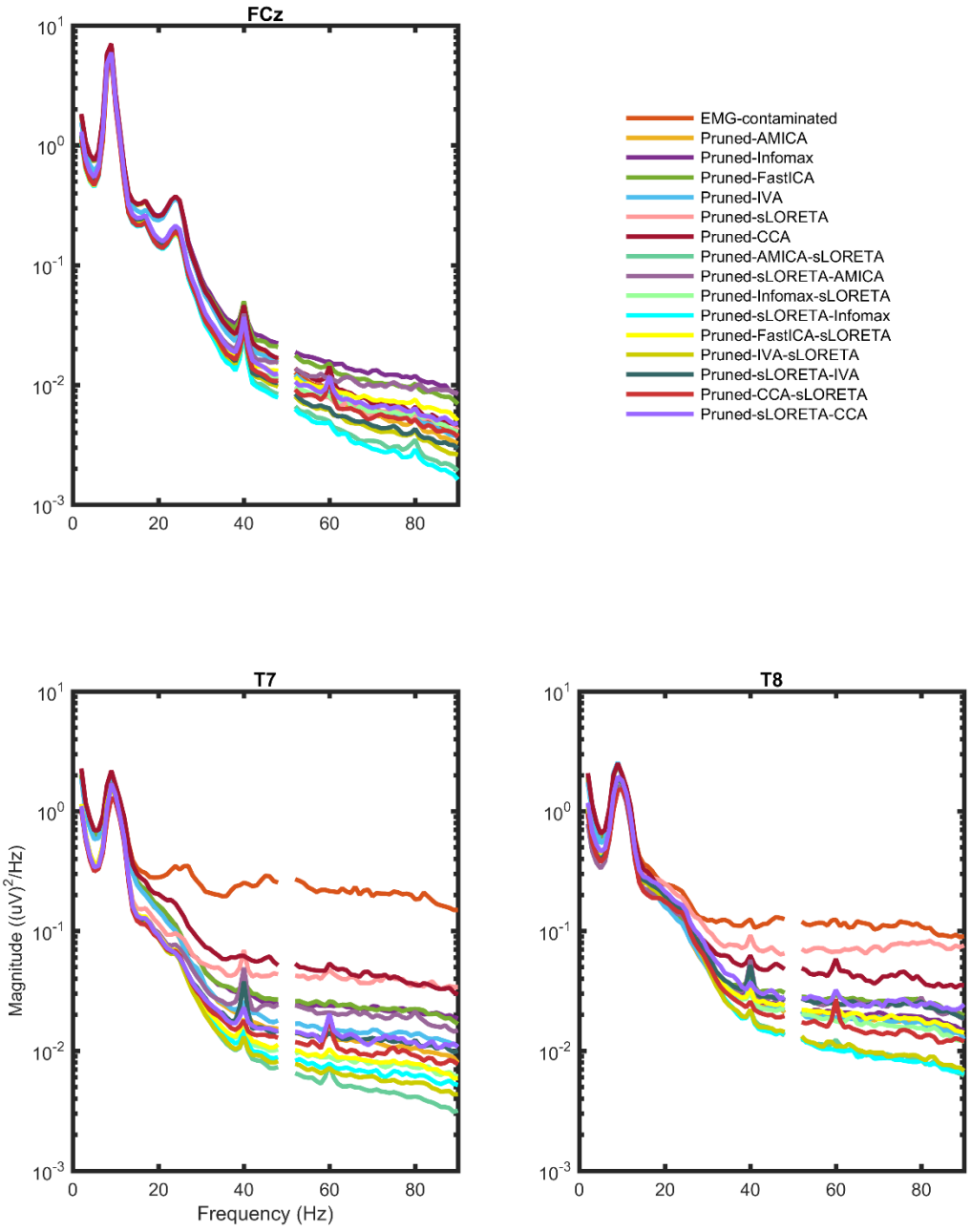

Figure 6-9: From dataset 2, mean of thirteen subjects' power spectra at T7 (left), FCz (middle), and T8 (right) in response to auditory simulation at 40 Hz. The steady state response peak is apparent in all single-pruned and double-pruned data, despite it not being apparent in EMG-contaminated spectra at peripheral channels. Note that the peak around 60 Hz which is disclosed in some double-pruned spectra is a VSSR due to the 60 Hz refresh rate of the monitor due to three subjects who opened their eyes during this task.

6.3.3 Large sample

To investigate the effect of the double-pruning approaches on a large sample, they were applied on dataset 3 consisting of a large number of healthy participants. Figure 6-10 shows the Berger effect, reduction of alpha activity (8-13 Hz) in eyes open task, and the VSSR caused by the 60 Hz refresh rate of the monitor, a peak at 60 Hz in the eyes open task. The 60

Hz VSSR peak is disclosed in the eyes open task in all pruned spectra except pruned-sLORETA. Figure 6-11 shows the relative spectra of eyes closed to eyes open to illustrate the Berger effect and 60 Hz VSSR more noticeably. The Berger effect is substantially unchanged by the double-pruning and single-pruning approaches, and the expected VSSR peak is enhanced by pruning.

ANOVA analysis showed that there is no significant effect for signal in the relative power in the alpha band ($F = 0.22$, $p = 0.99$). However, there is a significant difference in the height of the VSSR peak in the eyes open task ($F = 5.98$, $p < 0.001$). Post hoc results are shown at Table 6-6. EMG-contaminated and pruned-sLORETA are significantly different to all other pruned data, but no significant difference was found between pruned-sLORETA and EMG-contaminated. This indicates that other single-pruning and double-pruning approaches outperform sLORETA in disclosing brain activity. Moreover, pruned-Infomax-sLORETA was also significantly different to pruned-FastICA, Pruned-CCA, and pruned-IVA. This indicates that this double-pruning approach outperforms FastICA, CCA and IVA in disclosing brain activity. No significant difference was found between any other pairing of single-pruned or double-pruned data. These results are consistent with the double-pruning approaches reducing tonic muscle activity while keeping or disclosing brain neurophysiological responses.

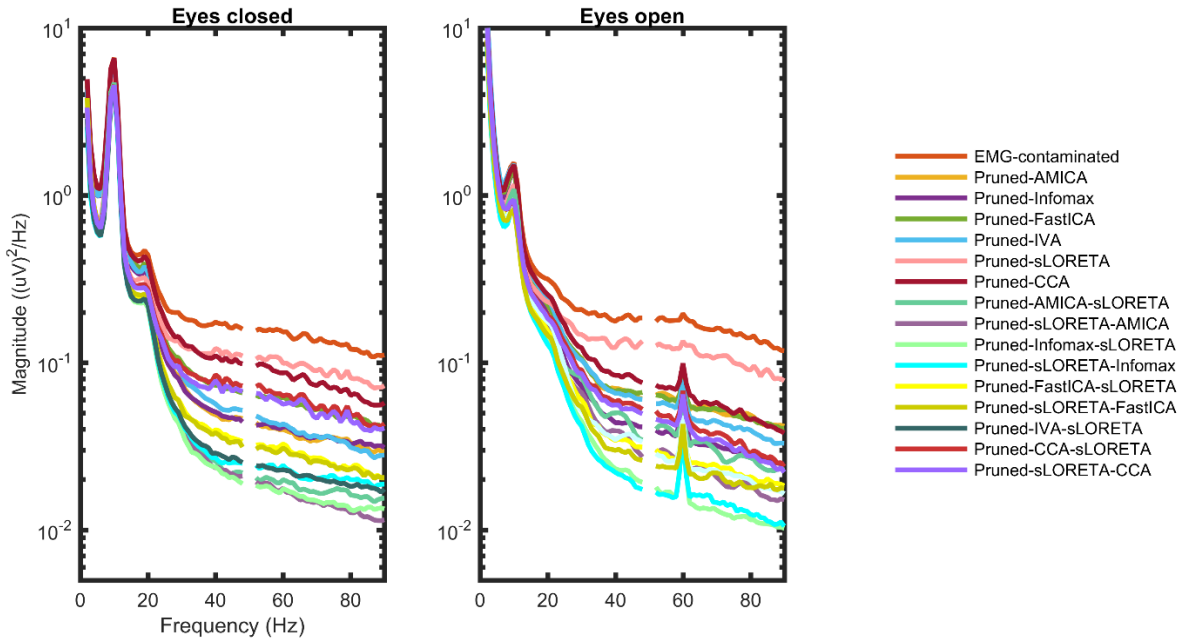

Figure 6-10: From dataset 3, mean of 93 subjects' spectra (eyes closed and eyes open) at Oz. The power at 10 Hz, alpha activity, is decreased in eyes open task. The 60 Hz VSSR peak is disclosed in eyes open task in all single-pruned and double-pruned spectra except pruned-sLORETA.

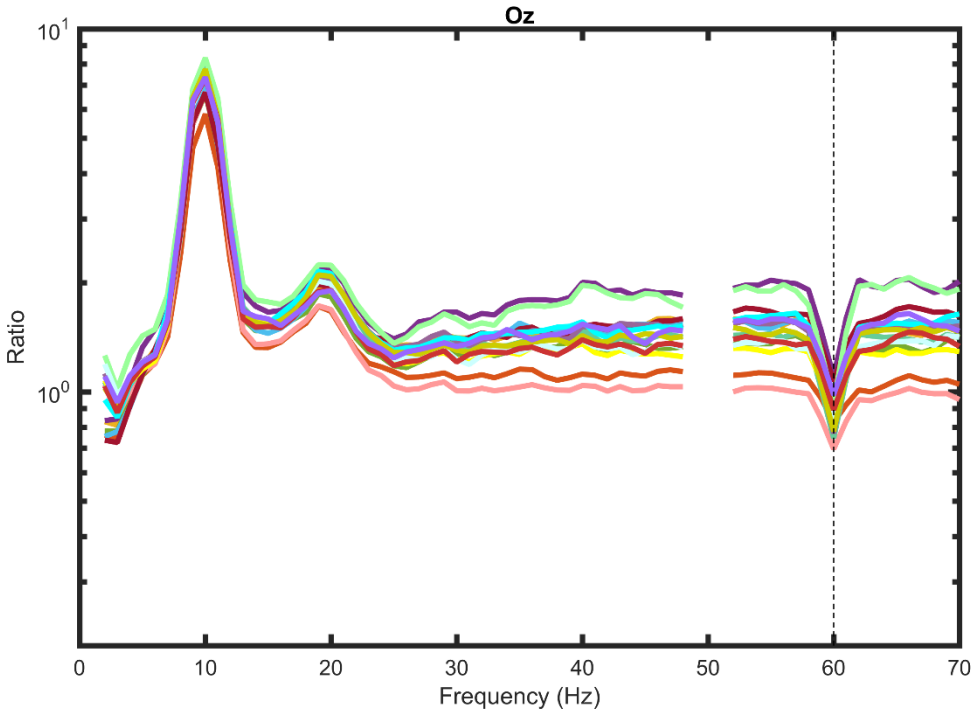

Figure 6-11: From dataset 3, averaged relative power spectra (eyes closed to eyes open) of healthy 93 subjects at Oz. The Berger effect is substantially unchanged by pruning, and the expected VSSR peak is enhanced by pruning.

Table 6-6: Post hoc results for the factor of signal for the VSSR peak in the eyes open task.

	EMG-contaminated	Pruned-AMICA	Pruned-Infomax	Pruned-FastICA	Pruned-IVA	Pruned-sLORETA	Pruned-CCA	Pruned-AMICA-sLORETA	Pruned-sLORETA-AMICA	Pruned-Infomax-sLORETA	Pruned-sLORETA-Infomax	Pruned-FastICA-sLORETA	Pruned-sLORETA-FastICA	Pruned-IVA-sLORETA	Pruned-sLORETA-IVA	Pruned-CCA-sLORETA	Pruned-sLORETA-CCA
EMG-contaminated		**0.03**	**0.002**	**0.03**	**0.01**	0.99	**0.04**	**<0.001**	**<0.001**	**<0.001**	**<0.001**	**0.04**	**0.004**	**0.001**	**<0.001**	**0.01**	**0.04**
Pruned-AMICA			1.00	0.99	1.00	**0.01**	0.99	0.85	0.82	0.15	1.00	1.00	1.00	1.00	1.00	1.00	1.00
Pruned-Infomax				0.69	0.99	**0.01**	0.88	0.99	0.99	0.56	0.95	1.00	1.00	1.00	1.00	1.00	1.00
Pruned-FastICA					0.99	**0.04**	1.00	0.06	0.06	**0.006**	0.14	0.97	0.74	0.54	0.82	0.99	0.98
Pruned-IVA						**0.04**	1.00	0.45	0.43	**0.03**	0.24	1.00	0.99	0.98	0.99	1.00	1.00
Pruned-sLORETA							**0.04**	**0.002**	**0.002**	**<0.001**	**<0.001**	**0.004**	**0.002**	**0.01**	**0.008**	**0.004**	**0.007**
Pruned-CCA								0.10	0.10	**0.002**	0.4	0.99	0.90	0.76	0.85	1.00	0.99
Pruned-AMICA-sLORETA									1.00	0.99	1.00	0.89	0.99	0.99	0.98	0.67	0.87
Pruned-sLORETA-AMICA										0.99	1.00	0.88	0.99	0.99	0.95	0.65	0.85
Pruned-Infomax-sLORETA											1.00	0.22	0.61	0.80	0.85	0.83	0.19
Pruned-sLORETA-Infomax												0.71	0.96	0.99	0.98	0.43	0.66
Pruned-FastICA-sLORETA													1.00	1.00	1.00	1.00	1.00
Pruned-sLORETA-FastICA														1.00	1.00	0.99	1.00
Pruned-IVA-sLORETA															0.99	0.99	0.99
Pruned-sLORETA-IVA																0.99	0.99
Pruned-CCA-sLORETA																	1.00
Pruned-sLORETA-CCA																	

6.4 Discussion and conclusion

The standard approaches to muscle reduction in different EEG toolboxes are the application of an ICA algorithm or BSS-CCA algorithm to SERs. Components are then classified by visual inspection of component properties such as their time-frequency characteristics or topographic maps (Delorme & Makeig 2004; Oostenveld et al. 2010). Those identified as muscle components are then discarded. My experience is that the application of multiple BSS algorithms to SERs (or multiple-pruning) is not normally possible, as the data is not full rank after the first pruning. Consistent with my experience, there are no publications presenting any such double-pruning approaches. Therefore, I have only tested combinations of single BSS algorithms with sLORETA.

Overall, double pruning approaches outperform single pruning approaches in removing tonic muscle contamination. Significant differences between double pruned and single pruned data are mostly found in higher frequency bands or at peripheral channels. This is due to greater muscle power in higher bands, and greater muscle contamination at peripheral channels which are located close to cranial and upper cervical muscles. Therefore, lower frequency bands or central channels are less affected by muscles, and hence fewer significant differences can be found between double-pruned and single-pruned data.

The literature reports that the traditional BSS-CCA methods outperform ICA methods in removing **phasic** muscle contamination from SERs (De Clercq et al. 2006; Gao, Zheng & Wang 2010; Karhunen, Hao & Ylipaavalniemi 2012). Phasic muscle signals are the result of voluntary muscle contraction and their spectra has high power in all frequency bands. (Goncharova et al. 2003). Therefore, phasic muscle signals are comparable to high frequency tonic muscle signals (>100 Hz). Under this comparison, I can conclude that my result is consistent with the literature. My finding was that, among the single pruning approaches, extended-CCA outperforms other approaches and is comparable to double pruning

approaches in removing **tonic** muscle contamination at **higher frequency bands** (>100 Hz). Hence, when there is more muscle power (phasic muscle or high frequency tonic muscle) extended-CCA outperforms ICA. However, when there is less muscle power (low frequency tonic muscle), I found that AMICA and Infomax beat extended-CCA. This indicates that findings on phasic muscle artefact do not completely apply to tonic muscle artefact, but there are some similarities.

Overall, it can be suggested that Infomax-sLORETA is the best double-pruning approach. No other algorithm removes more muscle contamination, and only AMICA-sLORETA equals it in pruning performance in all comparisons. Similarly, Infomax-sLORETA and AMICA-sLORETA perform equivalently in retaining brain neurophysiological responses. However, Infomax-sLORETA weakly outperforms AMICA-sLORETA in disclosing brain neurophysiological responses that are not visible in EMG-contaminated data. While the two approaches are not statistically significantly different, Infomax-sLORETA achieves significant differences to more single-pruning approaches than AMICA-sLORETA does.

In this study, I compared different single pruning and double pruning approaches based on the amount of muscle removal at various locations and frequency bands, and based on the retention or disclosure of brain neurophysiological responses. However, there are other factors that may influence the choice of a pruning approach for a particular study. Such factors may include memory requirements and computation time, and how they scale with both the number of channels and the number of samples. Consideration of all these factors in comparing algorithms is beyond the scope of this thesis and needs more investigation.

There are some research questions where it may be appropriate to use a single-pruning approach, for example, when there is little muscle artefact (e.g. where the research is considering only low frequency phenomena, such as alpha or lower frequencies), and when execution time is an issue (e.g. when there are many participants, or the analysis needs to

happen promptly on limited hardware). In such cases, Infomax and AMICA are the best choices. They are equal to each other in pruning performance and retention of brain neurophysiological responses in all comparisons. However, the general view and my experience is that Infomax converges faster that AMICA, and hence it is a better choice. Other research questions are focussed on higher frequencies, where the muscle artefact is large. For example, there are some studies, mostly on epileptic seizure spikes, that are interested in high frequency oscillations in the ripple band (80-250 Hz) of SERs (Kuhnke et al. 2018; Worrell 2012; Zijlmans et al. 2012). The speed of extended-CCA, combined with performance equal to double-pruning approaches at high frequency bands, would make it the best choice for these kinds of study.

Chapter 7

A new approach in quantifying cranial muscle activity

Previous chapters discussed using BSS to reduce cranial tonic muscle activity in SERs. However, in this chapter, I propose an inverted application of BSS algorithms. As discussed in Chapter 3, it is possible to identify and remove muscle activity from SERs using the BSS algorithms. Therefore, it is equally feasible to identify and retain muscle activity from SERs and accurately quantitate the power corresponding to muscle activity. In this chapter, I utilise the myogenic components from Infomax in a new approach to quantitate cranial and upper cervical muscle activity. This approach was firstly validated on disease groups generally known as having increased muscle tension, and then tested on migraineurs to address one of my revised research questions.[8]

7.1 Limitation of previous studies on cranial muscle activity of migraineurs

The International Classification of Headache Disorders (ICHD) considers muscle to be "the most significant abnormal finding" in tension-type headache, but the word "muscle" is not even mentioned in its definition of migraine (Headache Classification Committee of the International Headache 2013). There have been many studies since the 1970s examining the

[8] The published journal paper in Appendix A-3 contains a significant part of this chapter. The paper does not contain the validation on three disease groups (Section 7.7), nor the exploration on a further three disease groups (Section 7.9). Additionally, this chapter has an expanded discussion and conclusion.

role of muscle in migraine as well as in tension-type headache, mostly qualitative (Ahles et al. 1988; Bakal & Kaganov 1977; Bakke et al. 1982; Blaschek et al. 2012; Blau & MacGregor 1994; Burnett et al. 2000; Celentano, Stewart & Linet 1990; Clifford et al. 1982; Didier et al. 2015; Ebinger 2006; Fernández-de-las-Peñas et al. 2008; Hagen et al. 2002; Hung et al. 2008; Jensen et al. 1993; Landgraf et al. 2015; Lebbink, Spierings & Messinger 1991; Leistad et al. 2006; Lous & Olesen 1982; Oksanen et al. 2008; Tfelt-Hansen, Lous & Olesen 1981; Watson & Drummond 2012). Their conclusions disagree, but many do conclude there is a link between migraine and muscle activation. Here I limit myself to reviewing quantitative studies of migraine.

While many studies have focussed on tension-type headache, they sometimes have included migraine groups for comparison. The methods of quantitation of muscle activity in these studies differ, such that it is difficult to make robust comparisons and identify a clear conclusion. There are differences in recording EMG (surface or needle recordings), differences in muscles sampled, differences in headache phase (viz. inter-ictal, pre-ictal, ictal, post-ictal) and differences in activity state (at rest or during instructed contraction or during head postures). The extracted measures of EMG activity include median frequency, mean frequency and root mean square power.

The findings have not pointed to a consistent alteration in muscle activity. Bakal et al. (1977) reported migraine patients had higher frontalis EMG as well higher neck EMG activity than tension-type headache patients and headache-free controls. McArthur et al. (1980) reported migraine patients had higher frontalis EMG activity than tension-type headache patients and headache-free controls. Anderson et al. (1981) reported that frontalis EMG does not distinguish between tension-type and migraine headaches. Clifford (1982) reported that, during attacks, migraineurs had activity in the anterior temporal muscles which exceeded the patient's own baseline recordings and that all muscles were activated more strongly than in

the control period. Similarly, Bakke (1982), reported a rise in activity from control levels shortly before migraine patients self-reported experiencing maximal pain. Ahles et al. (1988) reported higher levels of muscle activity (frontalis, trapezius) in three headache groups (migraine with aura, migraine without aura, tension-type headache) compared to a non-headache group, but no difference between the three groups. Jensen et al. (1994) could not identify EMG measures that correlated with 'migraine severity in the previous year' (though increased EMG measures were seen in patients with 'chronic headache'), and there was no relationship between muscle activity and migraine generally.

7.2 New approach in quantitating cranial muscle activity

As discussed in Chapter 3, it is possible to identify and discard muscle activity from SERs using BSS algorithms, usually with the aim of extracting clean EEG. Therefore, it is equally feasible to retain muscle activity from SERs and accurately quantitate the power corresponding to muscle activity. In other words, the myogenic components from BSS can be utilised to quantitate cranial and upper cervical muscle activity. Hence this approach, unlike EMG recordings with surface or needle electrodes, is not restricted to recording the activity of individual muscles or the localised activity of some part of individual muscles. In contrast, it is possible to quantitate the combined activity of all cranial and upper cervical muscles using a high-density SER cap and a BSS algorithm. The cap covers the activity of all cranial and upper cervical muscles, for example, there are electrodes over frontalis, orbicularis and temporalis muscles, and also close to nuchal (upper cervical) muscles.

I utilised the myogenic components from Infomax to quantitate cranial and upper cervical muscle activity. I selected Infomax since it is a popular choice in neuroscience and provides a good separation of components in a reasonable time (Dharmaprani et al. 2016). This supported by the results in Chapter 3 and Chapter 6, which show that no other algorithm outperforms it.

To quantitate cranial muscle activity, all the procedures described in Section 3.2.2 were followed, but the identified muscle components were preserved while the remaining components were discarded. Then surface SER were reconstructed using the preserved muscle components and the mixing matrix.

Thus, the power of reconstructed SERs at each electrode location determines the contribution of cranial and upper cervical muscle activity to that specific location. I separated the SER channels into five groups for analysis based on their location in the 10-5 system as shown in Figure 7-1.

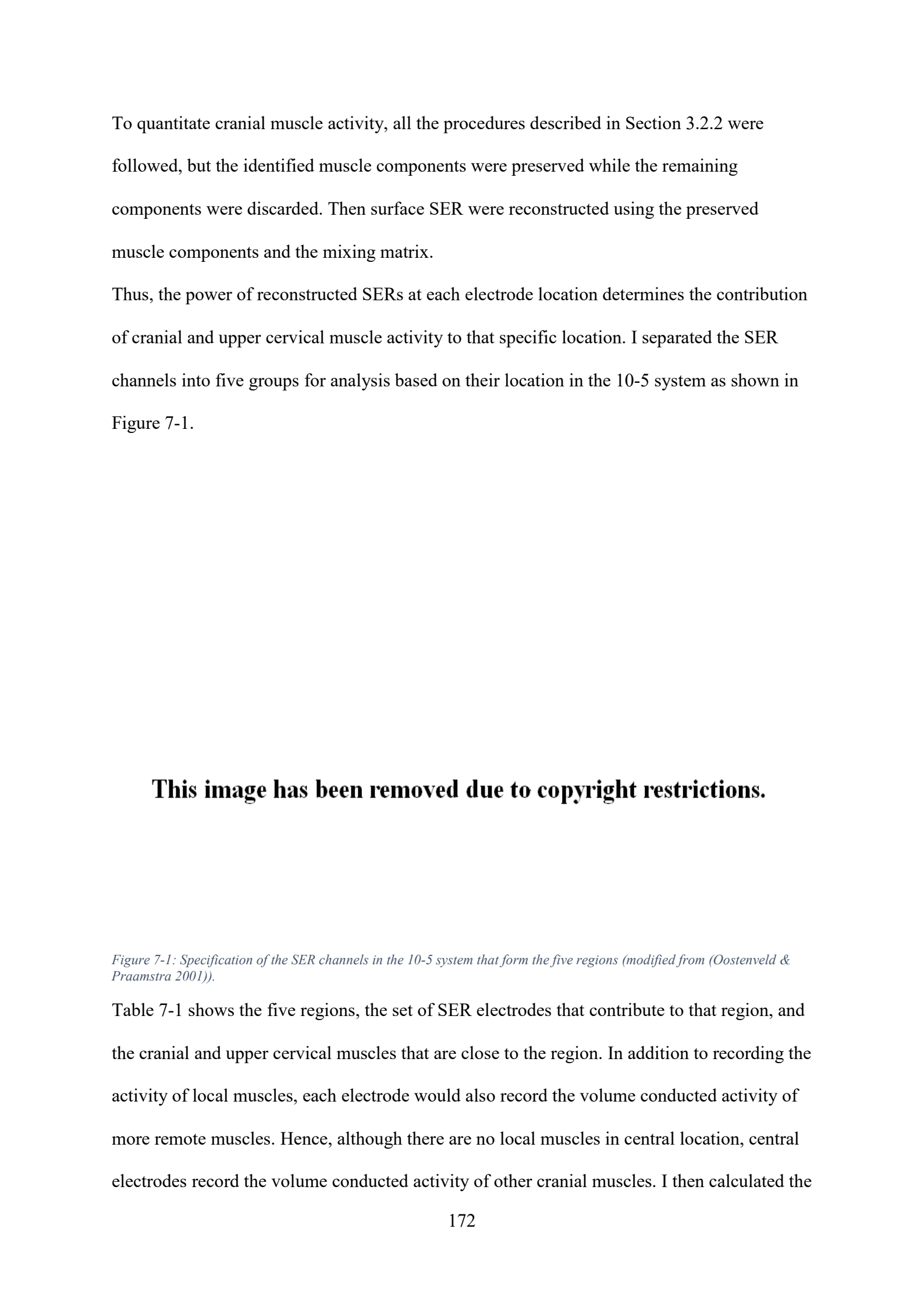

Figure 7-1: Specification of the SER channels in the 10-5 system that form the five regions (modified from (Oostenveld & Praamstra 2001)).

Table 7-1 shows the five regions, the set of SER electrodes that contribute to that region, and the cranial and upper cervical muscles that are close to the region. In addition to recording the activity of local muscles, each electrode would also record the volume conducted activity of more remote muscles. Hence, although there are no local muscles in central location, central electrodes record the volume conducted activity of other cranial muscles. I then calculated the

average power spectrum for each region, reported in dB (zero reference level 0 $dB = 1$ $(uV^2)/Hz$).

Table 7-1: Five regions, the SER electrodes within each region, and the local muscles that provide the strongest signals to recordings at these electrodes.

Regions	***SER electrodes***	***Local Muscles***
Frontal	Fp1, Fpz, Fp2, AFp1, AFp2, AF7, AF3, AFz, AF4, AF8, F3, F1, Fz, F2, F4	Frontalis, procerus, and orbicularis oculi
Left temporal	FT9, FT7, FTT9h, TPP9h, T9, T7, TP9, TP7	Temporalis and superior auricularis
Central	FC1, FCz, FC2, FCC1h, FCC2h, C1, Cz, C2, CCP1h, CCP2h, CP1, CPz, CP2	None
Right temporal	FT10, FT8, FTT10h, TPP10h, T10, T8, TP10, TP8.	Temporalis and superior auricularis
Occipital	O1, Oz, O2, O11h, O12h, PO9, I1, Iz, I2, PO10	Occipitalis, trapezius, splenius capitis and sub-occipital muscles

To validate the approach of cranial muscle quantitation, it was first applied to SERs of subjects suffering from diseases known to cause extra muscle tension. For example, one of the main symptoms of Parkinson's disease (PD) is muscle rigidity or stiffness which can affect 89% to 99% of patients (Gelb, Oliver & Gilman 1999; Louis et al. 1997; Martin et al. 1973). Moreover, studies have revealed that muscle tension is one of the main features of generalized anxiety disorder (Rowa & Antony 2008, Hazlett, 1994 #311), and the mean level of muscle activity is greater in people with anxiety than controls (Conrad & Roth 2007; Pluess, Conrad & Wilhelm 2009). Furthermore, spasticity and muscle contracture are recognized in many people following stroke (O'Dwyer, Ada & Neilson 1996; Sommerfeld et al. 2004; Watkins et al. 2002). Spasticity arises when there is damage to posture-governing

pathways arising from both forebrain and brainstem levels (Kandel et al. 2000) resulting in excessive contraction of agonist and/or antagonist muscles, causing increased muscle tone. After validating the cranial muscle quantitation approach, it was tested on migraine sufferers to explore if cranial and upper cervical muscle activity is increased in migraineurs.

7.3 Dataset

7.3.1 Subjects

As discussed in Section 3.1, I had access to three different datasets. Dataset 3 consists of 626 SERs collected from participants with a range of neurological and psychological disorders and controls, allowing the investigation of changes in brain rhythms with disease. All participants were recruited from the clinics and staff of the Flinders Medical Center, or their relatives, between 2004 to 2007. All patients were examined by a neurologist and those with a single neuro-psychiatric diagnosis were included. Note that some participants initially recruited as controls were diagnosed as migraineurs after the medical examination.

For this study, I only analyse the recorded data from migraineurs and from controls who had no history of headache. Sufficient clinical information was recorded for accurate diagnosis: migraine diaries were not used, so the full suite of migraine expression is not known. In addition, while all patients were without headache on the day of recording, it is not known how long they remained headache-free. Diagnosis was validated by another neurologist using the 2013 ICHD-III-beta diagnostic criteria (Headache Classification Committee of the International Headache 2013), based on a review of their records.

This resulted in a dataset consisting of different groups: 65 healthy participants with no history of headache, 26 migraine participants, 12 with PD, 9 with anxiety disorder, 13 with dementia, 10 with stroke, 18 with schizophrenia, and 24 with Childhood Absence Epilepsy (CAE). Table 7-2 shows the demographic details of the participants. Note that the gender distribution and age range of disease groups are close to the population expectations, for

example 67% of the migraineurs are female, and the Parkinson's disease participants have a higher average age. Given the high inter-individual variability of muscle activity, the maximum number of participants was included.

The migraine participants all described their pain intensity as three or four out of five (moderate or severe) with a mean intensity of 3.9. The maximum number of attacks per year was 104, about 70% of the migraine participants had a frequency of less than one attack in a month, and the mean frequency was 0.98 per month. 11 participants reported migraines lasting for a few hours, and 15 reported durations of a few days. 50% had migraine with aura. From the CAE group, 17 participants were using sedative drugs such as valproate, phenytoin, and carbamazepine, and the rest were drug-free or only on a non-sedative drug (lamotrigine).

Table 7-2: Subject Demographics

Participants	**Age (years)** (mean ± SEM)	**Females**	**Males**
Migraine	48.6 ± 13	19	7
PD	65 ± 8.1	3	9
Anxiety disorder	40.4 ± 14.6	4	5
Dementia	77.38 ± 8.9	6	7
Stroke	62.8 ± 14.6	2	8
Schizophrenia	46.9 ± 12	10	8
CAE	22.58 ± 11.9	18	6
Control	46.2 ± 17.2	33	32

Scalp electrical activity was recorded from each participant while sitting, head un-supported, in a stable 23-24º C temperature. One technician applied the electrodes and undertook recordings. No adaptation time was provided, nor judged to be necessary, as the recording environment was shown to participants before the electrode cap was applied – they knew where they would be sitting. Instructions were presented both verbal and written, using a computer-based bio-behavioural instruction program.

7.3.2 Migraine severity

I characterized migraine severity using three measures: duration, frequency and intensity. The patient-estimated duration was recorded as hours or days. Patient-estimated frequency was recorded as a count per year. Patient-estimated intensity was recorded on the scale 1-5, using descriptors dull, mild, moderate, severe or excruciating.

7.4 Power spectra

Welch's modified periodogram with one-second Hanning windows was implemented to compute the power spectra of components and also of reconstructed SERs. To estimate the level of muscle activity, I chose the average power in the band 52-98 Hz. This band, named as gamma 3 in Section 3.2.6, covers the frequencies where muscle power is highest, while avoiding mains power interference.

7.5 Statistical method

After confirming the data were normally distributed using a Lilliefors test, a regular four-way parametric ANOVA was used to compare the power of tonic muscle activity against factors of gender (female, male), task (eyes closed, eyes open), region (frontal, left-temporal, central, right-temporal, occipital) and condition (disease, control). Post hoc tests on significant factors used Tukey's honest significant difference criterion for the multiple comparisons. A five percent level of significance was utilized throughout.

7.6 Linear regression

Linear regression analysis was implemented to test for a relationship between the severity of the headache and the power of muscle activity. 89 of 91 participants reported intensity as none (controls) or severe, and duration was reported as either "hours" or "days", i.e. these measures provided only two sufficiently populated abscissa points. Hence I excluded intensity and duration from the linear regression analysis, retaining only frequency. Muscle

activity was regressed against frequency for all combinations of task and region, and adjusted for multiple comparisons using Bonferroni correction.

7.7 Validation of the proposed approach

To validate the approach of cranial muscle quantitation, it was applied on SERs of subjects suffering from diseases causing extra muscle tension. Finding significantly increased cranial and upper cervical muscle activity in these groups of patients would validate the efficacy of this new muscle quantitation approach.

7.7.1 PD vs control

The mean muscle power for each group (PD and control) and each baseline task (eyes closed and eyes open) at 52-98 Hz has been illustrated topographically in Figure 7-2. Dark red indicates the highest muscle power while dark blue indicates the least muscle power. Visual inspection reveals similar distributions of muscle power across the head, but with increased muscle power both centrally and peripherally in the Parkinson's group.

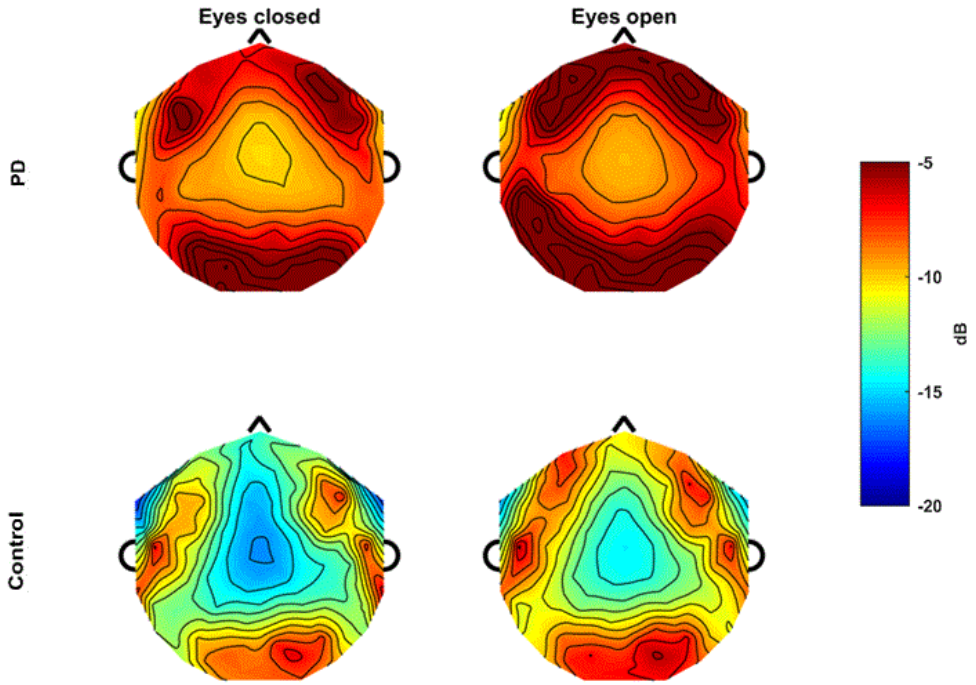

Figure 7-2: Mean muscle power in the gamma3 band for PD subjects (top row) and control subjects (bottom row) and eyes closed (left column) and eyes open tasks (right column).

Statistical analysis revealed a significant difference in muscle power based on condition, task, and location, but no significant differences were found for gender, nor in any interaction between the factors. I consider each significant factor in turn below.

Table 7-3 shows the result of the post hoc test comparing muscle activity between the PD and control groups. The muscle activity in the PD group is statistically greater than muscle activity in the control group ($F=55.15$, $p<0.001$). Overall, Parkinson subjects have 5dB or approximately three times more cranial and upper cervical muscle activity than control subjects. This result is consistent with rigidity and stiffness in PD sufferers.

Table 7-3: Mean muscle power (mean ± SEM) for each condition, and post hoc test p value comparing between conditions.

Condition	Number of participants	Mean of muscle power (dB)	p value
PD	12	-9.74 ± 0.68	**<0.001**
Control	65	-14.78 ± 0.25	

As shown in Table 7-4, the amount of muscle activity during eyes open is significantly more than in eyes closed ($F=11.2$, $p=0.001$), by 2.08 dB or approximately 61%.

Table 7-4: Mean muscle power (mean ± SEM) for each task, and post hoc test p value comparing between tasks.

Task	Mean of muscle power (dB)	p value
Eyes open	-13.30 ± 0.48	**0.001**
Eyes closed	-11.22 ± 0.48	

The muscle activity in the five regions (frontal, left temporal, central, right temporal, and occipital) was compared on a pairwise basis, shown in Table 7-5. The power in the occipital region is statistically greater than all other locations except frontally. Central power is also statistically less than frontal, consistent with the absence of local muscles in the central region.

Table 7-5: Mean muscle power (SEM = 0.74 dB) for each region, and post hoc test p values comparing between pairs of regions.

Region	Occipital	Right temporal	Central	Left temporal	Frontal
Power (dB)	-8.9	-13.04	-15.01	-12.93	-11.43
Frontal	0.1	0.52	**0.005**	0.59	
Left temporal	**0.009**	0.99	0.26		
Central	**< 0.001**	0.31			
Right temporal	**0.006**				

7.7.2 Anxiety vs control

Figure 7-3 shows the topographic map of the mean muscle power for each group (anxiety disorder and control) and each baseline task (eyes closed and eyes open) in the gamma3 band. Visually, the distribution of muscle power across the head is similar in both groups, but the anxiety disorder group has more muscle power, especially peripherally.

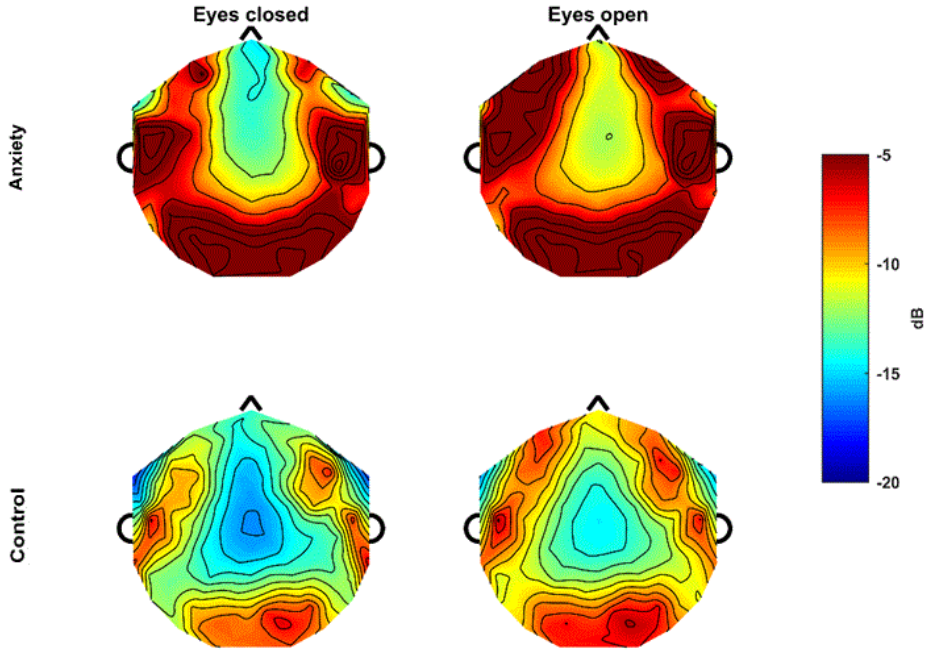

Figure 7-3: Mean muscle power in the gamma3 band for anxiety subjects (top row) and control subjects (bottom row) and eyes closed (left column) and eyes open tasks (right column).

Statistical analysis revealed a significant difference in muscle power based on condition, task, and location, but no significant differences were found for gender, nor in any interaction between the factors. Each significant factor is considered in turn below.

Table 7-6 shows the result of the post hoc test comparing muscle activity between the anxiety disorder and control groups. The muscle activity in the anxiety group is statistically greater than muscle activity in the control group ($F=63.92$, $p<0.001$). Overall, anxiety disorder subjects have 6.4 dB or approximately four times more cranial and upper cervical muscle activity than control subjects. This result is consistent with increased muscle tension in anxiety disorder.

Table 7-6: Mean muscle power (mean ± SEM) for each condition, and post hoc test p value comparing between conditions.

Condition	Number of Participants	Mean of muscle power (dB)	p value
Anxiety disorder	9	-8.41 ± 0.75	**<0.001**
Control	65	-14.78 ± 0.25	

As shown in Table 7-7, the amount of muscle activity during the baseline eyes open is significantly more than in the baseline eyes closed ($F=6.15$, $p=0.01$), by 1.9 dB or approximately 54%.

Table 7-7: Mean muscle power (mean ± SEM) for each task, and post hoc test p value comparing between tasks.

Task	Mean of muscle power (dB)	p value
Eyes open	-10.63 ± 0.55	**0.01**
Eyes closed	-12.56 ± 0.55	

The muscle activity in the five regions (frontal, left temporal, central, right temporal, and occipital) was compared on a pairwise basis, shown in Table 7-8. The power in the occipital region is statistically greater than all other locations. Central power is also statistically less than temporal, consistent with the absence of local muscles in the central region.

Table 7-8: Mean muscle power (SEM = 0.82 dB) for each region, and post hoc test p values comparing between pairs of regions.

Region	Occipital	Right temporal	Central	Left temporal	Frontal
Power (dB)	-7.71	-11.99	-14.72	-10.93	-12.62
Frontal	**0.006**	0.98	0.43	0.64	
Left temporal	**0.05**	0.97	**0.01**		
Central	**< 0.001**	**0.01**			
Right temporal	**0.004**				

7.7.3 Stroke vs control

The mean muscle power for each group (stroke and control) and each baseline task (eyes closed and eyes open) in the gamma3 band has been illustrated topographically in Figure 7-4. Visual inspection reveals more muscle activity in the stroke group, especially during the eyes open task, and some similarity in distribution between the groups, especially during eyes closed task.

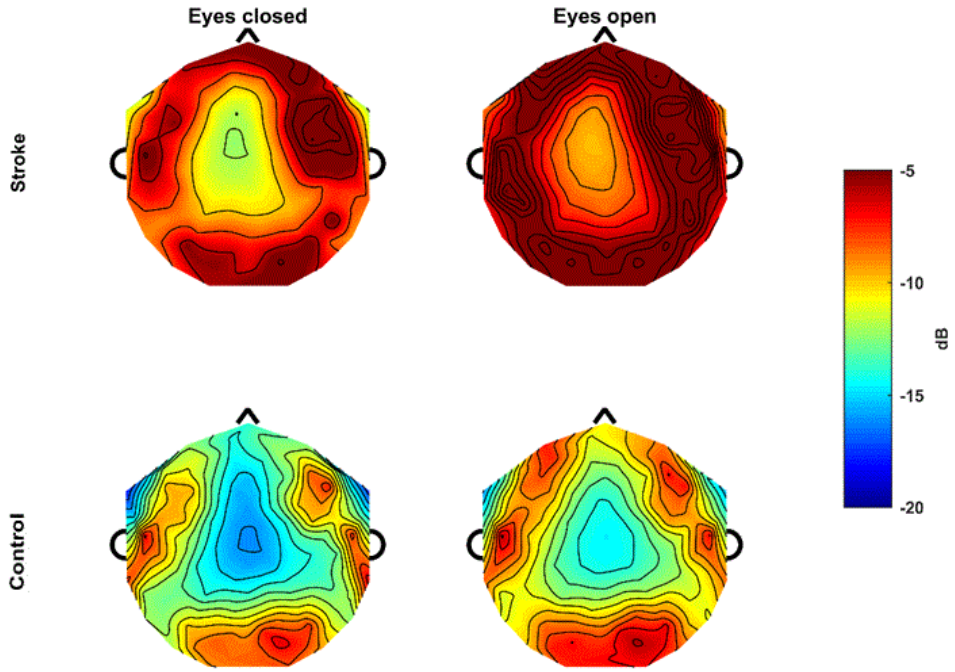

Figure 7-4: Mean muscle power in the gamma3 band for stroke subjects (top row) and control subjects (bottom row) and eyes closed (left column) and eyes open tasks (right column).

Statistical analysis revealed a significant difference in muscle power based on condition, task, and location, but no significant differences were found for gender, nor in any interaction between the factors. Each significant factor is considered in turn below.

Table 7-9 shows the result of the post hoc test comparing muscle activity between the stroke and control groups. The muscle activity in the stroke group is statistically greater than muscle activity in the control group ($F=24.78$, $p<0.001$). Overall, stroke subjects have 4.3 dB or 2.5 times more cranial and upper cervical muscle activity than control subjects. This result is consistent with spasticity and contracture that most people experiencing after the stroke.

Table 7-9: Mean muscle power (mean ± SEM) for each condition, and post hoc test p value comparing between conditions.

Condition	Number of Participants	Mean of muscle power (dB)	p value
Stroke	10	-10.49 ± 0.82	**<0.001**
Control	65	-14.78 ± 0.25	

As shown in Table 7-10, the amount of muscle activity during baseline eyes open is significantly more than in baseline eyes closed (F=6.75, p=0.009), by 1.9 dB or approximately 54%.

Table 7-10: Mean muscle power (mean ± SEM) for each task, and post hoc test p value comparing between tasks.

Task	Mean of muscle power (dB)	p value
Eyes open	-11.70 ± 0.56	**0.009**
Eyes closed	-13.57 ± 0.56	

The muscle activity in the five regions (frontal, left temporal, central, right temporal, and occipital) was compared on a pairwise basis, shown in Table 7-11. The power in the central region is statistically less than all other regions. This is consistent with the absence of local muscles in the central region.

Table 7-11: Mean muscle power (SEM = 0.84 dB) for each region, and post hoc test p values comparing between pairs of regions.

Region	Occipital	Right temporal	Central	Left temporal	Frontal
Power (dB)	-10.32	-12.87	-15.45	-12.32	-12.20
Frontal	0.46	0.97	**0.03**	0.99	
Left temporal	0.40	0.98	**0.04**		
Central	**< 0.001**	**0.04**			
Right temporal	0.16				

7.7.4 Validation results

Since the main purpose of this section was to validate the proposed muscle quantitation approach, the important part of the statistical analyses is the factor of condition. The literature reports an increase in muscle activity in each disease group compared to controls. All three disease groups showed a statistically significant increase in muscle activity compared to the control group, consistent with the literature. These results are strong evidence that the proposed muscle quantitation approach is appropriate to use prospectively on other disease

groups. However, none of the previous studies has reported on the cranial muscle topography or the size of cranial muscle increase in these diseases.

Additionally, significantly more cranial and upper cervical muscle activity in eyes open task is consistent with other reports. The significantly less muscle power in the central region is consistent with the absence of local muscles in the central region, and significantly greater muscle power in the occipital region is consistent with the activation of local occipital and upper cervical muscles even during the relaxed sitting task.

7.8 Testing of the proposed approach on migraineurs

After validating the proposed muscle quantitating approach, it was tested on the migraine group to compare their level of cranial and upper cervical muscle activity with the control group. Additionally, I tested for a linear relationship between the severity of the headache and the muscle power.

7.8.1 Migraine vs control

Figure 7-5 shows the topographic map of the mean muscle power for each group (migraine and control) and each baseline task (eyes closed and eyes open) in the gamma3 band. Visually, the distribution of muscle power across the head is similar in both groups, but migraineurs have more muscle power frontally and occipitally.

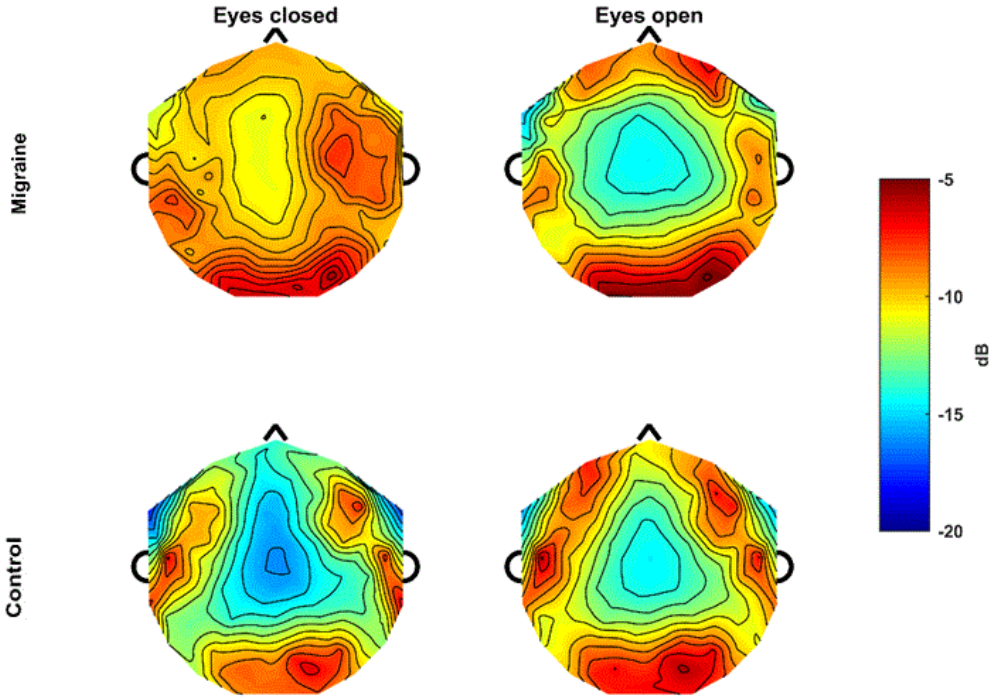

Figure 7-5: Mean muscle power in the gamma3 band for migraine subjects (top row) and control subjects (bottom row) and eyes closed (left column) and eyes open tasks (right column).

Statistical analysis revealed a significant difference in muscle power based on condition, task, and location, but no significant differences were found for gender, nor any interaction between the factors. Each significant factor is considered in turn below.

Table 7-12 shows the result of the post hoc test comparing muscle activity between the migraine and control groups. The muscle activity in the migraine group is statistically greater than muscle activity in the control group (F=4.85, p=0.02). Overall, migraine subjects have 1.2 dB or approximately 30% more cranial and upper cervical muscle activity than control subjects. This result provides preliminary evidence that increased cranial and upper cervical muscle activity is not restricted to tension-type headache, and there may be cranial muscle involvement in migraine.

Table 7-12: Mean muscle power (mean ± SEM) for each condition, and post hoc test p value comparing between conditions.

Condition	Number of Participants	Mean of muscle power (dB)	p value
Migraine	26	-13.61 ± 0.38	**0.02**
Control	65	-14.78 ± 0.25	

As shown in Table 7-13, the amount of muscle activity during baseline eyes open is significantly more than in baseline eyes closed (F=9.78, p=0.002), by 1.5 dB or approximately 40% more.

Table 7-13: Mean muscle power (mean ± SEM) for each task, and post hoc test p value comparing between tasks.

Task	Mean of muscle power (dB)	p value
Eyes open	-13.42 ± 0.30	**0.002**
Eyes closed	-14.92 ± 0.30	

The muscle activity in the five regions (frontal, left temporal, central, right temporal, and occipital) was compared on a pairwise basis, shown in Table 7-14. The power in the occipital region is statistically greater than all other regions. Central power is also statistically less than frontal and left temporal (and close to significantly different to right temporal), consistent with the absence of local muscles in the central region.

Table 7-14: Mean muscle power (SEM = 0.54 dB) for each region, and post hoc test p values comparing between pairs of regions.

Region	Occipital	Right temporal	Central	Left temporal	Frontal
Power (dB)	-11.21	-14.66	-16.64	-14.39	-13.42
Frontal	**0.002**	0.88	**0.003**	0.97	
Left temporal	**0.003**	0.99	**0.02**		
Central	**< 0.001**	0.06			
Right temporal	**< 0.001**				

7.8.2 Relation between muscle activity and severity of headache

Using linear regression, I tested for a relationship between frequency of headache and muscle activity. I pooled the data from males and females together since, based on the results of the ANOVA, no significant difference was found for the main factor of gender. As the factors of location and task were significant, I tested separately for each combination of location and task.

Tests were undertaken twice, once without control participants, and once including control participants with a frequency of zero since they had no history of headache. I decided to do the regression tests both with and without control subjects since I was not sure which one is

correct and including control participants could provide more subjects, and hence more power for the statistical analyses. However, no statistically significant relationship was found in any test (all $p>0.05$).

7.9 Exploration of the proposed method on other disease groups

I validated the proposed muscle quantitation approach by applying it to SERs of subjects suffering from diseases known to cause extra muscle tension. Then, this approach was tested on migraineurs to compare their level of cranial muscle activity with controls.

In our database, there are SERs of subjects suffering from other psychological diseases and brain disorders. There is some preliminary evidence that people suffering from some of these diseases may experience increased muscle tension. For example, it is reported that some cognitive and anxiety symptoms of dementia have overlap with generalized anxiety disorder, and some persons with dementia may also be recognized to suffer from anxiety (Calleo et al. 2011). Furthermore, anxiety disorder is often diagnosed among schizophrenia patients (Pallanti, Quercioli & Hollander 2004; Siris & Braga 2013), and progressive muscle relaxation is often effective in alleviating feelings of anxiety in these patients (Vancampfort et al. 2013; Vancampfort et al. 2011). Therefore, the proposed muscle quantitation approach was applied to the dementia and schizophrenia groups to compare their level of cranial and upper cervical muscle activity to controls to provide further evidence either for or against these hypotheses.

On the other hand, patients suffering from some brain diseases are prescribed sedative drugs that may relax the muscles. For example, some people with CAE are prescribed valproate, phenytoin, and carbamazepine. Valproate has sedative effect by enhancing GABA neurotransmission, resulting in a relaxing effect (Löscher 1999). Additionally, carbamazepine and phenytoin can both cause sedation as side effects by activing the GABA-induced current

in specific types of GABA receptors, namely the alpha 1, beta2, gamma2 receptor (Granger et al. 1995). Hence, the proposed muscle quantitation approach was applied to both sedative-free CAE patients and sedative-medicated[9] CAE patients to compare their level of cranial muscle power.

7.9.1 Dementia vs control

The mean muscle power for each group (dementia and control) and for each baseline task (eyes closed and eyes open) in the gamma3 band has been illustrated topographically in Figure 7-6. Visual inspection reveals similar distributions of muscle power across the head, but with increased muscle power in the dementia group.

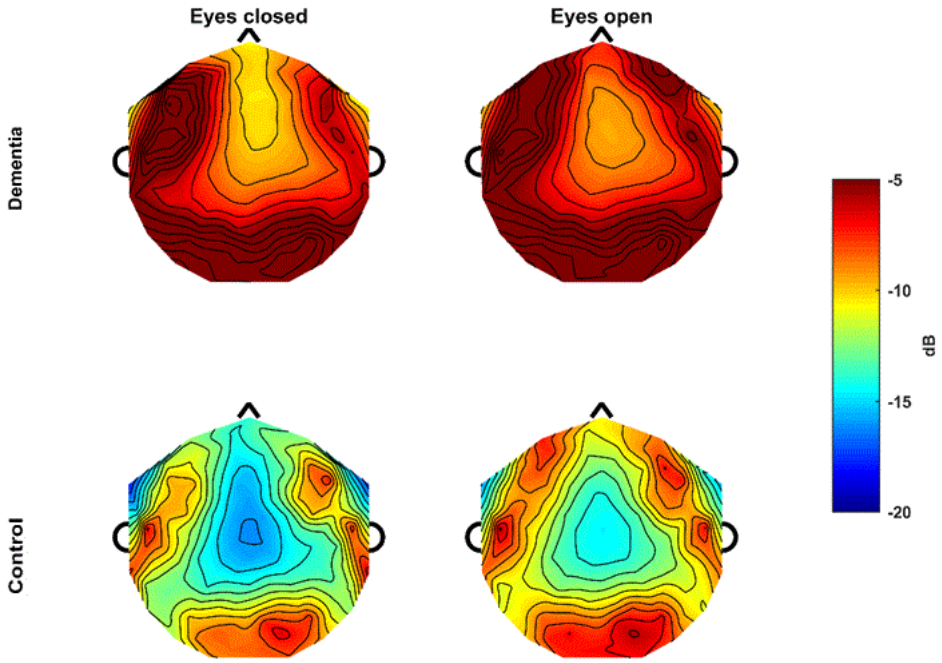

Figure 7-6: Mean muscle power in the gamma3 band for dementia subjects (top row) and control subjects (bottom row) and eyes closed (left column) and eyes open tasks (right column).

Statistical analysis revealed a significant difference in muscle power based on condition, task, and location, but no significant differences were found for gender, nor in any interaction between the factors. Each significant factor is considered in turn below.

[9] Here I use "sedative-medicated" to mean a patient whose medication includes at least one of the sedative drugs valproate, phenytoin and carbamazepine, but not lamotrigine.

Table 7-15 shows the result of the post hoc test comparing muscle activity between the dementia and control groups. The muscle activity in the dementia group is statistically greater than muscle activity in the control group ($F=71.88$, $p<0.001$). Overall, dementia subjects have 5.3 dB or approximately three times more cranial and upper cervical muscle activity than control subjects. This result shows that dementia patients exhibit significantly increased muscle tension. This is consistent with an aspect of dementia being similar to anxiety disorder, and suggests further research is warranted.

Table 7-15: Mean muscle power (mean ± SEM) for each condition, and post hoc test p value comparing between conditions.

Condition	Number of participants	Mean of muscle power (dB)	p value
Dementia	13	-9.44 ± 0.57	**<0.001**
Control	65	-14.78 ± 0.25	

As shown in Table 7-16, the amount of muscle activity during baseline eyes open is significantly more than in baseline eyes closed ($F=6.44$, $p=0.01$), by 1.6 dB or approximately 40%.

Table 7-16: Mean muscle power (mean ± SEM) for each task, and post hoc test p value comparing between tasks.

Task	Mean of muscle power (dB)	p value
Eyes open	-11.32 ± 0.44	**0.01**
Eyes closed	-12.91 ± 0.44	

The muscle activity in the five regions (frontal, left temporal, central, right temporal, and occipital) was compared on a pairwise basis, shown in Table 7-17. The power in the occipital region is statistically greater than all other regions. Central power is also statistically less than both temporal regions, consistent with the absence of muscle in the central region.

Table 7-17: Mean muscle power (SEM = 0.54 dB) for each region, and post hoc test p values comparing between pairs of regions.

Region	Occipital	Right temporal	Central	Left temporal	Frontal
Power (dB)	-8.01	-12.63	-15.31	-11.74	-12.87
Frontal	**<0.001**	0.89	0.10	0.78	
Left temporal	**0.001**	0.89	**0.003**		
Central	**< 0.001**	**0.04**			
Right temporal	**< 0.001**				

7.9.2 Schizophrenia vs control

Figure 7-7 shows the topographic map of the mean muscle power for each group (schizophrenia and control), and for each baseline task (eyes closed and eyes open) in the gamma3 band. Visually, schizophrenia group have more muscle power all over the head, especially during the eyes open task.

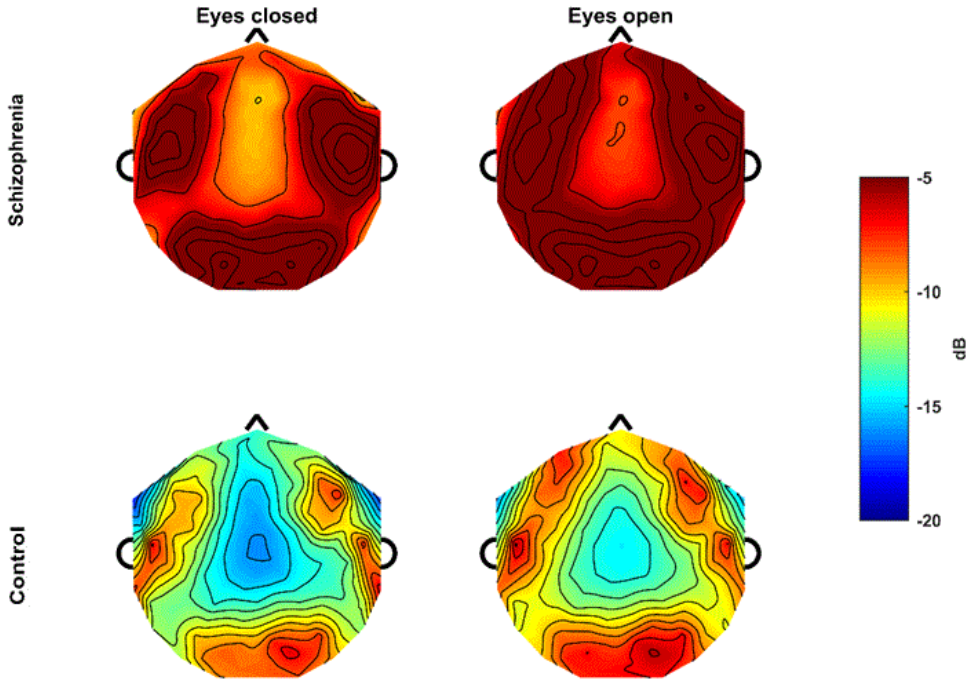

Figure 7-7: Mean muscle power in the gamma3 band for schizophrenia subjects (top row) and control subjects (bottom row) and eyes closed (left column) and eyes open tasks (right column).

Statistical analysis revealed a significant difference in muscle power based on condition, task, and location, but no significant differences were found for gender, nor in any interaction between the factors. Each significant factor is considered in turn below.

Table 7-18 shows the result of the post hoc test comparing muscle activity between the schizophrenia and control groups. The muscle activity in the schizophrenia group is statistically greater than the muscle activity in the control group ($F=30.62$, $p<0.001$). Overall, schizophrenia subjects have 3.2 dB or approximately twice the cranial and upper cervical muscle activity than control subjects. This result shows that schizophrenia patients experience significantly increased muscle tension. This is consistent with at least two hypotheses,

namely, that an aspect of schizophrenia is similar to anxiety disorder, or that medications used in treatment lead to increased muscle activity. Further research would be required to test these hypotheses.

Table 7-18: Mean muscle power (mean ± SEM) for each condition, and post hoc test p value comparing between conditions.

Condition	Number of participants	Mean of muscle power (dB)	p value
Schizophrenia	18	-11.59 ± 0.51	**<0.001**
Control	65	-14.78 ± 0.25	

As shown in Table 7-19, the amount of muscle activity during baseline eyes open is significantly more than in baseline eyes closed (F=13.67, p=0.002), by 2.2 dB or approximately 66%.

Table 7-19: Mean muscle power (mean ± SEM) for each task, and post hoc test p value comparing between tasks.

Task	Mean of muscle power (dB)	p value
Eyes open	-12.13 ± 0.40	**0.002**
Eyes closed	-14.25 ± 0.40	

The muscle activity in the five regions (frontal, left temporal, central, right temporal, and occipital) was compared on a pairwise basis, shown in Table 7-20. The power in the occipital region is statistically greater than all other locations. Central power is also statistically less than both temporal regions, consistent with the absence of muscle in the central region.

Table 7-20: Mean muscle power (SEM = 0.64 dB) for each region, and post hoc test p values comparing between pairs of regions.

Region	Occipital	Right temporal	Central	Left temporal	Frontal
Power (dB)	-9.62	-13.56	-15.94	-13.20	-13.61
Frontal	**0.001**	0.99	0.07	0.99	
Left temporal	**0.008**	0.99	**0.02**		
Central	**< 0.001**	**0.04**			
Right temporal	**0.001**				

7.9.3 Sedative-free CAE vs sedative-medicated CAE

The mean muscle power for each group (sedative-free CAE and sedative-medicated CAE), and for each baseline task (eyes closed and eyes open) in the gamma3 band has been

illustrated topographically in Figure 7-8. Visual inspection reveals much greater muscle power in the sedative-free CAE group, mostly peripherally.

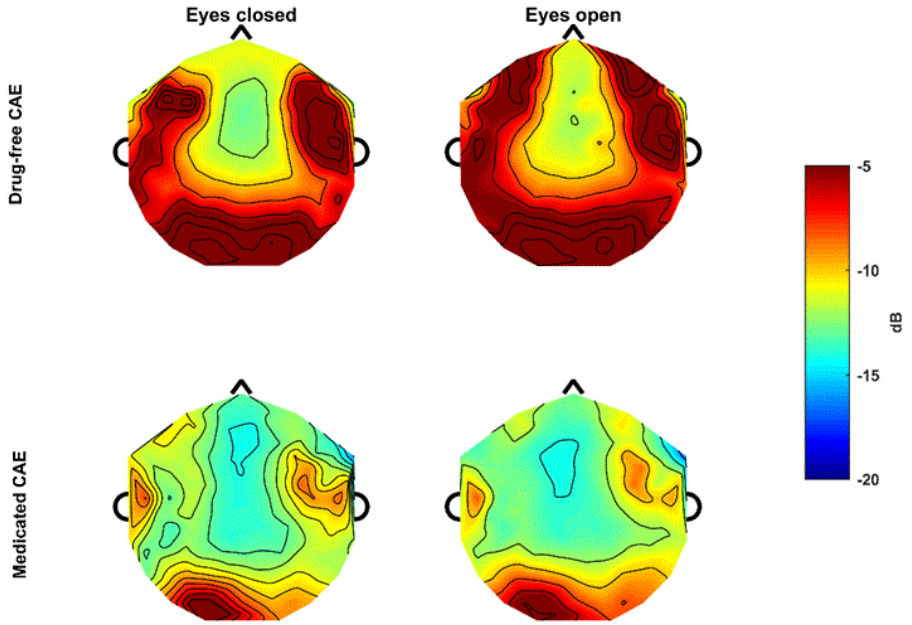

Figure 7-8: Mean muscle power in the gamma3 band for sedative-free CAE subjects (top row) and sedative-medicated CAE subjects (bottom row) and eyes closed (left column) and eyes open tasks (right column).

Statistical analysis only revealed a significant difference in muscle power based on region ($F=2.88$, $p=0.02$). Although, the factor of condition was not significant, it was very close to significant ($p=0.056$). As shown in Table 7-21 and Figure 7-9, the average muscle power in the sedative-medicated CAE group is 2.5 dB or about 77% less than the sedative-free CAE group. The number of subjects in the sedative-medicated CAE group is about 2.4 time greater than the number of subjects in the sedative-free CAE group. Hence, this near-significant result may be due to the small number of subjects in the sedative-free CAE group, and possibly the result would be significant with more subjects.

Table 7-21: Mean muscle power (mean ± SEM) for each condition, and post hoc test p value comparing between conditions.

Condition	Number of participants	Mean of muscle power (dB)	p value
Sedative-free CAE	7	-12.66 ± 0.99	**0.056**
Sedative-medicated CAE	17	-15.14 ± 0.82	

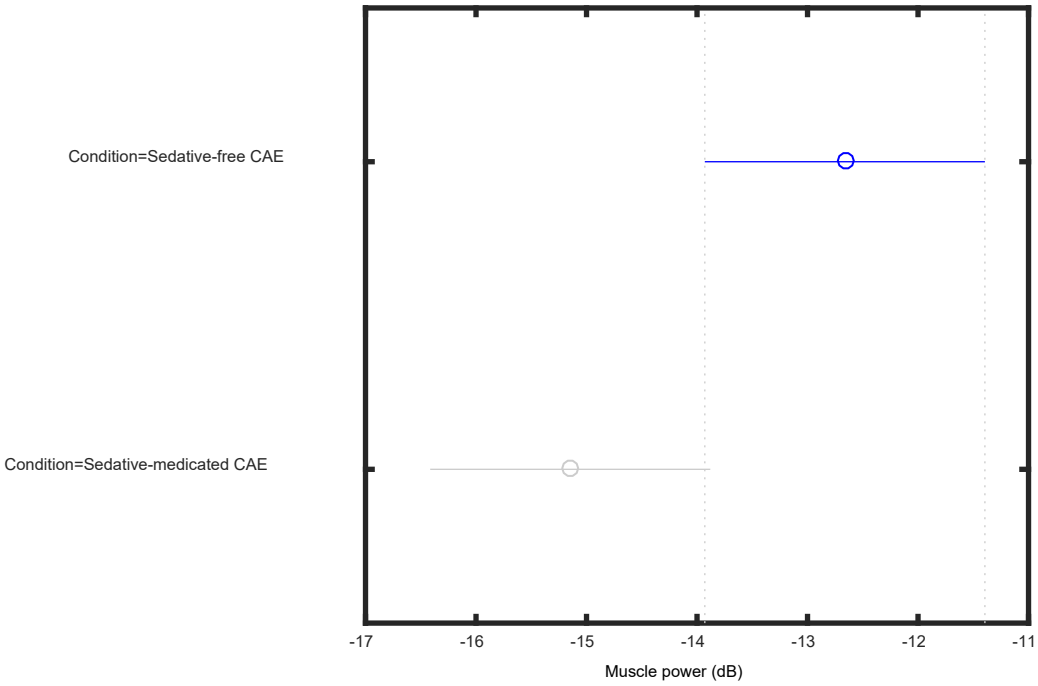

Figure 7-9: The average of muscle power in sedative-free CAE group versus sedative-medicated CAE group. Their mean difference is not significant, but close to significant. Red conditions are significantly different to the blue condition, and light grey conditions are not significantly different to the blue condition.

The muscle activity in the five regions (frontal, left temporal, central, right temporal, and occipital) was compared on a pairwise basis, shown in Table 7-22. The power in the occipital region is statistically greater than frontal and central regions.

Table 7-22: Mean muscle power (SEM = 1.42 dB) for each region, and post hoc test p values comparing between pairs of regions.

Region	Occipital	Right temporal	Central	Left temporal	Frontal
Power (dB)	-10.03	-13.37	-16.15	-14.42	-15.53
Frontal	**0.04**	0.82	0.99	0.98	
Left temporal	0.18	0.98	0.91		
Central	**0.01**	0.64			
Right temporal	0.45				

7.10 Discussion and conclusion

7.10.1 Contributions

I used a new approach to quantitate cranial and upper cervical muscle activity using SERs that are ordinarily used for measuring EEG. In this approach, a measure of muscle activity is presented that has a robust basis (ICA plus spectral slope plus muscle-frequency-band quantitation) combined with comprehensive topographic mapping. The use of a high-density SER cap gives good spatial coverage and avoids the issue of where to measure specific muscles. This enables me to evaluate the activity of all cranial and upper cervical muscles, not just one or two specific ones. This non-invasive topographic approach provides a new, holistic measure of cranial and upper cervical muscle activity.

To validate this new approach, it was first applied on SERs of subjects suffering from diseases known to cause extra muscle tension, namely PD, anxiety disorder, and stroke. Results showed that people suffering from these diseases experience significantly increased cranial and upper cervical muscle activity compared to controls. This is consistent with increased muscle tone in PD due to rigidity and stiffness (Gelb, Oliver & Gilman 1999; Louis et al. 1997; Martin et al. 1973), muscle tension and greater mean level of muscle activity in people suffering from anxiety disorder (Conrad & Roth 2007; Hazlett, McLeod & Hoehn-Saric 1994; Pluess, Conrad & Wilhelm 2009; Rowa & Antony 2008), and spasticity reported in many people following stroke (O'Dwyer, Ada & Neilson 1996; Sommerfeld et al. 2004; Watkins et al. 2002). This is strong evidence that the proposed muscle quantitation approach performs well on relaxed subjects.

After validating the efficacy of this new muscle quantitation approach, it was applied to SERs of migraineurs to compare their level of cranial and upper cervical muscle activity to controls. The main finding is that there is more cranial and upper cervical muscle activity in migraineurs than in controls. This is an important contribution to the literature for several

reasons. Firstly, previous studies (Anderson, CD & Franks 1981; Bakal & Kaganov 1977; McArthur & Cohen 1980) were on a sub-group of chronic migraineurs. In contrast, the migraine participants in our study were not selected for severity, and mostly had a frequency of headache less than one per month. This strengthens the finding because it is not limited to a chronic sub-group, and it would be unlikely to find a weaker level of muscle activity in chronic migraineurs. Secondly and similarly, the migraine participants were recorded in their non-headache phase, but, given others' work (Bakke et al. 1982; Clifford et al. 1982; McArthur & Cohen 1980), it would be surprising to find a reduced level during headache than that recorded in the headache-free period. Thirdly, the new proposed approach provides a more holistic measurement of cranial and upper cervical muscle activity due to good spatial coverage.

This result diminishes one of the accepted conceptual differences between migraine and tension-type headache. Although the result reveals an association between the diagnosis of migraine and resting muscle activity, the nature of this association is unknown. If the finding is of pathophysiological significance, it would provide some support to the now standard use of botulinum toxin in the treatment of severe migraine (Blumenfeld 2003; Diener et al. 2012; Dodick et al. 2005). Impaired sensory control by brainstem mechanisms (currently proposed as a primary feature in migraine (Goadsby et al. 2017) and possibly present in tension-type headache (Ashina, Bendtsen & Ashina 2012)) are thought to magnify trigeminal perivascular and other sensations. I speculate, therefore, that there might also be impaired brainstem control mechanisms for cranial muscle activity in migraine, driving muscle metabolism, possibly impacting on perivascular sensory nociceptive nerves. Another possible reason for increased cranial muscle activity might be that individuals who have experienced headaches learn (consciously or unconsciously) to use subtle adjustments of head posture or expression

as means to control the development of their headache (Bag & Karabulut 2005; Haque et al. 2012; Martins & Parreira 2001).

There were SERs of subjects suffering from other psychological diseases and brain disorders in the database described in Section 7.10. There is evidence in the literature (Calleo et al. 2011; Pallanti, Quercioli & Hollander 2004; Siris & Braga 2013; Vancampfort et al. 2013; Vancampfort et al. 2011) that there may be increased muscle tension in some of these disease groups. So, I tested this possibility by applying the proposed muscle quantitation method to their SERs to evaluate their level of muscle activity. The statistical results indicate that there are significantly increased cranial and upper cervical muscle activity in people suffering from dementia and schizophrenia compared to controls. This result is consistent with some evidence showing that an aspect of dementia and schizophrenia is similar to anxiety disorder, and people suffering from these disease are often recognized as having anxiety (Calleo et al. 2011; Pallanti, Quercioli & Hollander 2004; Siris & Braga 2013). Furthermore, drugs used in the treatment of schizophrenia (dopamine-blocking agents) do have mild parkinsonism (increased muscle tone) as a side-effect (Shin & Chung 2012).

In almost all comparisons, there was significantly more cranial and upper cervical muscle activity when the eyes were open than when the eyes were closed. This result is consistent with previous similar reports (Ben-Simon et al. 2013; Boĭtsova & Dan'ko 2009; Whitham, E. M. et al. 2008; Yilmaz et al. 2014). The findings show that the usual practice in SERs, with the eyes closed, does diminish EMG contamination. Possibly, the act of opening the eyes is an alerting process that incorporates readiness for fight or flight and, therefore, muscles are somewhat activated (Stemmler, Aue & Wacker 2007).

There were no differences between males and females in the amount of resting cranial and upper cervical muscle activity in any comparisons. However, the incidence of headache is twice as high in females and the percentage of females using botulinum toxin to treat their

headache is much higher than males (Aydinlar et al. 2017), rigidity is more frequent in males than females suffering from PD (Georgiev et al. 2017; Miller & Cronin-Golomb 2010), and anxiety disorder and stroke are more disabling in females than males (McLean et al. 2011; Petrea et al. 2009). My results suggest cranial and upper cervical muscle activation is not an important component of these gender differences.

In almost all statistical comparisons, there was greater muscle activity in the occipital region compared to frontal or temporal regions. This result is presumably due to EMG from the powerful trapezius, splenius capitis and sub-occipital muscles that insert along or under the nuchal ridge (Fehrenbach & Herring 2015; Johnson et al. 1994). These muscles maintain posture of the neck and head, and hence are active while sitting regardless of task. In contrast, the temporalis and frontalis muscle are small muscles, responsible for jaw position and facial expression and would be less active at rest.

7.10.2 Limitations and suggestions

This study did not address muscle activity during an acute headache, as the participants were studied during a non-ictal period. However, it was not documented when the patients experienced their next or previous migraine, so that some patients may have been pre-ictal when studied. Given the infrequent migraines in many of our cases, and the lack of relation of muscle activity to migraine frequency, I suggest this is unlikely. Moreover, this study had no participants with chronic migraine. Hence extending the finding would require testing with further studies. Studies comparing post-ictal, ictal, pre-ictal, and inter-ictal may reveal more about the nature of the association. Additionally, further studies are justified to apply the proposed muscle quantitation approach to SERs of people with different types of psychological diseases or brain disorders to evaluate their level of cranial or upper cervical muscle activity. This may help in the diagnosis of some diseases.

Chapter 8

Conclusion

The main focus of my study was cranial and upper cervical tonic muscle activity in resting subjects. As discussed in Chapter 2, generally, the amplitude of phasic muscle activity is sufficiently high that the activity can be detected easily by eye or mathematical algorithm. The standard remedy is to identify times when the activity occurs and to excise it from analysis, as phasic muscle activity dominates the SER. However, many cranial and upper cervical muscles produce continuing, gentle, involuntary contractions to maintain muscle tone even at rest. This tonic muscle activity occurs all the time, and so the traditional approach of excising times can never remove all tonic muscle activity. Hence, **reducing** the effect of **tonic** muscle activity from SERs without altering signals due to brain activity became the main aim of my thesis.

8.1 Contributions

- **Comparing efficacy of BSS algorithms in tonic muscle reduction using the paralysis database**

The effect of five BSS algorithms (AMICA, Infomax, FastICA, CCA, and IVA) in the **automated** removal of **tonic** cranial muscle activity was evaluated using the unique database of pharmacologically-induced **paralysed** subjects. The unique dataset of paralysed subjects provides many of the advantages of simulated data while retaining the advantage of being "real" data. The results of the pruned data were compared to EMG-free data (paralysis condition) and EMG-contaminated data (pre-paralysis condition). It is the first detailed

comparison of the efficacy of several important BSS algorithms in automatic tonic muscle removal, including testing for the retention of brain responses.

- **Comparing the effect of the number of SER channels in tonic muscle reduction**

Using the unique database of pharmacologically-induced paralysed subjects, I compared the effect of the **number of SER channels** used in Infomax in **reducing tonic muscle activity** of SERs. I showed that as the number of channels increases, the amount of muscle reduction increases, as does the range of frequencies achieving significant reduction. Hence, in studies where cranial muscle contamination is a significant issue, and more muscle reduction is a priority, the application of ICA with a higher number of SER channels (>64) is justified.

- **A new approach to tonic muscle reduction using minimum-norm beamforming**

I suggested a new approach applying minimum-norm beamforming to SERs. Using the sLORETA **minimum-norm beamforming** technique and a generic volume conduction model of the head (consisting of three layers: brain, skull, and scalp), the estimated sources **within the scalp volume** can be assumed to be muscular. I then showed that discarding these sources in forward modelling reduces tonic muscle activity of reconstructed SERs without affecting the brain neurophysiological responses.

- **Automating the BSS-CCA tonic muscle reduction algorithm**

I proposed an automated tonic muscle-removal approach by combining BSS-CCA with the spectral gradient of the derived components, and the unique database of pharmacologically-induced paralysed subjects. My investigations showed that the autocorrelation of tonic muscle sources revealed a negative correlation at a delays below 3 ms, maximum at 2 ms. This is not consistent with the published assumptions that muscle components are like white noise, i.e. have an autocorrelation which is zero at all delays except zero. Furthermore, my environmental noise test showed that components containing substantial mains power contamination (harmonics of 50 Hz) can have an autocorrelation coefficient as high as brain

or as low as muscle or white noise. In contrast, data free from substantial mains power contamination has a correlation coefficient below 0.19. Hence, I proposed a **double-stage** muscle pruning approach, based on **correlation coefficient** (first stage) and **spectral gradient** (second stage), applied to the components derived by BSS-CCA. The proposed pruning approach significantly reduces high frequency tonic muscle activity while preserving or even revealing cognitive activity.

- **Exploring the complementary effect of beamforming and BSS in tonic muscle reduction**

On the one hand, components derived by BSS approaches can be separated based on their spectral characteristics. On the other hand, the beamforming technique has location information, hence muscle sources can be discarded based on their location. So these two approaches, using different features, complement each other. I showed that **beamforming and BSS** approaches have a **complementary effect** in reducing tonic cranial muscle activity of SERs. Specifically, most of the combined approaches reduced tonic muscle activity significantly more than any single approach, and all the combined approaches did not significantly affect the measurement of brain activity.

- **Proposing a new cranial and upper cervical muscle quantitation approach**

I proposed a new approach to **quantitate cranial and upper cervical muscle activity** using SERs that are ordinarily used for measuring EEG. In this approach, unlike the typical use of ICA in SER analysis, the components identified as muscular are retained, not discarded. Hence, a comprehensive topographic map of muscle activity is quantitated that has a robust basis (ICA plus spectral gradient plus muscle-frequency-band quantitation). The use of a **high-density SER** cap gives good spatial coverage and avoids the issue of which specific muscle (or muscles) to measure, and where to measure it (them). This enables the user to evaluate the activity of all cranial and upper cervical muscles, not just a few specific ones.

This **non-invasive** topographic approach provides a new, holistic measure of cranial and upper cervical muscle activity.

- **Diminishing one of the accepted conceptual differences between migraine and tension-type headache**

For years, it was thought that increased pericranial muscle tenderness, which can be detected easily by palpation, is the most common abnormality in tension-type headache. Moreover, the ICHD currently considers muscle to be "the most significant abnormal finding" in tension-type headache. It uses other names such as muscle contraction headache and myogenic headache to refer to the tension-type headache, while the word "muscle" is not even mentioned in its definition of migraine. Therefore, it was commonly accepted that the difference between migraine and tension-type headache was the excessive muscle activity in tension-type headache. However, some studies have reported increased muscle activity in migraine sufferers. Hence, using my proposed holistic cranial and upper cervical muscle quantitation approach, I compared the muscle activity between migraine and control groups. My results revealed that there is **more cranial and upper cervical muscle activity in migraineurs** than in controls. My conclusion, supported by some previous studies, would weaken the thinking that increased muscle activity is a feature only of tension-type headache and, therefore, challenges current accepted beliefs about muscle tension and headache.

8.2 Suggestion for further studies

- **Need for a better algorithm to separate muscle and brain components**

My results showed that after using any BSS algorithm, there was still residual tonic muscle activity in pruned SERs compared to EMG-free data. Likely the most significant reason is that current algorithms do not provide a sufficient number of sufficiently pure muscle or pure brain components. At best, only 30% of the estimated components are pure, and about 70% of them are still a mixture of signals from different sources (e.g. neurogenic, myogenic, and

artefactual). Hence, there is a need for an algorithm that gives more components that are purely from one type of source. This could be achieved by a non-blind source separation algorithm. A negative spectral gradient is expected for purely neurogenic components, whereas purely myogenic components should have a positive gradient. This information could motivate a new non-blind algorithm that provides more components that are pure, and hence, more muscle reduction.

- **Testing the efficacy of minimum-norm beamforming in muscle reduction using individual, not generic, head models**

I showed the efficacy of sLORETA beamformer in reducing tonic muscle activity of SERs using a generic volume conduction model of the head. Although the muscle reduction was significant with this simple model of the head, better pruning results may be achieved with a more realistic head model using each subject's own sMRI. On the one hand, a realistic individual head model should provide more accurate computation of source locations and leadfields, which should yield better pruning. On the other hand, this requires an additional expense in recording the sMRI and is more time-consuming experimentally and computationally. Hence, if further research shows that the amount of muscle reduction using minimum-norm beamforming with the more realistic head model is significantly greater, its use could be justified, for example, in studies where cranial muscle contamination is a significant issue and more muscle reduction is a priority.

- **Comparing cranial muscle tension in different types of headache using the proposed holistic muscle quantitation method**

Using my proposed holistic muscle quantitation method, I showed there is more cranial and upper cervical muscle activity in non-chronic non-ictal migraineurs than controls. This result is important since it diminishes one of the accepted conceptual differences between migraine and tension-type headache. To expand this result, a comprehensive comparison study could

be conducted on the common types of headache, namely migraine with aura, migraine without aura, cervicogenic headache and tension-type headache. The results of these studies may help in a better understanding of the pathology of headache and classification or diagnosis of different types of headache.

- **Comparing cranial muscle tension in different phases of headache**

My study revealed an association between the diagnosis of migraine and resting muscle activity, but it did not address muscle activity during an acute headache. This finding could be extended by studies designed to compare post-ictal, inter-ictal, pre-ictal, and ictal muscle activity, which may reveal more about the nature of the association.

- **Further studies on gender difference in migraine**

My result showed that males and females exhibit the same amount of resting muscle activity, whether they have a migraine diagnosis or not. However, the percentage of females using botulinum toxin to treat their headache is much higher than males (85% vs 15%). There is a discrepancy between my non-significant gender difference result and the significant gender difference in treatment. Therefore, further studies looking for gender differences in social and physical characteristics of migraineurs are merited, and may improve our understanding of this disease.

8.3 Summary

My revised research question was: “How effectively can the current signal analysis methods reduce tonic muscle activity from scalp measurements without affecting brain activity, and can modified or new approaches with better effectiveness be proposed?”

My results showed that Infomax and AMICA are the best BSS algorithms in **automated tonic muscle artefact reduction** using the spectral gradient of components. Additionally, as the number of channels increases, the amount of muscle reduction increases, as does the

range of frequencies achieving significant reduction. However, none of the current algorithms can provide completely EMG-free SERs, likely due to the high percentage of mixed components.

In response to this finding, I proposed two new algorithms. Firstly, I detailed an automated extension of the traditional BSS-CCA approach that uses two stages, based on correlation coefficient (first stage) and spectral gradient (second stage). Secondly, I described a minimum-norm beamformer approach that reduces tonic muscle artefact at the sensor level. Additionally, I observed that beamforming and BSS approaches have a complementary effect in reducing tonic cranial muscle activity of SERs, and demonstrated that combining both approaches can reduce muscle activity significantly more than either approach alone.

I have also answered the reduced form of my initial research question: "Is resting muscle activity increased in migraineurs?". I described an "inverted" use of BSS, where components identified as myogenic are retained and neurogenic components are discarded. Hence I proposed a new holistic cranial and upper cervical muscle quantitation approach using a high-density SER cap. This approach was validated using SERs from subjects suffering from diseases associated with increased muscle tension. Applying this approach to SERs of non-chronic migraineurs and healthy controls showed that there is significantly more cranial and upper cervical muscle activity in migraineurs than in controls.

While I have answered my research questions, many more questions have arisen. Perhaps the two most important are: "Can a non-blind source separation algorithm reduce tonic muscle activity of SERs more significantly?" and "Can the beamforming muscle reduction approach reduce tonic muscle activity more significantly using individual head models?". Further studies are merited to answer these questions. On the one hand, they may provide better tonic muscle reduction algorithms, which would be valuable in EEG research and critically important for high-frequency EEG studies (e.g. gamma rhythms). On the other hand, they

may provide a better cranial and upper cervical muscle quantitation approach, which could be valuable for treatment and/or understanding of some medical conditions, such as headache or anxiety.

References

Abd, MD, Toh, CC, Mohd, SS & Azmi, AMI (2016), 'A study of blind source separation using nonnegative matrix factorization', *ARPN Journal of Engineering and Applied Sciences*, vol. 11, no. 18, pp. 10702-8.

Acharya, D & Panda, G (2008), 'A review of independent component analysis techniques and their applications', *IETE Technical Review*, vol. 25, no. 6, pp. 320-32.

Ahles, TA, Martin, JB, Gaulier, B, Cassens, HL, Andres, ML & Shariff, M (1988), 'Electromyographic and vasomotor activity in tension, migraine, and combined headache patients: The influence of postural variation', *Behaviour Research and Therapy*, vol. 26, no. 6, pp. 519-25.

Akay, M & Daubenspeck, JA (1999), 'Investigating the contamination of electroencephalograms by facial muscle electromyographic activity using matching pursuit', *Brain and Language*, vol. 66, no. 1, pp. 184-200.

Akhtar, MT, Jung, T-P, Makeig, S & Cauwenberghs, G (2012), 'Recursive independent component analysis for online blind source separation', in *Circuits and Systems (ISCAS), 2012 IEEE International Symposium on*, pp. 2813-6.

Albera, L, Kachenoura, A, Comon, P, Karfoul, A, Wendling, F, Senhadji, L & Merlet, I (2012), 'ICA-based EEG denoising: a comparative analysis of fifteen methods', *Bulletin of the Polish Academy of Sciences: Technical Sciences*, vol. 60, no. 3, pp. 407-18.

Anderer, P, Semlitsch, HV, Saletu, B & Barbanoj, MJ (1992), 'Artifact processing in topographic mapping of electroencephalographie activity in neuropsychopharmacology', *Psychiatry Research: Neuroimaging*, vol. 45, no. 2, pp. 79-93.

Anderson, CD & Franks, RD (1981), 'Migraine and tension headache: is there a physiological difference?', *Headache: The Journal of Head and Face Pain*, vol. 21, no. 2, pp. 63-71.

Anderson, M, Adali, T & Li, X-L (2012), 'Joint blind source separation with multivariate Gaussian model: Algorithms and performance analysis', *IEEE transactions on Signal Processing*, vol. 60, no. 4, pp. 1672-83.

Anderson, M, Fu, G-S, Phlypo, R & Adali, T (2013), 'Independent vector analysis, the Kotz distribution, and performance bounds', in *Acoustics, Speech and Signal Processing (ICASSP), 2013 IEEE International Conference on*, pp. 3243-7.

Anderson, M, Fu, G-S, Phlypo, R & Adali, T (2014), 'Independent vector analysis: Identification conditions and performance bounds', *IEEE transactions on Signal Processing*, vol. 62, no. 17, pp. 4399-410.

Ashina, S, Bendtsen, L & Ashina, M (2012), 'Pathophysiology of migraine and tension-type headache', *Techniques in Regional Anesthesia & Pain Management*, vol. 16, no. 1, pp. 14-8.

Aydinlar, EI, Dikmen, PY, Kosak, S & Kocaman, AS (2017), 'OnabotulinumtoxinA effectiveness on chronic migraine, negative emotional states and sleep quality: a single-center prospective cohort study', *J Headache Pain*, vol. 18, no. 1, p. 23.

Bag, B & Karabulut, N (2005), 'Pain-relieving factors in migraine and tension-type headache', *International journal of Clinical Practice*, vol. 59, no. 7, pp. 760-3.

Bakal, DA & Kaganov, JA (1977), 'Muscle contraction and migraine headache: psychophysiologic comparison', *Headache: The Journal of Head and Face Pain*, vol. 17, no. 5, pp. 208-15.

Bakke, M, Tfelt-Hansen, P, Olesen, J & Møller, E (1982), 'Action of some pericranial muscles during provoked attacks of common migraine', *Pain*, vol. 14, no. 2, pp. 121-35.

Barlow, JS (1993), *The electroencephalogram: its patterns and origins*, MIT press.

Bell, AJ & Sejnowski, TJ (1995), 'An information-maximization approach to blind separation and blind deconvolution', *Neural Computation*, vol. 7, no. 6, pp. 1129-59.

Belouchrani, A, Abed-Meraim, K, Cardoso, J-F & Moulines, E (1997), 'A blind source separation technique using second-order statistics', *IEEE transactions on Signal Processing*, vol. 45, no. 2, pp. 434-44.

Ben-Simon, E, Podlipsky, I, Okon-Singer, H, Gruberger, M, Cvetkovic, D, Intrator, N & Hendler, T (2013), 'The dark side of the alpha rhythm: fMRI evidence for induced alpha modulation during complete darkness', *European Journal of Neuroscience*, vol. 37, no. 5, pp. 795-803.

Berger, H (1929).'Über das Elektrenkephalogramm des Menschen', *Psychiatrie,* vol. 87, no. 527,pp. 35-6.

Bertrand, O & Tallon-Baudry, C (2000), 'Oscillatory gamma activity in humans: a possible role for object representation', *International Journal of Psychophysiology*, vol. 38, no. 3, pp. 211-23.

Blackwood, D & Muir, W (1990), 'Cognitive brain potentials and their application', *The British Journal of Psychiatry*, vol. 157, no. S9, pp. 96-101.

Blaschek, A, Milde-Busch, A, Straube, A, Schankin, C, Langhagen, T, Jahn, K, Schröder, SA, Reiter, K, von Kries, R & Heinen, F (2012), 'Self-reported muscle pain in adolescents with migraine and tension-type headache', *Cephalalgia*, vol. 32, no. 3, pp. 241-9.

Blau, J & MacGregor, E (1994), 'Migraine and the neck', *Headache: The Journal of Head and Face Pain*, vol. 34, no. 2, pp. 88-90.

Blumenfeld, A (2003), 'Botulinum toxin type A as an effective prophylactic treatment in primary headache disorders', *Headache: The Journal of Head and Face Pain*, vol. 43, no. 8, pp. 853-60.

Boĭtsova, I & Dan'ko, S (2009), 'EEG changes in comparison of rest states with open and closed eyes in complete darkness', *Fiziologiia cheloveka*, vol. 36, no. 3, pp. 138-41.

Brenner, CA, Krishnan, GP, Vohs, JL, Ahn, W-Y, Hetrick, WP, Morzorati, SL & O'Donnell, BF (2009), 'Steady state responses: electrophysiological assessment of sensory function in schizophrenia', *Schizophrenia bulletin*, vol. 35, no. 6, pp. 1065-77.

Brookes, MJ, Mullinger, KJ, Stevenson, CM, Morris, PG & Bowtell, R (2008), 'Simultaneous EEG source localisation and artifact rejection during concurrent fMRI by means of spatial filtering', *Neuroimage*, vol. 40, no. 3, pp. 1090-104.

Burnett, C, Fartash, L, Murray, B & Lamey, PJ (2000), 'Masseter and temporalis muscle EMG levels and bite force in migraineurs', *Headache: The Journal of Head and Face Pain*, vol. 40, no. 10, pp. 813-7.

Buzsáki, G, Anastassiou, CA & Koch, C (2012), 'The origin of extracellular fields and currents—EEG, ECoG, LFP and spikes', *Nature Reviews Neuroscience*, vol. 13, no. 6, p. 407.

Calleo, JS, Kunik, ME, Reid, D, Kraus-Schuman, C, Paukert, A, Regev, T, Wilson, N, Petersen, NJ, Snow, AL & Stanley, M (2011), 'Characteristics of generalized anxiety disorder in patients with dementia', *American Journal of Alzheimer's Disease & Other Dementias®*, vol. 26, no. 6, pp. 492-7.

Capizzi, G, Coco, S & Laudani, A (2007), 'A new tool for the identification and localization of electromagnetic sources by using independent component analysis', *IEEE transactions on magnetics*, vol. 43, no. 4, pp. 1625-8.

Cardoso, J-F & Souloumiac, A (1993), 'Blind beamforming for non-Gaussian signals', in *IEE proceedings F (radar and signal processing)*, vol. 140, pp. 362-70.

Celentano, DD, Stewart, WF & Linet, MS (1990), 'The relationship of headache symptoms with severity and duration of attacks', *J Clin Epidemiol.*, vol. 43, no. 9, pp. 983-94.

Charlton, SG & O'Brien, TG (2001), *Handbook of human factors testing and evaluation*, CRC Press.

Chen, X, He, C & Peng, H (2014), 'Removal of muscle artifacts from single-channel EEG based on ensemble empirical mode decomposition and multiset canonical correlation analysis', *Journal of Applied Mathematics*, vol. 2014.

Chen, X, Liu, A, Chen, Q, Liu, Y, Zou, L & McKeown, MJ (2017), 'Simultaneous ocular and muscle artifact removal from EEG data by exploiting diverse statistics', *Computers in Biology and Medicine*, vol. 88, pp. 1-10.

Chen, X, Liu, A, Peng, H & Ward, RK (2014), 'A preliminary study of muscular artifact cancellation in single-channel EEG', *Sensors*, vol. 14, no. 10, pp. 18370-89.

Chen, X, Peng, H, Yu, F & Wang, K (2017), 'Independent Vector Analysis Applied to Remove Muscle Artifacts in EEG Data', *IEEE Transactions on Instrumentation and Measurement*.

Chen, Y & Ostoja-Starzewski, M (2010), 'MRI-based finite element modeling of head trauma: spherically focusing shear waves', *Acta Mechanica*, vol. 213, no. 1-2, pp. 155-67.

Clifford, T, Lauritzen, M, Bakke, M, Olesen, J & Møller, E (1982), 'Electromyography of pericranial muscles during treatment of spontaneous common migraine attacks', *Pain*, vol. 14, no. 2, pp. 137-47.

Comon, P, Jutten, C & Herault, J (1991), 'Blind separation of sources, Part II: Problems statement', *Signal processing*, vol. 24, no. 1, pp. 11-20.

Conrad, A & Roth, WT (2007), 'Muscle relaxation therapy for anxiety disorders: It works but how?', *Journal of Anxiety Disorders*, vol. 21, no. 3, pp. 243-64.

Correa, AG, Laciar, E, Patino, H & Valentinuzzi, M (2007), 'Artifact removal from EEG signals using adaptive filters in cascade', in *Journal of Physics: Conference Series*, vol. 90, p. 012081.

Croft, RJ, Chandler, JS, Barry, RJ, Cooper, NR & Clarke, AR (2005), 'EOG correction: a comparison of four methods', *Psychophysiology*, vol. 42, no. 1, pp. 16-24.

De Clercq, W, Vergult, A, Vanrumste, B, Van Paesschen, W & Van Huffel, S (2006), 'Canonical correlation analysis applied to remove muscle artifacts from the electroencephalogram', *IEEE Transactions on Biomedical Engineering*, vol. 53, no. 12, pp. 2583-7.

Delorme, A & Makeig, S (2004), 'EEGLAB: an open source toolbox for analysis of single-trial EEG dynamics including independent component analysis', *Journal of Neuroscience Methods*, vol. 134, no. 1, pp. 9-21.

Delorme, A, Mullen, T, Kothe, C, Acar, ZA, Bigdely-Shamlo, N, Vankov, A & Makeig, S (2011), 'EEGLAB, SIFT, NFT, BCILAB, and ERICA: new tools for advanced EEG processing', *Computational Intelligence and Neuroscience*, vol. 2011, p. 10.

Delorme, A, Palmer, J, Onton, J, Oostenveld, R & Makeig, S (2012), 'Independent EEG sources are dipolar', *PloS one*, vol. 7, no. 2, p. e30135.

DeLosAngeles, D (2010), 'Electroencephalographic, Cognitive and Autonomic Correlates of States of Concentrative Meditation', Flinders University of South Australia.

DeLosAngeles, D, Williams, G, Burston, J, Fitzgibbon, SP, Lewis, TW, Grummett, TS, Clark, CR, Pope, KJ & Willoughby, JO (2016), 'Electroencephalographic correlates of states of concentrative meditation', *International Journal of Psychophysiology*, vol. 110, pp. 27-39.

Dharmaprani, D, Nguyen, HK, Lewis, TW, DeLosAngeles, D, Willoughby, JO & Pope, KJ (2016), 'A comparison of independent component analysis algorithms and measures to discriminate between EEG and artifact components', in *Engineering in Medicine and Biology Society (EMBC), 2016 IEEE 38th Annual International Conference of the*, pp. 825-8.

Didier, HA, Di Fiore, P, Marchetti, C, Tullo, V, Frediani, F, Arlotti, M, Gianni, AB & Bussone, G (2015), 'Electromyography data in chronic migraine patients by using neurostimulation with the Cefaly(R) device', *Neurol Sci*, vol. 36 Suppl 1, pp. 115-9.

Diener, H-C, Dodick, DW, Goadsby, PJ, Lipton, RB, Olesen, J & Silberstein, SD (2012), 'Chronic migraine—classification, characteristics and treatment', *Nature Reviews Neurology*, vol. 8, no. 3, p. 162.

Dimberg, U, Thunberg, M & Elmehed, K (2000), 'Unconscious facial reactions to emotional facial expressions', *Psychological Science*, vol. 11, no. 1, pp. 86-9.

Dodick, DW, Mauskop, A, Elkind, AH, DeGryse, R, Brin, MF, Silberstein, SD & Group, BCS (2005), 'Botulinum toxin type A for the prophylaxis of chronic daily headache: Subgroup analysis of patients not receiving other prophylactic medications: A randomized double-blind, placebo-controlled study', *Headache: The Journal of Head and Face Pain*, vol. 45, no. 4, pp. 315-24.

Ebinger, F (2006), 'Exteroceptive suppression of masseter muscle activity in juvenile migraineurs', *Cephalalgia*, vol. 26, no. 6, pp. 722-30.

Engel, AK, Fries, P, König, P, Brecht, M & Singer, W (1999), 'Temporal binding, binocular rivalry, and consciousness', *Consciousness and Cognition*, vol. 8, no. 2, pp. 128-51.

Engel, AK, König, P, Kreiter, AK, Schillen, TB & Singer, W (1992), 'Temporal coding in the visual cortex: new vistas on integration in the nervous system', *Trends in Neurosciences*, vol. 15, no. 6, pp. 218-26.

Fehrenbach, MJ & Herring, SW (2015), *Illustrated Anatomy of the Head and Neck-E-Book*, Elsevier Health Sciences.

Fernández-de-las-Peñas, C, Cuadrado, M, Arendt-Nielsen, L & Pareja, J (2008), 'Side-to-side differences in pressure pain thresholds and pericranial muscle tenderness in strictly unilateral migraine', *European Journal of Neurology*, vol. 15, no. 2, pp. 162-8.

Fitzgibbon, S, DeLosAngeles, D, Lewis, T, Powers, D, Grummett, T, Whitham, E, Ward, L, Willoughby, J & Pope, K (2016), 'Automatic determination of EMG-contaminated components and validation of independent component analysis using EEG during pharmacologic paralysis', *Clinical Neurophysiology*, vol. 127, no. 3, pp. 1781-93.

Fitzgibbon, SP, DeLosAngeles, D, Lewis, TW, Powers, DM, Whitham, EM, Willoughby, JO & Pope, KJ (2015), 'Surface Laplacian of scalp electrical signals and independent component analysis resolve EMG contamination of electroencephalogram', *Int J Psychophysiol*, vol. 97, no. 3, pp. 277-84.

Freeman, WJ, Holmes, MD, Burke, BC & Vanhatalo, S (2003), 'Spatial spectra of scalp EEG and EMG from awake humans', *Clinical Neurophysiology*, vol. 114, no. 6, pp. 1053-68.

Friman, O (2003), 'Adaptive analysis of functional MRI data', Linköpings Universitet.

Friman, O, Cedefamn, J, Lundberg, P, Borga, M & Knutsson, H (2001), 'Detection of neural activity in functional MRI using canonical correlation analysis', *Magnetic Resonance in Medicine*, vol. 45, no. 2, pp. 323-30.

Fu, MJ, Daly, JJ & Cavusoglu, MC (2006), 'A detection scheme for frontalis and temporalis muscle EMG contamination of EEG data', *Analysis*, vol. 5, p. 6.

g.tec (2018), *g.EEGsys*, viewed 20/11 2018, <http://www.gtec.at/Products/Complete-Solutions/g.EEGsys-Specs-Features>.

Gao, J, Zheng, C & Wang, P (2010), 'Online removal of muscle artifact from electroencephalogram signals based on canonical correlation analysis', *Clinical EEG and Neuroscience*, vol. 41, no. 1, pp. 53-9.

Gelb, DJ, Oliver, E & Gilman, S (1999), 'Diagnostic criteria for Parkinson disease', *Archives of Neurology*, vol. 56, no. 1, pp. 33-9.

Georgiev, D, Hamberg, K, Hariz, M, Forsgren, L & Hariz, GM (2017), 'Gender differences in Parkinson's disease: A clinical perspective', *Acta Neurologica Scandinavica*, vol. 136, no. 6, pp. 570-84.

Goadsby, PJ, Holland, PR, Martins-Oliveira, M, Hoffmann, J, Schankin, C & Akerman, S (2017), 'Pathophysiology of migraine: a disorder of sensory processing', *Physiological Reviews*, vol. 97, no. 2, pp. 553-622.

Goncharova, II, McFarland, DJ, Vaughan, TM & Wolpaw, JR (2003), 'EMG contamination of EEG: spectral and topographical characteristics', *Clinical Neurophysiology*, vol. 114, no. 9, pp. 1580-93.

Górriz, JM, Lang, EW & Ramírez, J (2011), *Recent Advances in Biomedical Signal Processing*, Bentham Science Publishers.

Granger, P, Biton, B, Faure, C, Vige, X, Depoortere, H, Graham, D, Langer, SZ, Scatton, B & Avenet, P (1995), 'Modulation of the gamma-aminobutyric acid type A receptor by the antiepileptic drugs carbamazepine and phenytoin', *Molecular Pharmacology*, vol. 47, no. 6, pp. 1189-96.

Grech, R, Cassar, T, Muscat, J, Camilleri, KP, Fabri, SG, Zervakis, M, Xanthopoulos, P, Sakkalis, V & Vanrumste, B (2008), 'Review on solving the inverse problem in EEG source analysis', *Journal of Neuroengineering and Rehabilitation*, vol. 5, no. 1, p. 1.

Gudmundsson, S, Runarsson, TP, Sigurdsson, S, Eiriksdottir, G & Johnsen, K (2007), 'Reliability of quantitative EEG features', *Clinical Neurophysiology*, vol. 118, no. 10, pp. 2162-71.

Haas, L (2003), 'Hans Berger (1873–1941), Richard Caton (1842–1926), and electroencephalography', *Journal of Neurology, Neurosurgery & Psychiatry*, vol. 74, no. 1, pp. 9-.

Hagen, K, Einarsen, C, Zwart, JA, Svebak, S & Bovim, G (2002), 'The co-occurrence of headache and musculoskeletal symptoms amongst 51 050 adults in Norway', *European Journal of Neurology*, vol. 9, no. 5, pp. 527-33.

Hallez, H, De Vos, M, Vanrumste, B, Van Hese, P, Assecondi, S, Van Laere, K, Dupont, P, Van Paesschen, W, Van Huffel, S & Lemahieu, I (2009), 'Removing muscle and eye artifacts using blind source separation techniques in ictal EEG source imaging', *Clinical Neurophysiology*, vol. 120, no. 7, pp. 1262-72.

Hämäläinen, MS & Ilmoniemi, RJ (1984), *Interpreting measured magnetic fields of the brain: estimates of current distributions*, Helsinki University of Technology, Department of Technical Physics.

Haque, B, Rahman, KM, Hoque, A, Hasan, AH, Chowdhury, RN, Khan, SU, Alam, MB, Habib, M & Mohammad, QD (2012), 'Precipitating and relieving factors of migraine versus tension type headache', *BMC neurology*, vol. 12, no. 1, p. 82.

Hazlett, RL, McLeod, DR & Hoehn-Saric, R (1994), 'Muscle tension in generalized anxiety disorder: Elevated muscle tonus or agitated movement?', *Psychophysiology*, vol. 31, no. 2, pp. 189-95.

Headache Classification Committee of the International Headache, S (2013), 'The International Classification of Headache Disorders, 3rd edition (beta version)', *Cephalalgia*, vol. 33, no. 9, pp. 629-808.

Hipp, JF, Engel, AK & Siegel, M (2011), 'Oscillatory synchronization in large-scale cortical networks predicts perception', *Neuron*, vol. 69, no. 2, pp. 387-96.

Hipp, JF & Siegel, M (2013), 'Dissociating neuronal gamma-band activity from cranial and ocular muscle activity in EEG', *Frontiers in Human Neuroscience*, vol. 7, p. 338.

Hotelling, H (1936), 'Relations between two sets of variates', *Biometrika*, vol. 28, no. 3/4, pp. 321-77.

Huang, MX, Shih, J, Lee, R, Harrington, D, Thoma, R, Weisend, M, Hanlon, F, Paulson, K, Li, T & Martin, K (2004a), 'Commonalities and differences among vectorized beamformers in electromagnetic source imaging', *Brain Topography*, vol. 16, no. 3, pp. 139-58.

Huang, MX, Shih, JJ, Lee, R, Harrington, D, Thoma, R, Weisend, M, Hanlon, F, Paulson, K, Li, T & Martin, K (2004b), 'Commonalities and differences among vectorized beamformers in electromagnetic source imaging', *Brain Topography*, vol. 16, no. 3, pp. 139-58.

Huang, Y, Dmochowski, JP, Su, Y, Datta, A, Rorden, C & Parra, LC (2013), 'Automated MRI segmentation for individualized modeling of current flow in the human head', *Journal of Neural Engineering*, vol. 10, no. 6, p. 066004.

Hughes, JR (2008), 'Gamma, fast, and ultrafast waves of the brain: their relationships with epilepsy and behavior', *Epilepsy & Behavior*, vol. 13, no. 1, pp. 25-31.

Hung, C-I, Liu, C-Y, Chen, J-J & Wang, S-J (2008), 'Migraine predicts self-reported muscle tension in patients with major depressive disorder', *Psychosomatics*, vol. 49, no. 6, pp. 502-10.

Hyvarinen, A (1999), 'Fast and robust fixed-point algorithms for independent component analysis', *IEEE transactions on Neural Networks*, vol. 10, no. 3, pp. 626-34.

Hyvärinen, A & Oja, E (2000), 'Independent component analysis: algorithms and applications', *Neural Networks*, vol. 13, no. 4, pp. 411-30.

Jensen, R, Fuglsang-Frederiksen, A & Olesen, J (1994), 'Quantitative surface EMG of pericranial muscles in headache. A population study', *Electroencephalography and Clinical Neurophysiology/Evoked Potentials Section*, vol. 93, no. 5, pp. 335-44.

Jensen, R, Rasmussen, BK, Pedersen, B & Olesen, J (1993), 'Muscle tenderness and pressure pain thresholds in headache. A population study', *Pain*, vol. 52, no. 2, pp. 193-9.

Jia, X & Kohn, A (2011), 'Primer Gamma Rhythms in the Brain'.

Johnson, G, Bogduk, N, Nowitzke, A & House, D (1994), 'Anatomy and actions of the trapezius muscle', *Clinical Biomechanics*, vol. 9, no. 1, pp. 44-50.

Jonmohamadi, Y, Poudel, G, Innes, C, Weiss, D, Krueger, R & Jones, R (2014), 'Comparison of beamformers for EEG source signal reconstruction', *Biomedical Signal Processing and Control*, vol. 14, pp. 175-88.

Jung, C-Y & Saikiran, SS (2016), 'A review on EEG artifacts and its different removal technique'.

Jung, T-P, Makeig, S, Humphries, C, Lee, T-W, Mckeown, MJ, Iragui, V & Sejnowski, TJ (2000), 'Removing electroencephalographic artifacts by blind source separation', *Psychophysiology*, vol. 37, no. 2, pp. 163-78.

Jutten, C & Herault, J (1991), 'Blind separation of sources, part I: An adaptive algorithm based on neuromimetic architecture', *Signal Processing*, vol. 24, no. 1, pp. 1-10.

Kandel, ER, Schwartz, JH, Jessell, TM, Biochemistry, Do, Jessell, MBT, Siegelbaum, S & Hudspeth, A (2000), *Principles of neural science*, vol. 4, McGraw-hill New York.

Kane, D, Balint, PV & Sturrock, RD (2003), 'Ultrasonography is superior to clinical examination in the detection and localization of knee joint effusion in rheumatoid arthritis', *The Journal of Rheumatology*, vol. 30, no. 5, pp. 966-71.

Karhunen, J, Hao, T & Ylipaavalniemi, J (2012), 'A generalized canonical correlation analysis based method for blind source separation from related data sets', in *Neural Networks (IJCNN), The 2012 International Joint Conference on*, pp. 1-9.

Kim, T, Attias, HT, Lee, S-Y & Lee, T-W (2007), 'Blind source separation exploiting higher-order frequency dependencies', *IEEE transactions on audio, speech, and language processing*, vol. 15, no. 1, pp. 70-9.

Kim, T, Eltoft, T & Lee, T-W (2006), 'Independent vector analysis: An extension of ICA to multivariate components', in *International Conference on Independent Component Analysis and Signal Separation*, pp. 165-72.

Kirmizi-Alsan, E, Bayraktaroglu, Z, Gurvit, H, Keskin, YH, Emre, M & Demiralp, T (2006), 'Comparative analysis of event-related potentials during Go/NoGo and CPT: decomposition of electrophysiological markers of response inhibition and sustained attention', *Brain Research*, vol. 1104, no. 1, pp. 114-28.

Kirschfeld, K (2005), 'The physical basis of alpha waves in the electroencephalogram and the origin of the "Berger effect"', *Biological Cybernetics*, vol. 92, no. 3, pp. 177-85.

Kisley, MA & Cornwell, ZM (2006), 'Gamma and beta neural activity evoked during a sensory gating paradigm: effects of auditory, somatosensory and cross-modal stimulation', *Clinical Neurophysiology*, vol. 117, no. 11, pp. 2549-63.

Kothe, CA & Makeig, S (2013), 'BCILAB: a platform for brain–computer interface development', *Journal of Neural Engineering*, vol. 10, no. 5, p. 056014.

Kuhnke, N, Schwind, J, Dümpelmann, M, Mader, M, Schulze-Bonhage, A & Jacobs, J (2018), 'High Frequency Oscillations in the Ripple Band (80–250 Hz) in Scalp EEG: Higher Density of Electrodes Allows for Better Localization of the Seizure Onset Zone', *Brain Topography*, vol. 31, no. 6, pp. 1059-72.

Kumar, S, Narayan, Y & Amell, T (2003), 'Power spectra of sternocleidomastoids, splenius capitis, and upper trapezius in oblique exertions', *The spine Journal*, vol. 3, no. 5, pp. 339-50.

Landgraf, MN, Ertl-Wagner, B, Koerte, IK, Thienel, J, Langhagen, T, Straube, A, von Kries, R, Reilich, P, Pomschar, A & Heinen, F (2015), 'Alterations in the trapezius muscle in young patients with migraine--a pilot case series with MRI', *Eur J Paediatr Neurol*, vol. 19, no. 3, pp. 372-6.

Laney, J, Westlake, KP, Ma, S, Woytowicz, E, Calhoun, VD & Adalı, T (2015), 'Capturing subject variability in fMRI data: A graph-theoretical analysis of GICA vs. IVA', *Journal of Neuroscience Methods*, vol. 247, pp. 32-40.

Lau, TM, Gwin, JT & Ferris, DP (2012), 'How many electrodes are really needed for EEG-based mobile brain imaging?', *Journal of Behavioral and Brain Science*, vol. 2, no. 03, p. 387.

Lebbink, J, Spierings, E & Messinger, HB (1991), 'A questionnaire survey of muscular symptoms in chronic headache. An age-and sex-controlled study', *The Clinical Journal of Pain*, vol. 7, no. 2, pp. 95-101.

Lee, I, Kim, T & Lee, T-W (2007), 'Fast fixed-point independent vector analysis algorithms for convolutive blind source separation', *Signal Processing*, vol. 87, no. 8, pp. 1859-71.

Leistad, R, Sand, T, Westgaard, R, Nilsen, K & Stovner, L (2006), 'Stress-induced pain and muscle activity in patients with migraine and tension-type headache', *Cephalalgia*, vol. 26, no. 1, pp. 64-73.

Leutheuser, H, Gabsteiger, F, Hebenstreit, F, Reis, P, Lochmann, M & Eskofier, B (2013), 'Comparison of the AMICA and the InfoMax algorithm for the reduction of electromyogenic artifacts in EEG data', in *Engineering in Medicine and Biology Society (EMBC), 2013 35th Annual International Conference of the IEEE*, pp. 6804-7.

Löscher, W (1999), 'Valproate: a reappraisal of its pharmacodynamic properties and mechanisms of action', *Progress in Neurobiology*, vol. 58, no. 1, pp. 31-59.

Louis, ED, Klatka, LA, Liu, Y & Fahn, S (1997), 'Comparison of extrapyramidal features in 31 pathologically confirmed cases of diffuse Lewy body disease and 34 pathologically confirmed cases of Parkinson's disease', *Neurology*, vol. 48, no. 2, pp. 376-80.

Lous, I & Olesen, J (1982), 'Evaluation of pericranial tenderness and oral function in patients with common migraine, muscle contraction headache and ‘combination headache’', *Pain*, vol. 12, no. 4, pp. 385-93.

Mansor, W, Rani, MSA & Wahy, N (2011), 'Integrating neural signal and embedded system for controlling small motor', in *Advances in Mechatronics*, InTech.

Martin, WE, Loewenson, RB, Resch, JA & Baker, AB (1973), 'Parkinson's disease Clinical analysis of 100 patients', *Neurology*, vol. 23, no. 8, pp. 783-.

Martins, IP & Parreira, E (2001), 'Behavioral Response to Headache: A Comparison Between Migraine and Tension-type Headache', *Headache: The Journal of Head and Face Pain*, vol. 41, no. 6, pp. 546-53.

McArthur, DL & Cohen, MJ (1980), 'Measures of forehead and finger temperature, frontalis EMG, heart rate and finger pulse amplitude during and between migraine headaches', *Headache: The Journal of Head and Face Pain*, vol. 20, no. 3, pp. 134-6.

McLean, CP, Asnaani, A, Litz, BT & Hofmann, SG (2011), 'Gender differences in anxiety disorders: prevalence, course of illness, comorbidity and burden of illness', *Journal of Psychiatric Research*, vol. 45, no. 8, pp. 1027-35.

McMenamin, BW, Shackman, AJ, Greischar, LL & Davidson, RJ (2011), 'Electromyogenic artifacts and electroencephalographic inferences revisited', *Neuroimage*, vol. 54, no. 1, pp. 4-9.

McMenamin, BW, Shackman, AJ, Maxwell, JS, Bachhuber, DR, Koppenhaver, AM, Greischar, LL & Davidson, RJ (2010), 'Validation of ICA-based myogenic artifact correction for scalp and source-localized EEG', *Neuroimage*, vol. 49, no. 3, pp. 2416-32.

Meirovitch, Y, Harris, H, Dayan, E, Arieli, A & Flash, T (2015), 'Alpha and beta band event-related desynchronization reflects kinematic regularities', *Journal of Neuroscience*, vol. 35, no. 4, pp. 1627-37.

Miller, IN & Cronin-Golomb, A (2010), 'Gender differences in Parkinson's disease: clinical characteristics and cognition', *Movement Disorders*, vol. 25, no. 16, pp. 2695-703.

Milstein, J, Mormann, F, Fried, I & Koch, C (2009), 'Neuronal shot noise and Brownian 1/f2 behavior in the local field potential', *PloS one*, vol. 4, no. 2, p. e4338.

Mognon, A, Jovicich, J, Bruzzone, L & Buiatti, M (2011), 'ADJUST: An automatic EEG artifact detector based on the joint use of spatial and temporal features', *Psychophysiology*, vol. 48, no. 2, pp. 229-40.

Møller, E (1976), *Evidence that the rest position is subject to servo-control*, Bristol: Wright.

Muthuraman, M, Tamás, G, Hellriegel, H, Deuschl, G & Raethjen, J (2012), 'Source analysis of beta-synchronisation and cortico-muscular coherence after movement termination based on high resolution electroencephalography', *PloS one*, vol. 7, no. 3, p. e33928.

Neugebauer, F, Möddel, G, Rampp, S, Burger, M & Wolters, CH (2017), 'The effect of head model simplification on beamformer source localization', *Frontiers in Neuroscience*, vol. 11, p. 625.

Niedermeyer, E (1997), 'Alpha rhythms as physiological and abnormal phenomena', *International Journal of Psychophysiology*, vol. 26, no. 1-3, pp. 31-49.

Niedermeyer, E & da Silva, FL (2005), *Electroencephalography: basic principles, clinical applications, and related fields*, Lippincott Williams & Wilkins.

O'Dwyer, N, Ada, L & Neilson, P (1996), 'Spasticity and muscle contracture following stroke', *Brain*, vol. 119, no. 5, pp. 1737-49.

Oksanen, A, Pöyhönen, T, Ylinen, JJ, Metsähonkala, L, Anttila, P, Laimi, K, Hiekkanen, H, Aromaa, M, Salminen, JJ & Sillanpää, M (2008), 'Force production and EMG activity of neck muscles in adolescent headache', *Disability and rehabilitation*, vol. 30, no. 3, pp. 231-9.

Olbrich, S & Arns, M (2013), 'EEG biomarkers in major depressive disorder: discriminative power and prediction of treatment response', *International Review of Psychiatry*, vol. 25, no. 5, pp. 604-18.

Oostenveld, R, Fries, P, Maris, E & Schoffelen, J-M (2010), 'FieldTrip: open source software for advanced analysis of MEG, EEG, and invasive electrophysiological data', *Computational Intelligence and Neuroscience*, vol. 2011.

—— (2011), 'FieldTrip: open source software for advanced analysis of MEG, EEG, and invasive electrophysiological data', *Computational Intelligence and Neuroscience*, vol. 2011, p. 1.

Oostenveld, R & Praamstra, P (2001), 'The five percent electrode system for high-resolution EEG and ERP measurements', *Clinical Neurophysiology*, vol. 112, no. 4, pp. 713-9.

Pallanti, S, Quercioli, L & Hollander, E (2004), 'Social anxiety in outpatients with schizophrenia: a relevant cause of disability', *American Journal of Psychiatry*, vol. 161, no. 1, pp. 53-8.

Palmer, JA, Kreutz-Delgado, K & Makeig, S (2012), 'AMICA: An adaptive mixture of independent component analyzers with shared components', *Swartz Center for Computatonal Neursoscience, University of California San Diego, Tech. Rep*.

Pascual-Marqui, RD (2002), 'Standardized low-resolution brain electromagnetic tomography (sLORETA): technical details', *Methods Find Exp Clin Pharmacol*, vol. 24, no. Suppl D, pp. 5-12.

Petrea, RE, Beiser, AS, Seshadri, S, Kelly-Hayes, M, Kase, CS & Wolf, PA (2009), 'Gender differences in stroke incidence and poststroke disability in the Framingham heart study', *Stroke*, vol. 40, no. 4, pp. 1032-7.

Petsche, H, Pockberger, H & Rappelsberger, P (1984), ' On the search for the sources of the electroencephalogram', *Neuroscience*, vol. 11, no. 1, pp. 1-27

Pham, TT, Croft, RJ, Cadusch, PJ & Barry, RJ (2011), 'A test of four EOG correction methods using an improved validation technique', *International Journal of Psychophysiology*, vol. 79, no. 2, pp. 203-10.

Pluess, M, Conrad, A & Wilhelm, FH (2009), 'Muscle tension in generalized anxiety disorder: a critical review of the literature', *Journal of Anxiety Disorders*, vol. 23, no. 1, pp. 1-11.

Pope, KJ & Bogner, RE (1996), 'Blind Signal Separation I. Linear, Instantaneous Combinations: I. Linear, Instantaneous Combinations', *Digital Signal Processing*, vol. 6, no. 1, pp. 5-16.

Pope, KJ, Fitzgibbon, SP, Lewis, TW, Whitham, EM & Willoughby, JO (2009), 'Relation of gamma oscillations in scalp recordings to muscular activity', *Brain Topogr*, vol. 22, no. 1, pp. 13-7.

Radüntz, T, Scouten, J, Hochmuth, O & Meffert, B (2015), 'EEG artifact elimination by extraction of ICA-component features using image processing algorithms', *Journal of Neuroscience Methods*, vol. 243, pp. 84-93.

Reddy, AG & Narava, S (2013), 'Artifact removal from EEG signals', *International Journal of Computer Applications*, vol. 77, no. 13.

Romero, S, Mañanas, MA & Barbanoj, MJ (2008), 'A comparative study of automatic techniques for ocular artifact reduction in spontaneous EEG signals based on clinical target variables: a simulation case', *Computers in Biology and Medicine*, vol. 38, no. 3, pp. 348-60.

Rowa, K & Antony, MM (2008), 'Generalized anxiety disorder', *Psychopathology: History, Diagnosis, and Empirical Foundations*, pp. 78-115.

Safieddine, D, Kachenoura, A, Albera, L, Birot, G, Karfoul, A, Pasnicu, A, Biraben, A, Wendling, F, Senhadji, L & Merlet, I (2012), 'Removal of muscle artifact from EEG data: comparison between stochastic (ICA and CCA) and deterministic (EMD and wavelet-based) approaches', *EURASIP Journal on Advances in Signal Processing*, vol. 2012, no. 1, p. 127.

Sahonero-Alvarez, G, La Paz, B-g, CALDERON, H & La Paz, B (2017), 'A Comparison of SOBI, FastICA, JADE and Infomax Algorithms'.

Sekihara, K, Nagarajan, SS, Poeppel, D, Marantz, A & Miyashita, Y (2001), 'Reconstructing spatio-temporal activities of neural sources using an MEG vector beamformer technique', *IEEE Transactions on Biomedical Engineering*, vol. 48, no. 7, pp. 760-71.

Sekihara, K, Sahani, M & Nagarajan, SS (2005), 'Localization bias and spatial resolution of adaptive and non-adaptive spatial filters for MEG source reconstruction', *Neuroimage*, vol. 25, no. 4, pp. 1056-67.

Shackman, AJ, McMenamin, BW, Slagter, HA, Maxwell, JS, Greischar, LL & Davidson, RJ (2009), 'Electromyogenic artifacts and electroencephalographic inferences', *Brain Topography*, vol. 22, no. 1, pp. 7-12.

Shim, M, Im, C & Lee, S (2017), 'Disrupted cortical brain network in post-traumatic stress disorder patients: a resting-state electroencephalographic study', *Translational Psychiatry*, vol. 7, no. 9, p. e1231.

Shin, H-W & Chung, SJ (2012), 'Drug-induced parkinsonism', *Journal of Clinical Neurology*, vol. 8, no. 1, pp. 15-21.

Siegmund, GP, Blouin, J-S, Brault, JR, Hedenstierna, S & Inglis, JT (2007), 'Electromyography of superficial and deep neck muscles during isometric, voluntary, and reflex contractions', *Journal of Biomechanical Engineering*, vol. 129, no. 1, pp. 66-77.

Singer, W (2001), 'Consciousness and the binding problem', *Annals of the New York Academy of Sciences*, vol. 929, no. 1, pp. 123-46.

Siris, SG & Braga, RJ (2013), 'Anxiety in Schizophrenia', *Retrieved on February*, vol. 15, p. 2014.

Sohrabpour, A, Lu, Y, Kankirawatana, P, Blount, J, Kim, H & He, B (2015), 'Effect of EEG electrode number on epileptic source localization in pediatric patients', *Clinical Neurophysiology*, vol. 126, no. 3, pp. 472-80.

Sommerfeld, DK, Eek, EU-B, Svensson, A-K, Holmqvist, LW & von Arbin, MH (2004), 'Spasticity after stroke: its occurrence and association with motor impairments and activity limitations', *Stroke*, vol. 35, no. 1, pp. 134-9.

Song, J, Davey, C, Poulsen, C, Luu, P, Turovets, S, Anderson, E, Li, K & Tucker, D (2015), 'EEG source localization: sensor density and head surface coverage', *Journal of Neuroscience Methods*, vol. 256, pp. 9-21.

Sörnmo, L & Laguna, P (2005), *Bioelectrical Signal Processing in Cardiac and Neurological applications*, vol. 8, Academic Press.

Stemmler, G, Aue, T & Wacker, J (2007), 'Anger and fear: Separable effects of emotion and motivational direction on somatovisceral responses', *International Journal of Psychophysiology*, vol. 66, no. 2, pp. 141-53.

Sur, S & Sinha, V (2009), 'Event-related potential: An overview', *Industrial Psychiatry Journal*, vol. 18, no. 1, p. 70.

Tatum, WO (2014), 'Ellen R. Grass Lecture: Extraordinary EEG', *The Neurodiagnostic Journal*, vol. 54, no. 1, pp. 3-21.

Teplan, M (2002), 'Fundamentals of EEG measurement', *Measurement Science Review*, vol. 2, no. 2, pp. 1-11.

Tfelt-Hansen, P, Lous, I & Olesen, J (1981), 'Prevalence and significance of muscle tenderness during common migraine attacks', *Headache: The Journal of Head and Face Pain*, vol. 21, no. 2, pp. 49-54.

Urigüen, JA & Garcia-Zapirain, B (2015), 'EEG artifact removal—state-of-the-art and guidelines', *Journal of Neural Engineering*, vol. 12, no. 3, p. 031001.

Van Oosterom, A (1991), 'History and evolution of methods for solving the inverse problem', *Journal of Clinical Neurophysiology*, vol. 8, no. 4, pp. 371-80.

Van Veen, BD & Buckley, KM (1988), 'Beamforming: A versatile approach to spatial filtering', *IEEE assp magazine*, vol. 5, no. 2, pp. 4-24.

Van Veen, BD, Van Drongelen, W, Yuchtman, M & Suzuki, A (1997), 'Localization of brain electrical activity via linearly constrained minimum variance spatial filtering', *IEEE Transactions on Biomedical Engineering*, vol. 44, no. 9, pp. 867-80.

Vancampfort, D, Correll, CU, Scheewe, TW, Probst, M, De Herdt, A, Knapen, J & De Hert, M (2013), 'Progressive muscle relaxation in persons with schizophrenia: a systematic review of randomized controlled trials', *Clinical Rehabilitation*, vol. 27, no. 4, pp. 291-8.

Vancampfort, D, De Hert, M, Knapen, J, Maurissen, K, Raepsaet, J, Deckx, S, Remans, S & Probst, M (2011), 'Effects of progressive muscle relaxation on state anxiety and subjective well-being in people with schizophrenia: a randomized controlled trial', *Clinical Rehabilitation*, vol. 25, no. 6, pp. 567-75.

Vanderwolf, C (2000), 'Are neocortical gamma waves related to consciousness?', *Brain Research*, vol. 855, no. 2, pp. 217-24.

Vergult, A, De Clercq, W, Palmini, A, Vanrumste, B, Dupont, P, Van Huffel, S & Van Paesschen, W (2007), 'Improving the interpretation of ictal scalp EEG: BSS–CCA algorithm for muscle artifact removal', *Epilepsia*, vol. 48, no. 5, pp. 950-8.

Vinhas, V, Oliveira, E & Reis, LP (2008), 'Realtime dynamic multimedia storyline based on online audience biometric information', in *New Directions in Intelligent Interactive Multimedia*, Springer, pp. 545-54.

Viola, FC, Thorne, J, Edmonds, B, Schneider, T, Eichele, T & Debener, S (2009), 'Semi-automatic identification of independent components representing EEG artifact', *Clinical Neurophysiology*, vol. 120, no. 5, pp. 868-77.

Watkins, C, Leathley, M, Gregson, J, Moore, A, Smith, T & Sharma, A (2002), 'Prevalence of spasticity post stroke', *Clinical Rehabilitation*, vol. 16, no. 5, pp. 515-22.

Watson, DH & Drummond, PD (2012), 'Head Pain Referral During Examination of the Neck in Migraine and Tension-Type Headache', *Headache: The Journal of Head and Face Pain*, vol. 52, no. 8, pp. 1226-35.

Welch, PD (1967), 'The use of fast Fourier transform for the estimation of power spectra: A method based on time averaging over short, modified periodograms', *IEEE Transactions on Audio and Electroacoustics*, vol. 15, no. 2, pp. 70-3.

Whitham, EM, Lewis, T, Pope, KJ, Fitzgibbon, SP, Clark, CR, Loveless, S, DeLosAngeles, D, Wallace, AK, Broberg, M & Willoughby, JO (2008), 'Thinking activates EMG in scalp electrical recordings', *Clin Neurophysiol*, vol. 119, no. 5, pp. 1166-75.

Whitham, EM, Pope, KJ, Fitzgibbon, SP, Lewis, T, Clark, CR, Loveless, S, Broberg, M, Wallace, A, DeLosAngeles, D & Lillie, P (2007), 'Scalp electrical recording during paralysis: quantitative evidence that EEG frequencies above 20Hz are contaminated by EMG', *Clinical Neurophysiology*, vol. 118, no. 8, pp. 1877-88.

Worrell, G (2012), 'High-frequency oscillations recorded on scalp EEG', *Epilepsy Currents*, vol. 12, no. 2, pp. 57-8.

Yilmaz, G, Ungan, P, Sebik, O, Uginčius, P & Türker, KS (2014), 'Interference of tonic muscle activity on the EEG: a single motor unit study', *Frontiers in human neuroscience*, vol. 8, p. 504.

Zijlmans, M, Jiruska, P, Zelmann, R, Leijten, FS, Jefferys, JG & Gotman, J (2012), 'High-frequency oscillations as a new biomarker in epilepsy', *Annals of Neurology*, vol. 71, no. 2, pp. 169-78.

Appendix A

First-author published journal papers

A-1 First paper

This paper is published in the Journal of Neuroscience Methods (https://doi.org/10.1016/j.jneumeth.2017.06.011) and covers much of Chapter 4. Chapter 4 contains some additional results, a more detailed statistical analysis, and an expanded discussion and conclusion. This article removed due to copyright restrictions.

A-2 Second paper

This paper is published in the Journal of Neuroscience Methods (https://doi.org/10.1016/j.jneumeth.2018.01.004) and covers much of Chapter 5. Chapter 5 contains some additional results, a more detailed statistical analysis, and an expanded discussion and conclusion. This article removed due to copyright restrictions.

A-3 Third paper

This paper is published in the Journal of Clinical Neurophysiology (https://doi.org/10.1016/j.clinph.2018.06.017) and covers much of Chapter 7. Chapter 7 contains some additional results, including the validation of the proposed method on three disease groups and the exploration of the proposed method on a further three disease groups. Additionally, Chapter 7 has an expanded discussion and conclusion. This article removed due to copyright restrictions.

Appendix B

First-author published conference papers

B-1 First paper

This paper is published in the 26th European Signal Processing Conference (EUSIPCO 2018, 10.23919/EUSIPCO.2018.8553261). A subset of Chapter 3, specifically the testing of the effect of the number of SER channels (Section 3.4 for dataset 1), is covered in this paper. Chapter 3 contains additional results, a more detailed statistical analysis, and an expanded discussion and conclusion. This article removed due to copyright restrictions.

B-2 Second paper

This paper is published in the 26th European Signal Processing Conference (EUSIPCO 2018, 10.23919/EUSIPCO.2018.8553014). This paper contains some of the results presented in Chapter 6, specifically it is restricted to using Infomax on dataset 1. Chapter 6 contains additional results using multiple BSS algorithms and multiple datasets, a more detailed statistical analysis, and an expanded discussion and conclusion. This article removed due to copyright restrictions.